DIFFERENTIAL REGULATION OF TWO- AND THREE-DIMENSIONAL CELL FUNCTION

by

Robert Grant Rowe

A dissertation submitted in partial fulfillment
of the requirements for the degree of
Doctor of Philosophy
(Cellular and Molecular Biology)
in The University of Michigan
2009

Doctoral Committee:

Professor Stephen J. Weiss, Chair
Professor James Douglas Engel
Professor Eric R. Fearon
Professor David Ginsburg
Professor Alan R. Saltiel

Acknowledgements

I thank my thesis mentor, Steve Weiss for constant feedback and criticism. I also thank my dissertation committee for guiding this work.

The discussion of basement membrane transmigration in Chapter 1 of this work has been published in *Trends in Cell Biology* with Stephen J. Weiss as co-author. The discussions regarding three-dimensional cell function and MT1-MMP structure, function, and regulation in Chapter 1 are under review for publication in *Annual Review of Cell and Developmental Biology* with Stephen J. Weiss as co-author.

For the work presented in Chapter 2, Ryoko Shimuzu-Hiraota assisted with intraperitoneal injections of transgenic mice, and Casey Hu processed liver tissue for cryosectioning. Joel Greenson of the Department of Pathology at the University of Michigan provided expertise related to assessment of liver inflammation. Eric G. Neilson of Vanderbilt University provided an essential reagent as well as critical input when writing this manuscript.

Chapter 4 has been published in *The Journal of Cell Biology*. I thank my co-authors Xiao-Yan Li and Casey Hu for performing and analyzing the chick chorioallantoic membrane assay; Thom Saunders and Eric Fearon for advice and support in generating conditional knock-out mice; Ismo Virtanen (University of Helsinki), Antonio Garcia de Herreros (Institut Municipal d'Investigació Mèdica Hospital del Mar Universitat Pompeu Fabra), and Karl-Friedrich Becker (Technical University of Munich) for providing anti-Snail1 antibodies, Signe Ingvarsen and Lars Engelholm (The Finsen Laboratory) for providing the anti-MT1-MMP antibody, and Guido Bommer for assistance in isolating and transforming mouse embryonic fibroblasts.

The data presented in Chapter 5 has been published in *Genes and Development*. I acknowledge my co-authors Xiaoming Zhou and Nobuaki Hiraoka for performing seminal experiments in this study, Jerry George and Dennis Wirtz (Johns Hopkins University) for three-dimensional ballistic nanorheology studies, Deane Mosher (University of Wisconsin) for providing the FUD peptide reagent, Ismo Virtanen (University of Helsinki) for tissue immunostaining, and Michael Chernousov (Weis Center for Research) for providing the L8 monoclonal antibody.

The data presented in Chapter 6 is currently under review. I acknowledge my co-authors Martin Ehrbar (University Hospital Zurich) and Matthias Lutolf (Ecole Polytechnique Federale de Lausanne) for assistance with 3-D poly(ethylene glycol) scaffolds, Heidi Fridolfsson and Daniel Starr (University of California, Davis) for providing the nesprin-3 antibody, Chris Chen and Colette Shen (University of Pennsylvania) for micropatterned cell culture substrata, Fei Liu and Dennis Tschumperlin (Harvard University) for performing atomic force microscopy measurements, and Deane Mosher for providing the FUD peptide reagent.

Tyler Dirda assisted with construction of the targeting vector to generate the MT2-MMP conditional knock-out mouse, and screened embryonic stem cell clones for targeting of the genes for MT1-MMP and MT2-MMP. Rosie Lemons and Changlian Lu performed crucial breeding and mouse husbandry for the MT1-MMP and MT2-MMP conditional knock-out mice. I thank Steve Lentz of the Michigan Diabetes Training Program Morphology and Image Analysis Core for assistance with confocal microscopy. The work in this dissertation was supported in part by the Cancer Biology Training Program and the Medical Scientist Training Program at The University of Michigan.

Table of Contents

List of Figures

List of Tables

Chapter 1: Introduction: 2-D to 3-D Transitions

In vivo, cell function is regulated not only by soluble biochemical signals, energy status, and oxygen availability, but also by the structural features and composition of the surrounding extracellular matrix (ECM) (1, 2, 3). The ECM is a crosslinked macromolecular network of proteins, glycoproteins, and proteoglycans that maintains tissue architecture while regulating cell function and fate (4, 5). Structural characteristics of ECMs vary as a function of ECM composition. One such characteristic is dimensionality; cells interface either with a two-dimensional (2-D) or three-dimensional (3-D) ECM (3, 5). The ability of a cell to sense and appropriately respond to dimensionality is essential for biologic development and tissue homeostasis. Consistent with this idea, a central aspect of cellular differentiation is the acquisition of the appropriate transcriptional programs and molecular machinery required for function either in 2-D or 3-D.

Though all cells are inherently 3-D structures at the subcellular level, cells residing within solid tissues can be classified as either 2-D or 3-D by considering the dimensionality of their respective ECM niches. 2-D cells form a tight monolayer lining all tubular organs such as the gastrointestinal tract, respiratory tract, glandular tissues, as well as the vasculature (3, 5). Under physiologic conditions, 2-D cells exhibit apical/basal polarity, are generally non-motile, quiescent, and tightly adherent to one another via interaction of multiprotein cell:cell junctional complexes. As such, epithelial, endothelial, and mesothelial cells can be classified as 2-D cells. The ECM that defines cellular two-dimensionality is the basement membrane (BM). 2-D cells reside atop this flat, sheet-like ECM which serves to confine such cells to tubular and glandular

lumina while acting as a structural scaffold for tissue organization and compartmentalization (5, 6). In many vertebrate tissues, the BM serves as a rugged barrier partitioning the second and third tissue dimensions (5, 6).

Beneath the epithelial BM lies the 3-D environment of the interstitial compartment. 3-D tissues – such as the mesenchyme of the dermis or colonic wall and soft tissues including muscle and adipose tissue - are predominately mesodermal or neural crest in origin. These tissues are populated by 3-D cells including fibroblasts, adipocytes, myocytes and peripheral neurons. Unlike 2-D cells, 3-D cells do not display apical/basal polarity, maintain the capacity to become highly motile and tissue-invasive, and do not typically exhibit homotypic adhesion. These cells are encased on all sides by a 3-D ECM dominated by mesh-like networks of collagens I and III in mature tissues or by scaffolds of fibrin and the fibrillar glycoprotein fibronectin in tissues undergoing active remodeling (2, 3, 7, 8).

A priori, since both 2-D and 3-D cells are derived from a common precursor - the 2-D, epithelial-like epiblast and hypoblast cells of the two-layered embryo in vertebrates – it follows that mechanisms must exist for interconversion of these two cell types. At the onset of gastrulation, 2-D epiblast cells residing atop a BM lose polarity and homotypic adhesion, invade the underlying ECM and assume a 3-D cell phenotype to form the earliest mesodermal precursors—a process that can be termed the 2-D to 3-D transition (9). This conversion from a 2-D to a 3-D phenotype is an important developmental paradigm that becomes inappropriately activated in several disease states. An essential requirement for a cell to change dimensionality is the ability to penetrate ECM barriers interposed between dimensions, such as the 2-D BM and the 3-D ECM of the interstitial compartment (Figure 1.1). Indeed, most 2-D-to-3-D transitions are a stepwise process beginning with perforation of epithelial or endothelial BMs, recruitment of the transcriptional programs required for execution of essential cell functions in 3-D, migration into 3-D, and establishment of a 3-D niche suitable for proliferation, differentiation, and survival (4, 5, 7, 10-12).

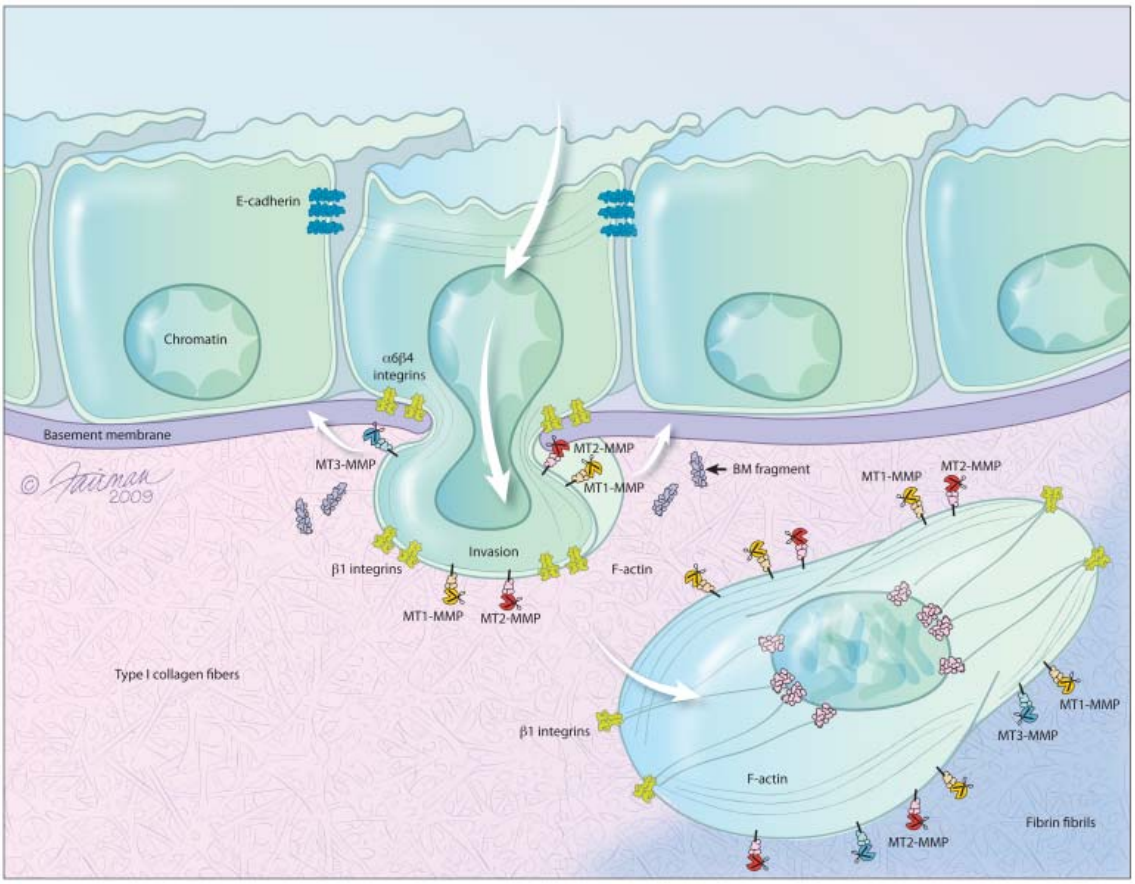

Figure 1.1. The 2-D-to-3-D transition

A differentiated epithelial cell normally exists atop the 2-D ECM of the BM. During carcinoma progression, a malignant epithelial cell punctures the BM via the action of MT1,2,3-MMPs and transmigrates into the 3-D environment of the interstitial ECM. BM degradation products with biological activity signal to the invading cell and host stroma to modulate cell function. Within the 3-D ECM, collagen fibrils are remodeled by MT1- and MT2- MMP, and fibrin fibrils via MT1,2,3-MMPs. This 2-D to 3-D transition process in accompanied by disruption of cell:cell adhesion complexes (including adherens junctions containing E-cadherin), loss of cell polarity, protease activation, cytoskeletal and nuclear remodeling, and integrin switching. Collectively, these phenotypic changes result in the malignant epithelial cell assuming a non-polar, mesenchymal-like phenotype for growth, migration, and survival within the 3-D interstitial ECM.

Herein I will discuss shifts in cellular dimensionality as events regulated by the capacity of a cell to modify and overcome ECM barriers in both development and disease. Furthermore, I will present recent studies that characterize the transcriptional regulators and ECM remodeling events recruited during 2-D-to-3-D transitions. Despite considerable variation in structure and composition

between 2-D and 3-D ECMs as well as the diversity of the cell lineages that undergo changes in dimensionality, a body of evidence suggests that a select group of transcriptional regulators of the Snail, ZEB, and basic helix-loop-helix family trigger the cell-intrinsic transcriptional reprogramming required for 2-D-to-3-D transitions (13). Additionally, a small family of membrane-tethered proteolytic effector enzymes, termed the membrane-type matrix metalloproteinases (MT-MMPs), serve as the minimal degradative machinery required for navigation and remodeling of both 2-D and 3-D ECM barriers (4, 5, 7, 8, 10, 14, 15). Hence, understanding the regulation, activity and pathophysiologic functions of this surprisingly small group of factors should provide a deeper understanding of the molecular mechanisms underlying the control of cell dimensionality during development and disease.

Changing Dimensionality in Development and Disease. Changes in cell dimensionality have long been known to occur during developmental events. During mammalian development, the early embryo consists of two apposed layers of 2-D epithelial cells. With the induction of gastrulation, genesis of the third germ layer, the mesoderm, occurs when epithelial cells within the epiblast at the primitive streak adopt mesenchymal (i.e., fibroblast-like) characteristics, penetrate the underlying BM and populate the intervening space to ultimately form the primitive mesoderm—the precursor to mature connective tissues (Figure 1.2A)(16-18). Similar programs are recruited during other developmental 2-D-to-3-D transitions. Specialized cells within the neuroepithelial layer of the ectoderm in the three-layered embryo – termed neural crest cells – delaminate, assume a 3-D phenotype, and migrate to distant sites where they differentiate into specialized tissues including craniofacial structures, peripheral nerves and pigmented cells (19-21).

2-D-to-3-D transitions occur during multiple stages of vascular development. During angiogenesis – the process of capillary sprouting from the mature vasculature – pro-angiogenic growth factors trigger endothelial cells to penetrate BM barriers, lose polarity, infiltrate the 3-D environment and eventually

coalesce to assemble a patent neovessel (5, 12, 14, 22) – a 2-D-to-3-D-to-2-D transition process. In adults, this developmental program is recruited to support vascularization of wounds, tumors, and sites of chronic inflammation (23, 24). Endothelial cells engage a similar program to form the cardiac valves when 2-D embryonic endocardial cells give rise to the 3-D mesenchymal cells populating the valve connective tissue (25-28). Furthermore, vascular pericytes and mural cells have been proposed to emerge from endothelial cells *via* a similar mechanism (29-33).

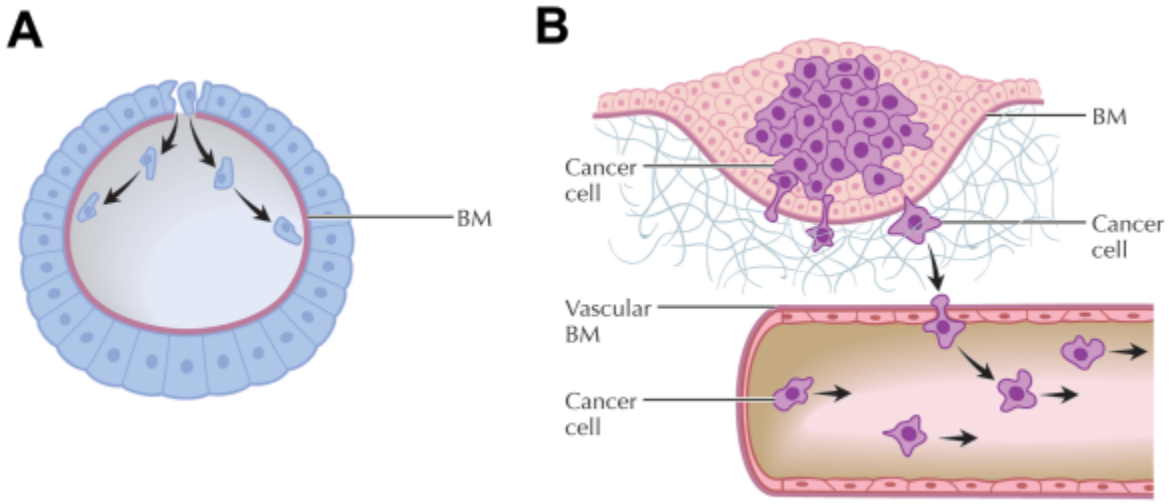

Figure 1.2. 2-D-to-3-D transitions

A. During gastrulation, epiblast cells invade at the primitive streak, penetrating the epithelial BM to populate the space beneath the germ layer to produce the mesoderm. **B.** At the initial phase of tumor invasion, tumor cells acquire the ability to breach epithelial BM barriers and migrate into the stromal matrix. After traversing the stroma, tumor cells cross the vascular BM both at the primary tumor site (termed intravasation) as well as at the site of metastasis (i.e., extravasation) to colonize distant organs.

With the exception of the 2-D/3-D transition events associated with reproduction in adult mammals – such as invasion of the endometrial decidua by trophoblast cells during blastocyst implantation – such programs do not seem to be re-engaged in the adult, save for pathologic conditions. 2-D-to-3-D transitions seem to play a major role in promoting cancer morbidity and mortality. During carcinoma progression, non-invasive, dysplastic 2-D epithelial cells proliferate locally as a lesion termed carcinoma *in situ*. Unchecked, the localized lesion will

acquire the capacity to perforate the subjacent BM barrier and invade the 3-D interstitium, thus becoming an invasive carcinoma (Figure 1.2B) (34, 35). Additionally, epithelial cells need not adopt a neoplastic status to display 2-D-to-3-D transitions. For example, recent studies demonstrate that in pathologic fibrotic disease states (e.g., most commonly affecting the liver, lungs or kidneys), epithelial cells adopt a 3-D mesenchymal, fibroblast-like phenotype as they traverse the underlying BM, infiltrate underlying stromal tissues and deposit an excess of interstitial matrix components (36-41). In addition, it has been proposed that endothelial cells can inappropriately recruit embryonic 2-D-to-3-D transition programs to contribute to the population of 3-D fibroblast-like cells found in fibrotic tissue and within the peritumoral stroma (42-44), as well as during atherosclerosis and pulmonary hypertension (45, 46)

Conversely, changes in dimensionality that occur during development and disease can also proceed from 3-D to 2-D. During nephrogenesis, condensation of the 3-D cells of the metanephric mesenchyme results in the differentiation of the 2-D epithelia of nephrons (38). Similar programs seem to be recruited during adenocarcinoma metastasis; though 2-D-to-3-D transition of neoplastic epithelial cells is required for local invasion at the primary tumor site, distant secondary tumor foci often contain well-differentiated 2-D epithelial glandular structures nearly identical to the tissue of origin (47). These findings suggest that cancer cells adopt a fibroblast-like phenotype in order to express invasive activity, but might re-assume an epithelial phenotype to support proliferation.

These examples underscore the fact that dimensional plasticity is a recurring theme in diverse developmental and pathologic events. Cellular dimensionality can be regulated at both the intrinsic and extrinsic levels. Intrinsic dimensionality refers to the transcriptional programs operating within the cell; cells typically express genes suited for function either in 2-D or 3-D. Extrinsic dimensionality is dictated by the ECM microenvironment; a cell either rests atop a 2-D substratum or is embedded within a surrounding 3-D ECM. To change in dimensionality within the context of complex tissues *in vivo*, the cell must both reprogram its intrinsic dimensionality and overcome extrinsic 2-D and 3-D ECM

barriers. Since intrinsic and extrinsic dimensionalities are often disconnected under artificial cell culture conditions (e.g. a fibroblast is programmed to function within the 3-D interstitium *in vivo*, not upon 2-D plastic or glass substrata used in standard tissue culture), most studies in the field of cell biology have failed to consider cell dimensionality. Hence, the two central questions of: i) how cells change their dimensional identity and ii) how dimensionality impacts important cell functions such as proliferation, migration, and survival remain largely unanswered. What work has recently been done to investigate how cells alter intrinsic and extrinsic dimensionality, as well as the mechanisms by which dimensionality regulates cell function?

Breaching the BM: the First Step Into 3-D.

BM Function and Structure: Impact on Cell Transmigration. Early in development animals ranging from flies to humans direct the embryonic epithelium to orchestrate the organization of an supramolecular network of proteins, glycoproteins, and proteoglycans, termed the basement membrane (BM) (48, 49). This conglomerate of structural macromolecules coalesces to form a dense, 100-300 nm-thick 2-D lamina that underlies all epithelia, and in higher organisms, ensheaths endothelial cells, nerves, smooth muscle cells and adipocytes (48, 50). The assembled BM provides adherent cells with structural support and functional cues by virtue of its biomechanical properties, display of adhesion receptor ligands and repertoire of matrix-bound growth factors (6, 50). With a pore size on the order of 50 nm, only small molecules are able to passively diffuse across this thin, but structurally rugged, barrier (6, 51, 52). Nonetheless, normal cells are able to traffic freely and rapidly across BMs by activating tissue-invasive programs during morphogenesis as well as immune surveillance (9, 16, 17, 53). Further, in a repetitive theme familiar to biologists, cell populations participating in pathologic events, such as cancer, can inappropriately co-opt “normal” BM transmigration programs to dire, and most often, lethal, consequence by driving the metastatic process (34).

Transmigration of cells across the BM plays an unquestionably important role in normal and neoplastic events, and has been the subject of thousands of reports – not to mention innumerable reviews - in the literature (6, 34, 48, 49). Nevertheless, it likely comes as a surprise that the mechanisms which allow cells to cross this structural barrier remain largely unknown and the subject of considerable debate. While the ability of a migrating cell to perforate the BM has been almost uniformly ascribed to proteolytic events, more than 500 proteinases are encoded within the mammalian genome, thus complicating efforts to identify a subset of critical, matrix-degrading enzymes (54). As such, using various model constructs designed to recapitulate BM structure *in vitro*, most investigators have, over the last 20 years, accepted a largely circumstantial premise that secreted proteinases play a dominant role in regulating

transmigration in both physiologic and pathologic states (55, 56). Very recently, however, evidence has begun to accumulate which suggests that accepted dogma may now be ripe for revisiting (4, 48, 57, 58). New insights into BM assembly and structure have raised serious concerns regarding the utility of most of the *in vitro* models used for analyzing invasion (59-61). Further, *in vivo* studies of mice harboring inactivating mutations of proteinases commonly implicated as the "usual suspects" in BM transmigration seldom appear to exhibit frank defects in BM invasion-associated events (62-65). Instead, recent studies support the contention that a small subset of membrane-anchored metalloproteases play a previously unrecognized role in this process (4). While we would be pleased to inform readers that solutions to all queries regarding BM invasion programs lie herein, this is far from the case and continued efforts will be required to build a definitive model of BM transmigration. Rather, it is our intent to highlight existing conundrums and caveats in the field, to pose possible solutions as to the means by which normal and neoplastic cells traverse BM barriers and to outline experimental systems where these hypotheses might be evaluated and tested in rigorous fashion.

BM Structure. Comprised of more than 50 distinct macromolecules, the predominant components of BMs are intertwined meshworks of polymeric laminin and type IV collagen (6, 49, 50). Distinct from all other BM constituents, only laminin and type IV collagen are able to self-assemble into polymers (50). Until recently, most models of BM organization assumed that type IV collagen serves as the major scaffolding upon which the laminin network is deposited. Newer studies suggest, however, that laminin polymers serve as the initial template for BM assembly (66, 67). Laminin isoforms are a family of 16 heterotrimeric glycoproteins composed generally of a 400 kD α chain, a 200 kD β chain and a 200 kD γ chain (68). The coalescence of α, β, and γ chains leads to the formation of a cruciform trimer with three long arms and one short arm stabilized by disulfide bonds (68). Supramolecular organization is triggered when laminins are concentrated at the plasma membrane of BM-associated cells via binding of long arm globular domains to cellular receptors that range, in a tissue-specific

fashion, from sulfated glycolipids to α-dystroglycan (66, 67). In turn, stable interactions between the short arm globular domains of adjacent laminin molecules allow for the organization of a single layer of obliquely-oriented laminin heterotrimers (66, 69).

Like the laminins, type IV collagens also assemble into a supramolecular network at the surface of epithelial and endothelial cells, adipocytes, muscle cells and nerves through processes either mediated directly by integrins (e.g., $\alpha_2\beta_1$ and $\alpha_1\beta_1$) or indirectly via type IV collagen binding interactions with laminin as well as other BM-associated macromolecules (49, 50). There are six distinct type IV collagen chains [α1-6(IV)] which display tissue-specific distribution patterns (49). In the trans-Golgi network, α(IV) chains form heterotrimeric protomers that contain a central discontinuous triple helical domain rich in Gly-X-Y motifs, where X and Y are often proline and hydroxyproline residues, as well as an N-terminal 7S domain and a C-terminal, globular NC1 domain (49). Following protomer secretion, dimeric associations between two NC1 trimers and tetrameric interactions between 7S domains promote the assembly of a polymeric meshwork (Figure 1.3) (49, 50). Remarkably, the six genetically distinct α chains assemble to form only three heterotrimers, i.e., α1α1α2, α3α4α5 or α5α5α6 (49). The α1(IV) and α2(IV) chains, the so-called “classic” chains, are present in the BM of all tissues whereas the other two heterotrimers display a more restricted pattern of distribution (49). Unlike the laminins, type IV collagen polymers are stabilized by a network of covalent crosslinks (49). Indeed, this structural characteristic likely provides the structural basis for the long-appreciated fact that type IV collagen cannot be extracted from BMs assembled *in vivo* unless the animals are fed a lathyrogen (i.e., a compound, such as β-aminopropionitrile, that prevents collagen crosslinking by inhibiting lysyl oxidase activity) and the tissues treated with a strong reducing agent (70). These observations support the contention that disulfide bonds and lysyl oxidase-catalyzed aldimines dominate intermolecular crosslinks generated within the 7S domain (70, 71). Further, more recent analyses of the type IV collagen NC1 domain have led to the novel demonstration of a new, and heretofore unprecedented, type of intermolecular,

thioether crosslink which is formed between specific methionine and hydroxylysine or lysine residues residing with apposing NC1 trimers (59, 61, 72). Hence, the highly-ordered and crosslinked nature of the type IV collagen network confers BMs with their structural integrity (73) and most likely presents migrating cells with their most formidable barrier during transmigration.

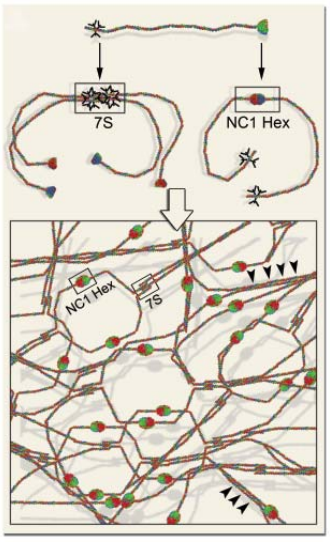

Figure 1.3. Type IV collagen network structure.

Type IV collagen protomers are triple-helical assemblies which contain N-terminal 7S domains that oligomerize to form 7S tetramers that are covalently stabilized by disulfide and (hydroxyl)lysine-derived crosslinks. The globular, C-terminal NC1 domains of two type IV collagen protomers also interact to form dimers composed of 6 individual collagen chains [termed NC1 hexamers (Hex)] that are held in association by strong non-covalent forces as well as (hydroxyl)lysine-methionine thioether crosslinks. Each individual collagen chain is synthesized with an N-terminal 7S domain that is decorated with a N-linked oligosaccharide (black, γ-shaped symbol). Formation of 7S domain tetramers and NC1 dimers support the assembly of a crosslinked, stabilized meshwork within the basement membrane that is reinforced by supramolecular twisting and lateral associations between the triple-helical collagenous domains (arrowheads).

Independent of the self-polymerizing properties of the laminins and type IV collagens, BM networks are further bridged by non-covalent interactions with nidogens 1 and 2, which in turn also bind the BM heparin sulfate proteoglycan, perlecan (6, 50). Perlecan, and other BM-associated proteoglycans, including collagens XV, XVIII and agrin may help confer charge-dependent selective

filtration properties to BMs and serve as reservoirs for heparin-binding growth factors including FGF-2, VEGF, and PDGF (74, 75).

Mechanisms of BM Transmigration: An Introduction. To probe mechanisms underlying BM transmigration events during the transition from 2-D to 3-D, we must first ask: what are the properties of BMs and the associated invasive cell populations that influence the transmigration process? From a structural perspective, the migrating cell will be confronted with a semi-permeable, type IV collagen-rich barrier whose pore size is dictated by both ECM density and crosslinking (4, 76). In turn, the degree to which the cell can deform its cytoplasm and nucleus to traverse a structural pore will determine whether proteolytic remodeling is a required step during BM transmigration (77-79). As migrating cells are unable to efficiently negotiate pores whose diameters are less than 2.0 μm in size (80, 81), a spatial limitation that exceeds BM pore size by a factor of ~40-fold (51, 52), it would seem that BM organization must be modulated to accommodate cell traffic. Larger BM discontinuities have been identified within distinct sites, such as the pulmonary bed, where circumscribed areas devoid of BM macromolecules have been detected, but their frequency and tissue-specific localization seem inconsistent with a more general role in providing unimpeded passageway for transmigrating cells (60, 82).

In normal tissue, BMs are subject to turnover at variable rates, presumably maintaining an equilibrium wherein macromolecular constituents are constantly removed and re-deposited in a dynamic process that preserves overall BM architecture (83). Therefore, in order to trigger 2-D-to-3D transitions, decreased BM synthesis or enhanced BM degradation would be predicted to tip this equilibrium in favor of BM removal and provide a mechanism for local BM effacement (5, 83). To effect such a process, increasing evidence suggests that cells re-activate programs normally reserved for use during embryonic development – a state wherein massive waves of cell migration are the rule rather than the exception (84, 85). How might BMs be remodeled to support transmigration during 2-D-to-3-D transitions? While attenuated BM production and assembly are likely contributing factors in the loss of an intact BM at the

tumor invasive front (35, 86), proteolytic machinery is also recruited to effect its removal (35, 87-91). BM pore size might be widened by proteolytic remodeling of BM superstructure, causing the localized dissolution of the BM at sites of cell invasion.

Protease-Dependent BM Transmigration. Evidence for proteolytic BM destruction during transmigration is supported by the observation that tissue-invasive events associated with 2-D-to-3-D transitions in developmental as well as disease states are characterized frequently by irreversible changes in BM structure (4, 9, 16, 18, 35, 48). Indeed BM discontinuities have been identified at sites of carcinoma invasion *in vivo* (35, 92, 93). Together, these observations have lent considerable support to the proposition that protease-dependent BM degradation is an event essential to transmigration (34, 48, 94). Accordingly, the expression of extracellular matrix (ECM)-degradative proteases has been documented in association with the tissue-invasive phenotype of both normal and neoplastic epithelial cells (34, 48, 57, 94). Nevertheless, the fact that the mammalian degradome is comprised of hundreds of proteases has led many to speculate whether the identification of those enzymes necessary and/or sufficient for BM transmigration may prove to be an impossible task (95, 96).

To date, *in vivo* models have implicated a confusing – and sometimes contradictory - array of serine proteases (97), cathepsins (98), and metalloproteases (95, 99) in tissue-invasive processes. Studies designed to identify roles of specific proteinases in ECM remodeling events associated with invasion *in vivo* must, however, be interpreted cautiously. In the *in vivo* setting, transmigration across an intact, crosslinked BM devoid of any preformed passageways is not only associated with the dissolution of the intervening barrier, but also the generation of multiple chemokines and mitogens, the inactivation of chemo-repulsive agents, the release or activation of matrix-bound growth factors as well as the unmasking of cryptic epitopes that can modify cell genotype/phenotype (57, 96, 100), the mechanistic interpretation of an “invasive” phenotype in the *in vivo* setting is challenging, if not problematic. Indeed, given the inherent complexities associated with whole animal studies, one might

realistically ask; i) is it possible to use *in vivo* models to identify the specific proteases involved directly in the BM remodeling program that specifically underlie invasion and ii) if not, how do we proceed?

From a reductionist perspective, an "ideal" model might rely on an *ex vivo* system wherein the ability of a normal or neoplastic cell type to traverse a BM barrier could be monitored directly. Studies initiated in the late 1970s used just such an approach with tissues isolated from donor organisms (55, 101). A popular source of tissue was the human placenta wherein the amniotic BM is sandwiched between an overlying layer of epithelial cells and a dense, underlying layer of interstitial collagen (dominated by an interwoven mat of fibrillar type I collagen) (101, 102). Following removal of the amniotic epithelial layer, a cell type of interest could be cultured atop the "naked" matrix and its invasion through the BM tracked (55, 103). Interestingly, such studies lent early support to the contention that BM invasion requires the mobilization of a subset of metalloenzymes encoded by the matrix metalloproteinase (MMP) gene family (55, 101, 103), a conclusion that may well hold 30 years later.

In search of the type IV collagenase(s). With close to 20,000 publications in the literature dedicated to the MMP family, it is perhaps less than surprising that these proteases have been associated with tissue-invasive and remodeling events in a variety of developmental and pathophysiologic states ranging across the evolutionary spectrum (48, 57, 58). In overview, MMPs are a class of 25 enzymes that are synthesized as latent zymogens (57, 95). When productive conformational changes occur between the autoinhibitory MMP prodomain and the catalytic domain, proteolytic activity is unmasked (104). MMPs are conveniently divided into two general classes; the secreted MMPs and membrane-type MMPs (MT-MMPs), with several subclass denominations based on domain composition (57, 95). Strikingly, despite the apparent complexity of the proteinase genome with all the complicating features of protease redundancy, compensation and adaptive development, recent work appears to narrow the cast of suspects to a small subclass of MMPs that serve as critical determinants of the BM transmigration program (4, 57, 58, 105).

A Novel BM Transmigration Program. Given a consensus that carcinoma cells as well as their normal counterparts mobilize similar machinery to traverse BMs (i.e., both cell populations employ analogous 2-D-to-3-D transition programs as they down-regulate cell:cell and cell:BM interactions, rearrange cytoskeletal elements and adopt a fibroblast-like motile phenotype (84)), *ex vivo* studies of pro-invasive activity were initiated to define the cancer cell-BM transmigration program (4). Using denuded peritoneal BM explants, multiple carcinoma cell lines (e.g., breast, prostate, pancreas, and squamous cell) exhibited invasive activity either "spontaneously" in response to motogenic signals generated by aberrant transcription factor expression or following the addition of pro-invasive growth factors (4, 84). In each case, carcinoma cells initiated invasion by first inserting pseudopod-like membrane extensions through the BM barrier in a manner that morphologically recapitulates cancer cell invasion *in vivo* (Figure 1.4A-B). Consistent with a protease-dependent mechanism, type IV collagen degradation products could also be identified in the perforated BM (4). While earlier studies had provided indirect evidence supporting a role for serine, cysteine or aspartyl proteinases during BM invasion programs (97, 98, 106), validated inhibitors of the respective proteinase families were unable to suppress invasive activity in this *ex vivo* model (4). In marked contrast, inhibitors directed against MMP family members not only ablated the cancer cell-mediated degradation of BM-associated type IV collagen, but transmigration as well (4). As proteolysis and invasion were unaffected by tissue inhibitor of metalloproteinases-1 (TIMP-1), an endogenous inhibitor specific for most secreted MMPs as well as the glycosylphosphatidylinositol (GPI)-anchored MMPs (i.e., MT4-MMP and MT6-MMP) (107), these data provided indirect support for the contention that BM remodeling might be mediated by one or more of the TIMP-1-insensitive MT-MMPs (i.e., MT1-MMP, MT2-MMP, MT3-MMP and MT5-MMP) (4), which are characterized by a type I transmembrane domain which tethers the MMP to the cell surface. Indeed, BM degradation and transmigration by cancer cells of epithelial, mesenchymal or neural crest origin were inhibited effectively by TIMP-2, a second member of the TIMP family that

targets all of the secreted as well as MT-MMP family members (4, 108). Most striking, perhaps, is the fact that cancer cells of multiple origins were unable to mobilize alternate proteolytic systems that supported BM invasion- even after 8 or more days in culture - when MMP activities were inhibited (4).

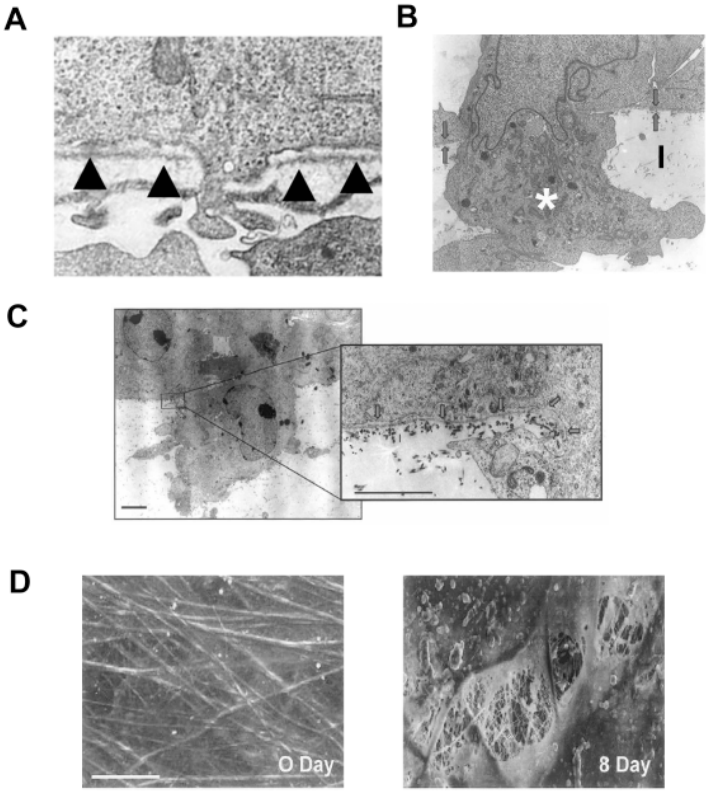

Figure 1.4. Proteolytic invasion of BM barriers

A. Transmission electron micrograph of a carcinoma cell extending an invadopodium-like process across a BM *in vivo* (from Kinjo et al. (1), with permission). Arrowheads mark the BM. **B.** Recapitulation of the *in vivo* BM transmigration program *in vitro* by culturing MDA-MB-231 breast carcinoma cells atop a peritoneal explant (from Hotary et al. (4); reprinted with permission). The invading cell extends an invadopodial process (asterisk) through the intact peritoneal BM into the underlying interstitial matrix (I). **C.** When engineered to express MT1-MMP, invasion-null COS-1 cells activate a BM transmigration program. Inset magnifies the discontinuous BM (arrows) associated with the COS-1 cell invadopodium.

In an effort to identify those MMPs that directly confer host cells with the ability to remodel or transmigrate BM barriers, a series of secreted or membrane-anchored MMPs were subsequently expressed in COS cells (i.e., an epithelial cell type that displays no BM degradative or invasive activity and no MMP

expression) (4). Independent of their secretion as latent or fully active enzymes, neither MMP-2, 3, 7, 9, 11 nor 13 endowed COS cells with BM remodeling activity (4). Though one cannot rule out the possibility that these proteinases hydrolyzed BM components at levels below the limits of morphologic or biochemical resolution used in these studies, none of the secreted MMPs tested conferred COS cells with BM pro-invasive potential (4). In marked contrast, however, three MT-MMP family members, i.e., MT1-MMP, MT2-MMP or MT3-MMP, conferred COS cells with the ability to both degrade and transmigrate the subjacent BM (Figure 1.4C) (4). BM remodeling activity did not, however, extend to MT4-MMP, MT5-MMP or MT6-MMP. Importantly, while it might be argued that a requirement for MT1, 2, 3 –MMPs during BM transmigration arose as a consequence of their ability to indirectly generate type IV collagenolytic activity by converting the MMP-2 zymogen to its active form (109), MT-MMP-dependent BM remodeling and invasion proceeded in an unabated fashion in the absence of active MMP-2 (4). Though these findings are limited to an experimental system wherein the implicated MT-MMPs were overexpressed in recipient COS cells, further studies demonstrated that specific MT-MMP silencing by small inhibitory RNAs (siRNAs) abrogated the ability of human cancer cells to traverse BMs isolated from either mouse, rat, canine or human sources (4). A required role for MT-MMPs must, of course, be validated in an *in vivo* system. While this work is ongoing, our preliminary data using the developing chick embryo as a host organism suggest that our *in vitro* findings might well prove applicable to complex *in vivo* settings. Nevertheless, the specific BM components cleaved by the MT-MMPs *in situ* remain to be characterized as does their role in promoting BM transmigration.

MT-MMPs Serve as Pro-Invasive Motors that Drive BM Transmigration. The ability of any single proteinase to effectively transform an invasion-null cell into a BM-invasive phenotype is, to say the least, surprising. Analyses of the structure/function relationships that underlie the ability of this subset of MT-MMPs to mediate BM remodeling and transmigration have yielded a number of insights into this process:

Firstly, MT1-MMP, MT2-MMP and MT3-MMP, though synthesized as latent enzymes, undergo intracellular activation prior to their display at the cell surface following the proteolytic removal of their respective prodomains by members of the ubiquitously expressed proprotein convertase family (109-111) .

Secondly, in the antiproteinase-rich extracellular environment of plasma, the active proteinases only display BM-degradative and pro-invasive activities when tethered to cell surface – a characteristic that may imbue these enzymes with unique activities (4, 112). For example, while soluble MMPs depend on diffusion to locate target substrates, the localization of MT-MMP catalytic activity to the cell surface provides for the direct apposition of enzyme and substrate at sites directed by the repertoire of receptors expressed on the cell membrane at the invasive front (113, 114). Additionally, MT-MMPs may be further concentrated at sites of active BM remodeling by trafficking to an actin-rich, adhesive cell protrusion termed, the invadopodium (113, 114). Though the precise mechanisms underlying MT-MMP trafficking to zones of BM effacement remain unclear, MT1-MMP cytoplasmic domain itself is dispensable, as cells expressing an MT1-MMP cytosolic tail-deletion mutant retain invasive activity while continuing to focus proteolytic activity to invadopodia (4, 112).

Thirdly, a recent elucidation of the biophysical mechanics underlying collagen degradation suggests that MT-MMPs may promote BM transmigration not only by dissolving ECM barriers, but also by acting as pro-invasive motors (115). In this model, MMPs display a proteolysis-dependent diffusion bias wherein the MMP affinity for native substrates exceeds that for degraded products, preventing retrograde diffusion of MMPs into sites depleted of targets in accordance with a “burnt bridge” model (115). Hence, MT-MMPs operating at the cell surface-BM interface may use a proteolysis-dependent diffusion mechanism to ‘pull’ the cell through the native ECM concurrently with matrix degradation, thus potentially integrating proteolysis and invasion into a single concerted process.

Of course, attempts to assign specific or direct-acting properties to the MT-MMPs are complicated by the fact that matrix proteolysis itself can exert

global effects on cell function. In the course of BM proteolysis, the MT-MMP-expressing cell would be bathed in a host of bioactive degradation products in association with fluctuations in local pH (6, 57, 96, 100, 116). Further, as new ligands are exposed (e.g., as the leading edge of the invading cell traverses the perforated BM, contact would be made with the underlying interstitial tissue), integrin usage would switch with attendant changes in downstream signaling and the application of cell-mediated mechanical forces (117, 118). Finally, changes in the biomechanical properties of the degraded BM itself would be expected to affect both cell shape and consequently, gene expression (2, 119, 120). Independent of the relative impact of these various signaling pathways on cellular behavior, MT1-, 2- and 3- MMPs appear unique relative to all other proteinases examined to date with regard to their ability to consolidate focal proteolysis with BM transmigration.

The Epithelial-Mesenchymal Transition (EMT): Changing Intrinsic Dimensionality

What is EMT? Under normal conditions, epithelial cells are intrinsically programmed for function in 2-D. Epithelial cells exhibit apical/basal polarity such that they bind the ECM of the BM on their basal aspect; they express integrin receptors specific for components of the 2-D BM, and typically do not proliferate or migrate. Following BM penetration, in order to acquire 3-D dimensionality, each of these facets of epithelial cell identity must be lost for proliferation, survival, and migration in 3-D. The transcriptional reprogramming and subsequent morphologic conversion of a 2-D epithelial cell into the phenotype of a 3-D cell is termed the epithelial-mesenchymal transition (EMT). In recent years, considerable insight has been gained into the signaling pathways and transcription factors that regulate EMT (11, 84, 121). However, since EMT studies are generally performed under classical, 2-D tissue culture conditions *in vitro*, the means by which EMT occurs within context of the ECM remodeling processes required for 2-D-to-3-D transitions remain largely unknown. While all of the known molecular regulators of EMT will not be discussed herein, I will discuss the key transcriptional changes that initiate EMT programs and begin to construct a model uniting EMT with the ECM remodeling events that occur during 2-D-to-3-D transitions.

EMT: Regulation. Several levels of control preserve the epithelial phenotype against mesenchymal differentiation. The ECM is a central regulator of epithelial plasticity. Indeed, epithelial cells must interface with an intact BM for maintenance of their differentiation state (17). Disruption of BM architecture and exposure of epithelial cells to 3-D ECMs seems to alter instrinsic dimensionality to contribute to the activation of pathologic EMTs (40, 122). These observations compel us to ask if, during 2-D-to-3-D transitions, proteolytic BM disruption and inhibition of BM deposition precedes EMT to drive transcriptional reprogramming toward a 3-D phenotype; or alternatively, if EMT results in the recruitment of degradative pathways necessary for BM penetration. Taken together with the observation that expression of BM-degradative enzymes is sufficient to drive 2-D-

to-3-D transitions in epithelial cells (4), the above studies suggest that that these two processes likely synergize in promoting gain of the 3-D phenotype, though the initiating step remains open to debate.

On a molecular level, a central mechanism for control of the epithelial phenotype seems to be regulation of epithelial cell-cell adhesion molecules of adherens junctions and tight junctions. Remarkably, the singlular loss of the adherens junction protein E-cadherin (gene name *CDH1* in humans) is sufficient to initiate the transcriptional reprogramming that characterizes EMT (123-125). Conversely, expression of E-cadherin in mesenchymal cells induces an epithelial-like phenotype (125). Hence, transcriptional repressors that bind the *CDH1* proximal promoter and inhibit RNA polymerase II-mediated transcription possess the intrinsic capacity to drive EMT on a transcriptional level. Indeed, expression of any one of a small family of transcriptional regulators seems to be sufficient to trigger the complex program of EMT, and therefore regulate intrinsic dimensionality.

Transcriptional repressors that drive EMT include those of the Snail zinc finger, zinc finger E-box-binding homeobox (ZEB), and basic helix-loop-helix family. In order to initiate EMT, these transcription factors bind to E-box elements within the proximal promoters of epithelial genes – including *CDH1* - and recruit co-repressors which result in the inhibition of mRNA transcription (84). During development, loss of E-cadherin is a required event for the progression of the epiblast EMT required for the formation of the primitive mesoderm (126). Gene targeting studies in mice have revealed a required role for one of these repressors - the Snail family member, Snail1 - in silencing epiblast E-cadherin at the primitive streak during gastrulation, with other *CDH1* repressors dispensable for this process (126). Further study has shown that Snail1 is aberrantly expressed in abnormal epithelium in several disease states including fibrosis and cancer, and the expression of Snail1 in 2-D cells is sufficient to drive complete EMT programs (127-132). Hence, Snail1 has taken center stage as a preeminent mediator of both developmental and pathologic EMTs. Our discussion will focus on Snail1 as a prototypical EMT-inducing factor.

Snail1: Regulation and Function. Like many transcription factors, Snail1 protein is regulated at both the transcriptional and post-translational levels (13). In epithelial cells, transcription of the gene encoding Snail1 (*Snai1*) is activated by a variety of extracellular stimuli and transcription factors, many of which are capable of initiating EMT. Signals from the ECM can activate cell surface integrins which in turn activate the integrin linked kinase (ILK), which can activate the Snail1 promoter (133). Furthermore, the presence of laminin-5 has been shown to induce Snail1 and EMT (134). Cytokines known to trigger EMT programs, such as TGFβ family members (135, 136), hepatocyte growth factor, (137), hedgehog/Gli (138, 139), and the Notch pathway (140) induce Snail1 transcription. Additionally, in the carcinomatous state, oncogenes such as H-Ras can induce Snail1 transcription (133, 141). Snail1 expression can also be activated by reactive oxygen species commonly found at sites of chronic inflammation and tissue remodeling (142). Not surprisingly, Snail1 transcription is also sensitive to negative regulation; e.g., activity of glycogen synthase kinase-3 (GSK3) acts to repress *Snai1* transcription (143) and Snail1 can bind to its own promoter and act as a repressor (144).

Independently of its regulation at the transcriptional level, Snail1 protein stability and subcellular localization are regulated *via* post-translational mechanisms. Phosphorylation of Snail1 is key means by which Snail1 protein function is modulated. A major regulator of Snail1 protein stability and localization is the activity of GSK3-β, a component of the canonical Wnt signaling pathway (145). In differentiated epithelial cells, Snail1 is constantly phosphorylated at serine residues near its N-terminus by GSK3-β, which targets Snail1 for polyubiquitination and proteasomal degradation (130, 146). Inactivation of GSK3-β activity *via* upstream signaling pathways – including the canonical Wnt pathway – results in Snail1 protein stabilization, *CDH1* repression, EMT, and subsequent tissue invasion (130, 146). Thus, Snail1 is a key mediator of Wnt-triggered EMTs. Furthermore, the canonical Wnt/β-catenin signaling pathway exerts control on Snail1 activity by regulating Snail1 nuclear localization. In differentiated epithelial cells, in the absence of canonical Wnt activity, nuclear

GSK3-β activity targets Snail1 protein for proteasomal destruction (131). Upon activation of the Wnt pathway and accumulation of nuclear β-catenin, the β-catenin/T-cell factor (TCF) transcriptional target Axin2 sequesters GSK3-β in the cytoplasm, stabilizing nuclear Snail1, and activating EMT programs (131). Furthermore, p21-activated kinase (PAK1) – pro-invasive factor in breast cancer – phosphorylates Snail1 to promote its accumulation within the nucleus (147). Recently, the small C-terminal domain phosphatase was identified as an antagonist of Snail1 phosphorylation by GSK3-β; possibly identifying a novel EMT-inducing pathway (148).

When Snail1 protein is stabilized within the nucleus, it binds E-box elements predominantly within the proximal promoters of target genes (84). The N-terminal SNAG domain serves to recruit various co-repressors required for gene silencing (149). The LIM protein, Ajuba, binds the Snail1 SNAG domain and recruits protein arginine methyltransferase—an event required for *CDH1* silencing (150, 151). Interestingly, Ajuba proteins are also components of adherens junctions, suggesting a potential positive feedback loop promoting adherens junction disassembly (151). Snail1 also recruits histone deacetylases 1 and 2, DNA methyltransferase 1, and Polycomb complex 2 for effective *CDH1* repression via promoter methylation and histone deacetylation (149, 152, 153). Furthermore, interaction with lysyl oxidase-like 2 seems to be required for effective repression of *CDH1* by Snail1 (154).

What are the consequences of Snail1 binding to promoters of target genes? In addition to repressing epithelial genes (e.g. *CDH1*) Snail1 modulates transcriptional programs that exert wide-reaching effects on cell function (Figure 1.5). EMT involves not only loss of epithelial characteristics, but also the gain of mesenchymal transcriptional programs which allow cells to function within the 3-D environment of the interstitial compartment. Hence, any stimulus that engages EMT must also imbue cells with a 3-D mesenchymal phenotype in order to create conditions permissive for the execution of an effective 2-D-to-3-D transition. Since Snail1 expression is sufficient to initiate a complete EMT and drive 2-D-to-3-D transitions (130, 131), Snail1 must possess the inherent capability to engage

mesenchymal genes. One potential mechanism involves Snail1 indirectly inducing mesenchymal genes in epithelial cells via direct repression of E-cadherin expression, and the consequent accumulation of free β-catenin liberated from adherens junctions that transactivates mesenchymal genes (124). Additionally, Snail1 expression in differentiated mesechymal cells recruits the migratory and proteolytic machinery required for navigation of 3-D interstitial ECMs (155). A further, though as yet uncharacterized, mechanism of mesenchymal gene activation by Snail1 might potentially involve Snail1 repression of microRNAs directed against mesenchymal genes.

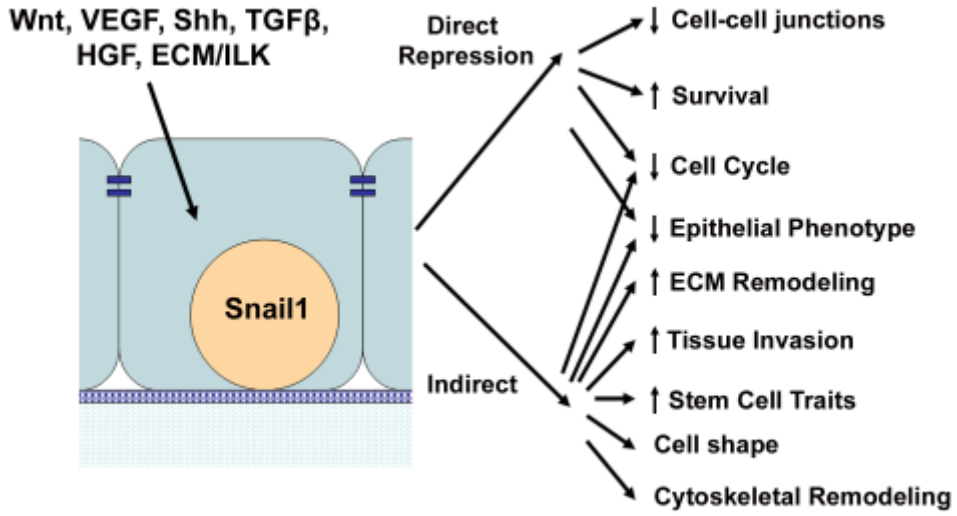

Figure 1.5. Regulation and Functions of Snail1

Snail1 protein accumulation in the nuclear compartment is induced by a variety of upstream signals. Snail1 activity regulates diverse cell functions during 2-D-to-3-D transitions via both direct repression of transcription as well as indirect mechanisms.

In addition to driving EMT at the transcriptional level, Snail1 expression regulates other cell functions relevant to development and disease. With particular relevance to cancer, Snail1 inhibits cell cycle progression and promotes resistance to radiation-induced apoptosis via repression of positive cell cycle regulators and pro-apoptotic genes (156, 157). Furthermore, ectopic Snail1 expression can drive both epithelial and mesenchymal primary tumorigenesis *in vivo*, suggesting crosstalk with oncogenic pathways (13, 139, 158-160). Additionally, in epithelial cells, Snail1-mediated EMT has been

proposed to confer stem-cell like properties, potentially contributing to secondary tumor formation in cancer (161). Consistent with this proposition, Snail1 expression is associated with carcinoma recurrence *in vivo* (162), and might therefore regulate secondary tumor latency (163, 164). Snail1 also seems to regulate tissue-invasive events in differentiated mesencyhmal cells and early mesodermal precursor cells during development, as well as mesenchymal cell tumors (155, 165). Accordingly, Snail1 is highly expressed in activated fibroblasts at sites of wound healing and tumor growth (128, 166). During development, Snail1 plays a role in body patterning by controlling left/right asymmetry (167). Further study will certainly identify additional EMT-independent functions for this transcription factor.

Snail1-mediated EMT during 2-D-to-3-D transitions in development and disease. Due to its ability to autonomously integrate complete EMT programs, Snail1 is a key mediator of physiologic and pathologic 2-D-to-3-D transition events. Perhaps most strikingly, global Snail1 deficiency in mice results in early embryonic lethality due to failure of gastrulation with defective silencing of *Cdh1* in epiblast cells at the primitive streak (126). Tissue-specific Snail1 ablation using Cre/loxp conditional deletion technology has revealed a role for Snail1 in craniofacial development, potentially playing a required role in EMT events during palatal fusion (168, 169). However, Snail1 seems to be dispensable for neural crest cell 2-D-to-3D transitions, which might be compensated by other *CDH1* repressors (126, 167, 169).

The endothelial-mesenchymal transition (EndoMT) is a program analogous to EMT that occurs in mature endothelial cells. In a similar manner as EMT, EndoMT involves loss of differentiated endothelial cell markers, such as platelet cell adhesion molecule (PECAM) and the homotypic cell-cell adhesion molecule vascular endothelial cadherin (VE-cadherin), and gain of mesenchymal markers such as the myofibroblast microfilament α-smooth muscle actin (αSMA) (170). EndoMT is a central process in the 2-D-to-3-D transitions required for neovessel sprouting, cardiac valve formation, and vascular mural cell differentiation (14, 22, 29, 45, 170, 171). Perhaps not surprisingly, Snail1 has

been implicated in EndoMT (136, 170). Snail1 transcription is engaged via Notch signaling during endocardial EndoMT and subsequent cardiac valve mesenchymal cell differentiation, and may play an important role in this process *via* direct repression of VE-cadherin (27, 172). Snail1 is required for activation of αSMA downstream of TGFβ signaling in embryonic endothelial cells (136). In support of a role for Snail1 in angiogenesis and vascular patterning, widespread Cre-mediated deletion of a loxp-flanked Snail1 allele during embryonic development results in cardiovascular defects, and Snail1 expression is activated in neovessels at sites of active tissue remodeling (24, 132, 167). Hence, the ability of Snail1 to regulate intrinsic dimensionality seems to extend to endothelial cells.

After completion of development, Snail1 does not seem to be expressed in healthy, mature tissues (166); however, differentiated cells retain the ability to express Snail1 and consequently recruit associated embryonic morphogenetic programs during the pathogenesis of certain diseases. Expression of Snail1 is thought to integrate EMT during the 2-D-to-3-D transitions that promote local invasion and distant metastasis in carcinoma cells (13). Consistent with this premise, Snail1 is expressed in invasive carcinoma cells at the tumor-stroma interface (128, 129, 132, 166), Snail1 expression is sufficient to induce carcinoma EMT *in vitro* as well as 2-D-to-3-D transitions *in vivo* (130, 131, 159, 162), and Snail1 positively regulates carcinoma lymph node metastasis (173). Within the peritumoral stroma, it has also been proposed that fibroblasts might arise from endothelial cells *via* EndoMT (42). Accordingly, since Snail1 is highly expressed within the tumor vasculature (24, 132), Snail1 might additionally play a role in this process.

EMT contributes significantly to the pathogenesis of organ fibrosis. Indeed, interstitial fibroblasts might arise from the tubular epithelium of the kidney (39), hepatocytes within the liver (41), and pneumocytes in the lung (40) as well as from the endothelium (43, 44). Perhaps not surprisingly, Snail1 expression is observed during fibrosis *in vivo* and is induced by pro-fibrogenic signals – including members of the TGFβ family – in normal epithelial cells *in vitro* (174-

176). Functionally, transgenic overexpression of Snail1 in the kidney epithelium results in tissue fibrosis (177). Though these data indicate that Snail1 expression alone might be sufficient to drive organ fibrosis, further work is required to assess the requirement for Snail1 during fibrosis pathogenesis in mouse models *in vivo*. Hence, models of Snail1 deficiency wherein Snail1 expression can be abrogated in a tissue-specific manner must be applied to validated disease systems to verify proposed roles for Snail1 in disease pathobiology.

Migration, Survival, and Growth in 3-D.

3-D Interstitial Barriers. Underlying the BM, the interstitial ECM is dominated by fibrillar networks of type I collagen (10, 178-181). Type I collagen-producing cells - primarily resident stromal fibroblasts - synthesize and assemble two α1 chains and one α2 chain into a heterotrimeric fibril with a central, continuous proline- and hydroxyproline-rich triple helix flanked by N- and C-terminal, non-helical domains termed telopeptides (181, 182). Type I collagen fibrils are deposited into the extracellular space following proteolytic maturation, and subsequent oxidation of telopeptide lysine residues by lysyl oxidase (LOX) enzymes (182). In a spontaneous process, staggered, lateral interactions of triple helical domains promote the assembly of a polymeric 3-D meshwork stabilized by intermolecular cross-links between oxidized lysine residues in the telopeptide regions (182, 183). In vivo, the type I collagen-rich stroma forms a structural barrier with effective pore sizes estimated to be on the order of 150 nm (184).

Navigating the 3-D Interstitium: A Proteolytic Process? As cells entering 3-D establish new contacts with type I collagen via integrins and discoidin domain receptors (tyrosine kinase collagen receptors), signal cascades are initiated which further promote EMT-like programs (117, 185). Cancer cells then proceed to invade stromal tissues in either a single cell fashion or as a cohesive network of cells (186). Both protease-dependent and protease-independent schemes have been proposed as the means by which advancing cells infiltrate and migrate within the interstitium (10, 15, 78, 118, 187-189). During protease-dependent invasion, cells recruit pericellular proteolytic systems that increase matrix pore size to a diameter permissive for cell passage by cleavage of impeding fibrils (10, 15, 181, 190-193). In contrast, protease-independent migration schemes involve displacement of ECM fibrils and acquisition of a round, ‘amoeboid’ cell phenotype characterized by increased cell deformability and decreased cell-ECM adhesion, a mode of migration similar to that used by leukocytes (78, 187, 189, 194). Interconversion of these two migratory phenotypes would be predicted to provide cells with an escape mechanism to

maintain effective 3-D migration in the absence of protease activity (187, 189). However, studies identifying proteinase-independent, amoeboid cell migration have used models wherein cells were cultured within hydrogels assembled from type I collagen molecules that had been proteolytically extracted from bovine tissues with pepsin, a protease that degrades the nonhelical telopeptides, rendering this construct deficient in the intermolecular crosslinks that stabilize the type I collagen network in vivo (78, 181, 187, 191, 194, 195). Indeed, in native, crosslinked type I collagen ECMs with intact telopeptides, compensatory amoeboid migration is not observed in the presence of broad-spectrum protease inhibitors (10, 15, 181, 191-193, 195). Similarly, the migration of 3-D cells within synthetic, protease-resistant poly(ethylene glycol) (PEG) hydrogels is inhibited as a function of increasing crosslink density (196).

The Proteolytic Players Within 3-D Collagen. Considerable attention has focused on both the cysteine proteinase and MMP families of collagenolytic enzymes as mediators of proteolytic cell traffic through 3-D, collagen-rich tissues. Cysteine proteinases are a family of 11 exopeptidases and endopeptidases localized preferentially within endolysosomal compartments (197). Recent genetic ablation studies have revealed that a subset of cathepsins are essential for carcinoma growth, invasion, and angiogenesis in vivo, in part due to their ability to cleave the cell:cell adhesion molecule E-cadherin and to generate anti-angiogenic, type IV collagen fragments (197). However, no clear role for tumor-derived cathepsins in type I collagen degradation has been forthcoming (10, 180, 192). Complicating interpretation of these in vivo studies, cysteine proteinases, like cathepsin L, can cleave transcription factors and histones, suggesting indirect roles in regulating tumor cell phenotype that do not necessarily involve ECM proteolysis (198, 199). Hence, it seems likely that cathepsins play important roles in 3-D cell function that operate independently of type I collagenolysis per se.

What evidence suggests that MMPs might contribute to the collagen-invasive program? MMPs have long been associated with type I collagenolysis; the first identified MMP, MMP-1, was isolated due to its ability to digest interstitial

collagen (200, 201). Inhibitor screens have demonstrated an essential role for MMPs during cell navigation of 3-D native type I collagen barriers - with negligible roles for other classes of collagenolytic proteases - results which have been extended to models using explants of live human tissue as well as ECM barriers in vivo (10, 180, 181, 190-193).

Which specific MMPs might act as central players during invasion of 3-D collagenous barriers? Not unexpectedly, considerable effort has focused on potential roles for those MMPs known to express type I collagenolytic activity as purified enzymes in cell-free systems - MMP-1, MMP-2, MMP-8, MMP-9, MMP-13, and MT1-MMP (109, 200, 202). Perhaps consistent with its lack of evolutionary conservation within vertebrates (no orthologous gene exists in mice), MMP-1 is not essential for tumor cell migration through 3-D collagen barriers and does not confer invasion-null cells with pro-invasive activity (57, 180, 181). Further, from the perspective that tumor cells are adept at hijacking mechanisms used by normal cells to remodel type I collagen, analyses of mice carrying targeted mutations in MMP-2, MMP-8 or MMP-9 reveal only subtle, nonlethal phenotypic defects, while MMP-13 deficient mice are viable with defects confined to bone development (203). Cells isolated from MMP-2, MMP-8, MMP-9, or MMP-13-deficient mice exhibit normal invasive activity through type I collagen barriers (10). Collectively, these observations suggest that secreted MMPs may not play essential roles in the focalized collagen hydrolysis required for 3-D cell migration while not precluding possible functions in bulk ECM turnover during tissue remodeling (200, 204-206).

For effective tissue invasion, proteolytic activity is likely confined to the leading edge of migrating cells in order to focally degrade impeding barriers while maintaining the overall structure of the 3-D ECM scaffold, though more complex distribution patterns of proteolytic activity have also been described (78, 191, 207, 208). Hence, MT1-MMP might be ideally suited for such activity by tethering type I collagenolytic activity to the cell surface. Indeed, cells isolated from MT1-MMP-deficient mice are unable to penetrate collagenous barriers or degrade subjacent type I collagen (10, 14, 209, 210), suggesting that MT1-MMP

is the dominant proteolytic effector mobilized during trafficking through 3-D interstitial barriers *in vivo* (211).

Protease-Dependent Fibrin Invasion. In addition to the ability to negotiate type I collagen lattices, tumor infiltrating cells must be equipped for migration-coupled fibrinolysis. In wound-like microenvironments, increases in vascular permeability disperse fibrinogen-rich plasma into the interstitium (212). Synthesized primarily in the liver, fibrinogen consists of six polypeptides: two disulfide-linked trimers each containing an Aα, Bβ and γ chain (213). Conversion of fibrinogen to fibrin occurs when cleavage of the N-terminal fibrinopeptide A from the Aα chain by the serine protease, thrombin, exposes a polymerization domain that initiates fibrillogenesis (213). Fibrils associate laterally and branch to form a 3-D network stabilized by the transglutaminase, factor XIII, which incorporates ε-(γ-glutamyl)lysine crosslinks between the assembled γ chains (213). The resulting fibrin clot contains pores estimated to be 0.1-1.0 μm in diameter (214, 215). The dense structure and small pore size of mature fibrin clots precludes mobilization of protease-independent migration schemes (8, 214, 216, 217). Efforts to identify the proteolytic pathways that govern this process have focused primarily on two axes: the plasminogen activator system and MMPs. Following processing of the circulating zymogen, plasminogen, to its active form by the plasminogen activators (i.e., either tissue-type plasminogen activator or urokinase type plasminogen activator; tPA and uPA, respectively), plasmin is responsible for bulk dissolution of fibrin clots during tissue repair (8, 218-220). However, during cell trafficking, unfocused plasmin-mediated fibrin degradation would not be predicted to support effective cell migration due to wholesale destruction of the supporting scaffold. While migrating cells can generate zones of juxtamembranous fibrinolysis by binding uPA to the membrane-tethered urokinase plasminogen activator receptor R (97), a requirement for this axis during cell trafficking through fibrin matrices may be questioned (8, 217). Fibroblasts as well as endothelial cells readily invade crosslinked fibrin gels in the absence of uPA, tPA or plasmin activity (8, 217). Furthermore, plasminogen-deficient mice, though displaying profound defects in thrombolysis, exhibit

unperturbed cell invasion through provisional fibrin matrices while plasminogen-deficient humans do not display overt signs of defective cell migration (217-219, 221). Hence, though plasmin unquestionably functions as a bulk fibrinolysin, the predominant proteolytic system mobilized for trafficking through fibrinous barriers may reside within other protease family members (8, 216, 217, 220).

Several MMPs possess hydrolytic activity toward fibrin, including MMPs-1, 2, 3, 7, 9, 11, and 13, as well as MT1-MMP (8, 216, 217, 220); among these candidates, however, only ectopic expression of MT1-MMP - and not secreted MMPs - was sufficient to drive cell invasion into 3-D fibrin barriers (8, 217). In contrast to results obtained with type I collagen invasion, MT1-MMP-deficient cells maintain the ability to invade fibrin barriers, albeit at slower rates than MT1-MMP-sufficient cells, suggesting that compensatory MT-MMP(s) may be mobilized when MT1-MMP function is compromised (8). Accordingly, MT2-MMP as well as MT3-MMP are likewise able to promote fibrin-invasive activity (8, 222). Taken together, these data reinforce the paradigm that pericellular hydrolysis of ECM barriers, rather than bulk ECM degradation, is a critical requirement for navigation of crosslinked 3-D ECMs, and that MT-MMPs are the ideal effectors of this process.

Growth Regulation Within the 3-D Interstitium. When cells find themselves embedded within a dense, 3-D ECM, the physical constraints exerted by the pericellular matrix must be circumvented to allow proliferating cells to expand (3, 7, 223, 224). Due to their ability to cleave both ECM and non-ECM growth regulatory targets, MT-MMPs have received significant attention as 3-D regulators of cell growth. MT-MMPs stimulate proliferation of cells embedded within 3-D ECMs of type I collagen (7, 211, 225). Several proposed functions of MT-MMPs in growth regulation may contribute to this 3-D growth stimulatory effect. Since MT1-MMP-mediated effects on cell growth in type I collagen-rich tissues correlates with type I collagen degradation, this suggests a simple model wherein collagenolytic removal of constraining barriers allows expansive cell growth (7). Furthermore, destruction of pericellular collagen attenuates anti-proliferative signaling derived from fibrillar collagen-mediated activation of the

tyrosine kinase receptor, DDR2 (224). Though Occam's razor might support this simple model, other evidence supports alternative mechanisms for MT1-MMP-mediated growth control.

Apart from ECM targets, MT1-MMP cleaves non-ECM growth regulatory targets in the intracellular as well as extracellular environments (190, 226-229). Furthermore, MT1-MMP can induce the shedding of the heparin sulfate proteoglycan, syndecan-1, from stromal cells to indirectly promote cell growth (230). MT1-MMP may also trigger TGFβ signaling, induce Wnt signaling and repress expression of anti-invasive factors (231-234). Within the cell, MT1-MMP traffics on the cytoskeleton to the centrosome where it cleaves pericentrin to induce chromosomal instability, potentially contributing to transformation in cancer cells (235). Together, these effects might collaborate to alter gene expression in MT1-MMP-expressing cells (232-234, 236). However, in native 3-D ECM, the requirement for MT1-MMP cleavage of type I collagen seems to predominate, as culture of cells in a 3-D, crosslinked ECM of MMP-resistant type I collagen (derived from a mouse strain carrying a knock-in mutation in the *Col1a1* gene rendering the product resistant to MMP-mediated degradation) abrogates MT1-MMP-stimulated 3-D proliferation (7). Additionally, MT1-MMP has been suggested to modulate cell growth independently of its catalytic activity via a process that is dependent on signaling through its cytoplasmic domain (237, 238). However, expression of an MT1-MMP construct lacking the cytoplasmic domain is sufficient for promoting 3-D growth while MT1-MMP mutants devoid of catalytic activity do not confer expressing cells with a growth advantage (7). Clearly, MT1-MMP is a potent regulator of growth, but further investigation is required to define the relative roles of these alternative pathways during cell proliferation within physiologically-relevant 3-D ECMs. Nevertheless, it should be stressed that under standard 2-D culture conditions or within ECMs devoid of covalent crosslinks (e.g. Vitrogen or Matrigel), MT1-MMP-null cells exhibit normal growth and migratory characteristics (10, 14, 209). A dominant role for MT1-MMP-dependent collagenolytic activity is also consistent with the fact that the lethal phenotype observed in MT1-MMP knockout zebrafish cannot

be rescued by expressing a catalytically-inactive MT1-MMP mutant (239). Further, mice develop normally in the absence of MT1-MMP and display no obvious phenotype until after the first week of postnatal life when the bulk of type I collagen deposition in maturing tissues is initiated (5, 10). Together, these observations favor the paradigm that MT-MMPs are required for cell growth and migration as a function of the structure of the ECM environment. In mature tissues, the dominant role of the MT-MMPs is most consistent with the proteolysis of physical barriers imposed by crosslinked, 3-D ECMs.

An MT-MMP-Centric View of 2-D-to-3-D Transitions.

Since MT-MMPs act as the central proteolytic effectors during 2-D-to-3-D transitions, attention has focused on characterizing the factors that regulate MT1-MMP expression, intracellular trafficking, and cell surface display, as well as the critical structural features that underlie its matrix-degradative capabilities (Figure 1.6).

MT-MMP Transcriptional Control. Transcriptional activation of MT1-MMP expression is mediated by several signaling axes. Not unexpectedly, transcription factors and signaling pathways associated with the induction of EMT (e.g., Snail, Wnt, TGFβ, etc.) can trigger MT1-MMP expression (88, 240-243). Loss of the epithelial cell-cell adhesion proteins E-cadherin and occludin - a hallmark of EMT - promotes MT1-MMP expression via de-repression of the transcription factor, hNanos1, and cytoplasmic localization of ZO1 to activate the β-catenin/TCF complex, respectively (244, 245). Having traversed the BM, exposure of cells to type I collagen further induces MT1-MMP expression via a TGFβ/SMAD-dependent pathway (241), suggesting a feedback loop wherein ECM barriers regulate expression of the proteolytic machinery necessary for invasion.

MT1-MMP Processing, Intracellular Traffic and Surface Localization.

Following synthesis of the MT1-MMP zymogen, protease function is regulated post-translationally via control of MT1-MMP activation, secretion, and surface localization. Whereas most proMMPs are activated extracellularly, a subset of MMPs are activated intracellularly by proprotein convertases (110, 111, 246, 247). Identification of an RX(K/R)R proprotein convertase recognition motif in the proMT1-MMP zymogen led to the discovery that multiple MT-MMP family members undergo intracellular activation prior to trafficking to the cell surface (57, 109, 110). Indeed, intracellular processing of MT-MMP family members to their active forms may also play a required role in controlling their trafficking to the cell surface (111).

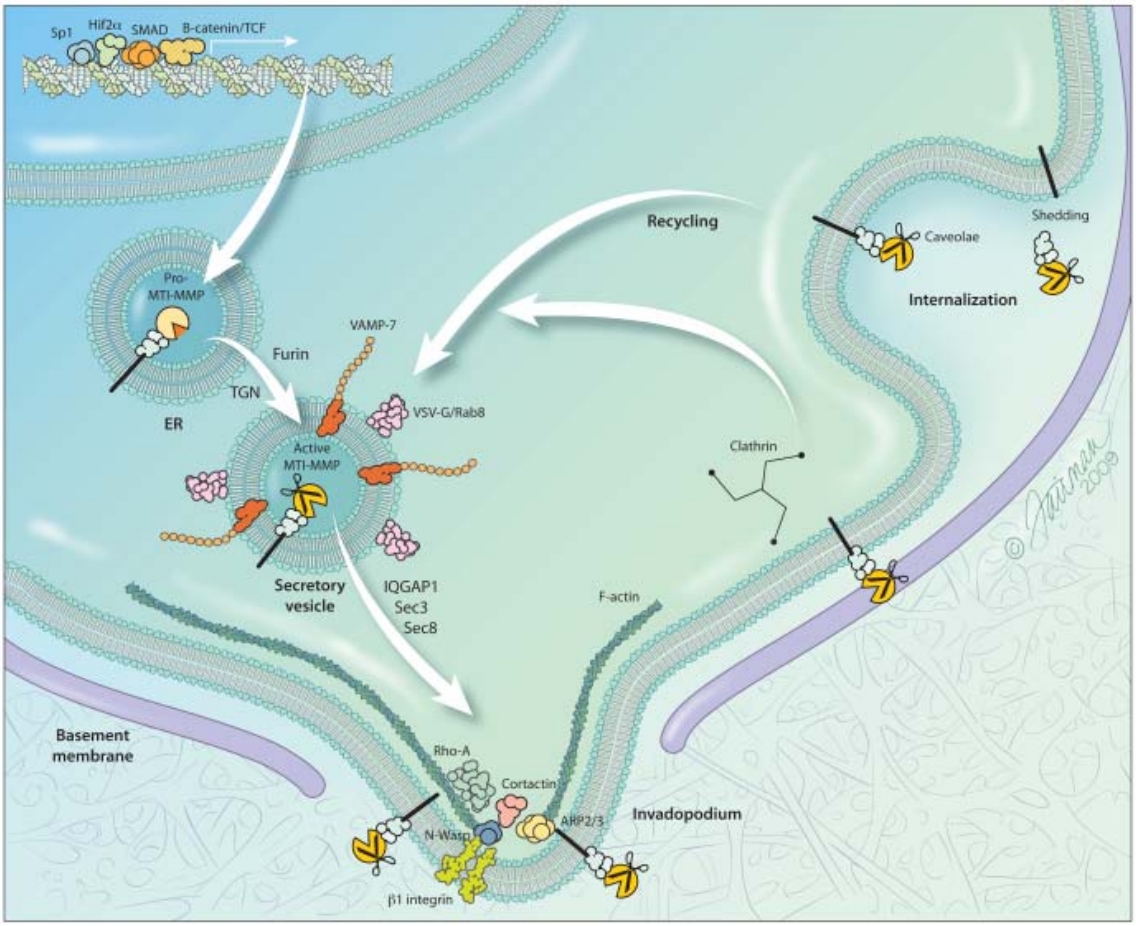

Figure 1.6. Regulation of MT1-MMP Expression, Processing, Traffic, and Activity at the Cell Surface

Triggered by a variety of signaling cascades, Pol II transcription at the *MMP14* gene and subsequent translation in the endoplasmic reticulum (ER) generates proMT1-MMP. ProMT1-MMP is proteolytically activated by proprotein convertases – such as furin – within the *trans*-Golgi network (TGN). MT1-MMP traffic to the cell surface is tightly regulated such that the active enzyme is delivered to focal zones of pericellular proteolysis that support 3-D growth and invasion. Vesicles containing active MT1-MMP are coated with VSV-G/Rab8 and trafficked via the exocyst complex to cortactin-rich invadopodia, where membrane fusion is mediated by VAMP-7. MT1-MMP activity at invadopodia coordinates cytoskeletal dynamics, adhesion, and proteolysis into a concerted invasion process. MT1-MMP cell surface activity is abrogated via mechanisms including endocytosis and shedding.

Unlike the pathways of constitutive secretion that control the export of soluble MMPs, secretory vesicles containing active MT1-MMP are delivered to the cell surface at sites of cell-ECM contact for effective invasion-coupled ECM proteolysis. Following activation, MT1-MMP is localized to VSV-G/Rab8-positive

vesicles that deliver the protease to invadopodia (248); specialized actin-rich cell membrane protrusions where integrins and pericellular proteases are concentrated to support proteolysis-driven adhesive migration through the ECM (113, 248, 249). During the initial phase of invadopodia assembly, integrin recognition of ECM ligands activates the N-WASP-Arp2/3-cortactin-dynamin complex which mediates actin polymerization to generate a leading edge, membrane protrusion (113). Rho GTPase activity at this site is a critical regulator of MT1-MMP invadopodial localization since p190B RhoGAP and RhoA/Cdc42 promote polarized trafficking of MT1-MMP-containing vesicles to invadopodia (249, 250). Fusion of MT1-MMP-containing vesicles to the invadopodial membrane is mediated by a v-SNARE TI-VAMP/VAMP-7 complex (251).

MT-MMP Functional Insights From Structural Studies. Clearly, by virtue of their broad substrate specificity, MT-MMPs are able to support invasion through structurally distinct and complex ECM barriers in order to support 2-D-to-3-D transitions. What structural characteristics imbue MT-MMPs with these novel characteristics?

A key aspect of MT-MMP-mediated tissue invasion is the ability to concentrate proteolytic activity at the cell surface, since expression of soluble, but catalytically active, forms of MT-MMPs does not support BM transmigration, invasion of interstitial ECMs, or 3-D growth (4, 7, 10, 180). Further, pericellular MT-MMP activity is critical for direct hydrolysis of ECM targets, rather than MT-MMP activation of protease cascades, since mutant forms of MT1-MMP deficient in proMMP-2 activation (but which retain catalytic activity), support trafficking through ECM barriers as do MMP-2-deficient cells (10, 180, 210, 252). Indeed, during traffic through 3-D type I collagen, only the pericellular type I collagenolytic functions of MT1-MMP are required, as replacement of the MT1-MMP catalytic domain with that of fibroblast collagenase (MMP-1) is sufficient to support 3-D invasion (180). This observation would seem to preclude the contention that MT1-MMP-mediated cleavage of motility-regulating cell surface molecules, such as E-cadherin, α_v integrin, CD44, or syndecan-1 represents major mechanisms

by which MT1-MMP drives 3-D ECM invasion (109, 180, 190). Taken together, this evidence supports the contention that membrane-associated, ECM-targeted proteolytic activity is the key functional feature of MT-MMPs during cell traffic through 3-D ECM.

Current Directions.

Intrinsic Regulation of Dimensionality. Since shifts in intrinsic dimensionality are governed in large part by EMT, what open questions remain in this field? As the preeminent *CDH1* repressor during development, Snail1 has received considerable attention as a mediator of EMT programs. Overexpression of Snail1 in adult mice *in vivo* is sufficient to drive organ fibrosis (160, 177). However, expression of Snail1 at levels never reached in development or disease might not accurately recapitulate naturally-occurring disease. Therefore, Snail1's necessity during the pathogenesis of any disease process *in vivo* remains an open question. Since Snail1 deficient mice die early in development (126), we have generated a conditional allele of *Snai1* using Cre recombinase /loxp technology. We have applied this allele to a validated mouse model of fibrosis to identify, for the first time, a required role for Snail1 during EMT in disease pathogenesis *in vivo*. Furthermore, we have defined novel roles for Snail1 in regulating differentiated mesenchymal cell function and EndoMT. Study using these models - coupled with mechanistic *in vitro* studies using physiologically-relevant ECM constructs – will allow investigators to rigorously assess the role of Snail1-mediated EMT and dimensionality shifts during disease.

Extrinsic Regulation of Dimensionality. Despite an increasing body of work pointing to the importance of multiple MT-MMP family members in tissue-invasive processes (109, 253), these findings beg the question as to how a single protease, even one such as MT1-MMP, could possibly exert such a range of important biological effects by "simply" cleaving impeding ECM molecules (57, 96, 254). Further insight into regulation of cell function by pericellular ECM remodeling is essential. Herein, we have found that pericellular ECM remodeling not only confers tissue-invasive potential, but also allows cells to adapt to new ECM environments by regulating the structure and function of the nuclear compartment.

Further studies in mouse models of MT-MMP deficiency should provide insight into the mechanisms underlying cellular dimensionality and *in vivo* verification of models derived from *ex vivo* and *in vitro* studies. Since the tools

available for genetic study of MT-MMPs in vivo are limited – MT1-MMP-null mice die within the first months of life and MT2-MMP-null mice have yet to be generated – novel models of MT-MMP conditional inactivation are essential to ablate MT-MMP expression with spatiotemporal specificity. We have generated and characterized mouse models of conditional MT1-MMP and MT2-MMP deficiency. Tissue-specific ablation of these proteases in development and disease will rigorously test their proposed roles in defining extrinsic dimensionality, and will provide deeper understanding of integration of pericellular ECM remodeling and EMT as a concerted 2-D-to-3-D transition process.

References.

1. Kinjo, M. 1978. Lodgement and extravasation of tumour cells in blood-borne metastasis: an electron microscope study. *Br J Cancer* 38:293-301.
2. Chun, T.H., Hotary, K.B., Sabeh, F., Saltiel, A.R., Allen, E.D., and Weiss, S.J. 2006. A pericellular collagenase directs the 3-dimensional development of white adipose tissue. *Cell* 125:577-591.
3. Yamada, K.M., and Cukierman, E. 2007. Modeling tissue morphogenesis and cancer in 3D. *Cell* 130:601-610.
4. Hotary, K., Li, X.Y., Allen, E., Stevens, S.L., and Weiss, S.J. 2006. A cancer cell metalloprotease triad regulates the basement membrane transmigration program. *Genes Dev* 20:2673-2686.
5. Rowe, R.G., and Weiss, S.J. 2008. Breaching the basement membrane: who, when and how? *Trends Cell Biol* 18:560-574.
6. Kalluri, R. 2003. Basement membranes: structure, assembly and role in tumour angiogenesis. *Nat Rev Cancer* 3:422-433.
7. Hotary, K.B., Allen, E.D., Brooks, P.C., Datta, N.S., Long, M.W., and Weiss, S.J. 2003. Membrane type I matrix metalloproteinase usurps tumor growth control imposed by the three-dimensional extracellular matrix. *Cell* 114:33-45.
8. Hotary, K.B., Yana, I., Sabeh, F., Li, X.Y., Holmbeck, K., Birkedal-Hansen, H., Allen, E.D., Hiraoka, N., and Weiss, S.J. 2002. Matrix metalloproteinases (MMPs) regulate fibrin-invasive activity via MT1-MMP-dependent and -independent processes. *J Exp Med* 195:295-308.
9. Viebahn, C. 1995. Epithelio-mesenchymal transformation during formation of the mesoderm in the mammalian embryo. *Acta Anat (Basel)* 154:79-97.
10. Sabeh, F., Ota, I., Holmbeck, K., Birkedal-Hansen, H., Soloway, P., Balbin, M., Lopez-Otin, C., Shapiro, S., Inada, M., Krane, S., et al. 2004. Tumor cell traffic through the extracellular matrix is controlled by the membrane-anchored collagenase MT1-MMP. *J Cell Biol* 167:769-781.
11. Thiery, J.P., and Sleeman, J.P. 2006. Complex networks orchestrate epithelial-mesenchymal transitions. *Nat Rev Mol Cell Biol* 7:131-142.
12. Zhou, X., Rowe, R.G., Hiraoka, N., George, J.P., Wirtz, D., Mosher, D.F., Virtanen, I., Chernousov, M.A., and Weiss, S.J. 2008. Fibronectin fibrillogenesis regulates three-dimensional neovessel formation. *Genes Dev* 22:1231-1243.
13. Peinado, H., Marin, F., Cubillo, E., Stark, H.J., Fusenig, N., Nieto, M.A., and Cano, A. 2004. Snail and E47 repressors of E-cadherin induce distinct invasive and angiogenic properties in vivo. *J Cell Sci* 117:2827-2839.

14. Chun, T.H., Sabeh, F., Ota, I., Murphy, H., McDonagh, K.T., Holmbeck, K., Birkedal-Hansen, H., Allen, E.D., and Weiss, S.J. 2004. MT1-MMP-dependent neovessel formation within the confines of the three-dimensional extracellular matrix. *J Cell Biol* 167:757-767.

15. Hotary, K., Allen, E., Punturieri, A., Yana, I., and Weiss, S.J. 2000. Regulation of cell invasion and morphogenesis in a three-dimensional type I collagen matrix by membrane-type matrix metalloproteinases 1, 2, and 3. *J Cell Biol* 149:1309-1323.

16. Viebahn, C., Mayer, B., and Miething, A. 1995. Morphology of incipient mesoderm formation in the rabbit embryo: a light- and retrospective electron-microscopic study. *Acta Anat (Basel)* 154:99-110.

17. Fujiwara, H., Hayashi, Y., Sanzen, N., Kobayashi, R., Weber, C.N., Emoto, T., Futaki, S., Niwa, H., Murray, P., Edgar, D., et al. 2007. Regulation of mesodermal differentiation of mouse embryonic stem cells by basement membranes. *J Biol Chem* 282:29701-29711.

18. Nakaya, Y., Sukowati, E.W., Wu, Y., and Sheng, G. 2008. RhoA and microtubule dynamics control cell-basement membrane interaction in EMT during gastrulation. *Nat Cell Biol* 10:765-775.

19. Baum, B., Settleman, J., and Quinlan, M.P. 2008. Transitions between epithelial and mesenchymal states in development and disease. *Semin Cell Dev Biol* 19:294-308.

20. Berndt, J.D., Clay, M.R., Langenberg, T., and Halloran, M.C. 2008. Rho-kinase and myosin II affect dynamic neural crest cell behaviors during epithelial to mesenchymal transition in vivo. *Dev Biol* 324:236-244.

21. Nieto, M.A., Sargent, M.G., Wilkinson, D.G., and Cooke, J. 1994. Control of cell behavior during vertebrate development by Slug, a zinc finger gene. *Science* 264:835-839.

22. Carmeliet, P., and Jain, R.K. 2000. Angiogenesis in cancer and other diseases. *Nature* 407:249-257.

23. Martin, P. 1997. Wound healing--aiming for perfect skin regeneration. *Science* 276:75-81.

24. Parker, B.S., Argani, P., Cook, B.P., Liangfeng, H., Chartrand, S.D., Zhang, M., Saha, S., Bardelli, A., Jiang, Y., St Martin, T.B., et al. 2004. Alterations in vascular gene expression in invasive breast carcinoma. *Cancer Res* 64:7857-7866.

25. Liebner, S., Cattelino, A., Gallini, R., Rudini, N., Iurlaro, M., Piccolo, S., and Dejana, E. 2004. Beta-catenin is required for endothelial-mesenchymal transformation during heart cushion development in the mouse. *J Cell Biol* 166:359-367.

26. Ma, L., Lu, M.F., Schwartz, R.J., and Martin, J.F. 2005. Bmp2 is essential for cardiac cushion epithelial-mesenchymal transition and myocardial patterning. *Development* 132:5601-5611.

27. Timmerman, L.A., Grego-Bessa, J., Raya, A., Bertran, E., Perez-Pomares, J.M., Diez, J., Aranda, S., Palomo, S., McCormick, F., Izpisua-Belmonte, J.C., et al. 2004. Notch promotes epithelial-mesenchymal transition during cardiac development and oncogenic transformation. *Genes Dev* 18:99-115.

28. Wang, J., Sridurongrit, S., Dudas, M., Thomas, P., Nagy, A., Schneider, M.D., Epstein, J.A., and Kaartinen, V. 2005. Atrioventricular cushion transformation is mediated by ALK2 in the developing mouse heart. *Dev Biol* 286:299-310.

29. Arciniegas, E., Ponce, L., Hartt, Y., Graterol, A., and Carlini, R.G. 2000. Intimal thickening involves transdifferentiation of embryonic endothelial cells. *Anat Rec* 258:47-57.

30. Arciniegas, E., Sutton, A.B., Allen, T.D., and Schor, A.M. 1992. Transforming growth factor beta 1 promotes the differentiation of endothelial cells into smooth muscle-like cells in vitro. *J Cell Sci* 103 (Pt 2):521-529.

31. DeRuiter, M.C., Poelmann, R.E., VanMunsteren, J.C., Mironov, V., Markwald, R.R., and Gittenberger-de Groot, A.C. 1997. Embryonic endothelial cells transdifferentiate into mesenchymal cells expressing smooth muscle actins in vivo and in vitro. *Circ Res* 80:444-451.

32. Frid, M.G., Kale, V.A., and Stenmark, K.R. 2002. Mature vascular endothelium can give rise to smooth muscle cells via endothelial-mesenchymal transdifferentiation: in vitro analysis. *Circ Res* 90:1189-1196.

33. Noseda, M., McLean, G., Niessen, K., Chang, L., Pollet, I., Montpetit, R., Shahidi, R., Dorovini-Zis, K., Li, L., Beckstead, B., et al. 2004. Notch activation results in phenotypic and functional changes consistent with endothelial-to-mesenchymal transformation. *Circ Res* 94:910-917.

34. Christofori, G. 2006. New signals from the invasive front. *Nature* 441:444-450.

35. Spaderna, S., Schmalhofer, O., Hlubek, F., Berx, G., Eger, A., Merkel, S., Jung, A., Kirchner, T., and Brabletz, T. 2006. A transient, EMT-linked loss of basement membranes indicates metastasis and poor survival in colorectal cancer. *Gastroenterology* 131:830-840.

36. Venkov, C.D., Link, A.J., Jennings, J.L., Plieth, D., Inoue, T., Nagai, K., Xu, C., Dimitrova, Y.N., Rauscher, F.J., and Neilson, E.G. 2007. A proximal activator of transcription in epithelial-mesenchymal transition. *J Clin Invest* 117:482-491.

37. Higgins, D.F., Kimura, K., Bernhardt, W.M., Shrimanker, N., Akai, Y., Hohenstein, B., Saito, Y., Johnson, R.S., Kretzler, M., Cohen, C.D., et al. 2007. Hypoxia promotes fibrogenesis in vivo via HIF-1 stimulation of epithelial-to-mesenchymal transition. *J Clin Invest* 117:3810-3820.

38. Barasch, J., Yang, J., Ware, C.B., Taga, T., Yoshida, K., Erdjument-Bromage, H., Tempst, P., Parravicini, E., Malach, S., Aranoff, T., et al. 1999. Mesenchymal to epithelial conversion in rat metanephros is induced by LIF. *Cell* 99:377-386.

39. Iwano, M., Plieth, D., Danoff, T.M., Xue, C., Okada, H., and Neilson, E.G. 2002. Evidence that fibroblasts derive from epithelium during tissue fibrosis. *J Clin Invest* 110:341-350.

40. Kim, K.K., Kugler, M.C., Wolters, P.J., Robillard, L., Galvez, M.G., Brumwell, A.N., Sheppard, D., and Chapman, H.A. 2006. Alveolar epithelial cell mesenchymal transition develops in vivo during pulmonary fibrosis and is regulated by the extracellular matrix. *Proc Natl Acad Sci U S A* 103:13180-13185.

41. Zeisberg, M., Yang, C., Martino, M., Duncan, M.B., Rieder, F., Tanjore, H., and Kalluri, R. 2007. Fibroblasts derive from hepatocytes in liver fibrosis via epithelial to mesenchymal transition. *J Biol Chem* 282:23337-23347.

42. Zeisberg, E.M., Potenta, S., Xie, L., Zeisberg, M., and Kalluri, R. 2007. Discovery of endothelial to mesenchymal transition as a source for carcinoma-associated fibroblasts. *Cancer Res* 67:10123-10128.

43. Zeisberg, E.M., Potenta, S.E., Sugimoto, H., Zeisberg, M., and Kalluri, R. 2008. Fibroblasts in kidney fibrosis emerge via endothelial-to-mesenchymal transition. *J Am Soc Nephrol* 19:2282-2287.

44. Zeisberg, E.M., Tarnavski, O., Zeisberg, M., Dorfman, A.L., McMullen, J.R., Gustafsson, E., Chandraker, A., Yuan, X., Pu, W.T., Roberts, A.B., et al. 2007. Endothelial-to-mesenchymal transition contributes to cardiac fibrosis. *Nat Med* 13:952-961.

45. Arciniegas, E., Frid, M.G., Douglas, I.S., and Stenmark, K.R. 2007. Perspectives on endothelial-to-mesenchymal transition: potential contribution to vascular remodeling in chronic pulmonary hypertension. *Am J Physiol Lung Cell Mol Physiol* 293:L1-8.

46. Beranek, J.T. 1995. Vascular endothelium-derived cells containing smooth muscle actin are present in restenosis. *Lab Invest* 72:771.

47. Brabletz, T., Jung, A., Spaderna, S., Hlubek, F., and Kirchner, T. 2005. Opinion: migrating cancer stem cells - an integrated concept of malignant tumour progression. *Nat Rev Cancer* 5:744-749.

48. Sherwood, D.R. 2006. Cell invasion through basement membranes: an anchor of understanding. *Trends Cell Biol* 16:250-256.

49. Khoshnoodi, J., Pedchenko, V., and Hudson, B.G. 2008. Mammalian collagen IV. *Microsc Res Tech* 71:357-370.

50. Yurchenco, P.D., Amenta, P.S., and Patton, B.L. 2004. Basement membrane assembly, stability and activities observed through a developmental lens. *Matrix Biol* 22:521-538.

51. Abrams, G.A., Schaus, S.S., Goodman, S.L., Nealey, P.F., and Murphy, C.J. 2000. Nanoscale topography of the corneal epithelial basement membrane and Descemet's membrane of the human. *Cornea* 19:57-64.

52. Abrams, G.A., Goodman, S.L., Nealey, P.F., Franco, M., and Murphy, C.J. 2000. Nanoscale topography of the basement membrane underlying the corneal epithelium of the rhesus macaque. *Cell Tissue Res* 299:39-46.

53. Huber, A.R., and Weiss, S.J. 1989. Disruption of the subendothelial basement membrane during neutrophil diapedesis in an in vitro construct of a blood vessel wall. *J Clin Invest* 83:1122-1136.

54. Puente, X.S., Sanchez, L.M., Overall, C.M., and Lopez-Otin, C. 2003. Human and mouse proteases: a comparative genomic approach. *Nat Rev Genet* 4:544-558.

55. Mignatti, P., Robbins, E., and Rifkin, D.B. 1986. Tumor invasion through the human amniotic membrane: requirement for a proteinase cascade. *Cell* 47:487-498.

56. Liotta, L.A., Tryggvason, K., Garbisa, S., Hart, I., Foltz, C.M., and Shafie, S. 1980. Metastatic potential correlates with enzymatic degradation of basement membrane collagen. *Nature* 284:67-68.

57. Page-McCaw, A., Ewald, A.J., and Werb, Z. 2007. Matrix metalloproteinases and the regulation of tissue remodelling. *Nat Rev Mol Cell Biol* 8:221-233.

58. Srivastava, A., Pastor-Pareja, J.C., Igaki, T., Pagliarini, R., and Xu, T. 2007. Basement membrane remodeling is essential for Drosophila disc eversion and tumor invasion. *Proc Natl Acad Sci U S A* 104:2721-2726.

59. Than, M.E., Henrich, S., Huber, R., Ries, A., Mann, K., Kuhn, K., Timpl, R., Bourenkov, G.P., Bartunik, H.D., and Bode, W. 2002. The 1.9-A crystal structure of the noncollagenous (NC1) domain of human placenta collagen IV shows stabilization via a novel type of covalent Met-Lys cross-link. *Proc Natl Acad Sci U S A* 99:6607-6612.

60. Howat, W.J., Holmes, J.A., Holgate, S.T., and Lackie, P.M. 2001. Basement membrane pores in human bronchial epithelium: a conduit for infiltrating cells? *Am J Pathol* 158:673-680.

61. Vanacore, R.M., Friedman, D.B., Ham, A.J., Sundaramoorthy, M., and Hudson, B.G. 2005. Identification of S-hydroxylysyl-methionine as the covalent cross-link of the noncollagenous (NC1) hexamer of the alpha1alpha1alpha2 collagen IV network: a role for the post-translational

modification of lysine 211 to hydroxylysine 211 in hexamer assembly. *J Biol Chem* 280:29300-29310.

62. Perez, S.E., Cano, D.A., Dao-Pick, T., Rougier, J.P., Werb, Z., and Hebrok, M. 2005. Matrix metalloproteinases 2 and 9 are dispensable for pancreatic islet formation and function in vivo. *Diabetes* 54:694-701.

63. Hamano, Y., Zeisberg, M., Sugimoto, H., Lively, J.C., Maeshima, Y., Yang, C., Hynes, R.O., Werb, Z., Sudhakar, A., and Kalluri, R. 2003. Physiological levels of tumstatin, a fragment of collagen IV alpha3 chain, are generated by MMP-9 proteolysis and suppress angiogenesis via alphaV beta3 integrin. *Cancer Cell* 3:589-601.

64. Baluk, P., Raymond, W.W., Ator, E., Coussens, L.M., McDonald, D.M., and Caughey, G.H. 2004. Matrix metalloproteinase-2 and -9 expression increases in Mycoplasma-infected airways but is not required for microvascular remodeling. *Am J Physiol Lung Cell Mol Physiol* 287:L307-317.

65. Itoh, T., Matsuda, H., Tanioka, M., Kuwabara, K., Itohara, S., and Suzuki, R. 2002. The role of matrix metalloproteinase-2 and matrix metalloproteinase-9 in antibody-induced arthritis. *J Immunol* 169:2643-2647.

66. McKee, K.K., Harrison, D., Capizzi, S., and Yurchenco, P.D. 2007. Role of laminin terminal globular domains in basement membrane assembly. *J Biol Chem* 282:21437-21447.

67. Li, S., Liquari, P., McKee, K.K., Harrison, D., Patel, R., Lee, S., and Yurchenco, P.D. 2005. Laminin-sulfatide binding initiates basement membrane assembly and enables receptor signaling in Schwann cells and fibroblasts. *J Cell Biol* 169:179-189.

68. Marinkovich, M.P. 2007. Tumour microenvironment: laminin 332 in squamous-cell carcinoma. *Nat Rev Cancer* 7:370-380.

69. McMillan, J.R., Akiyama, M., and Shimizu, H. 2003. Ultrastructural orientation of laminin 5 in the epidermal basement membrane: an updated model for basement membrane organization. *J Histochem Cytochem* 51:1299-1306.

70. Kleinman, H.K., McGarvey, M.L., Liotta, L.A., Robey, P.G., Tryggvason, K., and Martin, G.R. 1982. Isolation and characterization of type IV procollagen, laminin, and heparan sulfate proteoglycan from the EHS sarcoma. *Biochemistry* 21:6188-6193.

71. Reiser, K., McCormick, R.J., and Rucker, R.B. 1992. Enzymatic and nonenzymatic cross-linking of collagen and elastin. *Faseb J* 6:2439-2449.

72. Vanacore, R.M., Ham, A.J., Cartailler, J.P., Sundaramoorthy, M., Todd, P., Pedchenko, V., Sado, Y., Borza, D.B., and Hudson, B.G. 2008. A Role for Collagen IV Cross-links in Conferring Immune Privilege to the

Goodpasture Autoantigen: STRUCTURAL BASIS FOR THE CRYPTICITY OF B CELL EPITOPES. *J Biol Chem* 283:22737-22748.

73. Hu, J., Van den Steen, P.E., Sang, Q.X., and Opdenakker, G. 2007. Matrix metalloproteinase inhibitors as therapy for inflammatory and vascular diseases. *Nat Rev Drug Discov* 6:480-498.

74. Iozzo, R.V. 2005. Basement membrane proteoglycans: from cellar to ceiling. *Nat Rev Mol Cell Biol* 6:646-656.

75. Yang, B.G., Tanaka, T., Jang, M.H., Bai, Z., Hayasaka, H., and Miyasaka, M. 2007. Binding of lymphoid chemokines to collagen IV that accumulates in the basal lamina of high endothelial venules: its implications in lymphocyte trafficking. *J Immunol* 179:4376-4382.

76. Poschl, E., Schlotzer-Schrehardt, U., Brachvogel, B., Saito, K., Ninomiya, Y., and Mayer, U. 2004. Collagen IV is essential for basement membrane stability but dispensable for initiation of its assembly during early development. *Development* 131:1619-1628.

77. Pajerowski, J.D., Dahl, K.N., Zhong, F.L., Sammak, P.J., and Discher, D.E. 2007. Physical plasticity of the nucleus in stem cell differentiation. *Proc Natl Acad Sci U S A* 104:15619-15624.

78. Wolf, K., Wu, Y.I., Liu, Y., Geiger, J., Tam, E., Overall, C., Stack, M.S., and Friedl, P. 2007. Multi-step pericellular proteolysis controls the transition from individual to collective cancer cell invasion. *Nat Cell Biol* 9:893-904.

79. Nakayama, M., Amano, M., Katsumi, A., Kaneko, T., Kawabata, S., Takefuji, M., and Kaibuchi, K. 2005. Rho-kinase and myosin II activities are required for cell type and environment specific migration. *Genes Cells* 10:107-117.

80. Kuntz, R.M., and Saltzman, W.M. 1997. Neutrophil motility in extracellular matrix gels: mesh size and adhesion affect speed of migration. *Biophys J* 72:1472-1480.

81. Tucker, S.P., Melsen, L.R., and Compans, R.W. 1992. Migration of polarized epithelial cells through permeable membrane substrates of defined pore size. *Eur J Cell Biol* 58:280-290.

82. Warfel, K.A., and Hull, M.T. 1988. Basal lamina fenestrations in the human colon: transmission and scanning electron microscope study. *Anat Rec* 220:68-75.

83. Dingemans, K.P. 1988. What's new in the ultrastructure of tumor invasion in vivo? *Pathol Res Pract* 183:792-808.

84. Peinado, H., Olmeda, D., and Cano, A. 2007. Snail, Zeb and bHLH factors in tumour progression: an alliance against the epithelial phenotype? *Nat Rev Cancer* 7:415-428.

85. Yang, J., and Weinberg, R.A. 2008. Epithelial-mesenchymal transition: at the crossroads of development and tumor metastasis. *Dev Cell* 14:818-829.

86. Ikeda, K., Iyama, K., Ishikawa, N., Egami, H., Nakao, M., Sado, Y., Ninomiya, Y., and Baba, H. 2006. Loss of expression of type IV collagen alpha5 and alpha6 chains in colorectal cancer associated with the hypermethylation of their promoter region. *Am J Pathol* 168:856-865.

87. Murai, S., Umemiya, T., Seiki, M., and Harigaya, K. 2004. Expression and localization of membrane-type-1 matrix metalloproteinase, CD 44, and laminin-5gamma2 chain during colorectal carcinoma tumor progression. *Virchows Arch* 445:271-278.

88. Hlubek, F., Spaderna, S., Jung, A., Kirchner, T., and Brabletz, T. 2004. Beta-catenin activates a coordinated expression of the proinvasive factors laminin-5 gamma2 chain and MT1-MMP in colorectal carcinomas. *Int J Cancer* 108:321-326.

89. Franz, M., Richter, P., Geyer, C., Hansen, T., Acuna, L.D., Hyckel, P., Bohmer, F.D., Kosmehl, H., and Berndt, A. 2007. Mesenchymal cells contribute to the synthesis and deposition of the laminin-5 gamma2 chain in the invasive front of oral squamous cell carcinoma. *J Mol Histol* 38:183-190.

90. Takahashi, M., Tsunoda, T., Seiki, M., Nakamura, Y., and Furukawa, Y. 2002. Identification of membrane-type matrix metalloproteinase-1 as a target of the beta-catenin/Tcf4 complex in human colorectal cancers. *Oncogene* 21:5861-5867.

91. Bechetoille, N., Haftek, M., Staquet, M.J., Cochran, A.J., Schmitt, D., and Berthier-Vergnes, O. 2000. Penetration of human metastatic melanoma cells through an authentic dermal-epidermal junction is associated with dissolution of native collagen types IV and VII. *Melanoma Res* 10:427-434.

92. Frei, J.V. 1962. The fine structure of the basement membrane in epidermal tumors. *J Cell Biol* 15:335-342.

93. Birbeck, M.S., and Wheatley, D.N. 1965. An electron microscopic study of the invasion of ascites tumor cells into the abdominal wall. *Cancer Res* 25:490-497.

94. Liotta, L.A., and Kohn, E.C. 2001. The microenvironment of the tumour-host interface. *Nature* 411:375-379.

95. Overall, C.M., and Kleifeld, O. 2006. Tumour microenvironment - opinion: validating matrix metalloproteinases as drug targets and anti-targets for cancer therapy. *Nat Rev Cancer* 6:227-239.

96. Overall, C.M., and Blobel, C.P. 2007. In search of partners: linking extracellular proteases to substrates. *Nat Rev Mol Cell Biol* 8:245-257.

97. Pillay, V., Dass, C.R., and Choong, P.F. 2007. The urokinase plasminogen activator receptor as a gene therapy target for cancer. *Trends Biotechnol* 25:33-39.

98. Mohamed, M.M., and Sloane, B.F. 2006. Cysteine cathepsins: multifunctional enzymes in cancer. *Nat Rev Cancer* 6:764-775.

99. Martin, M.D., and Matrisian, L.M. 2007. The other side of MMPs: protective roles in tumor progression. *Cancer Metastasis Rev* 26:717-724.

100. Schenk, S., and Quaranta, V. 2003. Tales from the crypt[ic] sites of the extracellular matrix. *Trends Cell Biol* 13:366-375.

101. Liotta, L.A., Kleinerman, J., Catanzaro, P., and Rynbrandt, D. 1977. Degradation of basement membrane by murine tumor cells. *J Natl Cancer Inst* 58:1427-1431.

102. Aplin, J.D., Campbell, S., and Allen, T.D. 1985. The extracellular matrix of human amniotic epithelium: ultrastructure, composition and deposition. *J Cell Sci* 79:119-136.

103. Persky, B., Ostrowski, L.E., Pagast, P., Ahsan, A., and Schultz, R.M. 1986. Inhibition of proteolytic enzymes in the in vitro amnion model for basement membrane invasion. *Cancer Res* 46:4129-4134.

104. Fu, X., Parks, W.C., and Heinecke, J.W. 2008. Activation and silencing of matrix metalloproteinases. *Semin Cell Dev Biol* 19:2-13.

105. Margulis, A., Zhang, W., Alt-Holland, A., Crawford, H.C., Fusenig, N.E., and Garlick, J.A. 2005. E-cadherin suppression accelerates squamous cell carcinoma progression in three-dimensional, human tissue constructs. *Cancer Res* 65:1783-1791.

106. Wolf, K., Muller, R., Borgmann, S., Brocker, E.B., and Friedl, P. 2003. Amoeboid shape change and contact guidance: T-lymphocyte crawling through fibrillar collagen is independent of matrix remodeling by MMPs and other proteases. *Blood* 102:3262-3269.

107. English, J.L., Kassiri, Z., Koskivirta, I., Atkinson, S.J., Di Grappa, M., Soloway, P.D., Nagase, H., Vuorio, E., Murphy, G., and Khokha, R. 2006. Individual Timp deficiencies differentially impact pro-MMP-2 activation. *J Biol Chem* 281:10337-10346.

108. Zhao, H., Bernardo, M.M., Osenkowski, P., Sohail, A., Pei, D., Nagase, H., Kashiwagi, M., Soloway, P.D., DeClerck, Y.A., and Fridman, R. 2004. Differential inhibition of membrane type 3 (MT3)-matrix metalloproteinase (MMP) and MT1-MMP by tissue inhibitor of metalloproteinase (TIMP)-2 and TIMP-3 rgulates pro-MMP-2 activation. *J Biol Chem* 279:8592-8601.

109. Itoh, Y., and Seiki, M. 2006. MT1-MMP: a potent modifier of pericellular microenvironment. *J Cell Physiol* 206:1-8.

110. Yana, I., and Weiss, S.J. 2000. Regulation of membrane type-1 matrix metalloproteinase activation by proprotein convertases. *Mol Biol Cell* 11:2387-2401.

111. Wu, Y.I., Munshi, H.G., Snipas, S.J., Salvesen, G.S., Fridman, R., and Stack, M.S. 2007. Activation-coupled membrane-type 1 matrix metalloproteinase membrane trafficking. *Biochem J* 407:171-177.

112. Li, X.-Y., Ota, I., Yana, I., Sabeh, F., and Weiss, S.J. 2008. Molecular dissection of the structural machinery underlying the tissue-invasive activity of MT1-MMP. *Molecular Biology of the Cell* 19:3221-3233.

113. Artym, V.V., Zhang, Y., Seillier-Moiseiwitsch, F., Yamada, K.M., and Mueller, S.C. 2006. Dynamic interactions of cortactin and membrane type 1 matrix metalloproteinase at invadopodia: defining the stages of invadopodia formation and function. *Cancer Res* 66:3034-3043.

114. Linder, S. 2007. The matrix corroded: podosomes and invadopodia in extracellular matrix degradation. *Trends Cell Biol* 17:107-117.

115. Saffarian, S., Collier, I.E., Marmer, B.L., Elson, E.L., and Goldberg, G. 2004. Interstitial collagenase is a Brownian ratchet driven by proteolysis of collagen. *Science* 306:108-111.

116. Cardone, R.A., Casavola, V., and Reshkin, S.J. 2005. The role of disturbed pH dynamics and the Na+/H+ exchanger in metastasis. *Nat Rev Cancer* 5:786-795.

117. Shintani, Y., Fukumoto, Y., Chaika, N., Svoboda, R., Wheelock, M.J., and Johnson, K.R. 2008. Collagen I-mediated up-regulation of N-cadherin requires cooperative signals from integrins and discoidin domain receptor 1. *J Cell Biol* 180:1277-1289.

118. Gaggioli, C., Hooper, S., Hidalgo-Carcedo, C., Grosse, R., Marshall, J.F., Harrington, K., and Sahai, E. 2007. Fibroblast-led collective invasion of carcinoma cells with differing roles for RhoGTPases in leading and following cells. *Nat Cell Biol* 9:1392-1400.

119. Somogyi, K., and Rorth, P. 2004. Evidence for tension-based regulation of Drosophila MAL and SRF during invasive cell migration. *Dev Cell* 7:85-93.

120. Discher, D.E., Janmey, P., and Wang, Y.L. 2005. Tissue cells feel and respond to the stiffness of their substrate. *Science* 310:1139-1143.

121. Thiery, J.P. 2002. Epithelial-mesenchymal transitions in tumour progression. *Nat Rev Cancer* 2:442-454.

122. Zeisberg, M., Bonner, G., Maeshima, Y., Colorado, P., Muller, G.A., Strutz, F., and Kalluri, R. 2001. Renal fibrosis: collagen composition and assembly regulates epithelial-mesenchymal transdifferentiation. *Am J Pathol* 159:1313-1321.

123. Onder, T.T., Gupta, P.B., Mani, S.A., Yang, J., Lander, E.S., and Weinberg, R.A. 2008. Loss of E-cadherin promotes metastasis via multiple downstream transcriptional pathways. *Cancer Res* 68:3645-3654.

124. Solanas, G., Porta-de-la-Riva, M., Agusti, C., Casagolda, D., Sanchez-Aguilera, F., Larriba, M.J., Pons, F., Peiro, S., Escriva, M., Munoz, A., et al. 2008. E-cadherin controls beta-catenin and NF-kappaB transcriptional activity in mesenchymal gene expression. *J Cell Sci* 121:2224-2234.

125. Frixen, U.H., Behrens, J., Sachs, M., Eberle, G., Voss, B., Warda, A., Lochner, D., and Birchmeier, W. 1991. E-cadherin-mediated cell-cell adhesion prevents invasiveness of human carcinoma cells. *J Cell Biol* 113:173-185.

126. Carver, E.A., Jiang, R., Lan, Y., Oram, K.F., and Gridley, T. 2001. The mouse snail gene encodes a key regulator of the epithelial-mesenchymal transition. *Mol Cell Biol* 21:8184-8188.

127. Batlle, E., Sancho, E., Franci, C., Dominguez, D., Monfar, M., Baulida, J., and Garcia De Herreros, A. 2000. The transcription factor snail is a repressor of E-cadherin gene expression in epithelial tumour cells. *Nat Cell Biol* 2:84-89.

128. Blechschmidt, K., Sassen, S., Schmalfeldt, B., Schuster, T., Hofler, H., and Becker, K.F. 2008. The E-cadherin repressor Snail is associated with lower overall survival of ovarian cancer patients. *Br J Cancer* 98:489-495.

129. Cano, A., Perez-Moreno, M.A., Rodrigo, I., Locascio, A., Blanco, M.J., del Barrio, M.G., Portillo, F., and Nieto, M.A. 2000. The transcription factor snail controls epithelial-mesenchymal transitions by repressing E-cadherin expression. *Nat Cell Biol* 2:76-83.

130. Yook, J.I., Li, X.Y., Ota, I., Fearon, E.R., and Weiss, S.J. 2005. Wnt-dependent regulation of the E-cadherin repressor snail. *J Biol Chem* 280:11740-11748.

131. Yook, J.I., Li, X.Y., Ota, I., Hu, C., Kim, H.S., Kim, N.H., Cha, S.Y., Ryu, J.K., Choi, Y.J., Kim, J., et al. 2006. A Wnt-Axin2-GSK3beta cascade regulates Snail1 activity in breast cancer cells. *Nat Cell Biol* 8:1398-1406.

132. Zidar, N., Gale, N., Kojc, N., Volavsek, M., Cardesa, A., Alos, L., Hofler, H., Blechschmidt, K., and Becker, K.F. 2008. Cadherin-catenin complex and transcription factor Snail-1 in spindle cell carcinoma of the head and neck. *Virchows Arch* 453:267-274.

133. Barbera, M.J., Puig, I., Dominguez, D., Julien-Grille, S., Guaita-Esteruelas, S., Peiro, S., Baulida, J., Franci, C., Dedhar, S., Larue, L., et al. 2004. Regulation of Snail transcription during epithelial to mesenchymal transition of tumor cells. *Oncogene* 23:7345-7354.

134. Giannelli, G., Bergamini, C., Fransvea, E., Sgarra, C., and Antonaci, S. 2005. Laminin-5 with transforming growth factor-beta1 induces epithelial

to mesenchymal transition in hepatocellular carcinoma. *Gastroenterology* 129:1375-1383.

135. Peinado, H., Quintanilla, M., and Cano, A. 2003. Transforming growth factor beta-1 induces snail transcription factor in epithelial cell lines: mechanisms for epithelial mesenchymal transitions. *J Biol Chem* 278:21113-21123.

136. Kokudo, T., Suzuki, Y., Yoshimatsu, Y., Yamazaki, T., Watabe, T., and Miyazono, K. 2008. Snail is required for TGFbeta-induced endothelial-mesenchymal transition of embryonic stem cell-derived endothelial cells. *J Cell Sci* 121:3317-3324.

137. Grotegut, S., von Schweinitz, D., Christofori, G., and Lehembre, F. 2006. Hepatocyte growth factor induces cell scattering through MAPK/Egr-1-mediated upregulation of Snail. *Embo J* 25:3534-3545.

138. Li, X., Deng, W., Lobo-Ruppert, S.M., and Ruppert, J.M. 2007. Gli1 acts through Snail and E-cadherin to promote nuclear signaling by beta-catenin. *Oncogene* 26:4489-4498.

139. Li, X., Deng, W., Nail, C.D., Bailey, S.K., Kraus, M.H., Ruppert, J.M., and Lobo-Ruppert, S.M. 2006. Snail induction is an early response to Gli1 that determines the efficiency of epithelial transformation. *Oncogene* 25:609-621.

140. Sahlgren, C., Gustafsson, M.V., Jin, S., Poellinger, L., and Lendahl, U. 2008. Notch signaling mediates hypoxia-induced tumor cell migration and invasion. *Proc Natl Acad Sci U S A* 105:6392-6397.

141. Yang, A.D., Camp, E.R., Fan, F., Shen, L., Gray, M.J., Liu, W., Somcio, R., Bauer, T.W., Wu, Y., Hicklin, D.J., et al. 2006. Vascular endothelial growth factor receptor-1 activation mediates epithelial to mesenchymal transition in human pancreatic carcinoma cells. *Cancer Res* 66:46-51.

142. Radisky, D.C., Levy, D.D., Littlepage, L.E., Liu, H., Nelson, C.M., Fata, J.E., Leake, D., Godden, E.L., Albertson, D.G., Nieto, M.A., et al. 2005. Rac1b and reactive oxygen species mediate MMP-3-induced EMT and genomic instability. *Nature* 436:123-127.

143. Bachelder, R.E., Yoon, S.O., Franci, C., de Herreros, A.G., and Mercurio, A.M. 2005. Glycogen synthase kinase-3 is an endogenous inhibitor of Snail transcription: implications for the epithelial-mesenchymal transition. *J Cell Biol* 168:29-33.

144. Peiro, S., Escriva, M., Puig, I., Barbera, M.J., Dave, N., Herranz, N., Larriba, M.J., Takkunen, M., Franci, C., Munoz, A., et al. 2006. Snail1 transcriptional repressor binds to its own promoter and controls its expression. *Nucleic Acids Res* 34:2077-2084.

145. Clevers, H. 2006. Wnt/beta-catenin signaling in development and disease. *Cell* 127:469-480.

146. Zhou, B.P., Deng, J., Xia, W., Xu, J., Li, Y.M., Gunduz, M., and Hung, M.C. 2004. Dual regulation of Snail by GSK-3beta-mediated phosphorylation in control of epithelial-mesenchymal transition. *Nat Cell Biol* 6:931-940.

147. Yang, Z., Rayala, S., Nguyen, D., Vadlamudi, R.K., Chen, S., and Kumar, R. 2005. Pak1 phosphorylation of snail, a master regulator of epithelial-to-mesenchyme transition, modulates snail's subcellular localization and functions. *Cancer Res* 65:3179-3184.

148. Wu, Y., Evers, B.M., and Zhou, B.P. 2009. Small C-terminal domain phosphatase enhances snail activity through dephosphorylation. *J Biol Chem* 284:640-648.

149. Lim, S.O., Gu, J.M., Kim, M.S., Kim, H.S., Park, Y.N., Park, C.K., Cho, J.W., Park, Y.M., and Jung, G. 2008. Epigenetic changes induced by reactive oxygen species in hepatocellular carcinoma: methylation of the E-cadherin promoter. *Gastroenterology* 135:2128-2140, 2140 e2121-2128.

150. Hou, Z., Peng, H., Ayyanathan, K., Yan, K.P., Langer, E.M., Longmore, G.D., and Rauscher, F.J., 3rd. 2008. The LIM protein AJUBA recruits protein arginine methyltransferase 5 to mediate SNAIL-dependent transcriptional repression. *Mol Cell Biol* 28:3198-3207.

151. Langer, E.M., Feng, Y., Zhaoyuan, H., Rauscher, F.J., 3rd, Kroll, K.L., and Longmore, G.D. 2008. Ajuba LIM proteins are snail/slug corepressors required for neural crest development in Xenopus. *Dev Cell* 14:424-436.

152. Herranz, N., Pasini, D., Diaz, V.M., Franci, C., Gutierrez, A., Dave, N., Escriva, M., Hernandez-Munoz, I., Di Croce, L., Helin, K., et al. 2008. Polycomb complex 2 is required for E-cadherin repression by the Snail1 transcription factor. *Mol Cell Biol* 28:4772-4781.

153. Peinado, H., Ballestar, E., Esteller, M., and Cano, A. 2004. Snail mediates E-cadherin repression by the recruitment of the Sin3A/histone deacetylase 1 (HDAC1)/HDAC2 complex. *Mol Cell Biol* 24:306-319.

154. Peinado, H., Del Carmen Iglesias-de la Cruz, M., Olmeda, D., Csiszar, K., Fong, K.S., Vega, S., Nieto, M.A., Cano, A., and Portillo, F. 2005. A molecular role for lysyl oxidase-like 2 enzyme in snail regulation and tumor progression. *Embo J* 24:3446-3458.

155. Rowe, R.G., Li, X.Y., Hu, Y., Saunders, T.L., Virtanen, I., Garcia de Herreros, A., Becker, K.F., Ingvarsen, S., Engelholm, L.H., Bommer, G.T., et al. 2009. Mesenchymal cells reactivate Snail1 expression to drive three-dimensional invasion programs. *J Cell Biol* 184:399-408.

156. Vega, S., Morales, A.V., Ocana, O.H., Valdes, F., Fabregat, I., and Nieto, M.A. 2004. Snail blocks the cell cycle and confers resistance to cell death. *Genes Dev* 18:1131-1143.

157. Escriva, M., Peiro, S., Herranz, N., Villagrasa, P., Dave, N., Montserrat-Sentis, B., Murray, S.A., Franci, C., Gridley, T., Virtanen, I., et al. 2008.

Repression of PTEN phosphatase by Snail1 transcriptional factor during gamma radiation-induced apoptosis. *Mol Cell Biol* 28:1528-1540.

158. Olmeda, D., Jorda, M., Peinado, H., Fabra, A., and Cano, A. 2007. Snail silencing effectively suppresses tumour growth and invasiveness. *Oncogene* 26:1862-1874.

159. Olmeda, D., Montes, A., Moreno-Bueno, G., Flores, J.M., Portillo, F., and Cano, A. 2008. Snai1 and Snai2 collaborate on tumor growth and metastasis properties of mouse skin carcinoma cell lines. *Oncogene* 27:4690-4701.

160. Perez-Mancera, P.A., Perez-Caro, M., Gonzalez-Herrero, I., Flores, T., Orfao, A., de Herreros, A.G., Gutierrez-Adan, A., Pintado, B., Sagrera, A., Sanchez-Martin, M., et al. 2005. Cancer development induced by graded expression of Snail in mice. *Hum Mol Genet* 14:3449-3461.

161. Mani, S.A., Guo, W., Liao, M.J., Eaton, E.N., Ayyanan, A., Zhou, A.Y., Brooks, M., Reinhard, F., Zhang, C.C., Shipitsin, M., et al. 2008. The epithelial-mesenchymal transition generates cells with properties of stem cells. *Cell* 133:704-715.

162. Moody, S.E., Perez, D., Pan, T.C., Sarkisian, C.J., Portocarrero, C.P., Sterner, C.J., Notorfrancesco, K.L., Cardiff, R.D., and Chodosh, L.A. 2005. The transcriptional repressor Snail promotes mammary tumor recurrence. *Cancer Cell* 8:197-209.

163. Podsypanina, K., Du, Y.C., Jechlinger, M., Beverly, L.J., Hambardzumyan, D., and Varmus, H. 2008. Seeding and propagation of untransformed mouse mammary cells in the lung. *Science* 321:1841-1844.

164. Husemann, Y., Geigl, J.B., Schubert, F., Musiani, P., Meyer, M., Burghart, E., Forni, G., Eils, R., Fehm, T., Riethmuller, G., et al. 2008. Systemic spread is an early step in breast cancer. *Cancer Cell* 13:58-68.

165. Blanco, M.J., Barrallo-Gimeno, A., Acloque, H., Reyes, A.E., Tada, M., Allende, M.L., Mayor, R., and Nieto, M.A. 2007. Snail1a and Snail1b cooperate in the anterior migration of the axial mesendoderm in the zebrafish embryo. *Development* 134:4073-4081.

166. Franci, C., Takkunen, M., Dave, N., Alameda, F., Gomez, S., Rodriguez, R., Escriva, M., Montserrat-Sentis, B., Baro, T., Garrido, M., et al. 2006. Expression of Snail protein in tumor-stroma interface. *Oncogene* 25:5134-5144.

167. Murray, S.A., and Gridley, T. 2006. Snail family genes are required for left-right asymmetry determination, but not neural crest formation, in mice. *Proc Natl Acad Sci U S A* 103:10300-10304.

168. Fitchett, J.E., and Hay, E.D. 1989. Medial edge epithelium transforms to mesenchyme after embryonic palatal shelves fuse. *Dev Biol* 131:455-474.

169. Murray, S.A., Oram, K.F., and Gridley, T. 2007. Multiple functions of Snail family genes during palate development in mice. *Development* 134:1789-1797.

170. Potenta, S., Zeisberg, E., and Kalluri, R. 2008. The role of endothelial-to-mesenchymal transition in cancer progression. *Br J Cancer* 99:1375-1379.

171. Romano, L.A., and Runyan, R.B. 2000. Slug is an essential target of TGFbeta2 signaling in the developing chicken heart. *Dev Biol* 223:91-102.

172. Niessen, K., Fu, Y., Chang, L., Hoodless, P.A., McFadden, D., and Karsan, A. 2008. Slug is a direct Notch target required for initiation of cardiac cushion cellularization. *J Cell Biol* 182:315-325.

173. Olmeda, D., Moreno-Bueno, G., Flores, J.M., Fabra, A., Portillo, F., and Cano, A. 2007. SNAI1 is required for tumor growth and lymph node metastasis of human breast carcinoma MDA-MB-231 cells. *Cancer Res* 67:11721-11731.

174. Meindl-Beinker, N.M., and Dooley, S. 2008. Transforming growth factor-beta and hepatocyte transdifferentiation in liver fibrogenesis. *J Gastroenterol Hepatol* 23 Suppl 1:S122-127.

175. Yoshino, J., Monkawa, T., Tsuji, M., Inukai, M., Itoh, H., and Hayashi, M. 2007. Snail1 is involved in the renal epithelial-mesenchymal transition. *Biochem Biophys Res Commun* 362:63-68.

176. Dooley, S., Hamzavi, J., Ciuclan, L., Godoy, P., Ilkavets, I., Ehnert, S., Ueberham, E., Gebhardt, R., Kanzler, S., Geier, A., et al. 2008. Hepatocyte-specific Smad7 expression attenuates TGF-beta-mediated fibrogenesis and protects against liver damage. *Gastroenterology* 135:642-659.

177. Boutet, A., De Frutos, C.A., Maxwell, P.H., Mayol, M.J., Romero, J., and Nieto, M.A. 2006. Snail activation disrupts tissue homeostasis and induces fibrosis in the adult kidney. *Embo J* 25:5603-5613.

178. Perumal, S., Antipova, O., and Orgel, J.P. 2008. Collagen fibril architecture, domain organization, and triple-helical conformation govern its proteolysis. *Proc Natl Acad Sci U S A* 105:2824-2829.

179. Sweeney, S.M., Orgel, J.P., Fertala, A., McAuliffe, J.D., Turner, K.R., Di Lullo, G.A., Chen, S., Antipova, O., Perumal, S., Ala-Kokko, L., et al. 2008. Candidate cell and matrix interaction domains on the collagen fibril, the predominant protein of vertebrates. *J Biol Chem* 283:21187-21197.

180. Li, X.Y., Ota, I., Yana, I., Sabeh, F., and Weiss, S.J. 2008. Molecular Dissection of the Structural Machinery Underlying the Tissue-Invasive Activity of MT1-MMP. *Mol Biol Cell* 19:3221-3233.

181. Sabeh, F., Shimizu-Hirota, R., and Weiss, S.J. 2008. Protease-Dependent versus Independent Cancer Cell Invasion Programs: 3-Dimensional Amoeboid Movement Revisited. *J Biol Chem* In press.

182. Kadler, K.E., Holmes, D.F., Trotter, J.A., and Chapman, J.A. 1996. Collagen fibril formation. *Biochem J* 316 (Pt 1):1-11.

183. Sabeh, F., Shimizu-Hirota, R., and Weiss, S.J. 2009. Protease-dependent versus independent cancer cell invasion programs: 3-dimensional amoeboid movement revisited. *Journal of Cell Biology* accepted.

184. McKee, T.D., Grandi, P., Mok, W., Alexandrakis, G., Insin, N., Zimmer, J.P., Bawendi, M.G., Boucher, Y., Breakefield, X.O., and Jain, R.K. 2006. Degradation of fibrillar collagen in a human melanoma xenograft improves the efficacy of an oncolytic herpes simplex virus vector. *Cancer Res* 66:2509-2513.

185. Imamichi, Y., Konig, A., Gress, T., and Menke, A. 2007. Collagen type I-induced Smad-interacting protein 1 expression downregulates E-cadherin in pancreatic cancer. *Oncogene* 26:2381-2385.

186. Gavert, N., and Ben-Ze'ev, A. 2008. Epithelial-mesenchymal transition and the invasive potential of tumors. *Trends Mol Med* 14:199-209.

187. Wolf, K., Mazo, I., Leung, H., Engelke, K., von Andrian, U.H., Deryugina, E.I., Strongin, A.Y., Brocker, E.B., and Friedl, P. 2003. Compensation mechanism in tumor cell migration: mesenchymal-amoeboid transition after blocking of pericellular proteolysis. *J Cell Biol* 160:267-277.

188. Friedl, P., and Wolf, K. 2008. Tube travel: the role of proteases in individual and collective cancer cell invasion. *Cancer Res* 68:7247-7249.

189. Croft, D.R., and Olson, M.F. 2008. Regulating the conversion between rounded and elongated modes of cancer cell movement. *Cancer Cell* 14:349-351.

190. Barbolina, M.V., and Stack, M.S. 2008. Membrane type 1-matrix metalloproteinase: substrate diversity in pericellular proteolysis. *Semin Cell Dev Biol* 19:24-33.

191. Packard, B.Z., Artym, V.V., Komoriya, A., and Yamada, K.M. 2008. Direct visualization of protease activity on cells migrating in three-dimensions. *Matrix Biol* ePub October 29, 2008:doi:10.1016/j.matbio.2008.1010.1001.

192. Fisher, K.E., Pop, A., Koh, W., Anthis, N.J., Saunders, W.B., and Davis, G.E. 2006. Tumor cell invasion of collagen matrices requires coordinate lipid agonist-induced G-protein and membrane-type matrix metalloproteinase-1-dependent signaling. *Mol Cancer* 5:69.

193. Sodek, K.L., Ringuette, M.J., and Brown, T.J. 2007. MT1-MMP is the critical determinant of matrix degradation and invasion by ovarian cancer cells. *Br J Cancer* 97:358-367.

194. Sanz-Moreno, V., Gadea, G., Ahn, J., Paterson, H., Marra, P., Pinner, S., Sahai, E., and Marshall, C.J. 2008. Rac activation and inactivation control plasticity of tumor cell movement. *Cell* 135:510-523.

195. Demou, Z.N., Awad, M., McKee, T., Perentes, J.Y., Wang, X., Munn, L.L., Jain, R.K., and Boucher, Y. 2005. Lack of telopeptides in fibrillar collagen I promotes the invasion of a metastatic breast tumor cell line. *Cancer Res* 65:5674-5682.

196. Lutolf, M.P., Lauer-Fields, J.L., Schmoekel, H.G., Metters, A.T., Weber, F.E., Fields, G.B., and Hubbell, J.A. 2003. Synthetic matrix metalloproteinase-sensitive hydrogels for the conduction of tissue regeneration: engineering cell-invasion characteristics. *Proc Natl Acad Sci U S A* 100:5413-5418.

197. Palermo, C., and Joyce, J.A. 2008. Cysteine cathepsin proteases as pharmacological targets in cancer. *Trends Pharmacol Sci* 29:22-28.

198. Goulet, B., Baruch, A., Moon, N.S., Poirier, M., Sansregret, L.L., Erickson, A., Bogyo, M., and Nepveu, A. 2004. A cathepsin L isoform that is devoid of a signal peptide localizes to the nucleus in S phase and processes the CDP/Cux transcription factor. *Mol Cell* 14:207-219.

199. Duncan, E.M., Muratore-Schroeder, T.L., Cook, R.G., Garcia, B.A., Shabanowitz, J., Hunt, D.F., and Allis, C.D. 2008. Cathepsin L proteolytically processes histone H3 during mouse embryonic stem cell differentiation. *Cell* 135:284-294.

200. Sternlicht, M.D., and Werb, Z. 2001. How matrix metalloproteinases regulate cell behavior. *Annu Rev Cell Dev Biol* 17:463-516.

201. Gross, J., and Lapiere, C.M. 1962. Collagenolytic activity in amphibian tissues: a tissue culture assay. *Proc Natl Acad Sci U S A* 48:1014-1022.

202. Bigg, H.F., Rowan, A.D., Barker, M.D., and Cawston, T.E. 2007. Activity of matrix metalloproteinase-9 against native collagen types I and III. *Febs J* 274:1246-1255.

203. Krane, S.M., and Inada, M. 2008. Matrix metalloproteinases and bone. *Bone* 43:7-18.

204. Blackburn, J.S., and Brinckerhoff, C.E. 2008. Matrix metalloproteinase-1 and thrombin differentially activate gene expression in endothelial cells via PAR-1 and promote angiogenesis. *Am J Pathol* 173:1736-1746.

205. Blackburn, J.S., Rhodes, C.H., Coon, C.I., and Brinckerhoff, C.E. 2007. RNA interference inhibition of matrix metalloproteinase-1 prevents melanoma metastasis by reducing tumor collagenase activity and angiogenesis. *Cancer Res* 67:10849-10858.

206. Lanone, S., Zheng, T., Zhu, Z., Liu, W., Lee, C.G., Ma, B., Chen, Q., Homer, R.J., Wang, J., Rabach, L.A., et al. 2002. Overlapping and enzyme-specific contributions of matrix metalloproteinases-9 and -12 in IL-13-induced inflammation and remodeling. *J Clin Invest* 110:463-474.

207. Ouyang, M., Lu, S., Li, X.Y., Xu, J., Seong, J., Giepmans, B.N., Shyy, J.Y., Weiss, S.J., and Wang, Y. 2008. Visualization of polarized membrane type

1 matrix metalloproteinase activity in live cells by fluorescence resonance energy transfer imaging. *J Biol Chem* 283:17740-17748.

208. Wolf, K., and Friedl, P. 2008. Mapping proteolytic cancer cell-extracellular matrix interfaces. *Clin Exp Metastasis* ePub DOI 10.1007/s10585-008-9190-2.

209. Filippov, S., Koenig, G.C., Chun, T.H., Hotary, K.B., Ota, I., Bugge, T.H., Roberts, J.D., Fay, W.P., Birkedal-Hansen, H., Holmbeck, K., et al. 2005. MT1-matrix metalloproteinase directs arterial wall invasion and neointima formation by vascular smooth muscle cells. *J Exp Med* 202:663-671.

210. Lee, H., Overall, C.M., McCulloch, C.A., and Sodek, J. 2006. A critical role for the membrane-type 1 matrix metalloproteinase in collagen phagocytosis. *Mol Biol Cell* 17:4812-4826.

211. Devy, L., Huang, L., Naa, L., Yanamandra, N., Pieters, H., Frans, N., Chang, E., Tao, Q., Pham, M., Vanhove, M., et al. 2009. Selective inhibition of matrix metalloproteinase-14 (MMP-14) blocks tumor growth, invasion and angiogenesis. *Cancer Research* in press.

212. Schafer, M., and Werner, S. 2008. Cancer as an overhealing wound: an old hypothesis revisited. *Nat Rev Mol Cell Biol* 9:628-638.

213. Mosesson, M.W. 2005. Fibrinogen and fibrin structure and functions. *J Thromb Haemost* 3:1894-1904.

214. Lanir, N., Ciano, P.S., Van de Water, L., McDonagh, J., Dvorak, A.M., and Dvorak, H.F. 1988. Macrophage migration in fibrin gel matrices. II. Effects of clotting factor XIII, fibronectin, and glycosaminoglycan content on cell migration. *J Immunol* 140:2340-2349.

215. Raeber, G.P., Lutolf, M.P., and Hubbell, J.A. 2005. Molecularly engineered PEG hydrogels: a novel model system for proteolytically mediated cell migration. *Biophys J* 89:1374-1388.

216. van Hinsbergh, V.W., and Koolwijk, P. 2008. Endothelial sprouting and angiogenesis: matrix metalloproteinases in the lead. *Cardiovasc Res* 78:203-212.

217. Hiraoka, N., Allen, E., Apel, I.J., Gyetko, M.R., and Weiss, S.J. 1998. Matrix metalloproteinases regulate neovascularization by acting as pericellular fibrinolysins. *Cell* 95:365-377.

218. Bugge, T.H., Kombrinck, K.W., Xiao, Q., Holmback, K., Daugherty, C.C., Witte, D.P., and Degen, J.L. 1997. Growth and dissemination of Lewis lung carcinoma in plasminogen-deficient mice. *Blood* 90:4522-4531.

219. Romer, J., Bugge, T.H., Pyke, C., Lund, L.R., Flick, M.J., Degen, J.L., and Dano, K. 1996. Impaired wound healing in mice with a disrupted plasminogen gene. *Nat Med* 2:287-292.

220. Green, K.A., Almholt, K., Ploug, M., Rono, B., Castellino, F.J., Johnsen, M., Bugge, T.H., Romer, J., and Lund, L.R. 2008. Profibrinolytic effects of

metalloproteinases during skin wound healing in the absence of plasminogen. *J Invest Dermatol* 128:2092-2101.

221. Schuster, V., Hugle, B., and Tefs, K. 2007. Plasminogen deficiency. *J Thromb Haemost* 5:2315-2322.

222. Plaisier, M., Kapiteijn, K., Koolwijk, P., Fijten, C., Hanemaaijer, R., Grimbergen, J.M., Mulder-Stapel, A., Quax, P.H., Helmerhorst, F.M., and van Hinsbergh, V.W. 2004. Involvement of membrane-type matrix metalloproteinases (MT-MMPs) in capillary tube formation by human endometrial microvascular endothelial cells: role of MT3-MMP. *J Clin Endocrinol Metab* 89:5828-5836.

223. Even-Ram, S., and Yamada, K.M. 2005. Cell migration in 3D matrix. *Curr Opin Cell Biol* 17:524-532.

224. Wall, S.J., Werner, E., Werb, Z., and DeClerck, Y.A. 2005. Discoidin domain receptor 2 mediates tumor cell cycle arrest induced by fibrillar collagen. *J Biol Chem* 280:40187-40194.

225. Taniwaki, K., Fukamachi, H., Komori, K., Ohtake, Y., Nonaka, T., Sakamoto, T., Shiomi, T., Okada, Y., Itoh, T., Itohara, S., et al. 2007. Stroma-derived matrix metalloproteinase (MMP)-2 promotes membrane type 1-MMP-dependent tumor growth in mice. *Cancer Res* 67:4311-4319.

226. Li, Y., Aoki, T., Mori, Y., Ahmad, M., Miyamori, H., Takino, T., and Sato, H. 2004. Cleavage of lumican by membrane-type matrix metalloproteinase-1 abrogates this proteoglycan-mediated suppression of tumor cell colony formation in soft agar. *Cancer Res* 64:7058-7064.

227. Golubkov, V.S., Boyd, S., Savinov, A.Y., Chekanov, A.V., Osterman, A.L., Remacle, A., Rozanov, D.V., Doxsey, S.J., and Strongin, A.Y. 2005. Membrane type-1 matrix metalloproteinase (MT1-MMP) exhibits an important intracellular cleavage function and causes chromosome instability. *J Biol Chem* 280:25079-25086.

228. Abd El-Aziz, S.H., Endo, Y., Miyamaori, H., Takino, T., and Sato, H. 2007. Cleavage of growth differentiation factor 15 (GDF15) by membrane type 1-matrix metalloproteinase abrogates GDF15-mediated suppression of tumor cell growth. *Cancer Sci* 98:1330-1335.

229. Butler, G.S., Dean, R.A., Tam, E.M., and Overall, C.M. 2008. Pharmacoproteomics of a metalloproteinase hydroxamate inhibitor in breast cancer cells: dynamics of membrane type 1 matrix metalloproteinase-mediated membrane protein shedding. *Mol Cell Biol* 28:4896-4914.

230. Su, G., Blaine, S.A., Qiao, D., and Friedl, A. 2008. Membrane type 1 matrix metalloproteinase-mediated stromal syndecan-1 shedding stimulates breast carcinoma cell proliferation. *Cancer Res* 68:9558-9565.

231. Tatti, O., Vehvilainen, P., Lehti, K., and Keski-Oja, J. 2008. MT1-MMP releases latent TGF-beta1 from endothelial cell extracellular matrix via proteolytic processing of LTBP-1. *Exp Cell Res* 314:2501-2514.

232. Cao, J., Chiarelli, C., Richman, O., Zarrabi, K., Kozarekar, P., and Zucker, S. 2008. Membrane type 1 matrix metalloproteinase induces epithelial-to-mesenchymal transition in prostate cancer. *J Biol Chem* 283:6232-6240.

233. Saeb-Parsy, K., Veerakumarasivam, A., Wallard, M.J., Thorne, N., Kawano, Y., Murphy, G., Neal, D.E., Mills, I.G., and Kelly, J.D. 2008. MT1-MMP regulates urothelial cell invasion via transcriptional regulation of Dickkopf-3. *Br J Cancer* 99:663-669.

234. Freudenberg, J.A., and Chen, W.T. 2007. Induction of Smad1 by MT1-MMP contributes to tumor growth. *Int J Cancer* 121:966-977.

235. Golubkov, V.S., Chekanov, A.V., Savinov, A.Y., Rozanov, D.V., Golubkova, N.V., and Strongin, A.Y. 2006. Membrane type-1 matrix metalloproteinase confers aneuploidy and tumorigenicity on mammary epithelial cells. *Cancer Res* 66:10460-10465.

236. Rozanov, D.V., Savinov, A.Y., Williams, R., Liu, K., Golubkov, V.S., Krajewski, S., and Strongin, A.Y. 2008. Molecular signature of MT1-MMP: transactivation of the downstream universal gene network in cancer. *Cancer Res* 68:4086-4096.

237. D'Alessio, S., Ferrari, G., Cinnante, K., Scheerer, W., Galloway, A.C., Roses, D.F., Rozanov, D.V., Remacle, A.G., Oh, E.S., Shiryaev, S.A., et al. 2008. Tissue inhibitor of metalloproteinases-2 binding to membrane-type 1 matrix metalloproteinase induces MAPK activation and cell growth by a non-proteolytic mechanism. *J Biol Chem* 283:87-99.

238. Nyalendo, C., Beaulieu, E., Sartelet, H., Michaud, M., Fontaine, N., Gingras, D., and Beliveau, R. 2008. Impaired tyrosine phosphorylation of membrane type 1-matrix metalloproteinase reduces tumor cell proliferation in three-dimensional matrices and abrogates tumor growth in mice. *Carcinogenesis* 29:1655-1664.

239. Coyle, R.C., Latimer, A., and Jessen, J.R. 2008. Membrane-type 1 matrix metalloproteinase regulates cell migration during zebrafish gastrulation: evidence for an interaction with non-canonical Wnt signaling. *Exp Cell Res* 314:2150-2162.

240. Blavier, L., Lazaryev, A., Dorey, F., Shackleford, G.M., and DeClerck, Y.A. 2006. Matrix metalloproteinases play an active role in Wnt1-induced mammary tumorigenesis. *Cancer Res* 66:2691-2699.

241. Ottaviano, A.J., Sun, L., Ananthanarayanan, V., and Munshi, H.G. 2006. Extracellular matrix-mediated membrane-type 1 matrix metalloproteinase expression in pancreatic ductal cells is regulated by transforming growth factor-beta1. *Cancer Res* 66:7032-7040.

242. Miyoshi, A., Kitajima, Y., Kido, S., Shimonishi, T., Matsuyama, S., Kitahara, K., and Miyazaki, K. 2005. Snail accelerates cancer invasion by upregulating MMP expression and is associated with poor prognosis of hepatocellular carcinoma. *Br J Cancer* 92:252-258.

243. Labbe, E., Lock, L., Letamendia, A., Gorska, A.E., Gryfe, R., Gallinger, S., Moses, H.L., and Attisano, L. 2007. Transcriptional cooperation between the transforming growth factor-beta and Wnt pathways in mammary and intestinal tumorigenesis. *Cancer Res* 67:75-84.

244. Bonnomet, A., Polette, M., Strumane, K., Gilles, C., Dalstein, V., Kileztky, C., Berx, G., van Roy, F., Birembaut, P., and Nawrocki-Raby, B. 2008. The E-cadherin-repressed hNanos1 gene induces tumor cell invasion by upregulating MT1-MMP expression. *Oncogene* 27:3692-3699.

245. Polette, M., Gilles, C., Nawrocki-Raby, B., Lohi, J., Hunziker, W., Foidart, J.M., and Birembaut, P. 2005. Membrane-type 1 matrix metalloproteinase expression is regulated by zonula occludens-1 in human breast cancer cells. *Cancer Res* 65:7691-7698.

246. Pei, D., and Weiss, S.J. 1995. Furin-dependent intracellular activation of the human stromelysin-3 zymogen. *Nature* 375:244-247.

247. Mayer, G., Boileau, G., and Bendayan, M. 2003. Furin interacts with proMT1-MMP and integrin alphaV at specialized domains of renal cell plasma membrane. *J Cell Sci* 116:1763-1773.

248. Bravo-Cordero, J.J., Marrero-Diaz, R., Megias, D., Genis, L., Garcia-Grande, A., Garcia, M.A., Arroyo, A.G., and Montoya, M.C. 2007. MT1-MMP proinvasive activity is regulated by a novel Rab8-dependent exocytic pathway. *Embo J* 26:1499-1510.

249. Sakurai-Yageta, M., Recchi, C., Le Dez, G., Sibarita, J.B., Daviet, L., Camonis, J., D'Souza-Schorey, C., and Chavrier, P. 2008. The interaction of IQGAP1 with the exocyst complex is required for tumor cell invasion downstream of Cdc42 and RhoA. *J Cell Biol* 181:985-998.

250. Guegan, F., Tatin, F., Leste-Lasserre, T., Drutel, G., Genot, E., and Moreau, V. 2008. p190B RhoGAP regulates endothelial-cell-associated proteolysis through MT1-MMP and MMP2. *J Cell Sci* 121:2054-2061.

251. Steffen, A., Le Dez, G., Poincloux, R., Recchi, C., Nassoy, P., Rottner, K., Galli, T., and Chavrier, P. 2008. MT1-MMP-Dependent Invasion Is Regulated by TI-VAMP/VAMP7. *Curr Biol* 18:926-931.

252. Wu, Y.I., Munshi, H.G., Sen, R., Snipas, S.J., Salvesen, G.S., Fridman, R., and Stack, M.S. 2004. Glycosylation broadens the substrate profile of membrane type 1 matrix metalloproteinase. *J Biol Chem* 279:8278-8289.

253. Sohail, A., Sun, Q., Zhao, H., Bernardo, M.M., Cho, J.A., and Fridman, R. 2008. MT4-(MMP17) and MT6-MMP (MMP25), A unique set of membrane-anchored matrix metalloproteinases: properties and expression in cancer. *Cancer Metastasis Rev* 27:289-302.

254. O'Reilly, P.J., Gaggar, A., and Blalock, J.E. 2008. Interfering with extracellular matrix degradation to blunt inflammation. *Curr Opin Pharmacol* 8:242-248.

Chapter 2: Hepatocyte Snail1 Drives Liver Fibrogenesis

Introduction.

Plasticity of the epithelial phenotype is an absolute requirement for tissue morphogenesis within complex organisms (1, 2). Epithelial-mesenchymal transition (EMT) is one mechanism whereby epithelial cells shed differentiated characteristics such as homotypic adhesion and apicobasal polarity, coincident with the acquisition of mesenchymal or fibroblast traits, including multipolar shape, expression of interstitial extracellular matrix proteins, motility, and tissue invasion (1, 2). Though required for embryological development, morphogenetic EMT programs may be reactivated postnatally to induce epithelial transitions in disease states (2). Indeed, recent data suggest that mature epithelial cells engage EMT to generate significant numbers of fibroblasts that overpopulate the interstitial compartment during organ fibrogenesis, contributing to loss of tissue architecture and consequent physiologic dysfunction (3, 4).

A small group of transcriptional repressors – including members of the Snail and ZEB families – serves required functions in both developmental - and possibly pathologic - EMT (5, 6). One such member, Snail1, directly represses the homotypic cell:cell adhesion molecule E-cadherin in epithelial cells during gastrulation, and triggers the activation of genetic programs that govern the tissue-invasive processes characteristic of mesenchymal differentiation (7-10). Though not normally expressed in mature tissues, Snail1 is re-activated in a variety of pathologic conditions, including neoplasia and tissue fibrosis, where its expression is observed in transitioning epithelia (8-14). However, whether Snail serves an intravital role in EMT-associated events that arise during fibrogenesis remains unknown. Herein, we demonstrate that Snail1 is expressed in

hepatocytes during liver fibrogenesis *in vivo* where it plays a key role during liver fibrosis by serving as a critical mediator of hepatocyte EMT as well as associated inflammatory processes. The data provide the first evidence that Snail1 plays a required role in promoting EMT during fibrogenesis *in vivo*.

Materials and Methods.

Mice. To generate the *Snai1* conditional knockout mouse, a targeting vector was constructed consisting of an FRT-flanked PGK-neo cassette 3' to the loxp-flanked exon 3 of mouse *Snai1* (Figure 2.3). Approximately 4 kb of flanking genomic sequence was then inserted 5' and 3' of these sequences to promote homologous recombination. The linearized targeting vector was electroporated into W4 embryonic stem cells (15), and stable transfected clones were selected with G418. Clones were screened for targeting of the *Snai1* by Southern blotting, and recombination verified at both the 5' and 3' ends of the construct. Of 100 clones screened, 3 were identified with correct targeting and used for injection into C57BL/6NCrl x (C57BL/6J x DBA/2J)F1 blastocysts to produce chimeric mice. Out of three chimeric lines produced, two lines transmitted the targeted *Snai1* allele (*Snai1*^{tm1Stjw}) through the germline. Beta-actin FLPe mice (Jackson Laboratories Stock no. 003800) were backcrossed (> 10 generations) to C57BL/6J mice to generate a congenic strain prior to mating with chimeras for excision of the FRT-flanked PGK-neo cassette to generate the *Snai1*^{fl} (*Snai1*^{tm2Stjw}) allele. Albumin-Cre transgenic mice and R26R mice (*Gtrosa26*^{tm1Sor}) were obtained from Jackson Laboratories.

Model of liver fibrosis. Six week-old male mice were injected in the peritoneum with a 20% solution of carbon tetrachloride (CCl_4) in sterile mineral oil (4). Mice received a dose of 2.5 ml CCl_4 per kilogram body weight twice per week for two weeks. Mice were euthanized 72 hours after the final injection. Serum was collected by cardiac puncture. Trichrome-stained liver tissue was scored for liver fibrosis by a blinded investigator, with at least five random fields scored and averaged.

Tissue analysis. For the Masson trichrome and Sirius red stains, tissues were fixed in 4% paraformaldehyde and paraffin embedded, sectioned, and stained. For immunofluorescent staining of tissue, fresh liver tissue was frozen in OCT and sectioned, fixed with acetone at -20° for 10 minutes, blocked, and primary antibodies applied overnight. Tissue was then washed with phosphate buffered saline (PBS), the secondary antibody applied for 1-2 hours at room temperature

with TOTO-3 counterstain (Invitrogen), washed with PBS, and mounted. Antibodies used were: rabbit anti-Snail1 (10), rabbit anti-FSP1 (16), mouse anti-albumin (R and D systems), rabbit anti-collagen I (Abcam), rat anti-CD11b (Serotech) or goat anti-collagen III (Southern Biotechnology). Apoptosis was analyzed with the Roche in situ fluorescein cell death detection kit (Roche Diagnositcs).

Microscopy and image analysis. Confocal images of cells were acquired on an Olympus FV500 confocal microscope using a 60X water immersion lens with a 1.20 numerical aperture using Fluoview software (Olympus). Collagen deposition was measured by analyzing raw images with MetaMorph software (Molecular Devices).

Microarray analysis of gene expression. Labeled cRNA isolated from three mice for each treatment condition (WT and CKO mice with and without CCl_4 treatment) was hybridized to mouse 430 2.0 arrays (Affymetrix). Probe signals were transformed to expression values for each gene. Expression values were averaged within each treatment group. When comparing treatment groups, differentially expressed genes were selected with a fold change cutoff of 2.0 and a *P* value less than 0.05.

Hepatocyte isolation and culture. Livers were isolated from 6-8 week old male mice, minced, and digested in 0.5 mg/ml collagenase type I (Worthington). The cell suspension was filtered through a 100 μm pore, cells were washed, and plated on Matrigel (BD Biosciences) with F-12/DMEM 1:1 with 10% fetal bovine serum supplemented with insulin. In some experiments, cells were treated with 3 ng/ml recombinant human $TGF\beta_1$ (R and D Systems). To analyze protein expression, cells were immunostained with mouse monoclonal antibodies against Snail1 (8), or E-cadherin (Zymed Laboratories).

Results.

Snail1 is expressed in hepatocytes during liver fibrogenesis. To determine the relative functions of Snail1 and other EMT-inducing transcription factors during tissue fibrogenesis *in vivo*, a validated model of hepatic fibrosis was employed wherein mice are chronically treated with carbon tetrachloride (CCl_4). Following two weeks of exposure to CCl_4, the expression of *Snai1* is significantly elevated as assessed by quantitative RT-PCR (qRT-PCR) with a concomitant although lesser degree of induction of the Zeb family member, *Zeb2*, with no significant activation of *Snai2* or *Zeb1* (Figure 2.1A). To determine if hepatocytes increase the expression of Snail1 protein during fibrogenesis, uninjured and fibrotic tissues were double-immunostained with a Snail1-specific monoclonal antibody as well as an antibody against albumin to identify hepatocytes. In accordance with the hypothesis that hepatocytes activate EMT programs during liver fibrogenesis (4, 11), a strong induction of nuclear Snail1 expression is observed in the albumin-positive hepatocytes of fibrotic livers as compared to uninjured tissue (Figure 2.1B), in a fashion analogous to that observed in fibrotic human livers (11).

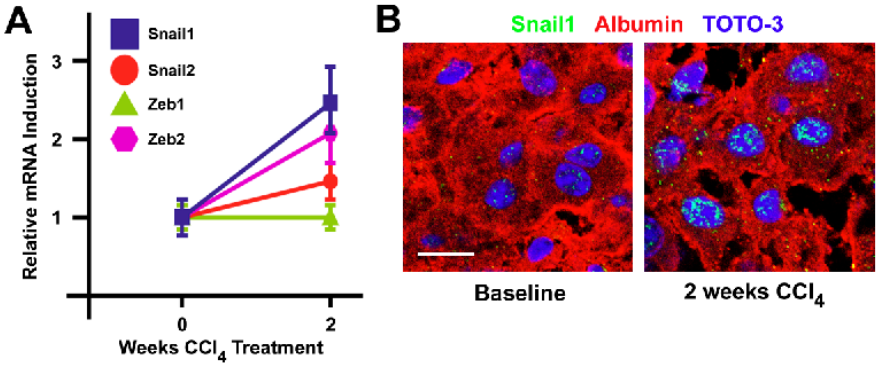

Figure 2.1. Analysis of EMT-inducing transcription factor expression during liver fibrogenesis

A. RNA was extracted from uninjured livers or from livers from mice treated with CCl_4 for two weeks. Levels of transcripts for Snail1, Snail2, Zeb1, and Zeb2 were analyzed by quantitative RT-PCR (qRT-PCR). **B.** Livers were isolated from uninjured mice or mice treated with CCl_4 for two weeks. Tissue was sectioned and co-immunostained with antibodies against albumin (red) and Snail1 (green). Nuclei were counterstained with TOTO-3 (blue; scale = 20 μm).

CCl_4 induces hepatic fibrosis through a process dependent on transforming growth factor β_1 (TGFβ_1), a potent EMT driver that induces *Snai1* expression in hepatocytes (17-20). To further verify the capacity of hepatocytes to activate Snail1 under fibrogenic conditions, mouse liver hepatocytes were isolated and incubated alone or with TGFβ_1 for 4 d. Under these conditions, TGFβ_1 treatment results in a marked induction of mRNA encoding *Snai1* mRNA as well as the accumulation of Snail1 protein in the nucleus (Figure 2.2C). Taken together, these results indicate that hepatocytes possess the capacity to reactivate Snail, raising the possibility that Snail1 mediates hepatocyte EMT during liver fibrosis.

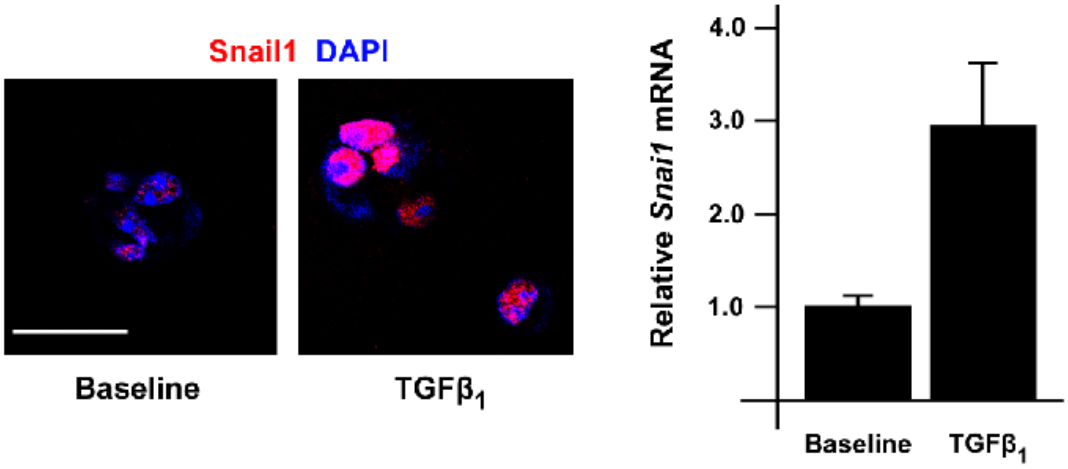

Figure 2.2. Snail1 is activated in hepatocytes in response to fibrogenic stimuli

(Left panels) Hepatocytes were isolated from wild-type mice and treated with or without 3 ng/ml recombinant TGFβ_1 for 4 days, at which time cells were immunostained for Snail1 (red). Nuclei were counterstained with DAPI (scale = 30 μm). (Right panels) RNA was isolated from hepatocytes and Snail1 mRNA levels measured by qRT-PCR.

Hepatocyte-specific ablation of the *Snai1* gene. To determine whether hepatocyte Snail1 serves a pro-fibrogenic role *in vivo*, we employed a recently characterized allele of mouse *Snai1* wherein the function of the *Snai1* gene is inactivated by Cre recombinase-mediated loss of loxp sites flanking the third exon of *Snai1* (*Snai1*^{loxp}; Figure 2.3, 2.4A) (8).

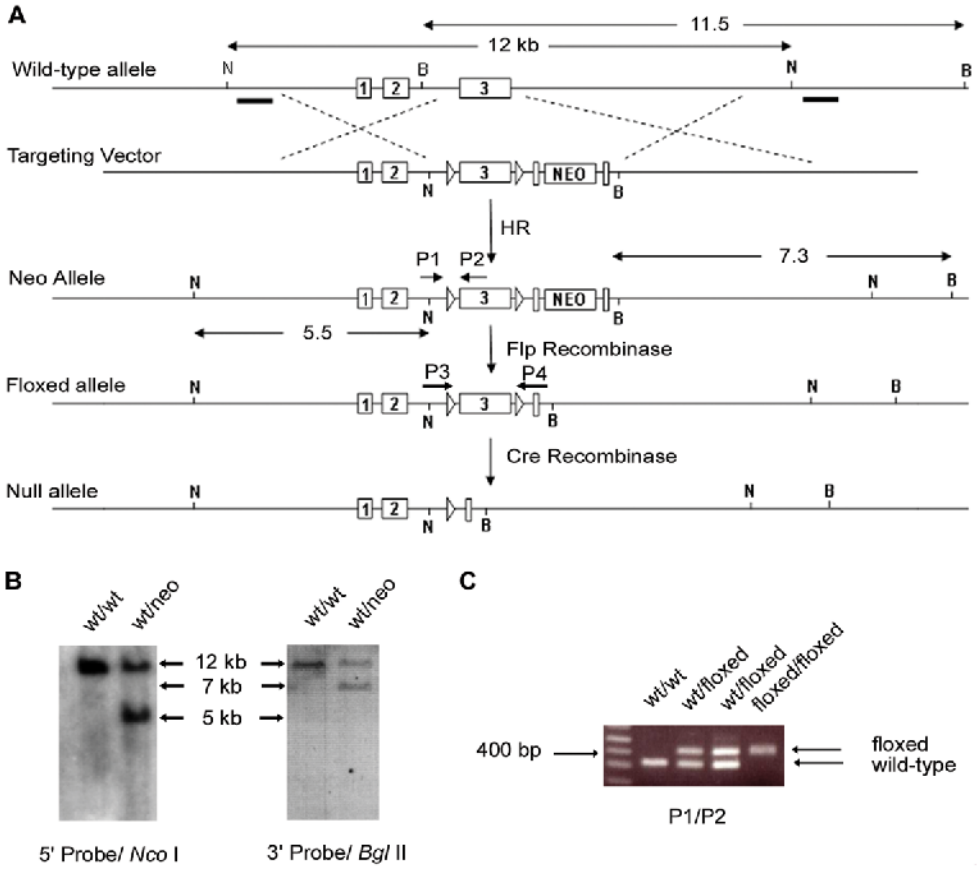

Figure 2.3. Targeting Snai1

A. Targeting schematic. A vector was constructed containing the third exon of Snail1 flanked by loxp sites. Four kilobases of upstream and downstream flanking sequences were inserted 5' and 3' to this cassette, respectively. **B.** The linearized targeting vector was transfected into embryonic stem cells, and stable transfectants screened for recombination with the indicated restriction endonucleases and probes. **C.** Example genotyping data demonstrating isolation of *Snai1*$^{fl/fl}$ adults.

To inactivate *Snai1* specifically in hepatocytes, the *Snai1*^{loxp} strain was bred with mice carrying the *Alb-Cre* transgene, where Cre recombinase is expressed under the control of the hepatocyte-specific *Albumin* promoter to generate *Alb-Cre*; *Snai1*$^{loxp/loxp}$ mice (hereafter termed CKO; Figure 2.4A)(21). Compared to wild-type (WT) littermates (*Snai1*$^{loxp/loxp}$), CKO mice are viable, display no overt defects, and survive up to six months with no ill effects (data not shown).

Following a two-week course of CCl_4 treatment, Snail1 protein is detected in the nucleus of hepatocytes of WT littermates, but not in CKO mice, confirming efficient hepatocyte-specific recombination of the *Snai1*^{loxp} allele (Figure 2.4B). CKO mice were then bred to the *Rosa26*-loxp-STOP-loxp-*lacZ* (*R26R*) reporter strain, wherein cells expressing Cre recombinase activity also excise the loxp-flanked DNA STOP sequence cassette in this allele to express β-galactosidase in cells containing the functional *Alb-Cre* transgene (Figure 2.4C). Staining of liver tissue from *Alb-Cre*; *Snai1*$^{loxp/loxp}$; *R26R* mice and control littermates reveal β-galactosidase activity in all hepatocytes, demonstrating that livers of CKO mice are not composed of Snail1-positive hepatocyte subpopulations with ineffective Cre-mediated recombination selected during liver development. That Snail1-deficient hepatocytes differentiate and function equivalently to WT littermates (Figure 2.4D) suggests that Snail1 is not necessary for organ expansion once primary liver tissue is formed.

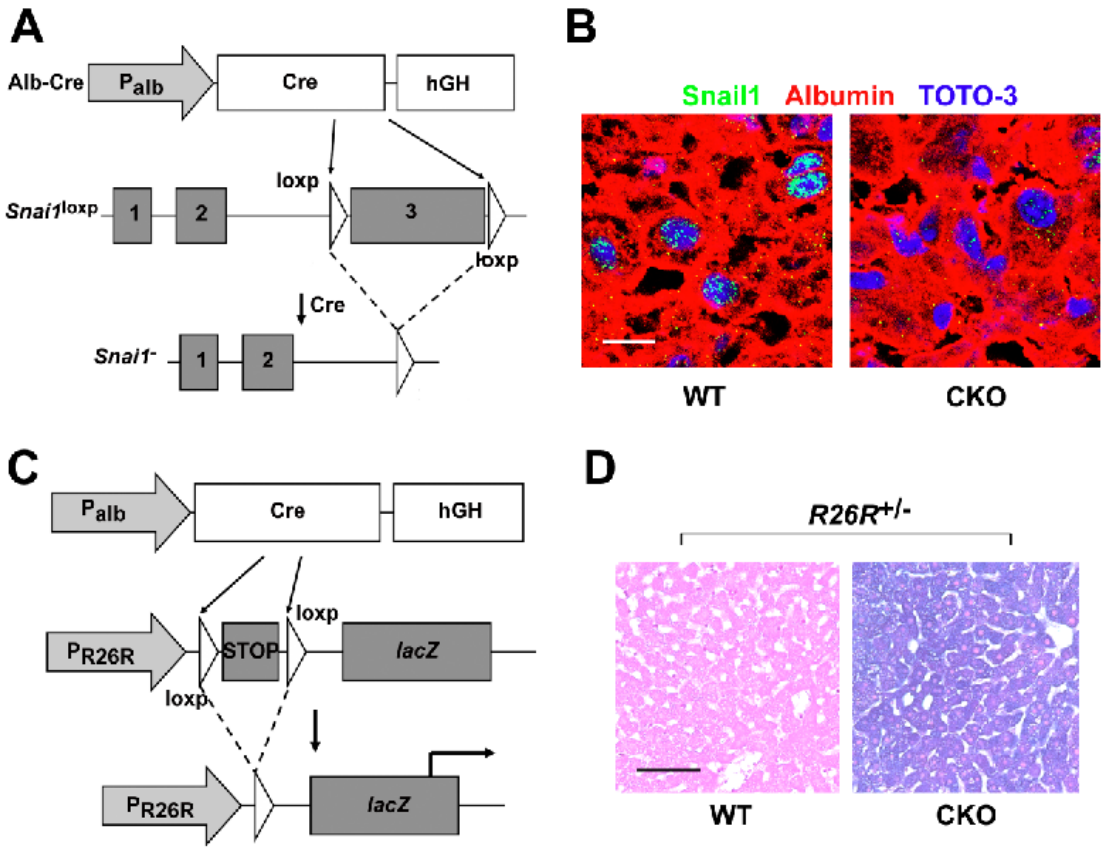

Figure 2.4. Hepatocyte-specific Snai1 deletion.

A. Mice carrying the *Snai1*^{fl} allele were bred with mice carrying the hepatocyte-specific Cre transgene, albumin-Cre (Alb-Cre). **B.** Liver tissue was isolated from *Snai1*$^{fl/fl}$ mice or Alb-Cre; *Snai1*$^{fl/fl}$ mice and co-immunostained with antibodies against albumin (red) and Snail1 (green), with nuclei counterstained with TOTO-3 (blue; scale = 20 μm). **C.** CKO mice were bred to the *R26R* reporter strain such that Albumin-Cre transgene activity would result in recombination of the loxp-flanked STOP cassette in the *R26R* allele, allowing *lacZ* gene expression and β-galactosidase activity in hepatocytes. **D.** Liver tissue was isolated from *R26R*$^{+/-}$; *Snai1*$^{loxp/loxp}$ mice with or without the Albumin-Cre transgene. Whole tissue was stained for β-galactosidase activity (blue staining), sectioned, and counterstained with eosin followed by examination by light microscopy. Scale = 50 μm.

Snail1 is required for the progression of liver fibrosis. As hepatocyte Snail1-deficient CKO mice are viable with no apparent defects, 6 week-old CKO mice and WT littermates were challenged with CCl_4. After treatment, livers were removed, sectioned, and processed for histopathological analysis or immunofluorescence microscopy. Whereas uninjured WT and CKO livers are morphologically identical, CCl_4-treated WT livers exhibited marked deposition of periportal and interlobular extracellular matrix fibrils (ECM) rich in collagen types I and III. Remarkably, this pathologic change is significantly attenuated in CCl_4-treated CKO livers (Figure 2.5A,B). Using validated criteria to quantify pathologic progression of liver fibrosis where a score of zero corresponds to a healthy liver, fibrosis is significantly reduced in CKO mice compared to WT littermates following CCl_4 treatment (WT 1.6 ± 0.2, CKO 0.8 ± 0.2; $P = 0.003$) (Figure 2.5A,C) (22), with no observed differences in hepatocyte apoptosis (data not shown). Since liver fibrosis is associated with chronic inflammation and massive influx of bone marrow-derived cells (23), hematoxylin and eosin-stained tissues were examined for inflammatory cell infiltration. The fibrotic interstitium of CCl_4-treated WT livers contain multinucleated macrophage giant cells, while CKO livers display an altered pattern of inflammation, limited to isolated clusters of mononuclear cells (Figure 2.5D). Accordingly, immunostaining for CD11b, a marker of monocytes and macrophages, reveals higher immunoreactivity in WT livers (25 ± 7 CD11b-positive cells per 60X field in WT versus 13 ± 2 cells in CKO mice; Figure 2.5D).

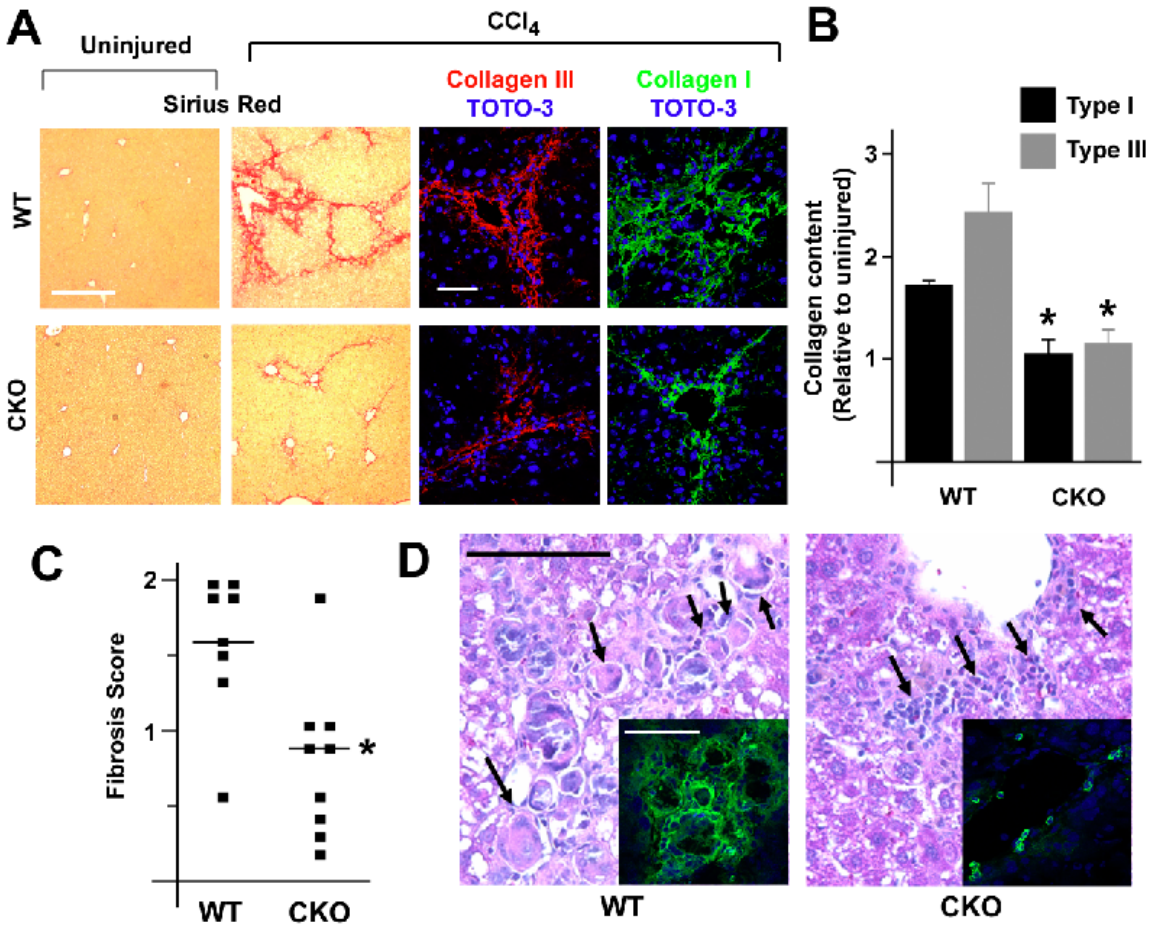

Figure 2.5. Hepatocyte Snail1 is required for efficient liver fibrogenesis.

A. Wild-type or CKO mice were treated with CCl_4 for two weeks, at which time liver tissue was isolated. Tissue was stained with Sirius red (left panels; scale = 200 μm), or immunostained for collagens III (red, middle panels) or I (green, right panels; scale = 50 μm) with TOTO-3 counterstaining. **B.** Induction of collagens I and III deposition versus uninjured liver was quantified by morphometric analysis (* $P < 0.05$). **C.** Scatter plot demonstrating distribution of fibrosis scores for each genotype (* $P = 0.003$). **D.** Hematoxylin and eosin-stained tissues from WT and CKO CCl_4-treated mice were examined to assess immune cell infiltration. Arrows indicate multinucleated giant cells in WT tissue (left) and mononuclear cell infiltrates in CKO tissue (right; scale = 50 μm)). (Insets) Tissues were stained for CD11b (green) and counterstained with TOTO-3 (blue; scale = 50 μm).

To further assess the role of hepatocyte Snail1 in liver fibrosis, mRNA from liver tissue was hybridized to cDNA microarrays for global analysis of gene expression. Compared to uninjured livers of the corresponding genotype, CCl_4-treated WT livers display significant changes in 846 unique genes (using a

significance cutoff of $P = 0.05$ with a minimum two-fold change in signal in KO versus WT). In WT livers, gene ontology (GO) analysis of altered transcripts reveal highly significant enrichment for biologic processes related to the immune response ($P = 0.00003$) and inflammation ($P = 0.000001$). In contrast, CKO livers display alterations in 487 transcripts versus genotype-matched uninjured livers in response to CCl_4, with a 2-3 log decrease in enrichment of GO terms related to immunity ($P = 0.001$) or inflammation ($P = 0.005$), consistent with the attenuated inflammatory response observed in these tissues (Figure 2.5D). Importantly, no significant differences in probe signal are observed between uninjured livers from WT and CKO mice. Analysis of a panel of genes known to contribute to the progression of liver fibrosis, including interstitial collagen types I and III (*Col1a1*, *Col1a2*, *Col3a1*), fibroblast markers (fibroblast-specific protein-1 (*FSP1; S100a4*), *Vimentin, and CD44*), signaling receptors (platelet-derived growth factor receptor β (*Pdgfbr*), leptin receptor (*Lpr*)), proteases (membrane-type I matrix metalloproteinase (*Mmp14*), cathepsin B (*Ctsb*)), soluble pro-fibrogenic signals (connective tissue growth factor (*Ctgf*)), and inflammatory effectors of oxidative stress (*Ncf1* and *Ncf2* subunits of NADPH oxidase) (4, 11, 23-27), reveal a stronger induction of these transcripts in response to CCl_4 in WT livers relative to CKO livers (Figure 2.6A). A compensatory induction of other EMT-inducing transcriptional repressors in fibrotic CKO livers is not observed under these conditions (Figure 2.6B). Taken together, these data support the proposition that hepatocyte Snail1 drives the progression of hepatic fibrosis.

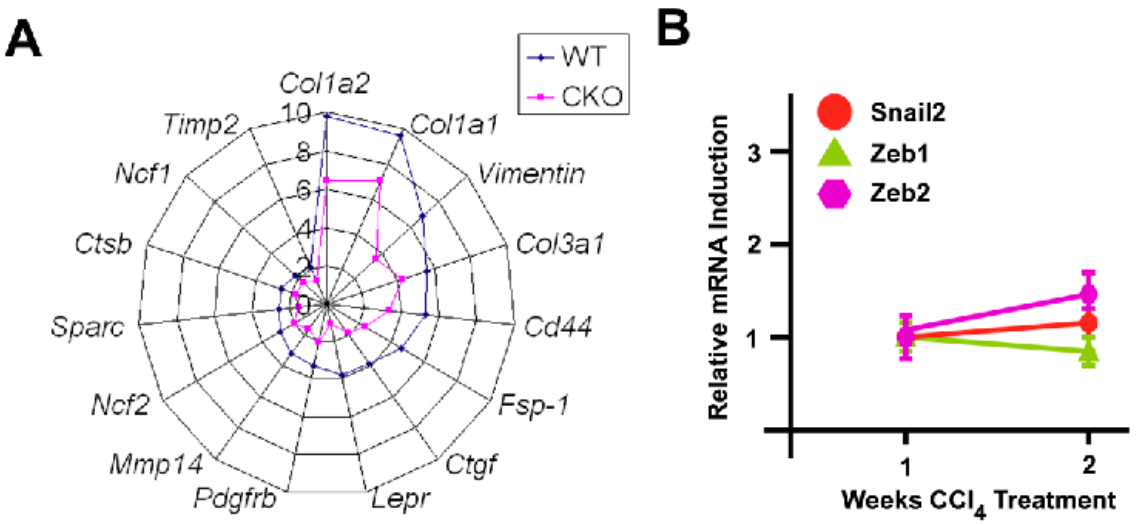

Figure 2.6. Snail1 drives pro-fibrogenic gene expression programs.

A. RNA was isolated from uninjured livers or from livers from mice treated with CCl_4 for two weeks. RNA was labeled and hybridized to Affymetrix microarrays for analysis of gene expression. Expression levels of a panel of genes associated with liver fibrosis are presented. **B.** Levels of mRNAs for Zeb1, Zeb2, and Snail1 were measured in uninjured CKO livers and in CKO livers treated with CCl_4 for two weeks.

Potential role for Snail1 in promoting hepatocyte EMT. Though the expression of Snail1 is required for efficient hepatic fibrogenesis, the mechanism by which Snail1 modulates fibrosis is unclear. To investigate hepatocyte EMT as a potential mechanism, we utilized a validated lineage tracing methodology whereby tissues are simultaneously immunostained with antibodies against a markers specific for both differentiated epithelial cells and fibroblasts to identify cells undergoing EMT, including those populations displaying an active 'transition state' wherein both epithelial and fibroblast markers are co-expressed (4, 28). Histologic sections of livers were double immunostained with antibodies specific for albumin (a marker of differentiated hepatocytes) and FSP1 (a marker of fibroblasts (16, 29)). Consistent with the observation that hepatocytes undergo EMT during liver fibrosis (4), we identified FSP1/albumin double-positive cells in CCl_4-treated, but not uninjured, WT livers (Figure 2.7A,B). Strikingly, in CCl_4-treated CKO livers, we observed significantly fewer FSP1/albumin double-positive cells, suggesting that Snail1-deficient hepatocytes are resistant to

fibrogenic EMT (Figure 2.7A,B). Furthermore, confirming our microarray data, CKO livers exhibit an attenuated induction of mRNAs encoding FSP1 in response to CCl_4 compared to WT livers (Figure 2.7C).

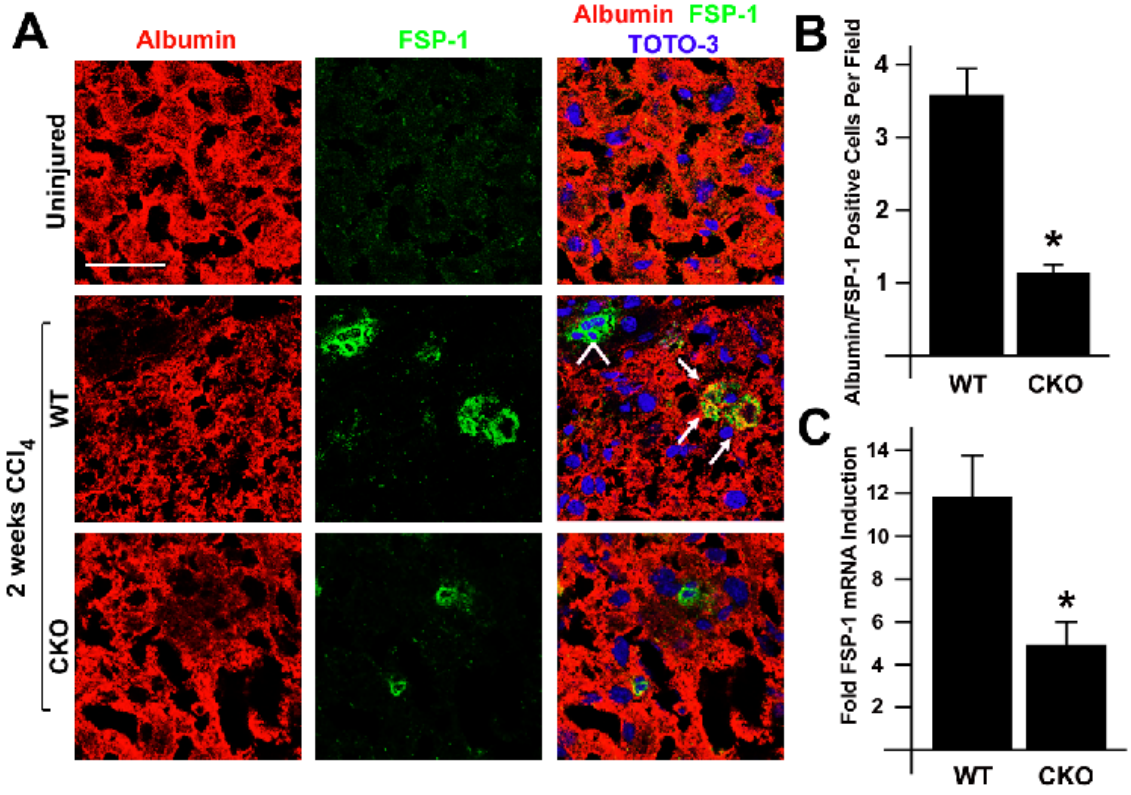

Figure 2.7. Potential role for Snail1 in mediating hepatocyte EMT during liver fibrogenesis in vivo.

A. Liver tissue was isolated from uninjured mice (top panels), wild-type mice treated with CCl_4 for two weeks (middle panels), or CKO mice treated with CCl_4 for two weeks (bottom panels). Frozen sections were co-immunostained with antibodies against albumin (red) and FSP1 (also known as S100A4; green), and nuclei were counterstained with TOTO-3. Albumin/FSP1 double-positive cells are indicated by arrowheads. Albumin-negative, FSP1-positive stellate cells are indicated by an arrowhead (blue; scale = 50 μm). **B.** The number of albumin/FSP1 double-positive cells per field was quantified (* P = 0.001). **C.** Fold-FSP1 mRNA induction in whole liver tissue (versus uninjured tissue of the corresponding genotype) was analyzed by qRT-PCR (* P = 0.02).

To further verify this proposed role for Snail1 in hepatocyte EMT during *in vivo* fibrogenesis, we isolated *Snai1*$^{loxp/loxp}$ hepatocytes and recombined the *Snai1*^{loxp} allele *in vitro* by transduction with an adenovirus carrying a cassette for

expression of Cre recombinase (adeno-Cre). Snail1 inactivation in hepatocyte cultures was verified by immunocytochemistry (Figure 2.8A). Whereas treatment of control (β-galactosidase (β-gal)) adenovirus infected-hepatocytes with TGFβ$_1$ results in a marked reduction of expression of the direct Snail1 target E-cadherin at the mRNA and protein levels, adeno-Cre-infected cells were unable to effectively silence E-cadherin expression with persistence of E-cadherin protein and message following TGFβ$_1$ treatment (Figure 2.8A,B), indicating that Snail1 plays a key role in mediating the proximal transcriptional changes that occur during hepatocyte EMT.

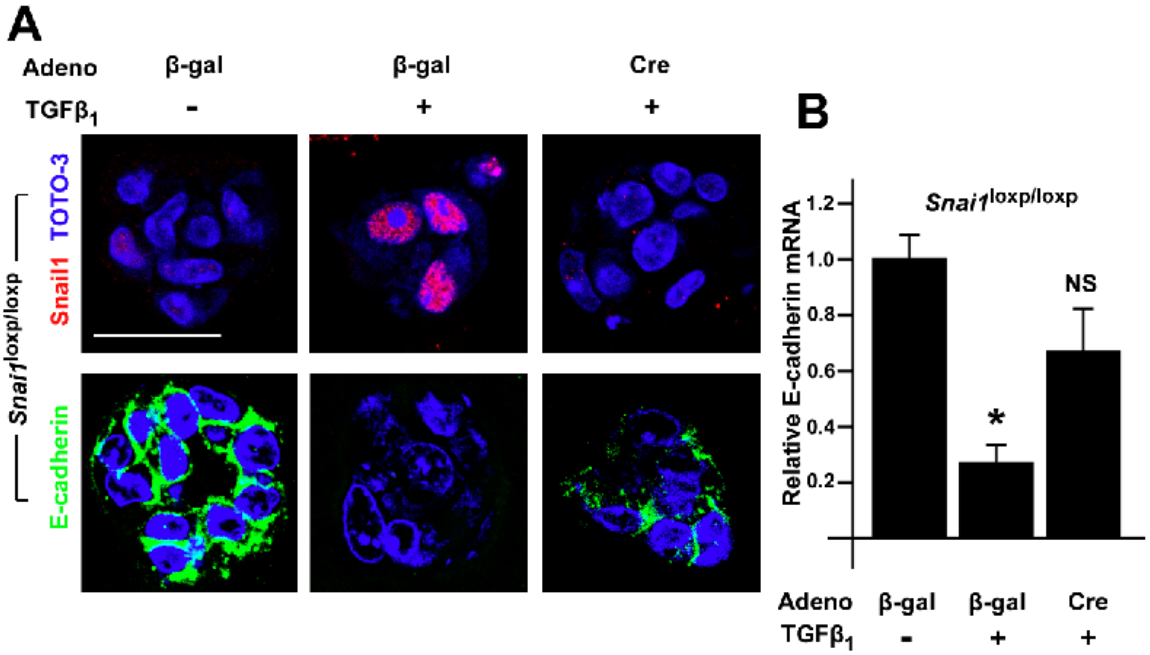

Figure 2.8. Snail1 regulates hepatocyte EMT.

A. *Snai1*$^{fl/fl}$ hepatocytes were infected either with a control adenovirus (β-gal) or a Cre adenovirus, and treated with or without 3 ng/ml TGFβ$_1$ for 4 days. Snail1 (red, upper panels) and E-cadherin (green, lower panels) protein expression was analyzed by immunofluorescent microscopy. Nuclei were counterstained with TOTO-3 (blue; scale = 30 μm). **B.** E-cadherin mRNA levels were analyzed by qRT-PCR (right panel) (* P < 0.0001; NS = not significant compared to adeno-β-gal without TGF β$_1$).

Discussion.

Snail factors have been implicated as central regulators of the transcriptional programs governing repression of the epithelial phenotype and engagement of fibroblastic traits (1, 5). Although a required role for Snail1-mediated EMT has been identified during development (7, 28, 30), studies focusing on diseases wherein Snail1-mediated EMT is prevented by deletion at the *Snai1* locus have not been described, with efforts to date confined to a single transgenic model of kidney-specific Snail1 overexpression (28). Recent work has identified EMT as a regulator of fibroblast abundance during tissue fibrogenesis (3, 4), and, consistent with this proposition, we observed a role for Snail1 in induction of FSP1 in hepatocytes as well as the loss of the epithelial adherens junction protein, E-cadherin. Though these results support the notion that hepatocyte reactivation of Snail1 is a central mechanism underlying fibrosis progression, the co-induction of the EMT-promoting factor, Zeb2, is also observed along with the recruitment of Snail1 during fibrosis *in vivo*. Zeb2 is a required mediator of neural crest EMT during development in humans and mice (31, 32), and its co-induction during CCl_4 treatment suggests a potential functional redundancy of these two factors during liver fibrogenesis. Interestingly, following Snail1 deletion, the reduction in fibrosis occurs in tandem with a loss of CCl_4-induced Zeb2 induction. As Snail1 has recently been characterized as a positive, post-transcriptional regulator of mRNA expression encoding Zeb2 (33), these data suggest that Snail1 acts as a proximal transcriptional and post-transcriptional regulator of Zeb2 activity during hepatocyte EMT.

Recent studies propose that approximately 30% of interstitial fibroblasts appear as a result of hepatocyte EMT (4). However, in our study, Snail1 deletion in hepatocytes attenuated fibrosis by 40-60%; a stronger effect than expected if Snail1 acts exclusively as a regulator of hepatocyte phenotype. In addition to hepatocyte EMT, other sources of overabundant myofibroblast-like cells in liver fibrosis have been identified, including the bone marrow, vascular pericytes, and activated hepatic stellate cells (23, 34, 35). Since the singular deletion of Snail1 in hepatocytes exerts wide-ranging effects on the pathobiology of hepatic

fibrosis, it is intriguing to speculate that hepatocyte Snail1 provides additional instructions during fibrogenesis, perhaps through control of paracrine signals that regulate fibrogenesis in non-hepatocyte cell populations. Indeed, histologic analyses, coupled with GO analysis of differentially expressed transcripts in whole liver tissue, demonstrate an attenuated CCl_4-induced inflammatory response in the absence of hepatocyte Snail1. As Snail1 acts as a regulator of global genetic programs apart from those directly related to EMT (8), including the immune response (36), we envision a model wherein Snail1-dependent EMT engages genetic programs in nascent transitioning hepatocytes that collaborate to promote further fibroblast accumulation and recruitment of inflammatory cells through the release of soluble signals, including CTGF, PDGF, and $TGF\beta_1$ family members (11, 20, 23, 25). Further, the recent observation that selective depletion of CD11b-positive macrophage populations in the liver confers a resistance to CCl_4-induced fibrosis (37) suggests that Snail1's pro-fibrogenic effects is mediated in part through recruitment and activation of mononuclear cells. Taken together, these results provide the first *in vivo* evidence of the required role for Snail1 in the evolution of EMT-associated pathology, and indicate that hepatocyte Snail1 acts as a proximal regulator of multiple phases of liver fibrosis.

References.

1. Kalluri, R., and E.G. Neilson. 2003. Epithelial-mesenchymal transition and its implications for fibrosis. *J Clin Invest* 112:1776-1784.

2. Neilson, E.G. 2006. Mechanisms of disease: Fibroblasts--a new look at an old problem. *Nat Reviews Nephrol* 2:101-108.

3. Iwano, M., D. Plieth, T.M. Danoff, C. Xue, H. Okada, and E.G. Neilson. 2002. Evidence that fibroblasts derive from epithelium during tissue fibrosis. *J Clin Invest* 110:341-350.

4. Zeisberg, M., C. Yang, M. Martino, M.B. Duncan, F. Rieder, H. Tanjore, and R. Kalluri. 2007. Fibroblasts derive from hepatocytes in liver fibrosis via epithelial to mesenchymal transition. *J Biol Chem* 282:23337-23347.

5. Peinado, H., D. Olmeda, and A. Cano. 2007. Snail, Zeb and bHLH factors in tumour progression: an alliance against the epithelial phenotype? *Nat Rev Cancer* 7:415-428.

6. Lee, J.M., S. Dedhar, R. Kalluri, and E.W. Thompson. 2006. The epithelial-mesenchymal transition: new insights in signaling, development, and disease. *J Cell Biol* 172:973-981.

7. Carver, E.A., R. Jiang, Y. Lan, K.F. Oram, and T. Gridley. 2001. The mouse snail gene encodes a key regulator of the epithelial-mesenchymal transition. *Mol Cell Biol* 21:8184-8188.

8. Rowe, R.G., X.Y. Li, Y. Hu, T.L. Saunders, I. Virtanen, A. Garcia de Herreros, K.F. Becker, S. Ingvarsen, L.H. Engelholm, G.T. Bommer, E.R. Fearon, and S.J. Weiss. 2009. Mesenchymal cells reactivate Snail1 expression to drive three-dimensional invasion programs. *J Cell Biol* 184:399-408.

9. Yook, J.I., X.Y. Li, I. Ota, E.R. Fearon, and S.J. Weiss. 2005. Wnt-dependent regulation of the E-cadherin repressor snail. *J Biol Chem* 280:11740-11748.

10. Yook, J.I., X.Y. Li, I. Ota, C. Hu, H.S. Kim, N.H. Kim, S.Y. Cha, J.K. Ryu, Y.J. Choi, J. Kim, E.R. Fearon, and S.J. Weiss. 2006. A Wnt-Axin2-GSK3beta cascade regulates Snail1 activity in breast cancer cells. *Nat Cell Biol* 8:1398-1406.

11. Dooley, S., J. Hamzavi, L. Ciuclan, P. Godoy, I. Ilkavets, S. Ehnert, E. Ueberham, R. Gebhardt, S. Kanzler, A. Geier, K. Breitkopf, H. Weng, and P.R. Mertens. 2008. Hepatocyte-specific Smad7 expression attenuates TGF-beta-mediated fibrogenesis and protects against liver damage. *Gastroenterology* 135:642-659.

12. Franci, C., M. Takkunen, N. Dave, F. Alameda, S. Gomez, R. Rodriguez, M. Escriva, B. Montserrat-Sentis, T. Baro, M. Garrido, F. Bonilla, I. Virtanen, and A. Garcia de Herreros. 2006. Expression of Snail protein in tumor-stroma interface. *Oncogene* 25:5134-5144.

13. Cano, A., M.A. Perez-Moreno, I. Rodrigo, A. Locascio, M.J. Blanco, M.G. del Barrio, F. Portillo, and M.A. Nieto. 2000. The transcription factor snail controls epithelial-mesenchymal transitions by repressing E-cadherin expression. *Nat Cell Biol* 2:76-83.

14. Yoshino, J., T. Monkawa, M. Tsuji, M. Inukai, H. Itoh, and M. Hayashi. 2007. Snail1 is involved in the renal epithelial-mesenchymal transition. *Biochem Biophys Res Commun* 362:63-68.

15. Auerbach, W., J.H. Dunmore, V. Fairchild-Huntress, Q. Fang, A.B. Auerbach, D. Huszar, and A.L. Joyner. 2000. Establishment and chimera analysis of 129/SvEv- and C57BL/6-derived mouse embryonic stem cell lines. *Biotechniques* 29:1024-1028, 1030, 1032.

16. Strutz, F., H. Okada, C.W. Lo, T. Danoff, R.L. Carone, J.E. Tomaszewski, and E.G. Neilson. 1995. Identification and characterization of a fibroblast marker: FSP1. *J Cell Biol* 130:393-405.

17. Del Castillo, G., M.M. Murillo, A. Alvarez-Barrientos, E. Bertran, M. Fernandez, A. Sanchez, and I. Fabregat. 2006. Autocrine production of TGF-beta confers resistance to apoptosis after an epithelial-mesenchymal transition process in hepatocytes: Role of EGF receptor ligands. *Exp Cell Res* 312:2860-2871.

18. Kaimori, A., J. Potter, J.Y. Kaimori, C. Wang, E. Mezey, and A. Koteish. 2007. Transforming growth factor-beta1 induces an epithelial-to-mesenchymal transition state in mouse hepatocytes in vitro. *J Biol Chem* 282:22089-22101.

19. Nitta, T., J.S. Kim, D. Mohuczy, and K.E. Behrns. 2008. Murine cirrhosis induces hepatocyte epithelial mesenchymal transition and alterations in survival signaling pathways. *Hepatology* 48:909-919.

20. Qi, Z., N. Atsuchi, A. Ooshima, A. Takeshita, and H. Ueno. 1999. Blockade of type beta transforming growth factor signaling prevents liver fibrosis and dysfunction in the rat. *Proc Natl Acad Sci U S A* 96:2345-2349.

21. Postic, C., M. Shiota, K.D. Niswender, T.L. Jetton, Y. Chen, J.M. Moates, K.D. Shelton, J. Lindner, A.D. Cherrington, and M.A. Magnuson. 1999. Dual roles for glucokinase in glucose homeostasis as determined by liver and pancreatic beta cell-specific gene knock-outs using Cre recombinase. *J Biol Chem* 274:305-315.

22. Scheuer, P.J. 1991. Classification of chronic viral hepatitis: a need for reassessment. *J Hepatol* 13:372-374.

23. Bataller, R., and D.A. Brenner. 2005. Liver fibrosis. *J Clin Invest* 115:209-218.

24. Bataller, R., R.F. Schwabe, Y.H. Choi, L. Yang, Y.H. Paik, J. Lindquist, T. Qian, R. Schoonhoven, C.H. Hagedorn, J.J. Lemasters, and D.A. Brenner. 2003. NADPH oxidase signal transduces angiotensin II in hepatic stellate cells and is critical in hepatic fibrosis. *J Clin Invest* 112:1383-1394.

25. Borkham-Kamphorst, E., J. Herrmann, D. Stoll, J. Treptau, A.M. Gressner, and R. Weiskirchen. 2004. Dominant-negative soluble PDGF-beta receptor inhibits hepatic stellate cell activation and attenuates liver fibrosis. *Lab Invest* 84:766-777.

26. Canbay, A., M.E. Guicciardi, H. Higuchi, A. Feldstein, S.F. Bronk, R. Rydzewski, M. Taniai, and G.J. Gores. 2003. Cathepsin B inactivation attenuates hepatic injury and fibrosis during cholestasis. *J Clin Invest* 112:152-159.

27. Ikejima, K., Y. Takei, H. Honda, M. Hirose, M. Yoshikawa, Y.J. Zhang, T. Lang, T. Fukuda, S. Yamashina, T. Kitamura, and N. Sato. 2002. Leptin receptor-mediated signaling regulates hepatic fibrogenesis and remodeling of extracellular matrix in the rat. *Gastroenterology* 122:1399-1410.

28. Boutet, A., C.A. De Frutos, P.H. Maxwell, M.J. Mayol, J. Romero, and M.A. Nieto. 2006. Snail activation disrupts tissue homeostasis and induces fibrosis in the adult kidney. *EMBO J* 25:5603-5613.

29. Venkov, C.D., A.J. Link, J.L. Jennings, D. Plieth, T. Inoue, K. Nagai, C. Xu, Y.N. Dimitrova, F.J. Rauscher, and E.G. Neilson. 2007. A proximal activator of transcription in epithelial-mesenchymal transition. *J Clin Invest* 117:482-491.

30. Murray, S.A., and T. Gridley. 2006. Snail family genes are required for left-right asymmetry determination, but not neural crest formation, in mice. *Proc Natl Acad Sci U S A* 103:10300-10304.

31. Van de Putte, T., M. Maruhashi, A. Francis, L. Nelles, H. Kondoh, D. Huylebroeck, and Y. Higashi. 2003. Mice lacking ZFHX1B, the gene that codes for Smad-interacting protein-1, reveal a role for multiple neural crest cell defects in the etiology of Hirschsprung disease-mental retardation syndrome. *Am J Hum Genet* 72:465-470.

32. Wakamatsu, N., Y. Yamada, K. Yamada, T. Ono, N. Nomura, H. Taniguchi, H. Kitoh, N. Mutoh, T. Yamanaka, K. Mushiake, K. Kato, S.

Sonta, and M. Nagaya. 2001. Mutations in SIP1, encoding Smad interacting protein-1, cause a form of Hirschsprung disease. *Nat Genet* 27:369-370.

33. Beltran, M., I. Puig, C. Pena, J.M. Garcia, A.B. Alvarez, R. Pena, F. Bonilla, and A.G. de Herreros. 2008. A natural antisense transcript regulates Zeb2/Sip1 gene expression during Snail1-induced epithelial-mesenchymal transition. *Genes Dev* 22:756-769.

34. Lin, S.L., T. Kisseleva, D.A. Brenner, and J.S. Duffield. 2008. Pericytes and perivascular fibroblasts are the primary source of collagen-producing cells in obstructive fibrosis of the kidney. *Am J Pathol* 173:1617-1627.

35. Russo, F.P., M.R. Alison, B.W. Bigger, E. Amofah, A. Florou, F. Amin, G. Bou-Gharios, R. Jeffery, J.P. Iredale, and S.J. Forbes. 2006. The bone marrow functionally contributes to liver fibrosis. *Gastroenterology* 130:1807-1821.

36. Kudo-Saito, C., H. Shirako, T. Takeuchi, and Y. Kawakami. 2009. Cancer metastasis is accelerated through immunosuppression during Snail-induced EMT of cancer cells. *Cancer Cell* 15:195-206.

37. Duffield, J.S., S.J. Forbes, C.M. Constandinou, S. Clay, M. Partolina, S. Vuthoori, S. Wu, R. Lang, and J.P. Iredale. 2005. Selective depletion of macrophages reveals distinct, opposing roles during liver injury and repair. *J Clin Invest* 115:56-65.

Chapter 3: Role of Snail1 in Endothelial-Mesenchymal Transition

Introduction.

Angiogenesis, the process of capillary sprouting from the existing vasculature, occurs when endothelial cells (ECs) lining mature blood vessels disrupt cell:cell junctions, degrade the vascular BM, delaminate and invade the underlying 3-D interstitial ECM (1-3). This morphogenetic event is accompanied by a shift in phenotype from an EC existing atop a BM substratum in a 2-D environment to a 3-D mesenchymal-like cell encased within a 3-D ECM—an event that can be termed the 2-D-to-3-D transition. This change in phenotype incorporates the endothelial-to-mesenchymal transition (EndoMT)—a redefining of cell identity wherein ECs integrate genetic programs characteristic of mesenchymal cells (4). Mechanistically, ECs undergoing EndoMT lose endothelial markers, such as CD31 (PECAM-1) and the adherens junction protein vascular endothelial (VE) cadherin, and gain mesenchymal markers, such as α-smooth muscle actin (αSMA) (4, 5).

EndoMT is a central process during cardiovascular development. In addition to promoting the initial steps of angiogenic sprouting, EndoMT occurs during formation of cardiac valves (6-9). When triggered with ligands of the Wnt, TGFβ, and Notch signaling pathways, ECs residing in the outflow tract of the primitive heart invade the proteoglycan-rich cardiac jelly to form the differentiated mesenchymal cells that populate mature valves (6-13). Furthermore, EndoMT might play a role in differentiation of vascular smooth muscle cells and pericytes from ECs (5, 14-17).

As in the case of morphogenetic epithelial-mesenchymal transition (EMT) programs, developmental EndoMT programs can be inappropriately activated to contribute to the pathobiology of several diseases (4). During carcinogenesis, stromal fibroblasts act as modulators of tumor progression (18, 19). It has been suggested that a significant proportion of tumor-associated fibroblasts arise via EndoMT within the tumor vasculature (20). Similarly, ECs might also provide a source of fibroblasts that overpopulate the interstitial compartment during fibrosis of the heart and kidney (21, 22). Furthermore, EndoMT events may produce excessive mural mesenchymal cells during vascular remodeling events in chronic pulmonary hypertension, atherosclerosis, and scarring (23-25).

As inducers of EMT, Snail family members have received considerable attention as potential mediators of EndoMT (8, 12, 26). Snail2 (Slug) is an effector of avian cardiac valve EndoMT, and has been suggested to serve a similar function in mammalian heart development (12, 13, 27). Interestingly, Snail1 acts as a direct repressor of VE-cadherin, and is highly expressed during valvular EndoMT in mice (8). Furthermore, Snail1 seems to be required for vascular development in early embryogenesis, and promotes EndoMT in embryonic ECs (26, 28). In support of a role during angiogenesis, Snail1 expression is induced by pro-angiogenic stimuli – including vascular endothelial growth factor (VEGF) and hepatocyte growth factor (HGF) - in epithelial cells (29, 30), suggesting that a similar mechanism might function in ECs. Additionally, Snail1 may be recruited to promote pathologic angiogenesis in adults, as its expression is enriched in the tumor-associated vasculature (31, 32).

Herein we have investigated the function of Snail1 in mediating EndoMT as well as its role in formation of the embryonic vasculature in mammals. We identify an essential role for Snail1 expression in the vasculature during mammalian development. We also find a requirement for Snail1 for acquisition of mesenchymal, smooth muscle-like characteristics in human ECs. Further, we show that Snail1 is regulated by pro-angiogenic stimuli in ECs. These studies have identified an intriguing role for Snail1 during EndoMT and vascular morphogenesis.

Materials and Methods.

Mice. Tie2-Cre transgenic mice on an inbred C57BL/6 background were purchased from Jackson Laboratories (Bar Harbor, ME). *Snai1*^{fl} targeted mice were described previously and were maintained on a mixed 129/C57BL/6 genetic background (33). All procedures were approved by the University of Michigan Committee regulating the care and use of animals.

EC isolation and culture. Human umbilical vein ECs were isolated and cultured in 20% human serum as described (34). ECs were treated with recombinant human TGFβ_2 (R and D Systems, Minneapolis, MN). ECs were transduced with recombinant control retroviruses or retroviruses bearing the cDNA for full-length human Snail1 in the presence of 6 μg/ml polybrene (Sigma, St. Louis, MO).

To silence Snail1 expression, ECs were transduced with recombinant lentiviruses encoding shRNAs specific for human Snail1 (provided by E. Fearon, University of Michigan). Lentiviruses were packaged in HEK293 cells transfected with lentiviral packaging vectors using Lipofectamine 2000 (Invitrogen, Carlsbad, CA) according to the manufacturer's instructions.

To induce a migratory phenotype in ECs, ECs were cultured to confluence in the presence of a glass coverslip. Following removal of the coverslip, ECs were allowed to migrate into the cell-free area for 12 hours, when they were fixed for immunocytochemistry.

Immunofluorescence microscopy. ECs were stained with antibodies specific for αSMA (Sigma, St. Louis, MO), Snail1 (35), or β-catenin (Cell Signaling Technologies, Danvers, MA). Subcellular protein localization was monitored by confocal laser microscopy using an Olympus FV500 microscope with a 60X water immersion lens (Olympus, Center Velley, PA). Cells were counterstained with DAPI (Invitrogen, Carlsbad, CA) to visualize nuclei.

Results.

Snail1 expression in the endothelium is required during murine development. Since Snail1 expression is associated with EC EndoMT (8, 26), and is recruited by vasculogenic signals in epithelial cells (29, 30), this suggests that Snail1 might function in vascular development by regulating EC function. To test this idea, we employed a previously-characterized mouse model of conditional Snail1 inactivation wherein the mouse *Snai1* gene contains loxp sites flanking the third exon such that messenger RNA expression is inactivated following Cre-mediated recombination of genomic DNA (*Snai1*^{fl})(33). For EC-specific Cre expression, we used the Tie2-Cre transgenic model (36) (Figure 3.1A).

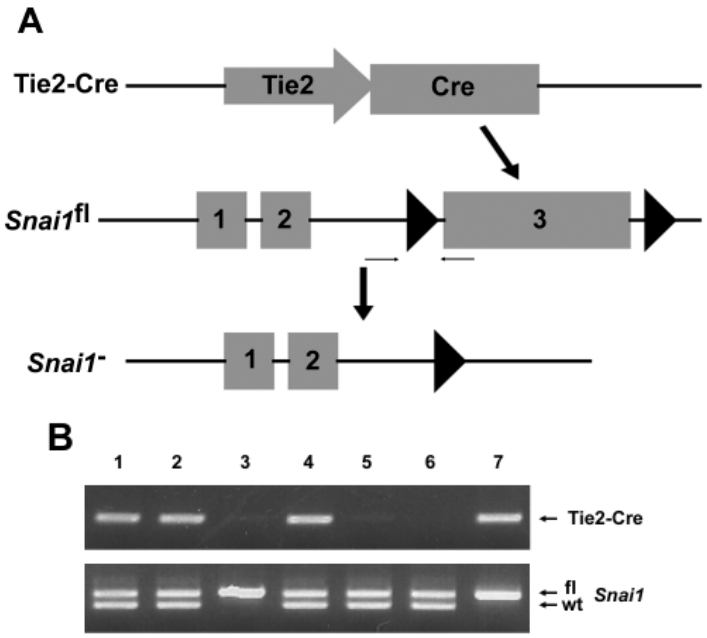

Figure 3.1. EC-specific deletion of Snai1

A. Tie2-Cre transgenic mice were crossed to mice bearing a conditional allele of the *Snai1* gene. EC-specific expression of Cre recombinase results in deletion of the loxp-flanked third exon within the *Snai1* gene. Primer locations for genotyping the *Snai1* locus are shown. **B.** *Tie2-Cre; Snai1*$^{+/fl}$ mice were crossed to *Snai1*$^{fl/fl}$ mice. Progeny were genotyped by tail biopsy for the Tie2-Cre transgene and the *Snai1*^{fl} allele at postnatal day 0. Lane 7: Tie2-Cre; *Snai1*$^{fl/fl}$ mouse deficient in EC Snail1 expression.

Mice carrying the *Snai1*^{loxp} allele were crossed to Tie2-Cre mice to generate Tie2-Cre; *Snai1*$^{+/loxp}$ mice (Figure 3.1B). Tie2-Cre; *Snai1*$^{+/loxp}$ mice were crossed to *Snai1*$^{loxp/loxp}$ mice, and progeny analyzed at postnatal day 0 to determine genotype distributions (Table 3.1). We found that progeny with EC-specific Snail1 deficiency were significantly under-represented at postnatal day 0 (chi-square = 14.2 for one degree of freedom; p = 0.0002) indicating a requirement for Snail1 during embryonic vascular development for mouse viability.

	P_0 genotypes			
	Snai1$^{fl/fl}$	*Snai1*$^{+/fl}$	Tie2-Cre; *Snai1*$^{+/fl}$	Tie2-Cre; *Snai1*$^{fl/fl}$
Obs	28	31	30	8
Exp	24	24	24	24

Table 3.1. Genotypes of offspring of Tie2-Cre; *Snai1*$^{+/fl}$ and *Snai1*$^{fl/fl}$ mice.

Potential role for Snail1 in EndoMT. To investigate potential roles for Snail1 during vascular morphogenesis, models of *in vitro* EndoMT were employed. TGFβ family members are activators of developmental and pathologic EndoMTs (7, 9, 11, 21, 22). In order to determine if human ECs underwent EndoMT in response to such signals, human umbilical vein ECs were treated with 2 ng/ml TGFβ$_2$ - a mediator of cardiac valve EndoMT (37) - and EndoMT was assessed by morphology and assessment of activation of the mesenchymal marker α-smooth muscle actin (αSMA). As shown in Figure 3.2A, 6 d TGFβ$_2$ treatment induced morphologic changes consistent with EndoMT; ECs transitioned from a tightly-packed, cobblestone morphology with clear cell:cell junctions to cells with a fibroblast-like, multipolar morphology. Furthermore, TGFβ$_2$-treated ECs exhibited a marked induction of αSMA expression at the protein and mRNA levels (Figure 3.2B-C).

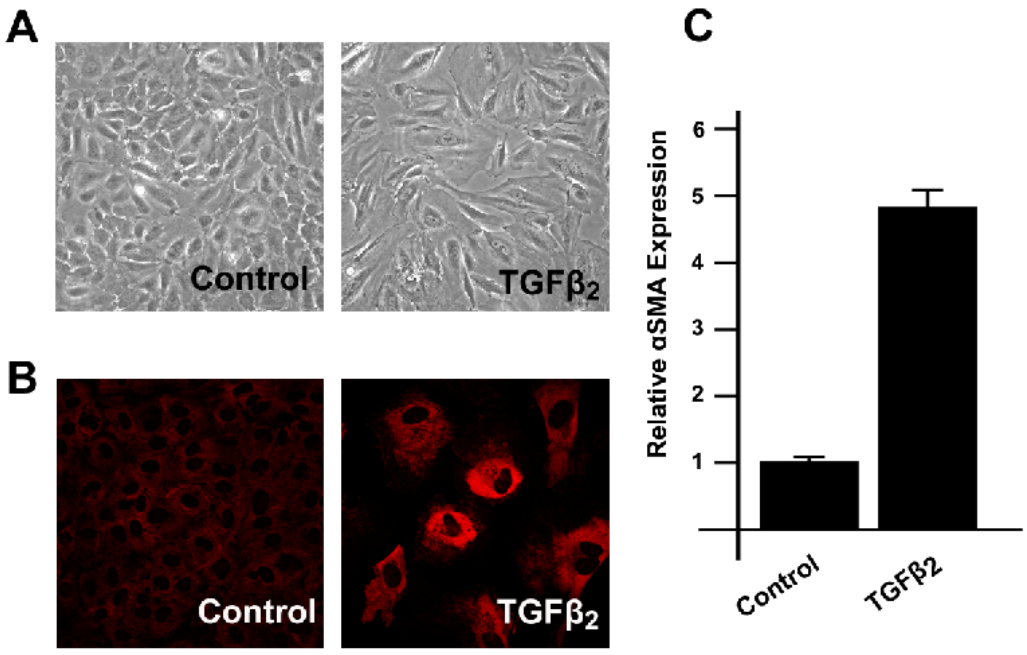

Figure 3.2. EndoMT

A. ECs were treated with or without $TGF\beta_2$ for 6 d, and cell morphology assessed by phase contrast microscopy.
B-C. ECs treated with or without $TGF\beta_2$ for 6 d and αSMA (red) expression assessed either by confocal laser microscopy (**B**) or quantitative reverse transcription PCR (qRT-PCR) (**C**).

In order to investigate a potential role for Snail1 in EndoMT in human cells, human umbilical vein ECs were treated with $TGF\beta_2$, and Snail1 induction measured. Treatment of ECs with 2 ng/ml $TGF\beta_2$ for 6 d induced Snail1 expression at both the mRNA and protein levels (Figure 3.3), indicating that Snail1 is a direct or indirect target of $TGF\beta_2$ in ECs, and suggesting Snail1 might be a candidate mediator of EndoMT in human cells.

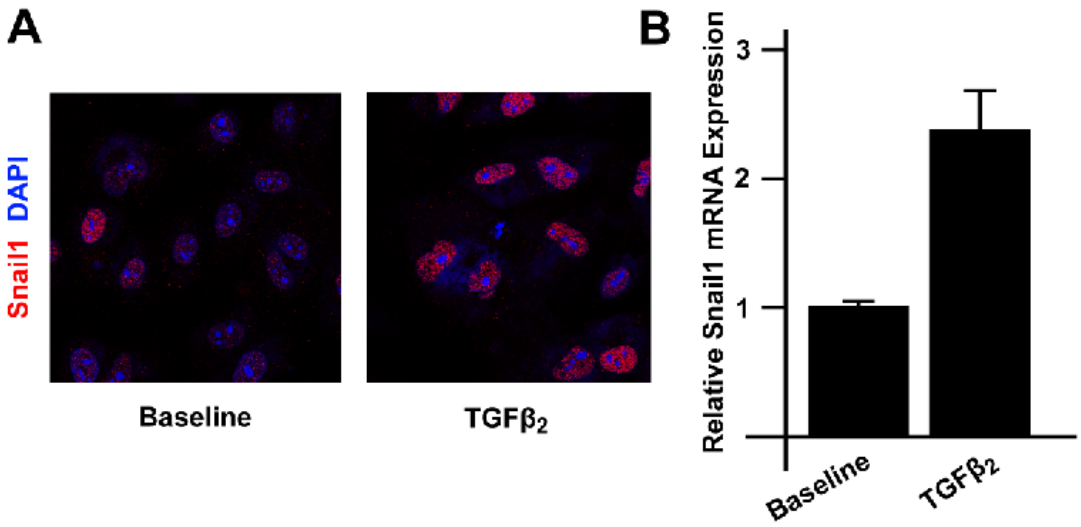

Figure 3.3. Snail1 is induced during EndoMT

A. ECs were treated with or without TGFβ$_2$ for 6 d and Snail1 protein (red) was measured by immunofluorescence and DAPI counterstaining (blue) followed by confocal laser microscopy. **B.** Snail1 mRNA was measured by quantitative RT-PCR.

To test if Snail1 expression promotes EndoMT, human ECs were infected with retroviruses bearing the full-length Snail1 cDNA (Figure 3.4A). Compared to ECs infected with a control virus, Snail1-expressing ECs exhibit an increased expression of αSMA (Figure 3.4B). These data suggest that activation of Snail1 expression in ECs might activate EndoMT programs.

To investigate if Snail1 plays a required role in TGFβ$_2$-mediated EndoMT, Snail1 expression was silenced in human endothelial cells via transduction with lentiviruses encoding small hairpin RNAs (shRNAs) directed against Snail1 as well as green fluorescent protein (GFP) to identify transduced cells. Transduction of ECs with two independent shRNA constructs resulted in an approximately 70% reduction in Snail1 mRNA in untreated cells and in cells treated with TGFβ$_2$ for 6 d using the Snail1-Sh4 construct (Figure 3.5A-B).

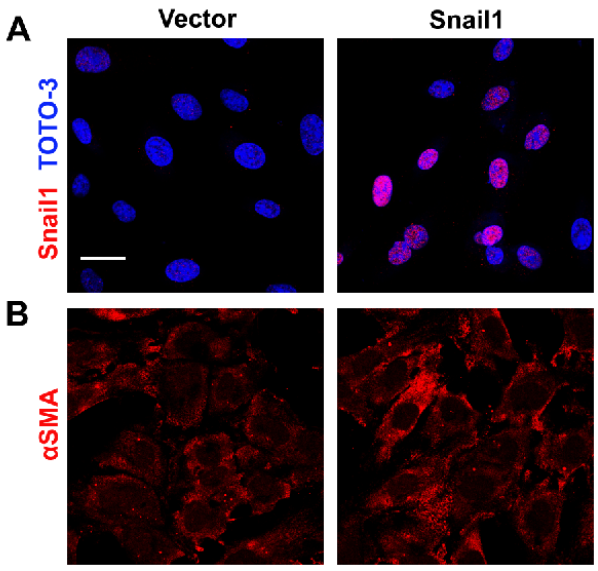

Figure 3.4. Snail1 expression promotes the EndoMT phenotype

A-B. Human ECs were infected with either a control retrovirus or a retrovirus bearing the cDNA for full-length human Snail1 and stained with antibodies against either Snail1 (**A**) or αSMA (**B**).

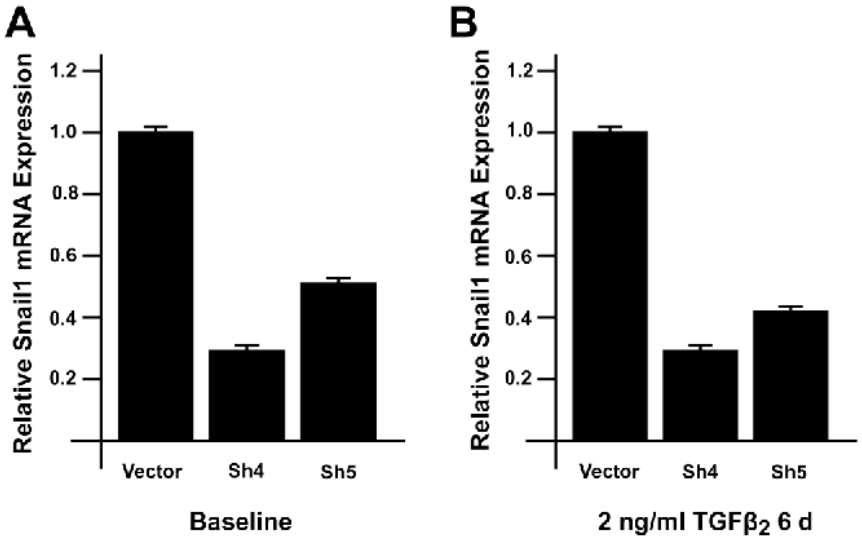

Figure 3.5. Silencing of Snail1 expression in human ECs by shRNA

A-B. Human ECs were infected with recombinant lentiviruses bearing constructs to express shRNAs directed against human Snail1. Levels of Snail1 transcripts were measured by qRT-PCR either at baseline (**A**) or after 6 d treatment with 2 ng/ml $TGF\beta_2$ (**B**).

To assess the role of Snail1 in EndoMT, αSMA induction by $TGF\beta_2$ treatment was measured in shRNA-expressing cells by immunocytochemistry.

We examined single cells due to the inability to transduce the complete EC population with 100% efficiency. ECs expressing the empty shRNA vector displayed a robust induction of αSMA in response to TGFβ$_2$ treatment, with many TGFβ$_2$-treated cells displaying double-positivity for GFP (identifying cells efficiently transduced with lentivirus) and αSMA (Figure 3.6). However, GFP-positive ECs expressing Snail1 shRNAs exhibited a weaker αSMA induction, with a significant reduction in GFP/αSMA-positive cells, suggesting an attenuated EndoMT response in the absence of wild-type levels of Snail1 expression (Figure 3.6).

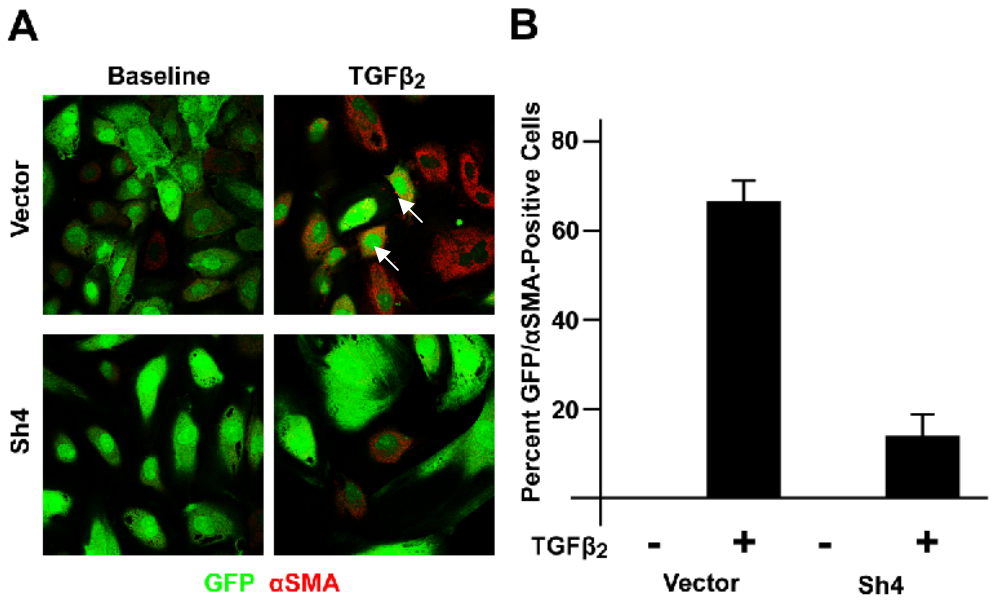

Figure 3.6. Snail1 is required for efficient TGFβ2-mediated αSMA induction in ECs

A. Human ECs were infected with lentiviruses to silence Snail1 expression. Following treatment with 2 ng/ml TGFβ$_2$ for 6 d, ECs were stained with an antibody against αSMA. Colocalization of green fluorescent protein (green, identifying transduced cells) and αSMA (red) was measured by confocal laser microscopy (arrows indicate double-positive cells. **B.** Per cent GFP/αSMA double positive cells were quantified.

Snail1 is regulated by pro-angiogenic signals. Vascular development is disrupted in mouse models of Snail1 deficiency (28), and data herein indicate that Snail1 plays a required role in ECs during vascular development, suggesting a role for Snail1 in angiogenic programs in ECs. Therefore, we next asked if

Snail1 protein levels could be modulated by pro-angiogenic signals. ECs were treated with the angiogenic factors VEGF and HGF and Snail1 protein levels assessed by Western blot and immunocytochemistry. As shown in Figure 3.7A, treatment of ECs with VEGF and HGF for 3 h was sufficient to induce transient Snail1 protein. Immunocytochemistry revealed that Snail1 protein increased within the nuclear compartment (Figure 3.7B). Hence, exposure of ECs to soluble pro-angiogenic signals induces Snail1 activation in ECs.

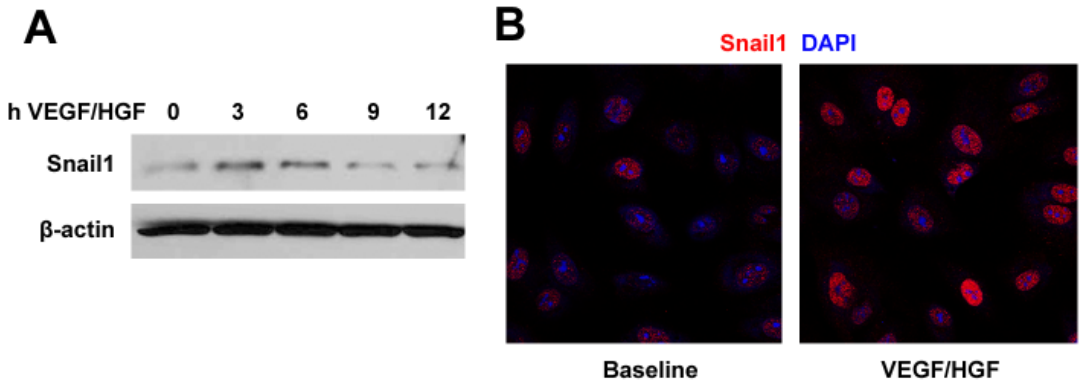

Figure 3.7. Snail1 expression is induced by pro-angiogenic signals

A. ECs were treated with 100 ng/ml VEGF and 50 ng/ml HGF for the indicated times and Snail1 protein levels measured by Western blot.
B. Human ECs were treated with or without VEGF and HGF for 6 h and Snail1 protein (red) localization assessed by immunocytochemistry and confocal laser microscopy following DAPI counterstaining.

At sites of tissue remodeling, ECs assume a migratory phenotype wherein they invade the surrounding environment on the path to forming capillary neovessels (1, 34). This scenario can be recapitulated *in vitro* through the use of an *in vitro* wounding assay wherein an EC monolayer is disrupted by removal of a glass coverslip, generating a cell-free area adjacent to the wound edge previously occupied by the coverslip. ECs immediately adjacent to the wound assume a migratory phenotype and begin to repopulate the cell-free area. We used this model as a second EC activation stimulus to assess Snail1 expression. Compared to an uninjured EC monolayer, ECs migrating into a wound relocalize the adherens junction protein β-catenin from cell-cell junctions to the nuclear compartment where it acts as a transcriptional regulator (Figure 3.8A), a pattern consistent with induction of an EMT-like program (38-40).

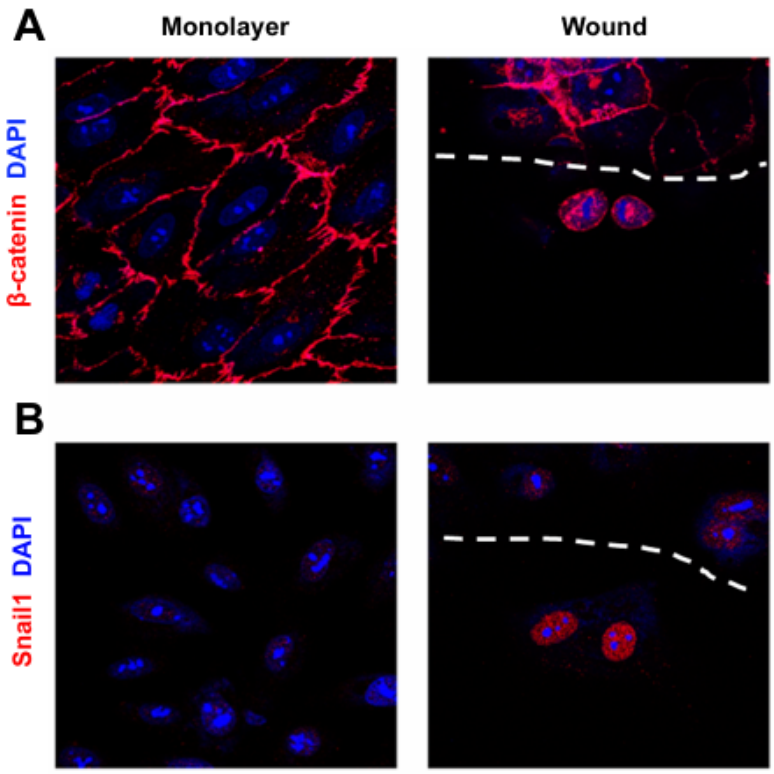

Figure 3.8. Snail1 expression is induced in migratory ECs

A-B. Human ECs were grown to confluence in the presence of a glass coverslip. After removal of the coverslip, ECs were allowed to migrate into the cell-free area for 12 h at which time localization of either β-catenin (**A**) or Snail1 (**B**) was examined by immunocytochemistry and confocal laser microscopy. Left panels display confluent cell monolayer, right panels display the edge of the cell-free area. Broken line demarcates wound edge.

Since Snail1 is both activated by pathways both upstream and downstream of β-catenin nuclear localization and transcriptional activity (41-43) and has been proposed to be a positive regulator of β-catenin signaling (44-47), and can be found in neovessels *in vivo* (31, 32), we examined Snail1 levels in ECs migrating in wounds. Compared to an uninjured EC monolayer - which expresses very low levels of nuclear Snail1 – migratory ECs at the wound edge display a strong induction of Snail1 protein within the nucleus (Figure 3.8B). Hence, Snail1 nuclear protein accumulation can be triggered by soluble pro-angiogenic signaling molecules as well as migratory cues from the tissue microenvironment.

Discussion.

Neovessel formation via the processes of angiogenesis and vasculogenesis requires a shift in EC phenotype from a quiescent, polarized cell existing within a 2-D monolayer to a migratory cell possessing the capacity to negotiate 3-D ECM barriers (1, 34, 48). Recently, considerable attention has focused on EndoMT as a mechanism of endothelial plasticity analogous EMT programs activated in epithelial cells (4, 49). Indeed, these two processes bear many similarities: characteristics of 2-D cells – such as tight homotypic cell-cell adhesion and apical/basolateral polarization – are lost, and traits of 3-D cells – including tissue-invasive capability and neo-ECM deposition – are gained (4, 34, 49, 50). Like EMT, EndoMT is triggered when activated ECs penetrate basement membrane barriers (3, 4, 41, 42, 51), suggesting that similar proximal signaling pathways and transcriptional regulators might be recruited to trigger both programs. Since repression of the epithelial phenotype seems to be the initiating step during EMT, attention has focused on the transcriptional repressors which act as master switches of the genetic programs governing EMT as inducers of EndoMT (33, 41, 42, 52, 53).

Accumulating data point to a central role for the Snail family of transcription factors in mediating EndoMT at a molecular level. Both Snail1 and Snail2 have been associated with endocardial EndoMT events that promote cardiac valve formation in vertebrates (8, 12, 13, 27). Triggered by TGFβ family members – which also act as initiators of EMTs - EndoMT-mediated cellularization of the cardiac valves is a required event during development (6, 7, 9, 11, 13, 54). Furthermore, Snail1 expression correlates with the 2-D-to-3-D transitions required for neovessel formation *in vivo* (31, 32). If Snail1 functions in EndoMT and 2-D-to-3-D transitions *in vivo*, Snail1 expression within ECs would be predicted to be required for cardiovascular development. Therefore, we used an endothelial-specific Tie2-Cre transgenic mouse line to inactivate *Snai1* mRNA expression within the vasculature during embryogenesis (33, 36). We found that endothelial Snail1 expression was required for mouse viability. Studies are ongoing to determine the precise role of Snail1 during vascular development.

In order to gain insight into *in vivo* functions of Snail1 in EC biology, we next investigated Snail1 function *in vitro*. First, we assessed expression of Snail1 in human ECs in response to stimuli known to promote EC EndoMTs. Accumulating evidence suggests that TGFβ family members initiate developmental and pathologic EndoMTs *in vivo* (11, 13). Therefore, we treated ECs with $TGF\beta_2$ and found an induction of Snail1 mRNA and protein during the induction of EndoMT, in accordance with the observation that Snail1 gene expression is activated during EndoMTs *in vivo* (8, 12). Consistent with this idea, expression of Snail1 in ECs resulted in the activation of the mesenchymal gene αSMA. To determine the functional role of Snail1 during $TGF\beta_2$-triggered EndoMT, we silenced Snail1 expression in ECs using lentiviral expression of anti-Snail1 shRNAs. Snail1-silenced ECs exhibited defective activation of αSMA compared to cells expressing a non-targeting shRNA, similar to results previously reported with embryonic ECs (26). Taken together, these data suggest that Snail1 might play a role during EndoMT events *in vivo*.

During angiogenic sprouting, ECs undergo an activation process wherein they perforate BM barriers, undergo an EndoMT in order to transcriptionally reprogram for function in 3-D, and invade 3-D ECM barriers— executing a 2-D-to-3-D transition process (2, 3, 34, 48, 55). Stimuli known to activate ECs include VEGF and HGF. To determine if Snail1 might function in VEGF/HGF-triggered EC activation and angiogenesis, human ECs were treated with VEGF and HGF, and Snail1 protein was found to accumulate. Consistent with this observation, VEGF can activate Snail1 expression in carcinoma cells, suggesting that this pattern of Snail1 regulation in ECs might be co-opted by carcinoma cells (30). Since Snail1 is regulated both at the transcriptional and post-translational levels (41-43), future study is required to determine the mechanism by which VEGF modulates signaling pathways known to control Snail1 protein levels. Furthermore, we found Snail1 protein accumulates in the nuclei of migratory ECs compared to quiescent ECs existing within a monolayer. This activation of Snail1 expression correlates with a shift in the adherens junction protein β-catenin to the nucleus, where it acts as a transcriptional regulator (56). Since endothelial β-

catenin is required for cardiovascular development (6, 10, 57), and Snail1 and β-catenin seem to exhibit reciprocal interactions (41, 42, 45, 58), this suggests an intriguing model wherein Snail1 and β-catenin might co-regulate EC function or exist within a linear pathway required for cardiovascular morphogenesis.

Taken together, these data demonstrate that Snail1 expression in ECs is required for vascular morphogenesis *in vivo*, and suggest that Snail1 might play an important role during EndoMTs and may also function in EC activation during angiogenic sprouting. Recent investigation has demonstrated parallels between EMT events that occur in epithelial cells and EndoMT in ECs (4). Indeed, both processes seem have similar molecular underpinnings, and might share common master transcriptional regulators including Snail family factors (4). Future study will define the precise *in vivo* function of Snail1 during vascular morphogenesis.

References

1. Chun, T.H., Sabeh, F., Ota, I., Murphy, H., McDonagh, K.T., Holmbeck, K., Birkedal-Hansen, H., Allen, E.D., and Weiss, S.J. 2004. MT1-MMP-dependent neovessel formation within the confines of the three-dimensional extracellular matrix. *J Cell Biol* 167:757-767.

2. Hiraoka, N., Allen, E., Apel, I.J., Gyetko, M.R., and Weiss, S.J. 1998. Matrix metalloproteinases regulate neovascularization by acting as pericellular fibrinolysins. *Cell* 95:365-377.

3. Rowe, R.G., and Weiss, S.J. 2008. Breaching the basement membrane: who, when and how? *Trends Cell Biol* 18:560-574.

4. Potenta, S., Zeisberg, E., and Kalluri, R. 2008. The role of endothelial-to-mesenchymal transition in cancer progression. *Br J Cancer* 99:1375-1379.

5. Noseda, M., McLean, G., Niessen, K., Chang, L., Pollet, I., Montpetit, R., Shahidi, R., Dorovini-Zis, K., Li, L., Beckstead, B., et al. 2004. Notch activation results in phenotypic and functional changes consistent with endothelial-to-mesenchymal transformation. *Circ Res* 94:910-917.

6. Liebner, S., Cattelino, A., Gallini, R., Rudini, N., Iurlaro, M., Piccolo, S., and Dejana, E. 2004. Beta-catenin is required for endothelial-mesenchymal transformation during heart cushion development in the mouse. *J Cell Biol* 166:359-367.

7. Ma, L., Lu, M.F., Schwartz, R.J., and Martin, J.F. 2005. Bmp2 is essential for cardiac cushion epithelial-mesenchymal transition and myocardial patterning. *Development* 132:5601-5611.

8. Timmerman, L.A., Grego-Bessa, J., Raya, A., Bertran, E., Perez-Pomares, J.M., Diez, J., Aranda, S., Palomo, S., McCormick, F., Izpisua-Belmonte, J.C., et al. 2004. Notch promotes epithelial-mesenchymal transition during cardiac development and oncogenic transformation. *Genes Dev* 18:99-115.

9. Wang, J., Sridurongrit, S., Dudas, M., Thomas, P., Nagy, A., Schneider, M.D., Epstein, J.A., and Kaartinen, V. 2005. Atrioventricular cushion transformation is mediated by ALK2 in the developing mouse heart. *Dev Biol* 286:299-310.

10. Hurlstone, A.F., Haramis, A.P., Wienholds, E., Begthel, H., Korving, J., Van Eeden, F., Cuppen, E., Zivkovic, D., Plasterk, R.H., and Clevers, H. 2003. The Wnt/beta-catenin pathway regulates cardiac valve formation. *Nature* 425:633-637.

11. Boyer, A.S., and Runyan, R.B. 2001. TGFbeta Type III and TGFbeta Type II receptors have distinct activities during epithelial-mesenchymal cell transformation in the embryonic heart. *Dev Dyn* 221:454-459.

12. Niessen, K., Fu, Y., Chang, L., Hoodless, P.A., McFadden, D., and Karsan, A. 2008. Slug is a direct Notch target required for initiation of cardiac cushion cellularization. *J Cell Biol* 182:315-325.

13. Romano, L.A., and Runyan, R.B. 2000. Slug is an essential target of TGFbeta2 signaling in the developing chicken heart. *Dev Biol* 223:91-102.

14. Arciniegas, E., Ponce, L., Hartt, Y., Graterol, A., and Carlini, R.G. 2000. Intimal thickening involves transdifferentiation of embryonic endothelial cells. *Anat Rec* 258:47-57.

15. Arciniegas, E., Sutton, A.B., Allen, T.D., and Schor, A.M. 1992. Transforming growth factor beta 1 promotes the differentiation of endothelial cells into smooth muscle-like cells in vitro. *J Cell Sci* 103 (Pt 2):521-529.

16. DeRuiter, M.C., Poelmann, R.E., VanMunsteren, J.C., Mironov, V., Markwald, R.R., and Gittenberger-de Groot, A.C. 1997. Embryonic endothelial cells transdifferentiate into mesenchymal cells expressing smooth muscle actins in vivo and in vitro. *Circ Res* 80:444-451.

17. Frid, M.G., Kale, V.A., and Stenmark, K.R. 2002. Mature vascular endothelium can give rise to smooth muscle cells via endothelial-mesenchymal transdifferentiation: in vitro analysis. *Circ Res* 90:1189-1196.

18. Kalluri, R., and Zeisberg, M. 2006. Fibroblasts in cancer. *Nat Rev Cancer* 6:392-401.

19. Karnoub, A.E., Dash, A.B., Vo, A.P., Sullivan, A., Brooks, M.W., Bell, G.W., Richardson, A.L., Polyak, K., Tubo, R., and Weinberg, R.A. 2007. Mesenchymal stem cells within tumour stroma promote breast cancer metastasis. *Nature* 449:557-563.

20. Zeisberg, E.M., Potenta, S., Xie, L., Zeisberg, M., and Kalluri, R. 2007. Discovery of endothelial to mesenchymal transition as a source for carcinoma-associated fibroblasts. *Cancer Res* 67:10123-10128.

21. Zeisberg, E.M., Potenta, S.E., Sugimoto, H., Zeisberg, M., and Kalluri, R. 2008. Fibroblasts in kidney fibrosis emerge via endothelial-to-mesenchymal transition. *J Am Soc Nephrol* 19:2282-2287.

22. Zeisberg, E.M., Tarnavski, O., Zeisberg, M., Dorfman, A.L., McMullen, J.R., Gustafsson, E., Chandraker, A., Yuan, X., Pu, W.T., Roberts, A.B., et

al. 2007. Endothelial-to-mesenchymal transition contributes to cardiac fibrosis. *Nat Med* 13:952-961.

23. Lee, J.G., and Kay, E.P. 2006. FGF-2-mediated signal transduction during endothelial mesenchymal transformation in corneal endothelial cells. *Exp Eye Res* 83:1309-1316.

24. Arciniegas, E., Frid, M.G., Douglas, I.S., and Stenmark, K.R. 2007. Perspectives on endothelial-to-mesenchymal transition: potential contribution to vascular remodeling in chronic pulmonary hypertension. *Am J Physiol Lung Cell Mol Physiol* 293:L1-8.

25. Beranek, J.T. 1995. Vascular endothelium-derived cells containing smooth muscle actin are present in restenosis. *Lab Invest* 72:771.

26. Kokudo, T., Suzuki, Y., Yoshimatsu, Y., Yamazaki, T., Watabe, T., and Miyazono, K. 2008. Snail is required for TGFbeta-induced endothelial-mesenchymal transition of embryonic stem cell-derived endothelial cells. *J Cell Sci* 121:3317-3324.

27. Carmona, R., Gonzalez-Iriarte, M., Macias, D., Perez-Pomares, J.M., Garcia-Garrido, L., and Munoz-Chapuli, R. 2000. Immunolocalization of the transcription factor Slug in the developing avian heart. *Anat Embryol (Berl)* 201:103-109.

28. Murray, S.A., and Gridley, T. 2006. Snail family genes are required for left-right asymmetry determination, but not neural crest formation, in mice. *Proc Natl Acad Sci U S A* 103:10300-10304.

29. Grotegut, S., von Schweinitz, D., Christofori, G., and Lehembre, F. 2006. Hepatocyte growth factor induces cell scattering through MAPK/Egr-1-mediated upregulation of Snail. *Embo J* 25:3534-3545.

30. Yang, A.D., Camp, E.R., Fan, F., Shen, L., Gray, M.J., Liu, W., Somcio, R., Bauer, T.W., Wu, Y., Hicklin, D.J., et al. 2006. Vascular endothelial growth factor receptor-1 activation mediates epithelial to mesenchymal transition in human pancreatic carcinoma cells. *Cancer Res* 66:46-51.

31. Parker, B.S., Argani, P., Cook, B.P., Liangfeng, H., Chartrand, S.D., Zhang, M., Saha, S., Bardelli, A., Jiang, Y., St Martin, T.B., et al. 2004. Alterations in vascular gene expression in invasive breast carcinoma. *Cancer Res* 64:7857-7866.

32. Zidar, N., Gale, N., Kojc, N., Volavsek, M., Cardesa, A., Alos, L., Hofler, H., Blechschmidt, K., and Becker, K.F. 2008. Cadherin-catenin complex and transcription factor Snail-1 in spindle cell carcinoma of the head and neck. *Virchows Arch* 453:267-274.

33. Rowe, R.G., Li, X.Y., Hu, Y., Saunders, T.L., Virtanen, I., de Herreros, A.G., Becker, K.F., Ingvarsen, S., Engelholm, L.H., Bommer, G.T., et al. 2009. Mesenchymal cells reactivate Snail1 expression to drive three-dimensional invasion programs. *J Cell Biol*.

34. Zhou, X., Rowe, R.G., Hiraoka, N., George, J.P., Wirtz, D., Mosher, D.F., Virtanen, I., Chernousov, M.A., and Weiss, S.J. 2008. Fibronectin fibrillogenesis regulates three-dimensional neovessel formation. *Genes Dev* 22:1231-1243.

35. Rosivatz, E., Becker, K.F., Kremmer, E., Schott, C., Blechschmidt, K., Hofler, H., and Sarbia, M. 2006. Expression and nuclear localization of Snail, an E-cadherin repressor, in adenocarcinomas of the upper gastrointestinal tract. *Virchows Arch* 448:277-287.

36. Koni, P.A., Joshi, S.K., Temann, U.A., Olson, D., Burkly, L., and Flavell, R.A. 2001. Conditional vascular cell adhesion molecule 1 deletion in mice: impaired lymphocyte migration to bone marrow. *J Exp Med* 193:741-754.

37. Azhar, M., Runyan, R.B., Gard, C., Sanford, L.P., Miller, M.L., Andringa, A., Pawlowski, S., Rajan, S., and Doetschman, T. 2009. Ligand-specific function of transforming growth factor beta in epithelial-mesenchymal transition in heart development. *Dev Dyn* 238:431-442.

38. Brabletz, T., Jung, A., Spaderna, S., Hlubek, F., and Kirchner, T. 2005. Opinion: migrating cancer stem cells - an integrated concept of malignant tumour progression. *Nat Rev Cancer* 5:744-749.

39. Schmalhofer, O., Brabletz, S., and Brabletz, T. 2009. E-cadherin, beta-catenin, and ZEB1 in malignant progression of cancer. *Cancer Metastasis Rev*.

40. Ivanova, L., Butt, M.J., and Matsell, D.G. 2008. Mesenchymal transition in kidney collecting duct epithelial cells. *Am J Physiol Renal Physiol* 294:F1238-1248.

41. Yook, J.I., Li, X.Y., Ota, I., Fearon, E.R., and Weiss, S.J. 2005. Wnt-dependent regulation of the E-cadherin repressor snail. *J Biol Chem* 280:11740-11748.

42. Yook, J.I., Li, X.Y., Ota, I., Hu, C., Kim, H.S., Kim, N.H., Cha, S.Y., Ryu, J.K., Choi, Y.J., Kim, J., et al. 2006. A Wnt-Axin2-GSK3beta cascade regulates Snail1 activity in breast cancer cells. *Nat Cell Biol* 8:1398-1406.

43. Zhou, B.P., Deng, J., Xia, W., Xu, J., Li, Y.M., Gunduz, M., and Hung, M.C. 2004. Dual regulation of Snail by GSK-3beta-mediated phosphorylation in control of epithelial-mesenchymal transition. *Nat Cell Biol* 6:931-940.

44. Li, X., Deng, W., Lobo-Ruppert, S.M., and Ruppert, J.M. 2007. Gli1 acts through Snail and E-cadherin to promote nuclear signaling by beta-catenin. *Oncogene* 26:4489-4498.

45. Stemmer, V., de Craene, B., Berx, G., and Behrens, J. 2008. Snail promotes Wnt target gene expression and interacts with beta-catenin. *Oncogene* 27:5075-5080.

46. Solanas, G., Porta-de-la-Riva, M., Agusti, C., Casagolda, D., Sanchez-Aguilera, F., Larriba, M.J., Pons, F., Peiro, S., Escriva, M., Munoz, A., et al. 2008. E-cadherin controls beta-catenin and NF-kappaB transcriptional activity in mesenchymal gene expression. *J Cell Sci* 121:2224-2234.

47. Medici, D., Hay, E.D., and Olsen, B.R. 2008. Snail and Slug promote epithelial-mesenchymal transition through beta-catenin-T-cell factor-4-dependent expression of transforming growth factor-beta3. *Mol Biol Cell* 19:4875-4887.

48. Carmeliet, P., and Jain, R.K. 2000. Angiogenesis in cancer and other diseases. *Nature* 407:249-257.

49. Thiery, J.P., and Sleeman, J.P. 2006. Complex networks orchestrate epithelial-mesenchymal transitions. *Nat Rev Mol Cell Biol* 7:131-142.

50. Yilmaz, M., and Christofori, G. 2009. EMT, the cytoskeleton, and cancer cell invasion. *Cancer Metastasis Rev*.

51. Zeisberg, M., Bonner, G., Maeshima, Y., Colorado, P., Muller, G.A., Strutz, F., and Kalluri, R. 2001. Renal fibrosis: collagen composition and assembly regulates epithelial-mesenchymal transdifferentiation. *Am J Pathol* 159:1313-1321.

52. Nieto, M.A. 2002. The snail superfamily of zinc-finger transcription factors. *Nat Rev Mol Cell Biol* 3:155-166.

53. Peinado, H., Olmeda, D., and Cano, A. 2007. Snail, Zeb and bHLH factors in tumour progression: an alliance against the epithelial phenotype? *Nat Rev Cancer* 7:415-428.

54. Camenisch, T.D., Molin, D.G., Person, A., Runyan, R.B., Gittenberger-de Groot, A.C., McDonald, J.A., and Klewer, S.E. 2002. Temporal and distinct TGFbeta ligand requirements during mouse and avian endocardial cushion morphogenesis. *Dev Biol* 248:170-181.

55. Chun, T.H., Hotary, K.B., Sabeh, F., Saltiel, A.R., Allen, E.D., and Weiss, S.J. 2006. A pericellular collagenase directs the 3-dimensional development of white adipose tissue. *Cell* 125:577-591.

56. Clevers, H. 2006. Wnt/beta-catenin signaling in development and disease. *Cell* 127:469-480.

57. Cattelino, A., Liebner, S., Gallini, R., Zanetti, A., Balconi, G., Corsi, A., Bianco, P., Wolburg, H., Moore, R., Oreda, B., et al. 2003. The conditional inactivation of the beta-catenin gene in endothelial cells causes a defective vascular pattern and increased vascular fragility. *J Cell Biol* 162:1111-1122.

58. Medici, D., Hay, E.D., and Goodenough, D.A. 2006. Cooperation between snail and LEF-1 transcription factors is essential for TGF-beta1-induced epithelial-mesenchymal transition. *Mol Biol Cell* 17:1871-1879.

Chapter 4: Mesenchymal Cells Reactivate Snail1 Expression to Mediate Tissue Invasion Programs

Introduction.

Snail1, a zinc-finger type transcriptional repressor, initiates an epithelial-mesenchymal transition (EMT) that is critical for the morphogenetic events which characterize developmental programs such as gastrulation (1-3). Snail1 triggers this transdifferentiation program, in part, by repressing epithelial markers and related cell-cell junction proteins while coordinately acting as a major cytoskeletal regulator (4-7). The aberrant postnatal expression of Snail1 is sufficient to confer a mesenchymal, fibroblast-like phenotype in differentiated epithelial cells during pathologic states associated with cancer and fibrosis (6-12).

At sites of active tissue remodeling, changes in vascular permeability disperse serum-derived soluble growth factors within the interstitial compartment which serve to activate signal transduction cascades in resident fibroblasts (13-17). Accordingly, these agonists trigger changes in gene expression programs that shift fibroblast phenotype from a quiescent status to an “activated” state characterized by increased proliferation, tissue-invasive activity, and the induction of angiogenesis (13, 15, 17-19). Growth factors capable of promoting the activated fibroblast phenotype, such as PDGF-BB, have been identified (14, 20), but key transcription factors that regulate downstream gene programs remain largely uncharacterized. Herein, we identify Snail1 as a critical regulator of fibroblast gene expression programs and function *in vitro* as well as *in vivo*. The results demonstrate that Snail1, a key regulator of EMT, continues to subserve vital cellular functions following mesenchymal cell terminal differentiation.

Materials and Methods.

Antibodies and reagents. The 173EC2, 173EC3, and Sn9H2 anti-Snail1, and anti-MT1-MMP mAb1 antibodies were prepared and characterized as described (21, 22). The anti-GSK3β phospho-serine 9 and anti-Akt phospho-serine 478 antibodies were obtained from Cell Signaling Technologies (Danvers, MA). The anti-cortactin, anti-actin and anti-Ki67 antibodies were from Santa Cruz Biotechnology (Santa Cruz, CA), Sigma (St. Louis, MO) and Abcam (Cambridge, MA), respectively. Adeno-β-gal and Adeno-Cre (transgenes driven by a CMV promoter) were obtained from the University of Michigan Vector Core. LY-294002 and MG132 were from Calbiochem (Gibbstown, NJ) and Sigma (St. Louis, MO), respectively. Apoptotic cell death was measured with the ApopTag Red *In Situ* Apoptosis Detection Kit according to the manufacturer's instructions (Chemicon/Millipore, Billerica, MA).

Western blotting. For western blotting, the following primary antibody dilutions were used: 173EC2 hybridoma supernatant 1:40; 173EC3 affinity-purified antibody, 1:10,000; anti-GSK3β phospho-serine 9 and anti-Akt phospho-serine 478 antibodies 1:1000; anti-actin 1:4000.

Quantitative PCR. Quantitative PCR was performed using the SYBR GREEN PCR master mix (Applied Biosystems, Foster City, CA) according to the manufacturer's instructions. Primers for mouse cortactin were F: 5' gcagccatcccaggtgttttagtt 3'; R: 5' ctttggtccccttttcctcctcttc 3'; mouse MT1-MMP primers were F: 5' tgattctgccgagccctggactgt 3'; R 5' tgaggggcatctttgtgggtgac 3'; mouse Snail primers were F: 5' ctgcttcgagccatagaactaaag 3'; R 5' gaggggaactattgcatagtctgt 3'; GAPDH primers were F: 5' ccaaggtcatccatgacaact 3'; R: 5' gtcataccaggaaatgagcttgaca 3'.

Immunofluorescence. For Snail1 immunocytochemistry, cells were fixed in 4% paraformaldehyde, permeabilized with 1% sodium dodecyl sulfate, denatured with 6M urea, 0.1% glycine, pH 3.5, blocked with 3% goat serum, incubated with either 173EC2 (1:5) or 173EC3 (1:1000) overnight, followed by detection with Alexa 488-labeled anti-mouse secondary antibody (Invitrogen, Carlsbad, CA). The Alexa-532-labeled anti-MT1-MMP mAb1 was used at 5 μg/ml and the anti-

cortactin antibody was used at a dilution of 1:40 following paraformaldehyde fixation and permeabilization with Triton X-100. The anti-cortactin antibody was detected with an Alexa-488-labeled, anti-rabbit secondary antibody (Invitrogen, Carlsbad, CA). Cells were counterstained either with 4´,6-diamidino-2-phenylindole or propidium iodide (Invitrogen, Carlsbad, CA). Confocal images of cells were acquired on an Olympus FV500 confocal microscope using a 60X water immersion lens with a 1.20 numerical aperture using Fluoview software (Olympus, Center Valley, PA). All images comparing Snail1 wild-type and deficient cells were acquired with equal photomultiplier tube intensity and gain settings. Phase contrast images were acquired with a Leica DM-ILB inverted microscope with a 20X objective and 0.40 numerical aperture, and CAM images were acquired on a Leica DM-LB microscope with a 20X objective and 0.50 numerical aperture (Leica Microsystems GmbH, Wetzlar, Germany). Phase contrast and CAM images were acquired and analyzed with SPOT cameras and software (Diagnostic Instruments, Sterling Heights, MI).

Image analysis. To analyze MT1-MMP in invadopodia, confocal cross-sections of invadopodia co-stained for MT1-MMP and cortactin were analyzed with MetaMorph software (Molecular Devices, Downingtown, PA). Invadopodial clusters were traced, and area containing MT1-MMP and cortactin co-localization were quantified.

Cell culture and invasion assays. To analyze 3-D invasion, 50,000 fibroblasts were embedded in 100 µl type I collagen gel (2.2 mg/ml) isolated from rat tail (19). After gelling, the plug was embedded in a cell-free, 500 µl collagen gel (2.2 mg/ml) cultured within a 24 well plate. After allowing the surrounding collagen matrix to gel (1 h at 37^{o} C), fibroblast invasion was stimulated with serum and 10 ng/ml PDGF-BB (Millipore, Bellerica, MA). Invasion distance from the inner collagen plug into the outer collagen gel was quantified. CAM invasion assays were conducted using 11-d-old chick embryos where fibroblasts labeled with fluoresbrite carboxylated nanospheres (Polysciences) were cultured atop the CAM for 24 h. Invasion depth was defined as the leading front of at least three invading cells in 10 fields in frozen sections (19). Invasion area was defined as

area occupied by invading cells in at least ten fields (19) while angiogenesis was quantified by type IV collagen staining (23). Snail1 conditional knock-out transformed fibroblasts were generated by isolating E13.5 mouse embryonic fibroblasts followed by serial retroviral introduction of the polyoma large T and activated Ras oncogenes (24).

Transcriptional Profiling. Total RNA was isolated from fibroblast cultures in 3-D collagen, labeled, and hybridized to Affymetrix Mouse 430 2.0 cDNA microarrays. Three replicates each of Snail1 wild-type and deficient cultures were analyzed by the University of Michigan Microarray Core. Differentially expressed probesets were determined using a minimum fold change of 1.5 and maximum p-value of 0.005. Gene ontology analysis was performed to identify biologic processes transcriptionally regulated by Snail. Gene Ontology coefficients were calculated as –log(p-value).

Results.

Snail1 expression is induced by fibroblast activating growth factors.

Under serum-free conditions, fibroblasts do not express detectable levels of Snail1 mRNA or protein (Figure 4.1A, B). By contrast, in the presence of 10% serum or PDGF-BB, both Snail1 mRNA and intranuclear protein levels are strongly induced in mouse as well as human fibroblasts (Figure 4.1A-C). In epithelial cells, Snail1 protein half-life is controlled by GSK3β- dependent and independent ubiquitination pathways that lead to proteasome-mediated Snail1 destruction (11, 12, 25, 26). As expected, blockade of fibroblast proteasome activity with the inhibitor, MG132, results in a marked accumulation of the Snail1 protein (Figure 4.1B). In the GSK3β-dependent pathway, Snail1 is marked for ubiquitination following phosphorylation of its N-terminal domain (12, 25, 26). As PDGF-BB signaling can inhibit GSK3β activity via the phosphatidylinositol 3-kinase (PI3K)/Akt-dependent phosphorylation of GSK3β serine 9 (Ser^9) (27), Akt phosphorylation, Ser^9 phosphorylation and Snail1 protein levels were monitored in fibroblasts in the absence or presence of the PI3K inhibitor, LY 294002. As predicted, treatment of serum-starved fibroblasts with PDGF-BB induces an increase in phospho-Akt and Ser^9 GSK3β levels in tandem with an increase in Snail1 protein (Figure 4.1D, E). In the presence of LY 294002, however, both Akt and Ser^9- GSK3β phosphorylation are blocked and Snail1 levels fall to undetectable levels (Figure 4.1D, E).

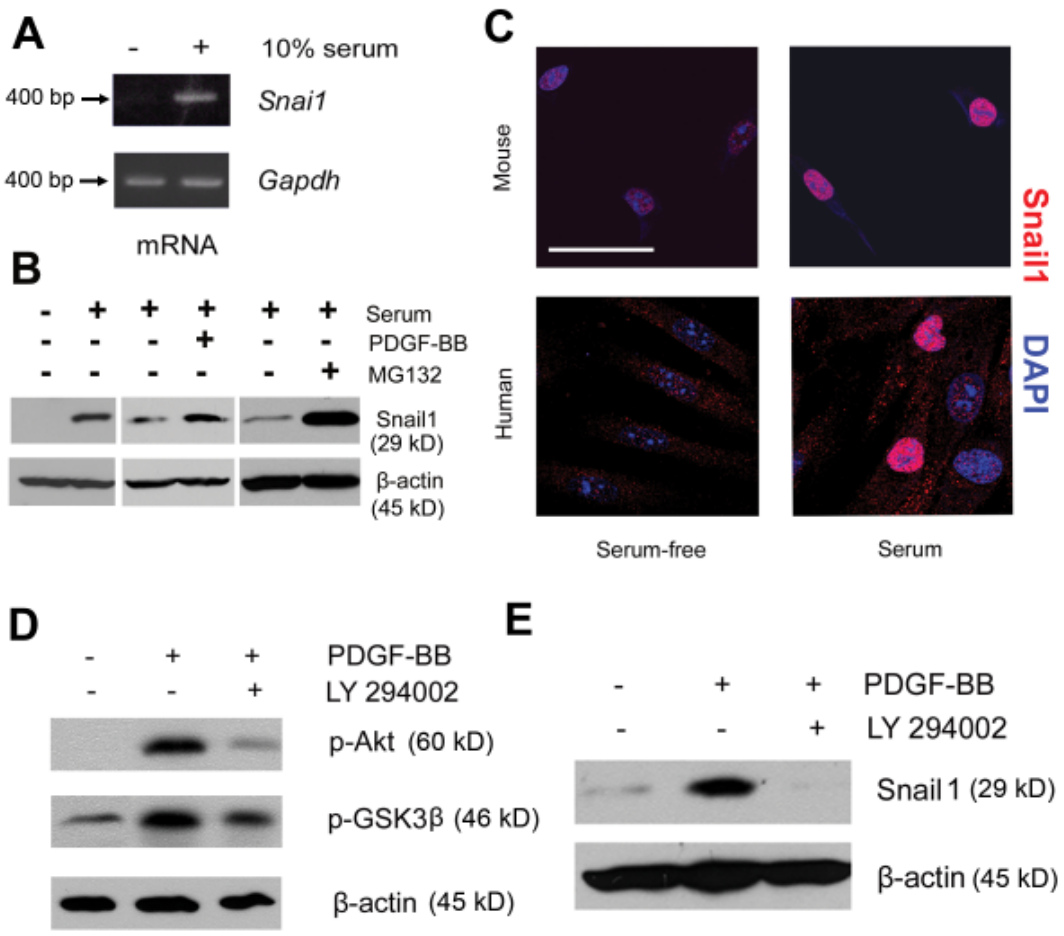

Figure 4.1. Expression and regulation of Snail1 in activated fibroblasts

A. Mouse dermal fibroblasts were cultured in the presence or absence of 10% serum for 24 h and Snail1 mRNA assessed by RT-PCR. **B.** Mouse dermal fibroblasts were cultured serum free, or in the presence of 10% serum, serum plus 10 ng/ml PDGF-BB, or serum plus 10 μM MG132 for 24 h, and Snail1 protein monitored by Western blot. **C.** Mouse fibroblasts (top panels) or human foreskin fibroblasts (bottom panels) were cultured serum-free or in the presence of 10% serum for 24 h, and Snail1 protein localized by immunocytochemistry with the anti-Snail1 173EC2 monoclonal antibody (mouse fibroblasts) or the Sn9H2 monoclonal antibody (human fibroblasts). Nuclei were stained with DAPI (blue). **D.** Mouse dermal fibroblasts were cultured serum-free for 48 h, followed by stimulation with PDGF-BB (10 ng/ml) in the presence or absence of LY294002 (10 μM) for 10 min. Levels of phospho-Ser^{478} Akt, phosho-Ser^{9} GSK3β, and β-actin were assessed by Western blot. **E.** Mouse dermal fibroblasts were cultured serum-free for 24 h, followed by stimulation with 10 ng/ml PDGF-BB for 12 h in the presence or absence of LY294002 and Snail1 protein levels determined by Western blot.

Generation and characterization of Snail1 deficient fibroblasts. *Snai1*-deficient mice die early in development prior to the differentiation of mesodermal lineages (1, 7). Hence, we analyzed fibroblast function in a mouse model wherein Snail1 can be conditionally inactivated via Cre/loxp-mediated recombination (Figure 4.2A-E). Fibroblasts isolated from a *Snai1*$^{+/fl}$ mouse were treated with an adenoviral Cre recombinase construct (adeno-Cre) or a control adenovirus [β-galactosidase (β-gal)], and recombination at the *Snai1* locus verified by PCR. As shown in Figure 4.2A, while adeno-βgal-infected fibroblasts yield P1/P2 amplicons corresponding to both the wild-type and loxp alleles of *Snai1*, adeno-Cre-infected fibroblasts yielded a single amplicon corresponding to the wild-type *Snai1* allele with P1 and P2, as well as a P3/P4 amplicon representing the *Snai1*$^{-}$ allele. Fibroblasts isolated from *Snai1*$^{fl/fl}$ mice and infected with adeno-Cre display a 95% reduction in Snail1 mRNA while Snail1 protein expression is undetectable by Western blot or immunocytochemistry (Figure 4.2B-D).

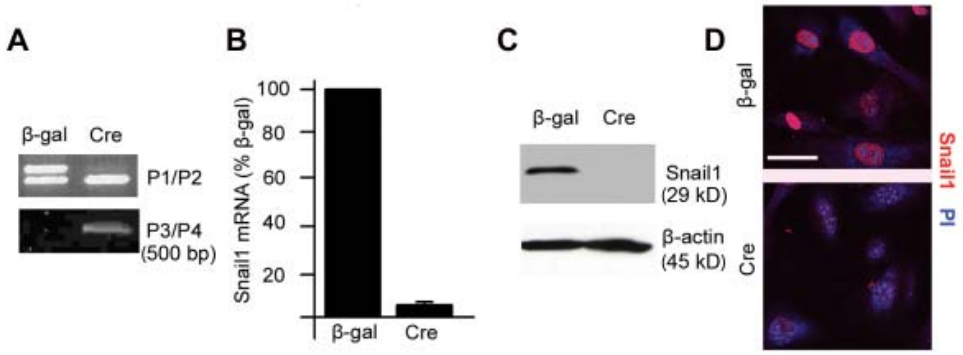

Figure 4.2. A model of Snail1 deficiency in mouse fibroblasts

A. *Snai1*$^{wt/fl}$ dermal fibroblasts were infected either with a control adenovirus (β-gal) or adeno-Cre, and recombination of the Snai1^{fl} allele assessed by the loss of the 420 base-pair amplicon when genomic DNA was amplified with P1 and P2 (top panel) and the appearance of a single amplicon with P3 and P4 (bottom panel). **B-D.** Snai1$^{fl/fl}$ dermal fibroblasts were infected with either a control adenovirus or a Cre adenovirus and Snai1 recombination assessed by quantitative PCR **(B)**, Western blot **(C)** or immunocytochemistry for Snail1 with mAb 173EC2 (red) with propidium iodide (PI) counterstaining (blue) **(D)**. Scale = 30 μm.

In addition to its well-defined role in promoting EMT, Snail1 has been suggested to regulate cell cycle progression and sensitivity to pro-apoptotic stresses (28-30). Snail1-deficient fibroblasts proliferate, however, at normal rates with no observed changes in apoptosis under serum-free conditions (Figure 4.3A-B). Furthermore, though Snail1 can promote a motile phenotype in epithelial cells (7, 30), Snail1-deleted fibroblasts migrate at rates comparable to wild-type fibroblasts in a 2-dimensional wound assay (Figure 4.4A). Likewise, whereas increased fibronectin synthesis and matrix assembly are characteristic features of EMT programs (7, 30), Snail1-deficient fibroblasts deposit a fibronectin matrix at rates comparable to control fibroblasts (Figure 4.4B). Consequently, insights into Snail1 function were alternatively sought by interrogating the gene expression patterns of Snail1-deleted fibroblasts.

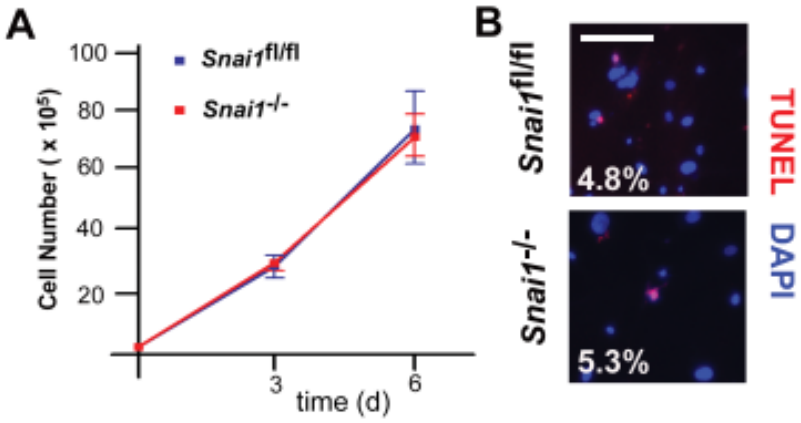

Figure 4.3. Snail1 does not regulate fibroblast 2-D proliferation or survival

A. Snail1 wild-type or deficient fibroblasts were cultured under traditional 2-D conditions. Cell number was counted at 3 d and 6 d incubation. **B.** Apoptosis of fibroblasts was measured by TUNEL stain following serum deprivation.

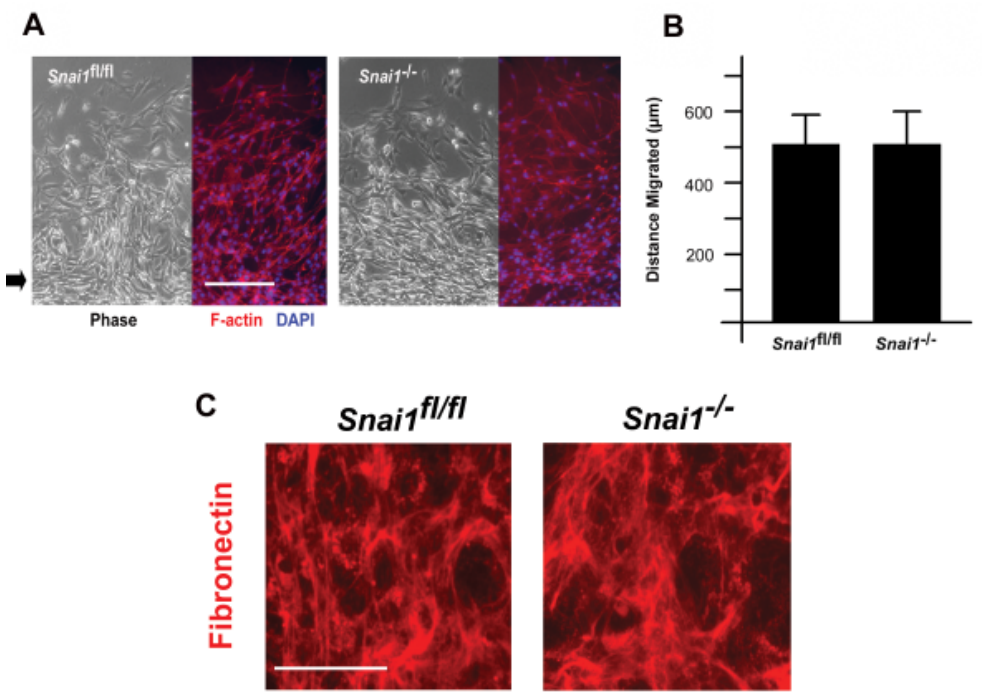

Figure 4.4. Snail1 does not regulate fibroblast 2-D motility or fibronectin deposition

A-B. Snail1 wild-type or deficient fibroblasts were cultured in the presence of a glass coverslip. After 24 h, the coverslip was removed, and migration into the cell-free area monitored. Scale = 100 μm. **C.** Fibroblasts were cultured in the presence of Alexa-594-labeled fibronectin, and fibril formation monitored by fluorescence microscopy.

Recent studies have demonstrated that cell behavior *in vitro* more closely recapitulates that observed *in vivo* when cells are cultured within a three-dimensional (3-D) extracellular matrix (ECM) (31-33). Hence, Snail1 wild-type and deficient cells were suspended in type I collagen matrices, the dominant matrix component of interstitial tissues (19, 34), and subjected to transcriptional profiling. Using cutoffs of $p \leq 0.005$ and a minimum fold-change of 1.5, Snail1 deficiency in fibroblasts exerts a global effect on transcription with over 1000 significant changes in gene expression detected (Figure 4.5A). Gene Ontology (GO) analysis further demonstrates that Snail1 governs multiple processes critical to fibroblast motile behavior, including adhesion, migration, and proteolysis (Figure 4.5B). Furthermore, Snail1 deficiency resulted in 32 microRNAs altered at least three-fold. Snail1 deletion did not trigger a

mesenchymal-to-epithelial transdifferentiation process as assessed by transcriptional analysis, suggesting that Snail1 is required for the induction, but not maintenance, of the mesenchymal phenotype during development.

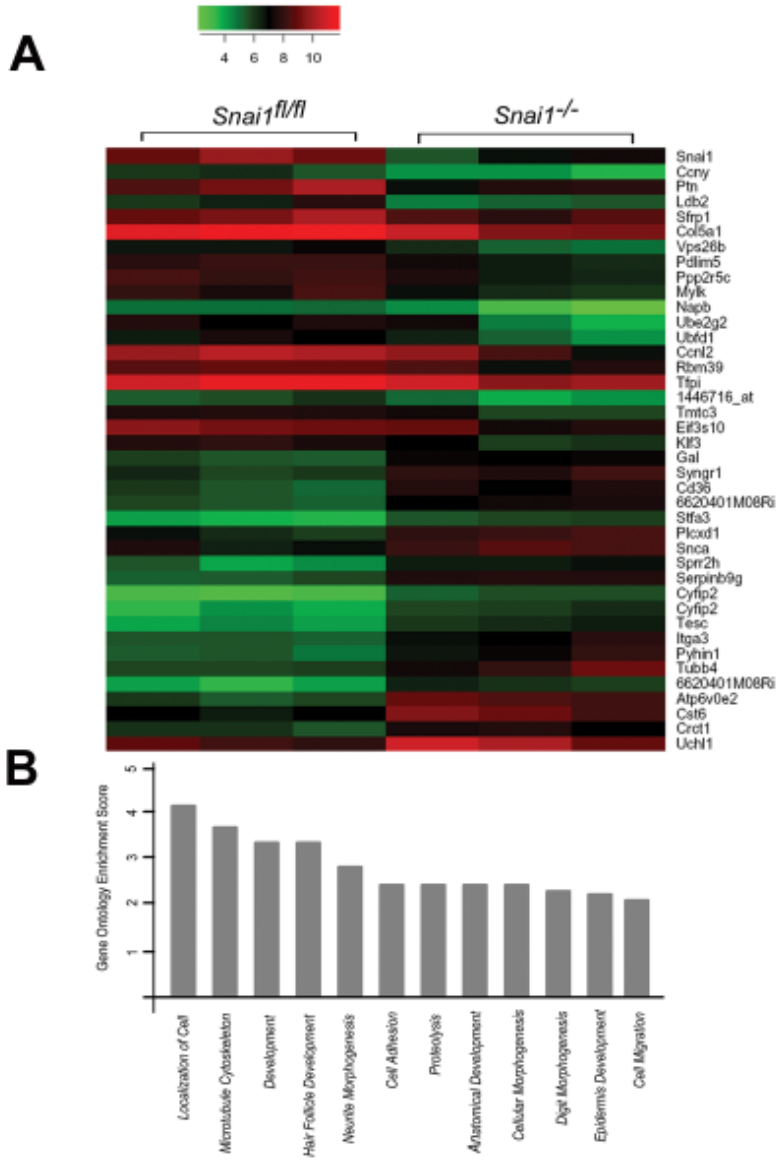

Figure 4.5. Snail1 is a master regulator of fibroblast gene expression programs

A. Heatmap of microarray data for three biologic replicates of Snail1$^{fl/fl}$ and Snail1$^{-/-}$ fibroblasts. The 20 most highly up-regulated and down-regulated transcripts in Snail1$^{-/-}$fibroblasts are presented. **B.** Gene ontology terms identifying biologic processes differentially expressed in *Snai1*$^{fl/fl}$ and deficient fibroblasts.

Snail1 regulates tissue invasive programs in mesenchymal cells. To assess the consequences of Snail1 loss on 3-D ECM invasion, a critical component of fibroblast wound and tumor responses (15-17, 19, 34), cells were embedded within a 3-D bed of type I collagen. Snail1-deleted, but not Snail1-rescued, fibroblasts displayed a significant defect in their ability to negotiate the type I collagen barrier (Figure 4.6A-B).

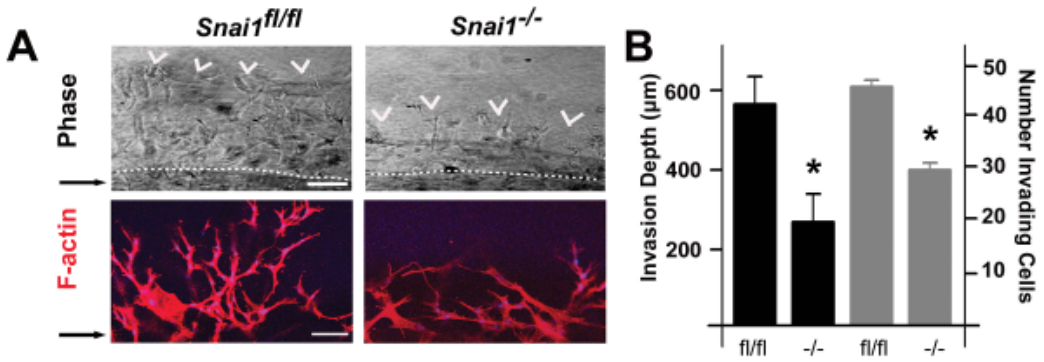

Figure 4.6. Snail1 regulates the 3-D invasive activities of fibroblasts

A. *Snai1*$^{fl/fl}$ or *Snai1*$^{-/-}$ fibroblasts were embedded in a 100 μl plug of cross-linked, fibrillar type I collagen (2.2 mg/ml) which was embedded within a larger, cell-free collagen matrix in the presence of 10 ng/ml PDGF-BB and 10% serum. Migration was monitored over a 6 d culture period by phase contrast microscopy with arrowheads marking the advance of the invading front and the dotted line indicating the boundary between the inner and outer collagen gels (scale = 200 μm; upper row of panels in *A*) or following phalloidin staining in the lower panels (red; scale = 100 μm). **B.** 3-D invasion depth and the number of invading cells were measured after a 6 d culture period (n = 3; mean ± SEM). *p < 0.01.

Focusing on candidate genes implicated previously in 3-D cell motility and invasion (35-37), probesets corresponding to transcripts for cortactin (*Cttn*), enabled homolog (*Enah*), ezrin, moesin, rhoA, ROCK1, myosin light chain kinase, tropomyosin and MT1-MMP (*Mmp14*) are significantly altered in Snail1-deficient fibroblasts (Table 4.1).

Gene Symbol	Gene Name	p-value	Fold-change
Cttn	cortactin	0.003	-1.74
Enah	enabled homolog	0	-2.27
Ezr	ezrin	0	2.6
Msn	moesin	0.001	-2
Rhoa	Ras homolog gene family, member A	0	-1.99
Rock1	Rho-associated coiled-coil containing protein kinase 1	0.004	-1.71
Mylk	myosin, light polypeptide kinase	0	-2.3
Tpm1	tropomyosin 1, alpha	0	-2.08
Mmp14	matrix metallopeptidase 14 (membrane-inserted)	0.003	-1.88

Table 4.1. Motility-associated genes deregulated in Snail1-deficient fibroblasts in 3-D.

Consistent with the altered patterns of gene expression revealed by the microarray data and confirmed by quantitative PCR (Figure 4.7), Snail1-deficient fibroblasts exhibit a significant reduction in the cortactin-rich membrane protrusions that mark invadopodia – actin-rich, cellular processes that focus proteolytic activity at sites of cell:ECM contact (i.e., 83.3 ± 8.3% cortactin-positive processes in wild-type fibroblasts vs 31.2 ± 13.2% in Snail1-deleted fibroblasts, $p < 0.01$; Figure 4.8A) (38).

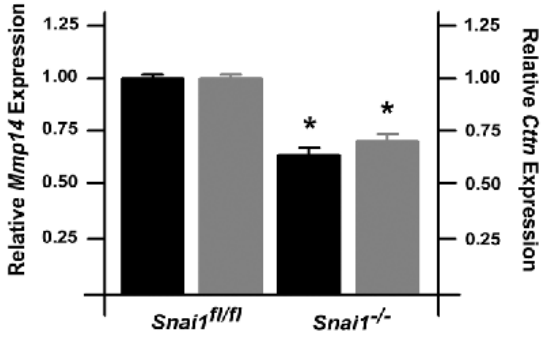

Figure 4.7. Snail1 controls mRNA expression of 3-D invasion-associated genes

Messenger RNA levels of the transcripts for cortactin (*Cttn*) or MT1-MMP (*Mmp14*) were measured in *Snail1*$^{fl/fl}$ or *Snail1*$^{-/-}$ fibroblasts by quantitative PCR.

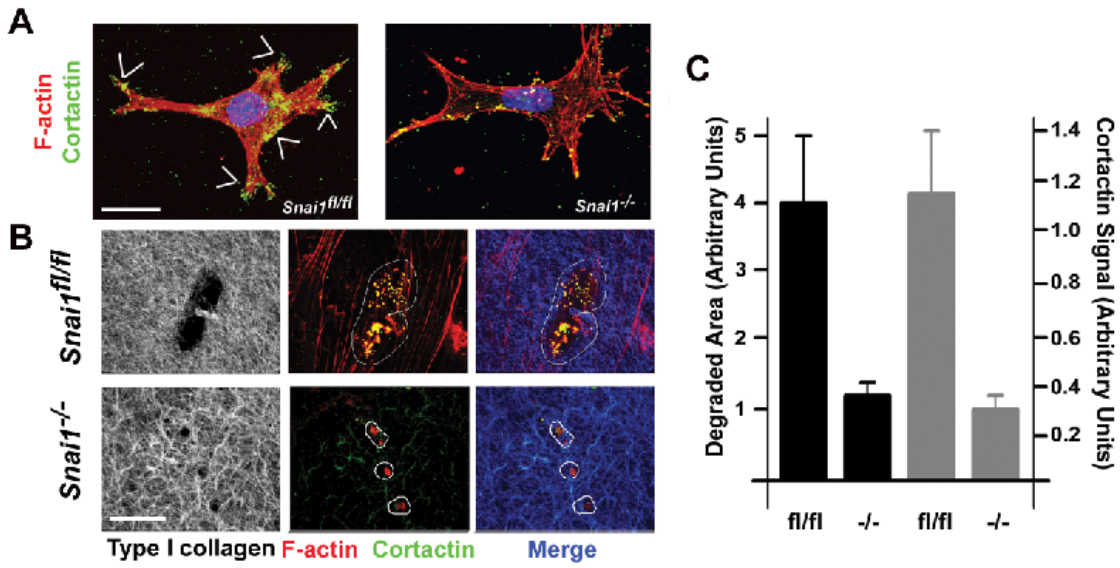

Figure 4.8. Snail1 regulates fibroblast cortactin localization and collagen degradation

A. Snail1$^{fl/fl}$ or Snail1$^{-/-}$ fibroblasts were cultured in 3-D collagen for 48 h and stained for cortactin (green), F-actin (red) and nuclei (DAPI, blue) and images captured by confocal laser microscopy. Scale = 10 μm. Cortactin-rich cellular processes are marked by arrowheads. **B-C.** Fibroblasts were cultured atop a 3-D bed of Alexa-594-labeled type I collagen (grey, left panels; blue, right panels) for 5 d and collagen degradation monitored by confocal laser microscopy in sections co-stained for cortactin (green) and F-actin (red, middle and right panels) (**B**) and quantified using Imagequant software in the photomicrographs (**C**). Degraded areas in left panels are demarcated by broken lines in the middle and right panels. Scale = 10 μm. (**C**) Degraded area and relative cortactin signal are presented as representative results of three experiments with the mean ± SEM (* $p < 0.05$).

As cortactin-rich invadopodia play a critical role in recruiting MT1-MMP, a membrane-anchored collagenase critical for cell invasion, to zones of pericellular proteolysis (39-41), wild-type and Snail1-deficient fibroblasts were cultured with Alexa-594-labeled type I collagen, and collagenolysis monitored (19). Whereas wild-type fibroblasts generate collagenolytic zones that are associated with adhesive sites enriched for actin spikes and cortactin, Snail1-deficient fibroblasts exhibit a significantly diminished ability to degrade collagen or mobilize invadopodia (Figure 4.8B). In accordance with these collagenolytic defects, invadopodial clusters of MT1-MMP and cortactin localized at the fibroblast-collagen interface are reduced by ~80% in Snail1-deficient cells (Figure 4.9).

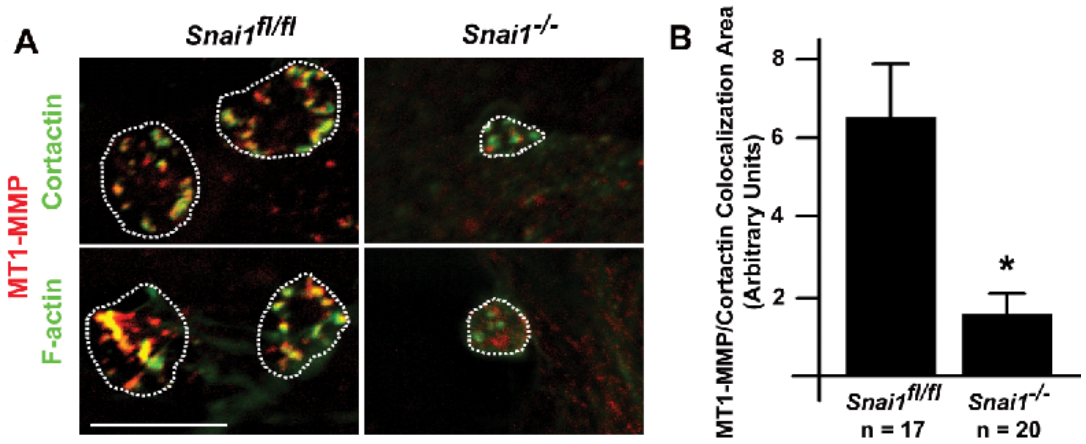

Figure 4.9. Snail1 regulates cortactin and MT1-MMP localization at invadopodia

A. *Snail1*$^{fl/fl}$ or Snail1$^{-/-}$ fibroblasts were cultured on a bed of type I collagen and co-stained for MT1-MMP (red) and either cortactin (green, upper panels) or F-actin (green, lower panels; 60X magnification, scale = 5 μm). **B.** MT1-MMP signal co-localizing with cortactin and actin within invadopodia clusters was quantified using Metamorph software.

Reconstitution of Snail1-deficient fibroblasts with full-length human Snail1 normalizes expression of cortactin and MT1-MMP and rescues the collagen-invasive phenotype (Figure 4.10). Further, consistent with a GO enrichment scores that did not detect changes in cell cycle or apoptosis regulation, wild-type or Snail1-deleted fibroblasts embedded within 3-D collagen gels proliferate at indistinguishable rates (7.8% ± 3.2% Ki67-positive for Snail1 wild-type cells versus 8.1 ± 1.4% Ki67-positive for Snail1-null cells, n = 3) and display similar low levels of apoptosis (Snail1 wild-type: 1.6 ± 0.8%; Snail1-null: 1.4 ± 1.4%, assessed by TUNEL; n = 3).

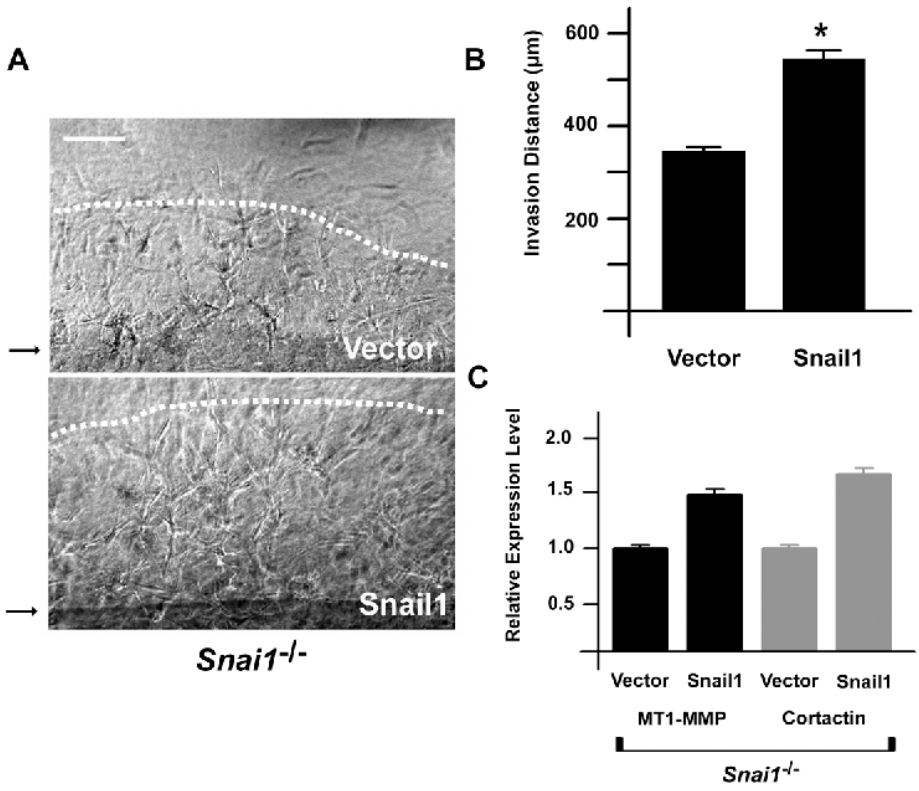

Figure 4.10. Rescue of cortactin and MT1-MMP expression and 3-D invasion by reconstitution with Snail1

A-B. Snail1-deficient fibroblasts were engineered to express full-length, wild-type Snail1 and 3-D type I collagen invasion monitored. Scale = 200 μm. **C.** Snail1-deficient fibroblasts were engineered to express full-length, wild-type Snail1, and levels of *Cttn* and *Mmp14* were measured by quantitative PCR.

Snail1 regulates invasion of ECM barriers *in vivo.* Though Snail1-deficient cells display defects in the pericellular proteolysis and invasion of homogeneous collagenous barriers *in vitro,* connective tissue barriers *in vivo* are complex, multi-molecular composites of ECM macromolecules (31-34). As such, wild-type and Snail1-deleted fibroblasts were cultured atop the chorioallantoic membrane (CAM) of live chick embryos (19), a tissue characterized by a type IV collagen-rich basement membrane and an underlying interstitium containing both type I and type III collagens (the stroma also contains blood vessels circumscribed by type IV collagen-positive basement membranes) (Figure 4.11).

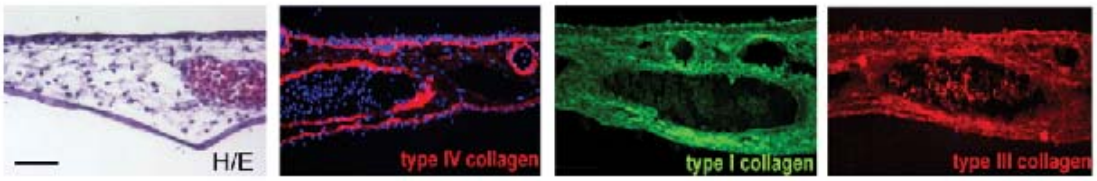

Figure 4.11. Components of the CAM ECM barrier

CAM sections were stained with (left to right) hematoxylin and eosin, or antibodies against type IV, I, and III collagens and photographed using light or fluorescence microscopy. Scale = 100 μm.

While wild-type fibroblasts efficiently breach the CAM basement membrane and invade into the underlying stroma, Snail1-deficient fibroblasts exhibit a complete defect in invasion and fail to penetrate the CAM surface (Figure 4.12A-B) – a phenotype identical to that reported previously for MT1-MMP-null fibroblasts (19). *In vivo*, fibroblasts can initiate neovascularization during wound healing *in vivo* (15), but Snail1-deficient fibroblasts also demonstrate a significantly attenuated ability to induce neovessel formation (Figure 4.12A, C). Neither proliferative nor apoptotic indices of the fibroblasts are affected in the CAM model (Figure 4.13). Taken together, the data identify Snail1 as a master regulator of activated fibroblast function *in vivo* by controlling tissue-invasive as well as pro-angiogenic functions.

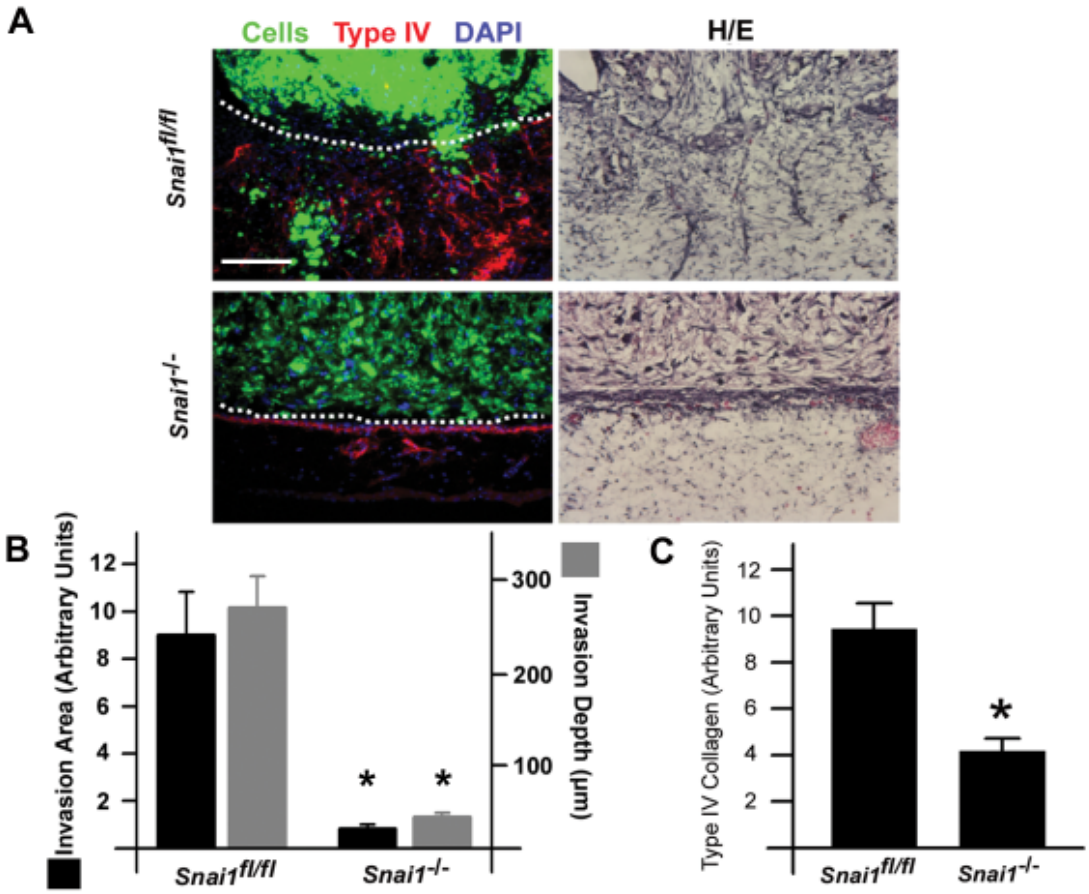

Figure 4.12. Snail1 and the fibroblast wound response in vivo

A. *Snai1*$^{fl/fl}$ or *Snai1*$^{-/-}$ fibroblasts were labeled with green fluorescent nanobeads, and cultured atop the live CAM. After 24 h, CAMs were sectioned and assessed for invasion by fluorescence microscopy for labeled cells (green), type IV collagen (red), cell nuclei (blue, left panels) or H/E staining (right panels). The broken line marks the upper surface of the CAM. Scale bar = 100 μm. **B.** CAM invasion was quantified by measuring invasive area demarcated by distribution of fluorescent beads in the CAM stroma or depth of the invasive front (n = 5; mean ± SEM). *p = 0.02 for invasion area and *p = 0.01 for invasion depth. **C.** Utilizing type IV collagen signal in the CAM interstitium as an index of neovessel formation, CAM stromal angiogenesis was quantified (n = 11 for wild-type, n = 9 for null; mean ± SEM, *p < 0.01).

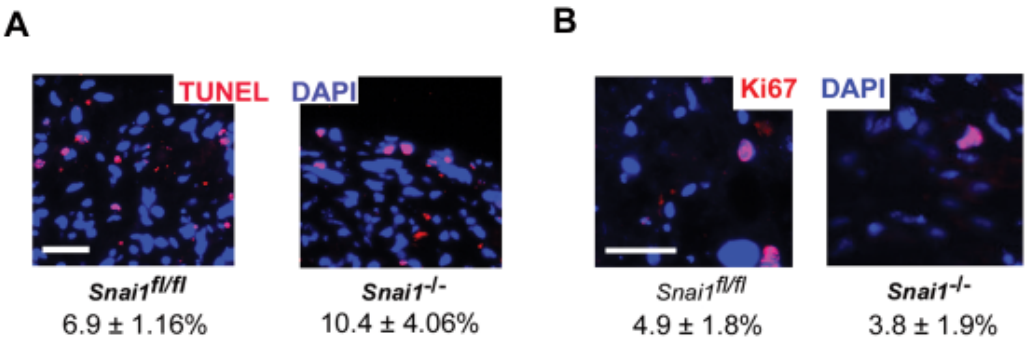

Figure 4.13. Fibroblast proliferation and survival on the CAM are independent of Snail1 function

A. CAM sections were stained for the apoptosis marker, TUNEL (red) and counterstained with DAPI (blue), and % TUNEL-positive cells were quantified (n = 3; mean ± SEM). **B.** CAM sections were stained for the proliferation marker Ki67 (red), nuclei counterstained with DAPI (blue) and % Ki67-positive nuclei quantified (n = 3; mean ± SEM). Scale bar = 50 μm for **A,B**.

Discussion.

Snail1 exerts global effects on epithelial cell gene expression by binding consensus sequences within the promoter regions of target genes while recruiting histone deactylases, arginine methyltransferase, and DNA methyltransferases to chromatin remodeling complexes (7, 42, 43). Despite the remarkable range of Snail1's impact on epithelial cell fate determination, a functional role for Snail1 in terminally differentiated mesenchymal cells has not been explored previously. Unexpectedly, under 3-D culture conditions, GO analyses revealed that major shifts had occurred in fibroblast behavior in the absence of Snail1 expression with changes concentrated in functional programs tightly linked to cell adhesion, migration, proteolysis and morphogenesis. Among Snail1-regulated targets, cortactin has been reported to regulate MT1-MMP-dependent proteolysis, an activity critical for mesenchymal cell trafficking through ECM barriers (19, 39, 40, 44-46). As such, the defects in cortactin and MT1-MMP expression and function observed in Snail1-deficient fibroblasts, in tandem with predicted changes in accessory molecules such as rhoA, ROCK, myosin light chain kinase and tropomyosin, correlated with a marked loss in collagenolytic potential as well tissue-invasive activity *in vitro* and *in vivo*. Snail1-deleted fibroblasts were also unable to initiate an angiogenic response, a result likely consistent with the ability of MT1-MMP to induce angiogenesis by generating bioactive collagen fragments, regulating VEGF expression or mediating semiphorin 4D shedding (47-49).

To date, analyses of Snail1 function in mammalian cells have focused on the ability of the transcription factor to initiate the transdifferentiation of normal or neoplastic epithelial cells. The findings presented herein, coupled with the fact that Snail1 protein is expressed in fibroblasts localized at damaged or carcinomatous tissues *in vivo* (21, 22), demonstrate that Snail1 activity is not confined to epithelial cells alone. While our studies have focused on the role of Snail1 in regulating fibroblast function, it is intriguing to note that Snail1 may also be expressed in the neoplastic mesenchyme (22), suggesting a potential role in mesenchymal tumors. Hence, in addition to its essential roles in EMT, we

propose that Snail1 now be considered as a transcription factor capable of exerting key regulatory effects in the mesenchyme during development as well as disease.

References.

1. Carver, E.A., Jiang, R., Lan, Y., Oram, K.F., and Gridley, T. 2001. The mouse snail gene encodes a key regulator of the epithelial-mesenchymal transition. *Mol Cell Biol* 21:8184-8188.

2. Nieto, M.A. 2002. The snail superfamily of zinc-finger transcription factors. *Nat Rev Mol Cell Biol* 3:155-166.

3. Murray, S.A., Oram, K.F., and Gridley, T. 2007. Multiple functions of Snail family genes during palate development in mice. *Development* 134:1789-1797.

4. Batlle, E., Sancho, E., Franci, C., Dominguez, D., Monfar, M., Baulida, J., and Garcia De Herreros, A. 2000. The transcription factor snail is a repressor of E-cadherin gene expression in epithelial tumour cells. *Nat Cell Biol* 2:84-89.

5. Cano, A., Perez-Moreno, M.A., Rodrigo, I., Locascio, A., Blanco, M.J., del Barrio, M.G., Portillo, F., and Nieto, M.A. 2000. The transcription factor snail controls epithelial-mesenchymal transitions by repressing E-cadherin expression. *Nat Cell Biol* 2:76-83.

6. Moreno-Bueno, G., Cubillo, E., Sarrio, D., Peinado, H., Rodriguez-Pinilla, S.M., Villa, S., Bolos, V., Jorda, M., Fabra, A., Portillo, F., et al. 2006. Genetic profiling of epithelial cells expressing E-cadherin repressors reveals a distinct role for Snail, Slug, and E47 factors in epithelial-mesenchymal transition. *Cancer Res* 66:9543-9556.

7. Peinado, H., Olmeda, D., and Cano, A. 2007. Snail, Zeb and bHLH factors in tumour progression: an alliance against the epithelial phenotype? *Nat Rev Cancer* 7:415-428.

8. Boutet, A., De Frutos, C.A., Maxwell, P.H., Mayol, M.J., Romero, J., and Nieto, M.A. 2006. Snail activation disrupts tissue homeostasis and induces fibrosis in the adult kidney. *Embo J* 25:5603-5613.

9. Olmeda, D., Jorda, M., Peinado, H., Fabra, A., and Cano, A. 2007. Snail silencing effectively suppresses tumour growth and invasiveness. *Oncogene* 26:1862-1874.

10. Olmeda, D., Moreno-Bueno, G., Flores, J.M., Fabra, A., Portillo, F., and Cano, A. 2007. SNAI1 is required for tumor growth and lymph node metastasis of human breast carcinoma MDA-MB-231 cells. *Cancer Res* 67:11721-11731.

11. Yook, J.I., Li, X.Y., Ota, I., Fearon, E.R., and Weiss, S.J. 2005. Wnt-dependent regulation of the E-cadherin repressor snail. *J Biol Chem* 280:11740-11748.

12. Yook, J.I., Li, X.Y., Ota, I., Hu, C., Kim, H.S., Kim, N.H., Cha, S.Y., Ryu, J.K., Choi, Y.J., Kim, J., et al. 2006. A Wnt-Axin2-GSK3beta cascade regulates Snail1 activity in breast cancer cells. *Nat Cell Biol* 8:1398-1406.

13. Klapholz-Brown, Z., Walmsley, G.G., Nusse, Y.M., Nusse, R., and Brown, P.O. 2007. Transcriptional program induced by Wnt protein in human fibroblasts suggests mechanisms for cell cooperativity in defining tissue microenvironments. *PLoS ONE* 2:e945.

14. Dong, J., Grunstein, J., Tejada, M., Peale, F., Frantz, G., Liang, W.C., Bai, W., Yu, L., Kowalski, J., Liang, X., et al. 2004. VEGF-null cells require PDGFR alpha signaling-mediated stromal fibroblast recruitment for tumorigenesis. *Embo J* 23:2800-2810.

15. Martin, P. 1997. Wound healing--aiming for perfect skin regeneration. *Science* 276:75-81.

16. Orimo, A., Gupta, P.B., Sgroi, D.C., Arenzana-Seisdedos, F., Delaunay, T., Naeem, R., Carey, V.J., Richardson, A.L., and Weinberg, R.A. 2005. Stromal fibroblasts present in invasive human breast carcinomas promote tumor growth and angiogenesis through elevated SDF-1/CXCL12 secretion. *Cell* 121:335-348.

17. Bhowmick, N.A., Neilson, E.G., and Moses, H.L. 2004. Stromal fibroblasts in cancer initiation and progression. *Nature* 432:332-337.

18. Iyer, V.R., Eisen, M.B., Ross, D.T., Schuler, G., Moore, T., Lee, J.C., Trent, J.M., Staudt, L.M., Hudson, J., Jr., Boguski, M.S., et al. 1999. The transcriptional program in the response of human fibroblasts to serum. *Science* 283:83-87.

19. Sabeh, F., Ota, I., Holmbeck, K., Birkedal-Hansen, H., Soloway, P., Balbin, M., Lopez-Otin, C., Shapiro, S., Inada, M., Krane, S., et al. 2004. Tumor cell traffic through the extracellular matrix is controlled by the membrane-anchored collagenase MT1-MMP. *J Cell Biol* 167:769-781.

20. Gao, Z., Sasaoka, T., Fujimori, T., Oya, T., Ishii, Y., Sabit, H., Kawaguchi, M., Kurotaki, Y., Naito, M., Wada, T., et al. 2005. Deletion of the PDGFR-beta gene affects key fibroblast functions important for wound healing. *J Biol Chem* 280:9375-9389.

21. Rosivatz, E., Becker, K.F., Kremmer, E., Schott, C., Blechschmidt, K., Hofler, H., and Sarbia, M. 2006. Expression and nuclear localization of

Snail, an E-cadherin repressor, in adenocarcinomas of the upper gastrointestinal tract. *Virchows Arch* 448:277-287.

22. Franci, C., Takkunen, M., Dave, N., Alameda, F., Gomez, S., Rodriguez, R., Escriva, M., Montserrat-Sentis, B., Baro, T., Garrido, M., et al. 2006. Expression of Snail protein in tumor-stroma interface. *Oncogene* 25:5134-5144.

23. Bajou, K., Masson, V., Gerard, R.D., Schmitt, P.M., Albert, V., Praus, M., Lund, L.R., Frandsen, T.L., Brunner, N., Dano, K., et al. 2001. The plasminogen activator inhibitor PAI-1 controls in vivo tumor vascularization by interaction with proteases, not vitronectin. Implications for antiangiogenic strategies. *J Cell Biol* 152:777-784.

24. Land, H., Parada, L.F., and Weinberg, R.A. 1983. Tumorigenic conversion of primary embryo fibroblasts requires at least two cooperating oncogenes. *Nature* 304:596-602.

25. Zhou, B.P., Deng, J., Xia, W., Xu, J., Li, Y.M., Gunduz, M., and Hung, M.C. 2004. Dual regulation of Snail by GSK-3beta-mediated phosphorylation in control of epithelial-mesenchymal transition. *Nat Cell Biol* 6:931-940.

26. Vernon, A.E., and LaBonne, C. 2006. Slug stability is dynamically regulated during neural crest development by the F-box protein Ppa. *Development* 133:3359-3370.

27. Julien, S., Puig, I., Caretti, E., Bonaventure, J., Nelles, L., van Roy, F., Dargemont, C., de Herreros, A.G., Bellacosa, A., and Larue, L. 2007. Activation of NF-kappaB by Akt upregulates Snail expression and induces epithelium mesenchyme transition. *Oncogene* 26:7445-7456.

28. Escriva, M., Peiro, S., Herranz, N., Villagrasa, P., Dave, N., Montserrat-Sentis, B., Murray, S.A., Franci, C., Gridley, T., Virtanen, I., et al. 2008. Repression of PTEN phosphatase by Snail1 transcriptional factor during gamma radiation-induced apoptosis. *Mol Cell Biol* 28:1528-1540.

29. Vega, S., Morales, A.V., Ocana, O.H., Valdes, F., Fabregat, I., and Nieto, M.A. 2004. Snail blocks the cell cycle and confers resistance to cell death. *Genes Dev* 18:1131-1143.

30. Barrallo-Gimeno, A., and Nieto, M.A. 2005. The Snail genes as inducers of cell movement and survival: implications in development and cancer. *Development* 132:3151-3161.

31. Yamada, K.M., and Cukierman, E. 2007. Modeling tissue morphogenesis and cancer in 3D. *Cell* 130:601-610.

32. Hotary, K.B., Allen, E.D., Brooks, P.C., Datta, N.S., Long, M.W., and Weiss, S.J. 2003. Membrane type I matrix metalloproteinase usurps tumor growth control imposed by the three-dimensional extracellular matrix. *Cell* 114:33-45.

33. Zhou, X., Rowe, R.G., Hiraoka, N., George, J.P., Wirtz, D., Mosher, D.F., Virtanen, I., Chernousov, M.A., and Weiss, S.J. 2008. Fibronectin fibrillogenesis regulates three-dimensional neovessel formation. *Genes Dev* 22:1231-1243.

34. Grinnell, F. 2003. Fibroblast biology in three-dimensional collagen matrices. *Trends Cell Biol* 13:264-269.

35. Yamaguchi, H., and Condeelis, J. 2007. Regulation of the actin cytoskeleton in cancer cell migration and invasion. *Biochim Biophys Acta* 1773:642-652.

36. Olson, M.F., and Sahai, E. 2008. The actin cytoskeleton in cancer cell motility. *Clin Exp Metastasis*.

37. Sakurai-Yageta, M., Recchi, C., Le Dez, G., Sibarita, J.B., Daviet, L., Camonis, J., D'Souza-Schorey, C., and Chavrier, P. 2008. The interaction of IQGAP1 with the exocyst complex is required for tumor cell invasion downstream of Cdc42 and RhoA. *J Cell Biol* 181:985-998.

38. Gimona, M., Buccione, R., Courtneidge, S.A., and Linder, S. 2008. Assembly and biological role of podosomes and invadopodia. *Curr Opin Cell Biol* 20:235-241.

39. Clark, E.S., Whigham, A.S., Yarbrough, W.G., and Weaver, A.M. 2007. Cortactin is an essential regulator of matrix metalloproteinase secretion and extracellular matrix degradation in invadopodia. *Cancer Res* 67:4227-4235.

40. Artym, V.V., Zhang, Y., Seillier-Moiseiwitsch, F., Yamada, K.M., and Mueller, S.C. 2006. Dynamic interactions of cortactin and membrane type 1 matrix metalloproteinase at invadopodia: defining the stages of invadopodia formation and function. *Cancer Res* 66:3034-3043.

41. Li, X.Y., Ota, I., Yana, I., Sabeh, F., and Weiss, S.J. 2008. Molecular Dissection of the Structural Machinery Underlying the Tissue-Invasive Activity of MT1-MMP. *Mol Biol Cell* 19:3221-3233.

42. Herranz, N., Pasini, D., Diaz, V.M., Franci, C., Gutierrez, A., Dave, N., Escriva, M., Hernandez-Munoz, I., Di Croce, L., Helin, K., et al. 2008. Polycomb complex 2 is required for E-cadherin repression by the Snail1 transcription factor. *Mol Cell Biol* 28:4772-4781.

43. Hou, Z., Peng, H., Ayyanathan, K., Yan, K.P., Langer, E.M., Longmore, G.D., and Rauscher, F.J., 3rd. 2008. The LIM protein AJUBA recruits protein arginine methyltransferase 5 to mediate SNAIL-dependent transcriptional repression. *Mol Cell Biol* 28:3198-3207.

44. Hotary, K., Li, X.Y., Allen, E., Stevens, S.L., and Weiss, S.J. 2006. A cancer cell metalloprotease triad regulates the basement membrane transmigration program. *Genes Dev* 20:2673-2686.

45. Chun, T.H., Sabeh, F., Ota, I., Murphy, H., McDonagh, K.T., Holmbeck, K., Birkedal-Hansen, H., Allen, E.D., and Weiss, S.J. 2004. MT1-MMP-dependent neovessel formation within the confines of the three-dimensional extracellular matrix. *J Cell Biol* 167:757-767.

46. Filippov, S., Koenig, G.C., Chun, T.H., Hotary, K.B., Ota, I., Bugge, T.H., Roberts, J.D., Fay, W.P., Birkedal-Hansen, H., Holmbeck, K., et al. 2005. MT1-matrix metalloproteinase directs arterial wall invasion and neointima formation by vascular smooth muscle cells. *J Exp Med* 202:663-671.

47. Basile, J.R., Holmbeck, K., Bugge, T.H., and Gutkind, J.S. 2007. MT1-MMP controls tumor-induced angiogenesis through the release of semaphorin 4D. *J Biol Chem* 282:6899-6905.

48. Weathington, N.M., van Houwelingen, A.H., Noerager, B.D., Jackson, P.L., Kraneveld, A.D., Galin, F.S., Folkerts, G., Nijkamp, F.P., and Blalock, J.E. 2006. A novel peptide CXCR ligand derived from extracellular matrix degradation during airway inflammation. *Nat Med* 12:317-323.

49. Sounni, N.E., Roghi, C., Chabottaux, V., Janssen, M., Munaut, C., Maquoi, E., Galvez, B.G., Gilles, C., Frankenne, F., Murphy, G., et al. 2004. Up-regulation of vascular endothelial growth factor-A by active membrane-type 1 matrix metalloproteinase through activation of Src-tyrosine kinases. *J Biol Chem* 279:13564-13574.

Chapter 5: Fibronectin Fibrillogenesis Regulates 3-D Neovessel Formation

Introduction.

Under quiescent conditions, the endothelium of the patent vasculature exists as a 2-dimensional (2-D) monolayer that rests atop a self-organized basement membrane which serves to separate the cells from the underlying interstitial matrix (1, 2). During angiogenesis and vasculogenesis, this structural arrangement is disrupted as endothelial cells embed themselves within a 3-dimensional (3-D) ECM dominated by either crosslinked networks of the clotting protein, fibrin, or the triple-helical matrix molecule, type I collagen (1, 2). Within this extrinsic matrix, endothelial cells are exposed to angiogenic growth factors that initiate the migratory, proliferative and tubulogenic responses required for the development of the neovasculature (1, 2). Growth factors acting alone, however, are unable to trigger angiogenesis (3-6). Endothelial cells must concurrently establish productive integrin-mediated adhesive interactions with matrix-bound ligands and undergo shape changes critical to the activation of actomyosin-dependent contractile responses which serve to trigger the motogenic, proliferative and morphogenic programs that underlie neovascularization (3-8).

Using traditional, 2-D culture systems, the responsiveness of adherent cell populations to soluble growth factors is modulated by the composition, density and topology of adhesive ligands as well as the mechanical properties of the supporting matrix itself (7-10). However, an increasing body of evidence indicates that standard 2-D culture systems do not recapitulate accurately cell behavior displayed in the 3-D *in vivo* setting (11-15). Indeed, when cells are cultured within the confines of 3-D extracellular matrices *in vitro*, cell-matrix adhesive interactions are established that more closely approximate those observed *in vivo,* and in coincident fashion, the cell cytoskeleton reorganizes into

patterns that mimic those exhibited by intact tissues (11-14, 16-18). Despite the described contrasts between 2-D and 3-D cell behavior, the mechanisms by which pro-angiogenic endothelial cells remodel the surrounding 3-D ECM to generate an adhesive platform that allows them to interpret the biochemical and mechanical inputs critical to neovessel formation remain undefined. Herein, we demonstrate that the endothelial cell-dependent unfolding and pericellular polymerization of the soluble glycoprotein, fibronectin (Fn), plays a required - and 3-D-specific - role in triggering neovascularization. By constructing a pericellular scaffold of polymerized Fn fibrils, endothelial cells are able to assemble a functional cytoskeletal-actomyosin complex and modulate their intracellular viscoelastic properties to engage the mechanotransduction-sensitive programs that drive 3-D neovessel formation.

Materials and Methods.

Endothelial Cell Isolation and 2-D/3-D Culture. Endothelial cells were isolated from human umbilical cord veins by collagenase digestion and cultured in Medium 199 (Gibco) containing 20% human serum, 50 µg/ml endothelial cell growth supplement (BD Biosciences), 100 U/ml penicillin, and 100 µg/ml streptomycin (Hiraoka et al., 1998). For 2-D/3-D culture, endothelial cell monolayers (no later than third passage) were suspended by mild trypsinization and dispersed within or plated atop fibrin (3 mg/ml) or collagen (2.2 mg/ml) gels (prepared as described; Hiraoka et al., 1998; Hotary et al., 2003), and stimulated with a cocktail of growth factors including 100 ng/ml human vascular endothelial growth factor (Genentech), 50 ng/ml human hepatocyte growth factor (Genentech), 10 ng/ml human TGFα (Biosource), 0.5 ng/ml TGFβ1 (R and D Systems), and 100 µg/ml heparin (Sigma). In selected experiments, endothelial cell spheroids were prepared and suspended in 3-D fibrin gels.

To monitor Fn matrix assembly or to assess the impact of inhibiting Fn matrix assembly on endothelial cell function, human serum was depleted of Fn by gelatin-sepharose affinity chromatography (Amersham) and supplemented with either 20 µg/ml of human plasma Fn (Sigma) or FITC-labeled Fn. Where indicated, endothelial cells were incubated with mouse IgG (Pierce), monoclonal antibody L8, monoclonal antibody 9D2 (final concentration of 100 µg/ml), the 70 kD Fn fragment (Sigma; 75 µg/ml), the FUD peptide (250 n*M*), ± Blebbistatin (Calbiochem; 50 µ*M*), or cytochalasin D (Sigma; 10 µ*M*) during 3-D culture. Cell number in 3-D cultures was determined by hemacytometry after dissolving gels with 2 mg/ml bacterial collagenase (Worthington) while the number of patent tubules was determined in randomly selected cross-sections.

To monitor endothelial cell contractility, 2-D or 3-D cultures cast in 24 well plates at 2 d incubation (prior to commencement of 3-D proliferation) were detached from the tissue culture plate and cells were allowed to contract the matrices for 10 h, at which time gel diameter was measured. To assess migration in 2-D, endothelial cells were plated atop a fibrin substratum in the presence of a glass coverslip. After attachment, the coverslip was removed and

migration into the cell-free area monitored over 2 d. To monitor 3-D migration, endothelial cells were suspended in 3-D fibrin gels in 96-well tissue culture plates. After formation of the fibrin gel, the gels were removed and embedded within fibrin gels in 24-well plates. Migration from the inner into the outer gel was monitored over 6 d.

Antibody Purification and Fluorescent Fibronectin Labeling. 9D2 monoclonal antibody was purified from the 9D2 hybridoma cell line (Sottile et al., 1998) by Staph protein A/G affinity chromatography following the manufacturer's protocol (Pierce). The L8 monoclonal was purified as described previously (Chernousov et al., 1991). Human plasma Fn (Sigma) was labeled with fluorescein isothiocyanate (FITC) as described (McKeown-Longo and Mosher, 1985).

Western Blot and Immunofluorescence. For western blotting, the following antibodies were used: ERK1/2 (Santa Cruz), phospho-p42/44 MAP kinase (Thr 202/Tyr 204), phospho-p38 MAP kinase (Thr180/Tyr182), β-actin, α-actinin (Cell Signaling Technologies), NMMIIA, and NMMIIB (Covance). Phosphorylated JNK was detected following pull-down with c-Jun fusion protein beads (Cell Signaling Technologies) and probed with phospho-SAPK/JNK1/2 (Thr183/Tyr185) polyclonal antibody (Cell Signaling Technologies).

For active β_1 integrin immunofluorescence, 3-D cultures were fixed in 4% formaldehyde, permeabilized with 0.25% Triton X-100, and incubated overnight with an anti-active β_1 monoclonal antibody (Chemicon) followed by an Alexa 488-conjugated secondary antibody (Molecular Probes). For visualization of the F-actin cytoskeleton, cultures were stained with Alexa 594- or Alexa 488-conjugated phalloidin (Molecular Probes) following permeabilization. To examine the 3-D Fn matrix, fibrin gels supplemented with 20 μg/ml FITC-labeled Fn were fixed with 4% formaldehyde. All 3-D gels were analyzed by confocal microscopy.

Histology and Transmission Electron Microscopy (TEM). 3-D cultures were fixed in 4% formaldehyde, processed for paraffin-embedded sectioning and standard haematoxylin and eosin (H&E) staining. TEM was carried out as described previously (Hiraoka et al., 1998; Hotary et al., 2003).

Plasmid Constructs and Transfection. The pRK/EGFP-vinculin vector was introduced into endothelial cells by lipofectamine-mediated transfection (Invitrogen). Cells were used for 3-D culture 24 hours following transfection.

Chorioallantoic Membrane Angiogenesis Assay. 3-D matrices of type I collagen or a type I collagen/fibrin composite matrix were cast in transwell tissue culture inserts (24 well size) perforated with a 25 gauge needle. A 30 µl Matrigel (BD Biosciences) reservoir was placed atop the matrix containing 200 ng VEGF, 100 ng HGF, and either the del29 or FUD peptides. The entire apparatus was placed atop the dropped CAM of 10-11 d old fertile chicken eggs. Following incubation in a humidified incubator at 37° for 3 d, the matrices were harvested and processed for sectioning and H&E staining.

3-D Intracellular Microrheology. The micromechanical properties of the cytoplasm of endothelial cells embedded in the 3-D were measured using the method of ballistic intracellular nanorheology (19, 20). To our knowledge, this is the only method capable of probing the intracellular micro-mechanics of single cells embedded inside a 3-D matrix. Briefly, 100-nm diameter polystyrene fluorescent beads were ballistically injected in the cytoplasm of cells using biolistic particle delivery system (Bio-Rad, Hercules, CA) (21). The cells were then incorporated in the 3-D fibrin matrix. After 72 h incubation, the beads (between 5 and 10 per cell) had dispersed uniformly in the cytoplasm and their centroids were tracked for 20 seconds with high spatial (~5 nm) and temporal (33 ms) resolutions using a Cascade 1k CCD camera (Roper Scientific, Tucson AZ) mounted on a Nikon Eclipse TE2000-E epifluorescence microscope and controlled by the software Metaview (Universal Imaging). The mean-squared displacement (MSDs) of individual beads were computed from the time-dependent (x,y) coordinates of the beads' centroid displacements. The MSDs were verified to have a slope lower than 1, i.e. no directed motion of the beads was ever observed. A simple mathematical manipulation detailed in (22) was used to transform MSDs into elastic modulus (reported here) and viscous modulus of the cytoplasm. The number of individual cells and total number of beads tracked for each type of cell is indicated in the caption of Fig. 6. Mean

values, standard error of measurement (SEM), and statistical analysis of bead displacements were calculated and plotted using Graphpad Prism (Graphpad Software, San Diego, CA). Two-tailed unpaired *t* tests were conducted to determine significance, which was indicated using the standard Michelin Guide scale.

Results.

Endothelial Cell Tubulogenesis in 3-D. When embedded in a 3-D gel of cross-linked fibrin and stimulated with a cocktail of pro-angiogenic factors in serum-containing media, human endothelial cells assume a spheroid configuration during the first 8-12 h of culture (Fig. 5.1A). Consistent with reports that endothelial cell rounding is incompatible with proliferative activity (3, 6, 23), no increase in cell number is detected until after a 48 h culture period whereupon the embedded cells display a stretched phenotype (Figure 5.1A,B). Endothelial cell number subsequently increases after the 2 d lag period, and a tubulogenic program is engaged which leads to the formation of an anastomosing network of patent neovessels by day 6 (Figure 5.1B and C). Neovessel formation *in vitro* recapitulates the *in vivo* program which is dependent upon both $\alpha_5\beta_1$, a Fn-specific integrin, as well as the Fn RGD domain contained within its primary cell-adhesion module (Figure 5.2) (24-27). Furthermore, as observed *in vivo* (28-30), endothelial cell morphogenesis occurs in tandem with the assembly of a network of Fn fibrils that not only enmesh the stretched endothelial cells observed at 48 h, but also ensheath the tubules formed at the end of the 6 d culture period (Figure 5.1D).

The 3-D-Specific Regulation of Endothelial Cell Function by Fn Fibrillogenesis. Under 2-D culture conditions, cell shape changes critical to signal transduction, migration and proliferation are dictated by the composition, organization, and rigidity of the surrounding ECM (3, 7, 8, 31, 32). As changes in the morphology of 3-D embedded endothelial cells correlate with Fn matrix assembly, we first sought to characterize the functional role that the fibrillogenic process plays in the tubulogenic program.

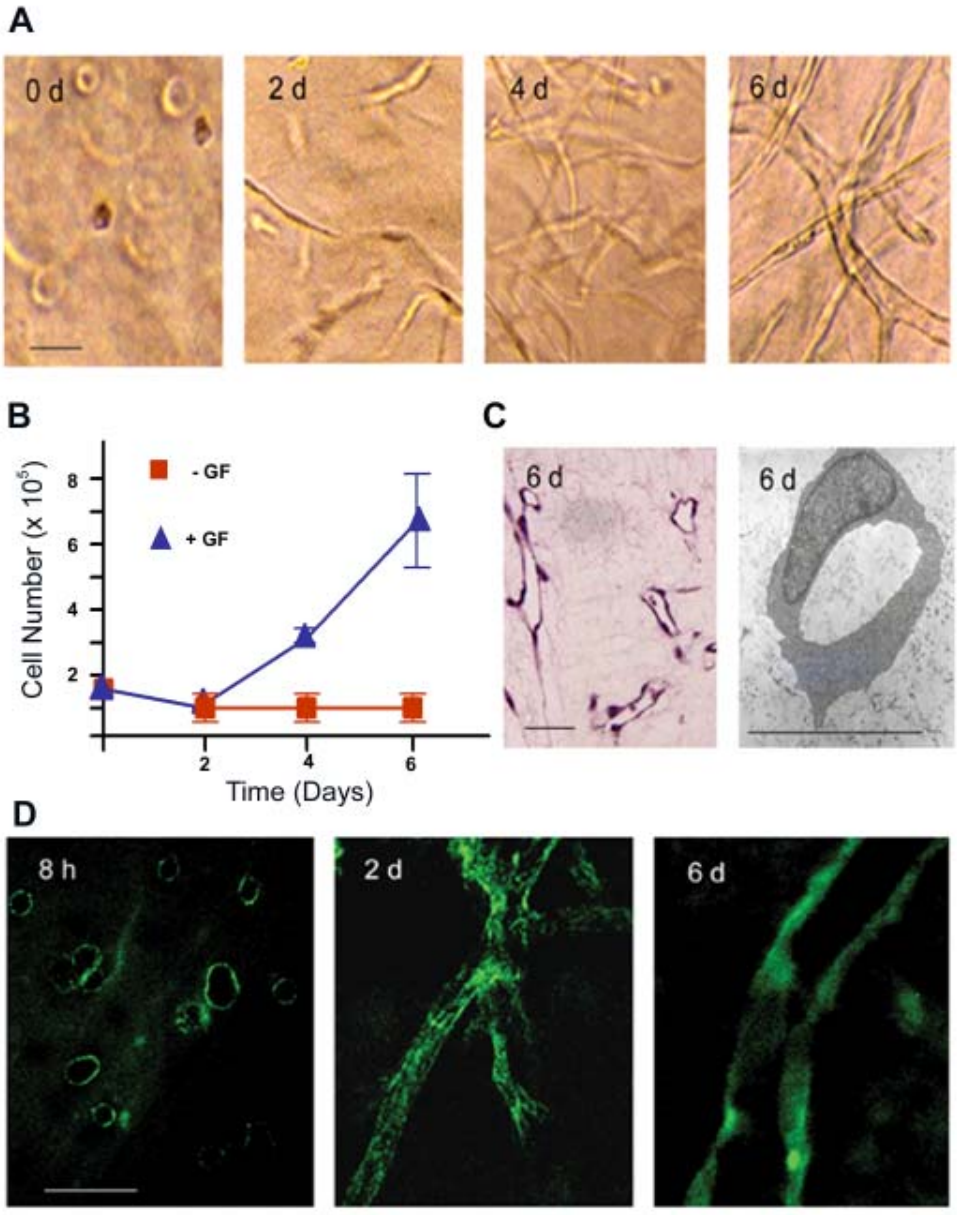

Figure 5.1. Endothelial cell tubulogenesis and Fn matrix assembly

A. Endothelial cells (1.5 x 10^5) were embedded in a 3-D fibrin gel in the presence of 20% human serum and a cocktail of VEGF, HGF, TGFα, TGFβ_1, and heparin. Phase contrast micrographs are shown following 0, 2, 4 and 6 d in culture. **B.** Endothelial cell growth in the presence or absence of the pro-vasculogenic cocktail was assessed by protease digestion of the 3-D fibrin matrix followed by counting of cells. **C.** Following 6 d in culture, patent endothelial cell tubules are formed as assessed in H&E stained cross-sections or transmission electron micrographs. **D.** Confocal laser micrographs of pericellular assembly of FITC-labeled Fn matrix following 8 h, 2 d and 6 d of culture. Scale bar, 30 μm.

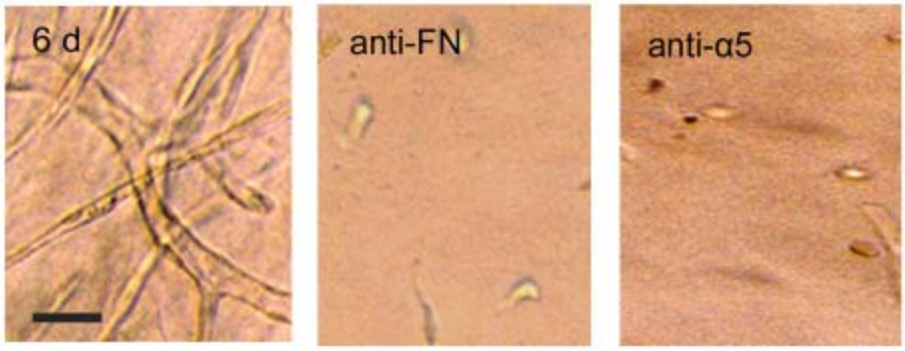

Figure 5.2. Interactions the RGD motif of Fn with α5β1 integrin are required for 3-D EC survivial

ECs were cultured in 3-D fibrin under control conditions (left panel) or with an antibody against the RGD domain of Fn (middle panel) or an antibody against α_5 integrin, and tubulogenesis assessed after 6 d culture (scale = 100 μm).

To block Fn matrix assembly without affecting the initial binding of soluble Fn binding to $\alpha_5\beta_1$, endothelial cells were incubated with i) monoclonal antibodies directed against Fn domains embedded within, or near, the Fn $III_{1,2}$ modules that are critical for regulating Fn-Fn interactions (i.e., monoclonal antibody L8 or 9D2), ii) a 70 kDa aminoterminal Fn fragment that interferes with the polymerization of intact Fn dimers by competing for matrix assembly sites on the endothelial cell surface or iii) a 49mer peptide (termed the functional upstream domain or FUD) derived from the Streptococcus pyogenes adhesion F1 protein which binds directly to the N-terminal matrix assembly domain of Fn (33-36). As exemplified by the addition of FUD (but not the control peptide, Del29, wherein FUD residue 29 is deleted), the ability of fibrin-embedded endothelial cells to assemble a Fn matrix is blocked completely in the presence of inhibitors of Fn fibrillogenesis (Figure 5.3A). In the absence of Fn fibrillogenesis – and despite the presence of a surrounding 3-D fibrin matrix, serum and exogenously provided pro-angiogenic growth factors – the endothelial cells are unable to undergo the expected shape change and retain a spherical morphology (Figure 5.3A).

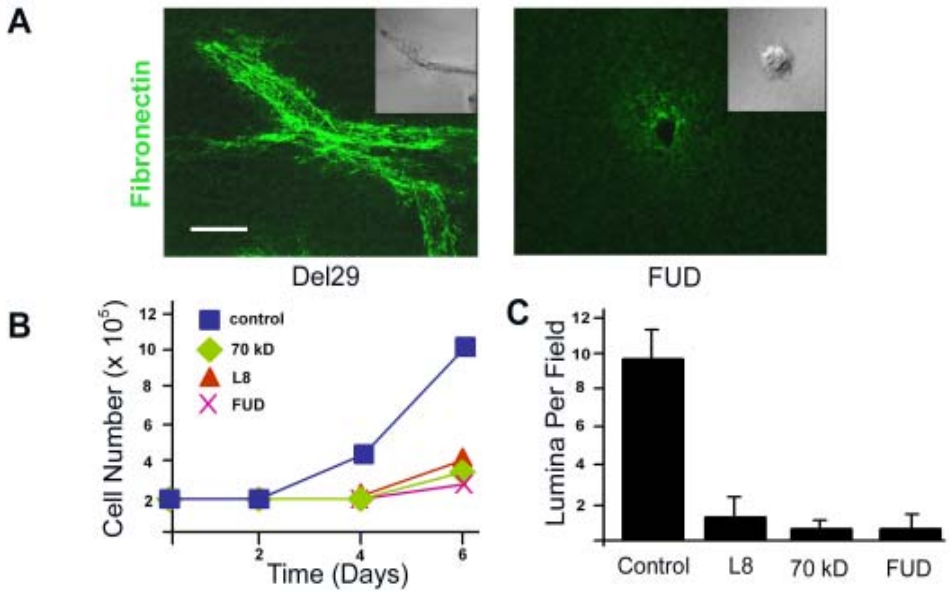

Figure 5.3. Fn matrix assembly regulates endothelial cell 3-D morphogenesis

A. Endothelial cells were suspended in 3-D fibrin gels with FITC-labeled Fn in the absence or presence of the FUD peptide (250 n*M*) with matrix assembly and cell morphology monitored by confocal laser microscopy. Scale bar 20 μm. **B.** Endothelial cells were cultured within 3-D fibrin matrices for six days in the presence or absence of Fn matrix inhibitors. Cell number was quantified following gel digestion with collagenase. **C.** Endothelial cells were cultured in 3-D fibrin gels under control conditions or in the presence of various Fn matrix assembly inhibitors for 6 d and tubulogenesis was assessed by sectioning and H&E staining of the matrices followed by lumen quantification.

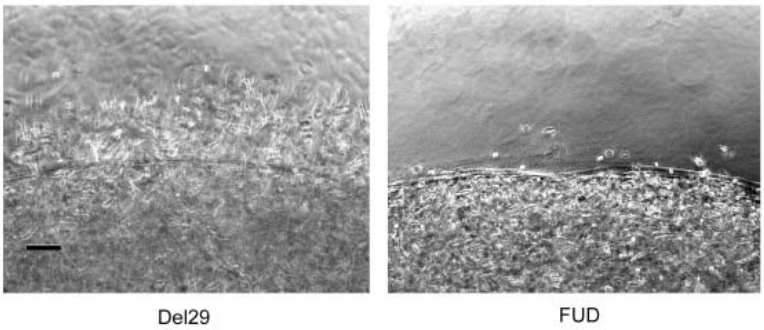

Figure 5.4. Fn matrix assembly is required for 3-D endothelial cell migration

Endothelial cells were cultured in 3-D within a 100 μl fibrin gel embedded within a larger cell free fibrin gel. Migration from the inner to the outer gel was induced by treatment with VEGF and HGF in the presence of the Del29 or FUD peptides (scale = 100 μm).

Coincident with the block in Fn matrix deposition, the 3-D migratory and proliferative responses of the embedded endothelial cells are blunted significantly and tubulogenesis is effectively terminated (Figure 5.3B and C; Figure 5.4). Under these conditions where Fn/$\alpha_5\beta_1$ interactions are left intact, no increase in apoptosis (as assessed by TUNEL staining) is detected in the absence of Fn fibrillogenesis (data not shown). Further, the ability of Fn matrix inhibitors to block neovessel formation is not restricted to the specific use of fibrin gel suspension system. Similar, if not identical, results are obtained when neovessel formation is initiated with spheroids of endothelial cells embedded in 3-D fibrin gels (37) or alternatively, when type I collagen, the major ECM macromolecule found in mammalian tissues (12, 14, 38), is used as the supporting matrix (Figure 5.5A-B). Though Fn matrix assembly can regulate type I collagen deposition (39) neovessel formation is unaffected in the presence of the collagen synthesis inhibitor, *cis*-hydroxyproline (data not shown).

While the findings presented thus far support a required role for Fn fibrillogenesis in regulating endothelial cell behavior within the confines of a 3-D ECM, endothelial cells are likewise able to assemble Fn matrices when cultured atop physiologic substrata (40, 41)(Figure 5.5). Consistent, however, with the fact that cell behavior can be affected differentially under 2-D versus 3-D culture conditions (11-14, 18, 42), the inhibition of Fn matrix assembly during endothelial cell culture atop fibrin gels did not affect cell shape, migration or proliferation (Figure 5.5C-E).

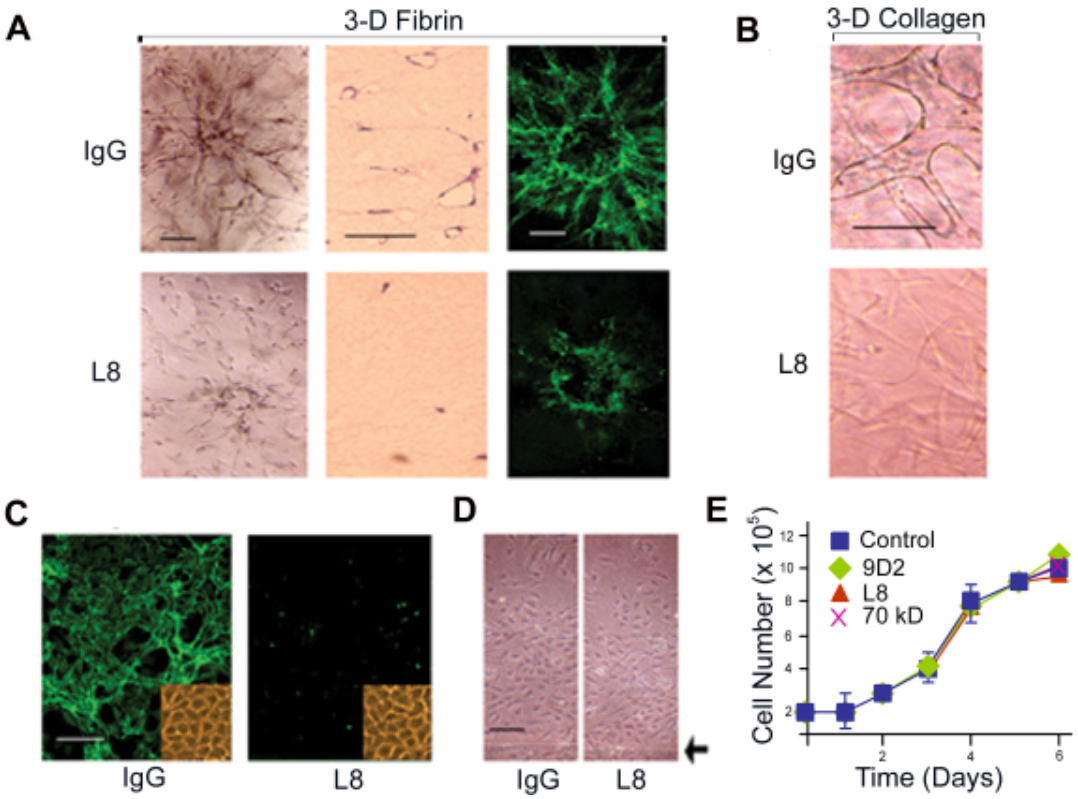

Figure 5.5. Fn fibrillogenesis and 3-D specific regulation of endothelial cell function

A. Endothelial cells spheroids were embedded in gels of 3-D fibrin and cultured for 6 d in the absence or presence of mAb L8 (100 μg/ul) and tubulogenesis assessed by phase contrast microscopy (left panels in the upper and lower series) or light microscopy (H&E-stained cross sections in the middle column). The assembly of a FITC-labeled Fn matrix was monitored by confocal laser microscopy (right panels). Scale bar, 50 μm. **B.** Endothelial cells were cultured within a matrix of type I collagen in the presence or absence of mAb L8 and tubulogenesis assessed at 6 d by phase contrast microscopy. Scale bar, 50 μm. **C.** Endothelial cells were cultured atop 3-D fibrin gels for 6 d in the presence of L8 or control IgG. Assembly of FITC-Fn into a fibrillar matrix was monitored by fluorescence microscopy and cell morphology was assessed by phase contrast microscopy (inset). **D.** Endothelial cell 2-D migration (middle panels) was assessed atop a fibrin-coated substratum in the presence of IgG or L8 (arrowhead marks the edge of the monolayer at the start of the 2 d culture period). **E.** Endothelial cell growth was monitored during a 6 d culture period in the presence of mAb L8, mAb 9D2, or the 70 kD Fn fragment relative to an IgG control. Scale bar 100 μm.

Given the demonstrated requirement for Fn matrix assembly in 3-D neovessel formation *in vitro*, a functional role for fibrillogenesis in tissue sites

undergoing active angiogenesis *in vivo* was assessed. To this end, 3-D composite gels of fibrin and type I collagen were placed atop the chorioallantoic membrane of live chicks and angiogenesis initiated by the application of a cocktail of growth factors in the presence of FUD or the Del29 peptide control. Under control conditions, angiogenic vessels infiltrated the ECM construct in tandem with the deposition of a dense network of Fn fibrils (Figure 5.6). In the presence of FUD, however, Fn matrix assembly is almost completely inhibited and neovessel formation is ablated (Figure 5.6).

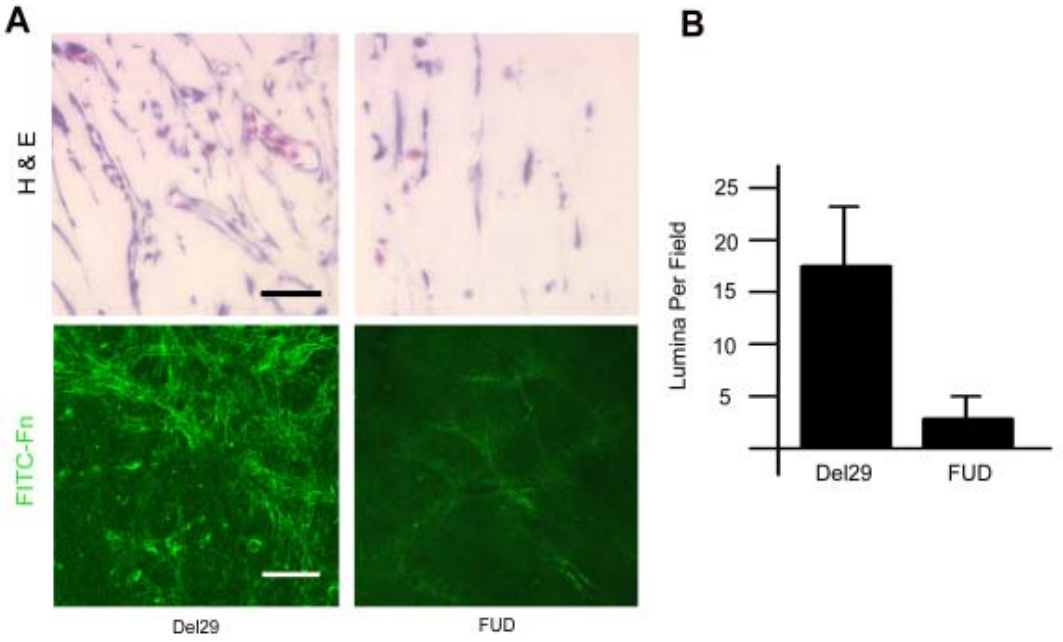

Figure 5.6. Fn matrix assembly is required for angiogenesis in vivo

A. Type I collagen/Fn composite gels polymerized in perforated Transwell chambers were prepared. A Matrigel reservoir containing 200 ng VEGF and 100 ng HGF with either the Del29 control peptide or the FUD peptide was placed atop the matrix. The apparatus was placed atop the dropped CAM, and angiogenesis was allowed to proceed. After 3 d, the gels were harvested and vascular ingrowth was monitored by light microscopy following H&E staining (top panels, scale bar 40 μm). In some experiments, FITC-Fn was supplemented in the matrices during the culture period, and Fn fibrillogenesis within the gels was monitored by confocal laser microscopy (lower panels, scale bar 50 μm). **B.** After sectioning, lumina per 40X field were counted.

As monoclonal antibody L8 only recognizes unfolded Fn epitopes that are exposed during Fn fibrillogenesis (33, 43), Fn matrix assembly in the context of

human tumor angiogenesis was also assessed. Immunostaining of a series of renal cell carcinomas (stages GI-III; n=18) and invasive ductal breast carcinomas (n=8) demonstrates that vascular wall L8 immunoreactivity is dramatically increased in tissues undergoing active vasculo/angiogenesis (Figure 5.7). In both renal cell carcinoma and invasive ductal breast carcinoma specimens, all blood vessels and vascular channels are strongly L8-reactive with additional stromal staining seen in some cases of breast cancer (Figure 5.7). In normal tissues, immunoreactivity for the L8 Fn epitope is observed infrequently as small streaks in fewer than 10% of the vessels (Figure 5.7).

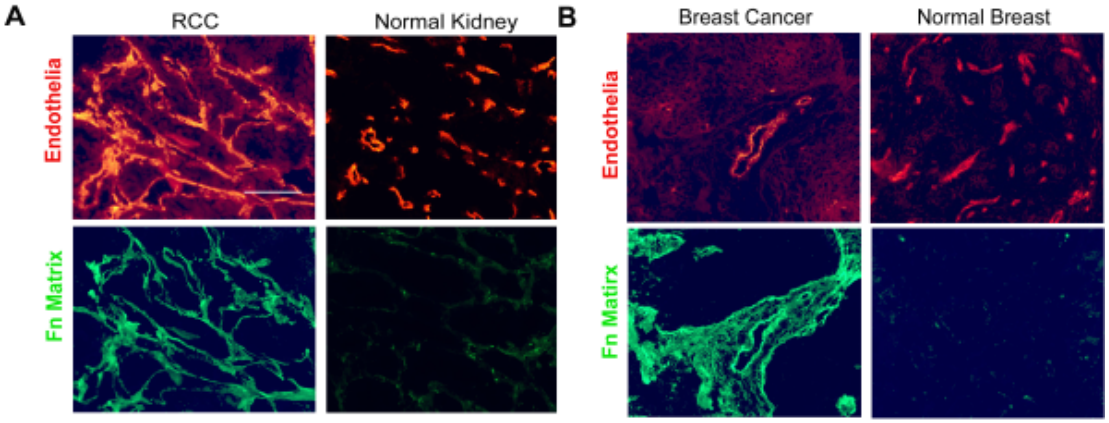

Figure 5.7. Fn matrix assembly is restricted to human neovessels in vivo

A. Renal cell carcinoma (left panels) or normal kidney (right panels; n=8) were stained for UEA-1 (top panels, red) or with mAb L8 (bottom panels, green). **B.** Breast carcinoma (left panels) was stained for UEA-1 (top left panel, red), or with mAb L8 (bottom left panel, green). Normal breast (n=8) was stained for FVIIIRAg (top right panel, red), or with mAb L8 (bottom right panel, green).

Fn Fibrillogenesis and Endothelial Cell Cytoskeletal Organization. Changes in cell geometry impact on the signaling cascades that control cell migration, proliferation and morphogenesis (3, 6, 9, 44). *In vivo,* integrins and growth factors collaborate in the activation of MAPK pathways which regulate the angiogenic response (5, 6, 45, 46). To determine the degree to which endothelial cell responses to growth factor and integrin-ligand signals are linked to Fn matrix assembly, the phosphorylation of the MAP kinases, ERK1 and 2, JNK and p38 were monitored in the absence or presence of fibrillogenesis inhibitors during the 48 h period that precedes proliferative responses. In control

cultures, sustained MAP kinase activation is maintained throughout the 48 h incubation period in a fashion that recapitulates the *in vivo* setting (45, 47)(Figure 5.8A). However, independent of the marked changes in endothelial cell morphology and cytoskeletal organization associated with the inhibition of Fn fibrillogenesis, phosphorylation patterns of ERK1/2, JNK and p38 are largely unaffected (Figure 5.8A).

Despite the comparable initiation of signal transduction cascades in endothelial cells competent or incompetent for Fn matrix assembly, cell responses to integrin and growth factor-mediated signals are also dictated by the organization of actin cytoskeletal architecture (3, 4, 6, 32). In tandem with the ability of growth factor-stimulated endothelial cells to adopt an elongated phenotype in 3-D culture, a reticulated pattern of well-organized stress fibers is resolved by F-actin phalloidin staining when cells are cultured in the presence of the Del29 control peptide (Figure 5.8B). In 3-D culture, stress fibers terminate at specialized β_1 integrin- and vinculin-rich sites of cell-matrix interactions termed 3-D adhesions (5, 42). As such, endothelial cells transduced with a GFP-tagged vinculin expression vector or alternatively immunostained with an activated β_1 integrin-specific monoclonal antibody, target both vinculin as well as activated β_1 integrins into stitch-like structures at the endothelial cell periphery (Figure 5.8C). In the absence of Fn fibrillogenesis, however, stress fiber formation is suppressed completely and actin staining is confined to the cortical envelope in a punctate network (Figure 5.8B). Further, specific interactions between either activated β_1 integrins or vinculin and F-actin networks can no longer be discerned (Figure 5.8C). Endothelial cells alternatively cultured *atop* fibrin matrices in a 2-D configuration assemble a well-organized stress fiber-focal adhesion network whose organization is unaffected by inhibitors of Fn fibrillogenesis (Figure 5.8D).

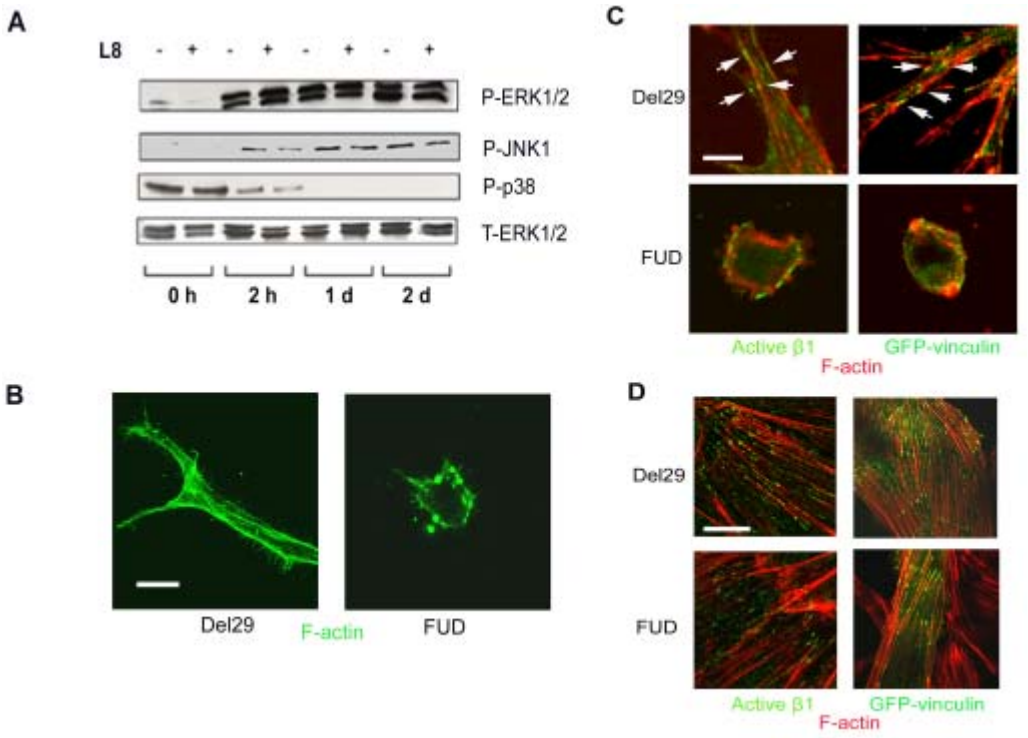

Figure 5.8. The 3-D Fn matrix is required for endothelial cell cytoskeletal organization and adhesion

A. Levels of phosphorylated ERK1/2, JNK and p38 were determined by immunoblot analysis in lysates of endothelial cells embedded in fibrin gels in the presence of either control IgG or mAb L8 for 0 h, 2 h, 1 d or 2 d. Total ERK1/2 serves as the loading control. **B.** Endothelial cells were cultured within 3-D fibrin gels in the presence of the FUD or control peptides for 2 d. F-actin cytoskeletal organization was monitored following staining with Alexa 488-conjugated phalloidin and confocal laser microscopy. Scale bar, 20 μm. **C.** Endothelial cells in 3-D fibrin matrices in the presence or absence of FUD were either stained with an antibody against activated β_1 integrin (green, left panels) or transfected with a GFP-tagged vinculin expression vector (pRK-vinculin-EGFP, green, right panels). Following counterstaining with Alexa 594-labeled phalloidin (red), fluorescence was monitored by confocal laser microscopy. Scale bar, 10 μm. **D.** Endothelial cells were cultured atop a 2-D fibrin gel for 2 d in the presence of either Del29 or FUD peptides. In tandem with staining with Alexa 594-labeled phalloidin to monitor cytoskeletal organization, actve β_1 integrin and vinculin distribution were monitored by staining with an antibody against active β_1 integrin (left panels) or assessing GFP-vinculin localization (right panels), respectively, by confocal microscopy. Scale bar, 20 μm.

Fn Matrix Assembly Induces Myosin-Dependent Tractional Forces.
Adhesive interactions between cells and their surrounding matrix allow for the generation of tractional forces that regulate cell fate and function (7-10, 13, 42). Given a 3-D-specific requirement for Fn matrix deposition in the assembly of organized cell-matrix adhesive sites, the ability of embedded endothelial cells to generate tractional forces on the fibrin matrix was determined in the presence or absence of Fn fibrillogenesis inhibitors. In stressed ECM gels wherein cells are permitted to exert isometric tension, the degree of force exerted by cells on the surrounding fibrillar network can be assessed by monitoring gel contraction after the matrix is released from the surrounding culture dish (48, 49). As shown in Figure 5.9A, growth factor-stimulated endothelial cells cultured in control gels for 48 h were able to actively contract the released fibrin gel. By contrast, each of the Fn fibrillogenesis inhibitors markedly attenuated the ability of the embedded endothelial cells to generate tractional forces under 3-D (Figure 5.9A), but not 2-D (data not shown), culture conditions

Tractional forces exerted at cell-matrix adhesion sites require the activation of an actinomyosin motor complex whose assembly is tightly linked to actin cytoskeleton organization, non-muscle myosin II isoform expression and the rigidity of the surrounding substratum (10, 17, 49, 50). Given that Fn matrix rigidity or adhesivity can affect the expression of gene products critical to the generation of tractional forces (10, 51, 52), we monitored β-actin, α-actinin, myosin light chain-2 (MLC2) as well as non-muscle myosin IIA and IIB isoforms (NMMIIA and NMMIIB, respectively) protein levels in 3-D embedded endothelial cells (Figure 5.9B). Significantly, whereas each cytoskeletal component is expressed in growth factor-stimulated endothelial cells actively assembling a Fn matrix, endothelial cells cultured in the presence of FUD or L8 express markedly reduced levels of β-actin, α-actinin and MLC2 (Figure 5.9B)(10, 49, 53).

.

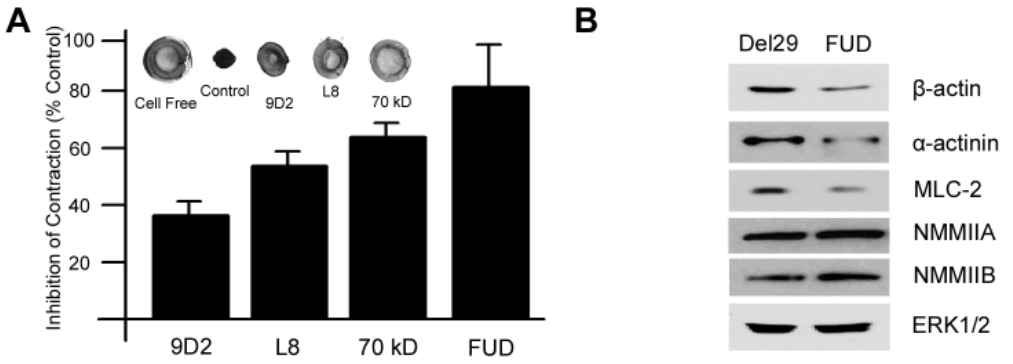

Figure 5.9. Fn Matrix Assembly Regulates the Generation of 3-D Tension

A. 3-D fibrin gels were cast in individual wells of 24-well plates and cultured alone or in the presence of embedded endothelial cells for 2 d in the presence of control IgG, mAb L8, mAb 9D2, the 70 kD Fn fragment, or the FUD peptide. Gels were detached from the edges of the culture wells and contraction monitored after an additional incubation period of 10 h at 37° C. The percent inhibition of gel contraction (measured as the change in gel diameter) relative to and IgG control is presented. Inset shows photographs (from left to right) of a cell-free fibrin gel, a gel contracted by embedded endothelial cells, and gels contracted by endothelial cells cultured in the presence of either mAb L8 or the 70 kD Fn fragment. **B.** Endothelial cells were cultured in 3-D fibrin gels for 2 d with either the FUD peptide or the control Del29 peptide. Levels of β-actin, α-actinin, NMMIIA, NMMIIB, and MLC2 were measured by Western blot, with ERK1/2 serving as the loading control. As assessed by semi-quantitative densitometry, the levels of β-actin, actinin and MLC2 were 58±7% (n=5; mean±1 SD), 62% (n=2), and 60±12% (n=3; mean±1 SD) of control.

Sensing Extracellular Stiffness Through Fn Fibrillogenesis. Endothelial cells cultured atop highly malleable surfaces retain a spheroid configuration, fail to organize stress fibers and are unable to exert tractional forces (3, 10, 23, 54) - a phenotype identical to that observed in 3-D-embedded, Fn matrix assembly-incompetent endothelial cells. As the cell's internal stiffness, a viscoelastic property governed by cytoskeletal assembly, actin crosslinking and the production of actomyosin-dependent stress, changes as a function of the perceived stiffness of the surrounding substratum (55), intracellular nanorheology was used to monitor the micromechanical properties of 3-D-embedded endothelial cells. 100-nm diameter fluorescent polystyrene beads were ballistically injected into the endothelial cell cytoplasm before the cells were cultured within the 3-D fibrin matrix to circumvent the endocytic pathway and

subsequent directed motion of the beads (22). After 72 h, beads dispersed uniformly in the cytoplasm (e.g., Figure 5.10A) and their (random) displacements within the cytoplasm (Figure 5.10B) were analyzed with the appropriate software (see details in Materials and Methods). As shown in Figure 5.10C, relative to control endothelial cells, the mean square displacement (MSD) of the beads is significantly increased in cells treated with the FUD peptide, indicating a significant relative cytoplasmic softening compared to that of cells where Fn matrix assembly is intact. Elastic moduli (G', expressed in dyn/cm^2), which quantify the local resistance of the cytoplasm against small random forces acting on the surface of the beads, were derived from MSD curves to quantify cellular mechanical properties. The elastic modulus of the cytoplasm of FUD-treated cells is significantly lower than that of control cells ($P<0.001$), indicating a pronounced defect in internal stiffness and the cell's ability to sense a sufficiently rigid substratum (Figure 5.10D).

In the absence of Fn fibrillogenesis, an impaired ability of embedded endothelial cells to generate myosin-dependent forces and increase cytoplasmic stiffness would be predicted to affect both Fn unfolding (43, 50, 56, 57) as well as the ability of the cells to properly register the mechanical properties of the surrounding substratum (8, 10). As such, the rheological and functional characteristics of endothelial cells were assessed in the presence of the specific myosin ATPase inhibitor, blebbistatin (10, 53). Blebbistatin-treated endothelial cells phenocopy Fn matrix assembly-incompetent cells and fail to increase cytoplasmic stiffness, undergo cell shape change, assemble a pericellular Fn matrix or reorganize cytoskeletal architecture (Figure 5.10E-F; Figure 5.11A). Consequently, endothelial cell tubulogenesis is blocked completely (Figure 5.11B). Hence, myosin ATPase activity and Fn matrix assembly each play required roles in regulating the endothelial cell's ability to match internal stiffness with that of the surrounding substratum so as to propagate the mechanotransduction-initiated signals critical to neovessel formation.

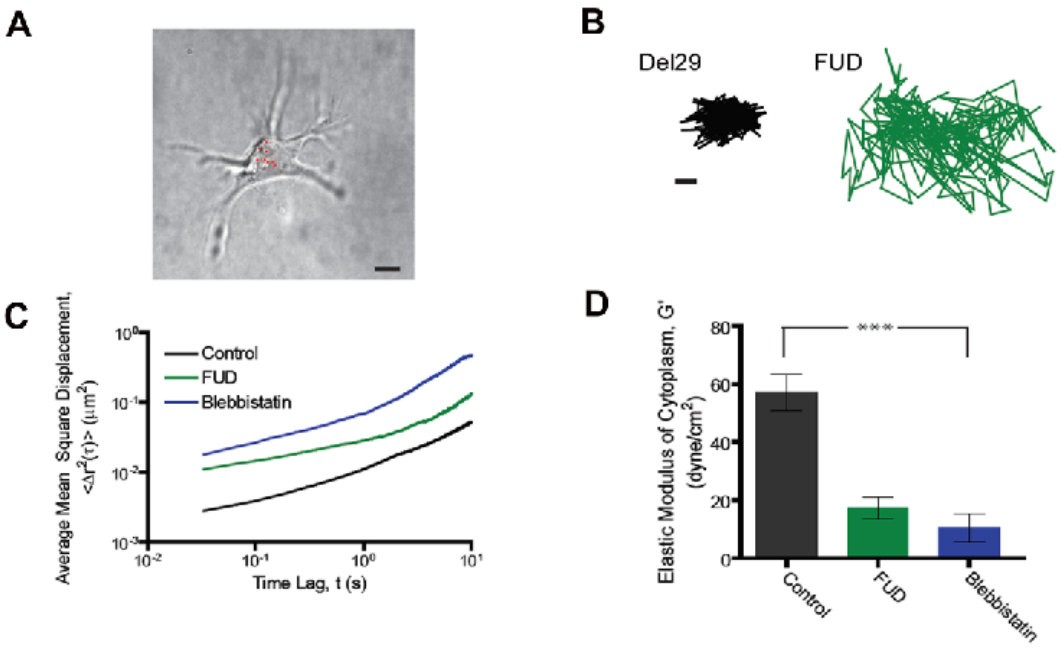

Figure 5.10. The 3-D Fn matrix regulates intracellular nanorheology

A. Prior to embedding in the 3-D fibrin matrix, endothelial cells were ballistically microinjected with 100 nm polystyrene beads. After 3 d incubation, the beads dispersed in the cytoplasm and their centroids were tracked with high spatial and temporal resolution using fluorescence microscopy. Scale bar, 10 μm. **B.** Typical trajectories of beads in the cytoplasm of 3-D embedded cells, under control conditions (black, left panel) and in the presence of FUD (green, right panel). Time of movie capture, 20 s. Scale bar, 50 nm. **C.** Ensemble-averaged mean squared displacements (MSDs) of beads in the cytoplasm of 3-D embedded endothelial cells under control conditions (black curve), in the presence of FUD (green curve) or blebbistatin (blue curve). MSDs were computed from displacements of the beads such as shown in panel **A**. At least 110 beads in at least 10 cells were tracked for each condition. **D.** Averaged elastic modulus of cells under control conditions or in the presence FUD or blebbistatin. ***: $P < 0.001$.

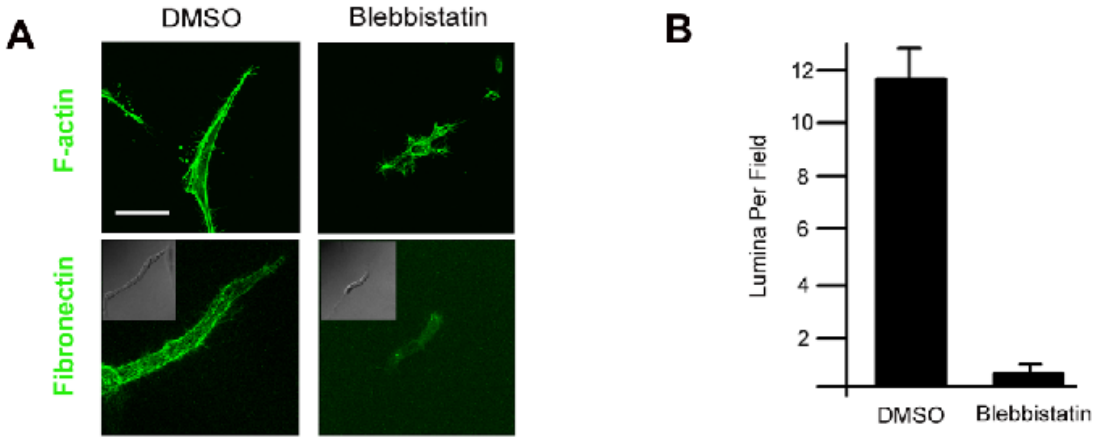

Figure 5.11. Regulation of 3-D endothelial cell function by myosin-dependent forces

A. Endothelial cells were cultured in 3-D fibrin gels for 2 d in the presence or absence of 50 μ*M* ± blebbistatin and F-actin organization and Fn matrix assembly was monitored by confocal laser microscopy. F-actin organization was monitored by staining with Alexa 488-conjugated phalloidin (top panels). Fn matrix assembly was assessed by culture in the presence of FITC-conjugated Fn (bottom panels). Scale bar, 20 μm. **B.** Endothelial cells were cultured in 3-D fibrin gels for 6 d under pro-vasculogenic conditions in the presence of 50 μ*M* ± blebbistatin or vehicle (DMSO). Tubulogenesis was monitored following sectioning, H&E staining, and lumen quantification.

Discussion.

By modulating the responsiveness of endothelial cells to soluble agonists, the biomechanical properties of the ECM play critical roles in regulating vasculogenesis and angiogenesis (3, 4, 6, 8, 54). Herein, we have demonstrated that endothelial cell function within the specific confines of the 3-D ECM is unexpectedly regulated by Fn fibrillogenesis. Fn, a disulfide-linked dimer of subunits composed of 3 types of repeating modules (i.e., type I, II and III repeats), binds to the endothelial cell surface by displaying a dominant cell-adhesive domain (module $III_{9,10}$), a carboxyterminal heparin-binding domain (module $III_{12\text{-}14}$) and a 70 kDa aminoterminal domain that are recognized, respectively, by integrins, syndecans and Fn matrix assembly sites (34, 35). Once the soluble Fn dimer engages adhesion molecules on the endothelial cell surface, signaling cascades are triggered that initiate the unfolding of the globular glycoprotein and the consequent exposure of cryptic domains which then serve to support Fn polymerization and matrix assembly (5, 34, 35). As observed during both vasculogenesis and angiogenesis *in vivo* (24-26, 28-30), endothelial cells embedded in 3-D fibrin or collagen-rich gels rapidly assemble a pericellular Fn matrix following stimulation with pro-angiogenic growth factors. While $\alpha_5\beta_1$-Fn interactions have been established previously to regulate vascular development *in vivo* by heretofore undefined mechanisms, Fn monomers are known to initiate $\alpha_5\beta_1$-dependent signaling cascades that operate independently of the polymerization process per se (5, 42). As such, a specific role for Fn fibrillogenesis in 3-D neovessel formation has not been considered previously. Though earlier reports concluded that endothelial cell signaling in 2-D culture is dependent upon Fn matrix assembly (41), these studies employed a Fn-derived peptide as an inhibitory fragment that has since been shown to modulate cell function independently of effects on Fn fibrillogenesis (58). Indeed, our findings, as well as those of others (36, 59), demonstrate that under 2-D conditions, cell adhesion, migration and proliferation proceed independently of Fn matrix assembly.

Optimal cell-matrix adhesive interactions induce the assembly of a cytoskeletal network that is required for the support of cell shape changes which, in turn, activate mechanotransduction-sensitive signaling cascades (7, 8, 60-62). If, however, endothelial cell shape changes are prevented under planar conditions (e.g., by altering ligand topology or decreasing matrix rigidity), the adherent cells are unable to rearrange their cytoskeletal architecture to exert tractional forces on the underlying substratum, and either senesce or undergo apoptosis (3, 4, 23, 54). In 3-D culture, endothelial cell responses to pro-angiogenic agonists are similarly disengaged when pericellular Fn matrix assembly is blocked and the cells are unable to use the multiple ligands presented by dense matrices of fibrin or type I collagen as structural platforms in either the *in vitro* or *in vivo* settings. Recent studies demonstrate that cells "sense" the mechanical properties of the surrounding matrix via a myosin II-dependent pathway (8, 55). Consequently, the adherent cells alter their intracellular stiffness to match that of the supporting ECM in order to initiate the appropriate acytomyosin-dependent responses (8, 10, 55). Given that i) the 3-D behavior of Fn fibrillogenesis-incompetent endothelial cells phenocopies that of cells cultured atop suboptimal substrata and ii) internal cellular stiffness is modulated as a function of the perceived stiffness of the extracellular substratum (10, 55), we reasoned that 3-D analyses of microrheological responsiveness might uncover a required role for Fn matrix assembly in allowing endothelial cells to discern the biomechanical characteristics of the pericellular environment. Embedded in a 3-D matrix, cells are inaccessible to conventional physical probes, including atomic force microscopy, glass microneedles, membrane-bound magnetic beads or micropipette suction (22). Using intracellular nanorheology, however, the random movements of submicron particles microinjected into the cytoplasm can be monitored as a means to determine local viscoelasticity (19, 22). Based on such analyses, we demonstrate that 3-D-embedded endothelial cells sense and respond to a sufficiently rigid scaffolding only when a network of Fn polymers is interposed between the cell and surrounding matrix of fibrin and/or type I collagen.

The ability of Fn matrix assembly to regulate endothelial cell mechanotransduction signaling is likely ascribed to either of two, though not necessarily mutually exclusive, processes. First, as Fn fibrils are crosslinked into insoluble mats by both covalent and non-covalent interactions (34), the assembled matrix may increase local mechanical rigidity to a degree necessary to support the tractional forces and intracellular stiffening generated during cell spreading (63). Indeed, in preliminary studies designed to directly monitor changes in the rigidity of the pericellular matrix, we have found that endothelial cells modulate the local mechanical rigidity of the ECM by a process dependent on fibronectin fibrillogenesis (unpublished observation). Second, Fn matrix assembly allows for an increase in the local concentration and order of potential $\alpha_5\beta_1$ integrin-binding sites that would serve as a structural platform for cell spreading (5, 34). Unfolded Fn molecules could further alter cell function by displaying matricryptic heparin-binding sites (64). As neither mechanically soft matrices displaying high adhesivity nor rigid matrices decorated with suboptimal levels of pro-adhesive binding sites will induce changes in cytoskeletal architecture and intracellular stiffness (8, 55), endothelial cells apparently use Fn matrix assembly to purposefully deposit an elastic layer of pro-adhesive binding sites whose concentration and topology support neovessel formation.

In vivo, Fn is expressed transiently around the developing vasculature during both vasculogenesis and angiogenesis (28-30). As the vasculature matures, Fn expression wanes, and the maturing blood vessels are invested with a type IV collagen/laminin-rich basement membrane (1, 29). Fn is, however, re-expressed in the neovasculature surrounding wound sites or tumors (30). Significantly, large deposits of unfolded Fn could be detected in association with neovessels infiltrating cancerous tissues. While Fn fibrils are also found, as expected, in association with fibroblasts, it is important to stress that we were unable to identify a similarly critical role for Fn matrix assembly in fibroblast function - under either 2-D or 3-D culture conditions (Figure 5.12). These findings reinforce earlier reports where inhibitors of Fn fibrillogenesis did not affect fibroblast behavior in 3-D collagen gels (65). Similar analyses of Fn matrix assembly in

wild-type and Fn knockout embryos indicate that distinct differences exist between embryonic fibroblast and endothelial cell behavior *in vivo* and *in vitro* (25, 51, 66-69). Cell type-specific responses to Fn fibrillogenesis are likewise consistent with more recent findings that mesenchymal cell populations display singular mechanical requirements for optimizing their responses to matrix-derived signals (9, 10, 54). Interestingly, a unique role for Fn in the specific regulation of endothelial cell behavior is supported by the fact that unlike most ECM molecules, Fn expression is limited to vertebrates and its appearance in evolution coincides with the appearance of the vasculature (70).

With increasing frequency, the morphology, adhesive interactions and behavior of cells are recognized as being uniquely affected by the dimensionality of their surrounding matrix environment (12-15, 18). Under 3-D conditions, we posit that the random intertwining of the surrounding fibrin or collagen fibrils precludes the high density, planar display of adhesive ligands on a rigid template that can support integrin clustering and/or cellular traction. These data are consistent with a model wherein the endothelial cell has elected to assemble its own pericellular matrix of polymerized Fn to meet the spatial and structural constraints placed on transmitting extracellular signals to intracellular compartments and effectors. By regulating cell shape, stiffness sensing and mechanotransduction, Fn matrix assembly is shown to serve as a multifaceted, and 3-D-specific, regulator of neovessel formation that may prove useful as a target for therapeutic intervention in pathologic states.

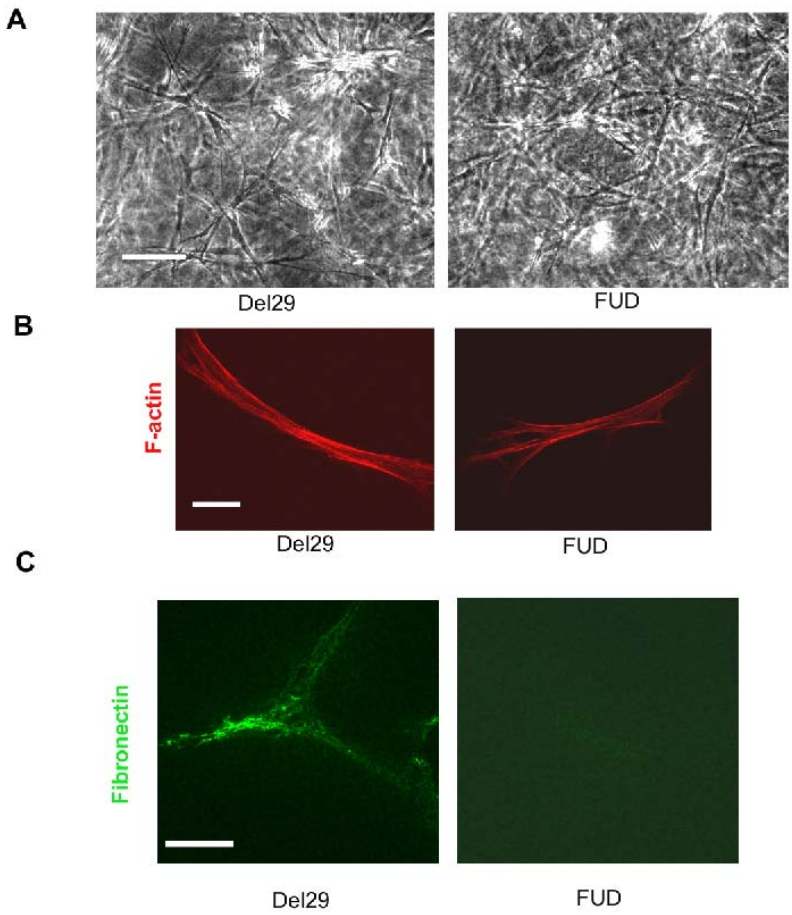

Figure 5.12. Fn fibrillogenesis does not regulate 3-D fibroblast function

A. Human fibroblasts were cultured in 3-D fibrin gels in the presence of the Del29 or FUD peptides for 6 d, and cell shape monitored by phase contrast microscopy (scale = 100 μm). **B.** Human fibroblasts were cultured in 3-D fibrin in the presence of Del29 or FUD and cytoskeletal organization examined following staining with Alexa-594-labeled phalloidin and confocal laser microscopy (scale = 20 μm). **C.** Human fibroblasts were cultured in 3-D fibrin in the presence of Del29 or FUD as well as FITC-Fn, and Fn fibrillogenesis assessed by confocal laser microscopy (scale = 30 μm).

References.

1. Jain, R.K. 2003. Molecular regulation of vessel maturation. *Nat Med* 9:685-693.

2. Carmeliet, P. 2005. Angiogenesis in life, disease and medicine. *Nature* 438:932-936.

3. Chen, C.S., Mrksich, M., Huang, S., Whitesides, G.M., and Ingber, D.E. 1997. Geometric control of cell life and death. *Science* 276:1425-1428.

4. Huang, S., Chen, C.S., and Ingber, D.E. 1998. Control of cyclin D1, p27(Kip1), and cell cycle progression in human capillary endothelial cells by cell shape and cytoskeletal tension. *Mol Biol Cell* 9:3179-3193.

5. Geiger, B., Bershadsky, A., Pankov, R., and Yamada, K.M. 2001. Transmembrane crosstalk between the extracellular matrix--cytoskeleton crosstalk. *Nat Rev Mol Cell Biol* 2:793-805.

6. Ingber, D.E. 2006. Cellular mechanotransduction: putting all the pieces together again. *Faseb J* 20:811-827.

7. Vogel, V., and Sheetz, M. 2006. Local force and geometry sensing regulate cell functions. *Nat Rev Mol Cell Biol* 7:265-275.

8. Discher, D.E., Janmey, P., and Wang, Y.L. 2005. Tissue cells feel and respond to the stiffness of their substrate. *Science* 310:1139-1143.

9. McBeath, R., Pirone, D.M., Nelson, C.M., Bhadriraju, K., and Chen, C.S. 2004. Cell shape, cytoskeletal tension, and RhoA regulate stem cell lineage commitment. *Dev Cell* 6:483-495.

10. Engler, A.J., Sen, S., Sweeney, H.L., and Discher, D.E. 2006. Matrix elasticity directs stem cell lineage specification. *Cell* 126:677-689.

11. Walpita, D., and Hay, E. 2002. Studying actin-dependent processes in tissue culture. *Nat Rev Mol Cell Biol* 3:137-141.

12. Chun, T.H., Hotary, K.B., Sabeh, F., Saltiel, A.R., Allen, E.D., and Weiss, S.J. 2006. A pericellular collagenase directs the 3-dimensional development of white adipose tissue. *Cell* 125:577-591.

13. Yamada, K.M., and Cukierman, E. 2007. Modeling tissue morphogenesis and cancer in 3D. *Cell* 130:601-610.

14. Hotary, K.B., Allen, E.D., Brooks, P.C., Datta, N.S., Long, M.W., and Weiss, S.J. 2003. Membrane type I matrix metalloproteinase usurps tumor

growth control imposed by the three-dimensional extracellular matrix. *Cell* 114:33-45.

15. Nelson, C.M., and Bissell, M.J. 2006. Of extracellular matrix, scaffolds, and signaling: tissue architecture regulates development, homeostasis, and cancer. *Annu Rev Cell Dev Biol* 22:287-309.

16. Beningo, K.A., Dembo, M., and Wang, Y.L. 2004. Responses of fibroblasts to anchorage of dorsal extracellular matrix receptors. *Proc Natl Acad Sci U S A* 101:18024-18029.

17. Meshel, A.S., Wei, Q., Adelstein, R.S., and Sheetz, M.P. 2005. Basic mechanism of three-dimensional collagen fibre transport by fibroblasts. *Nat Cell Biol* 7:157-164.

18. Debnath, J., and Brugge, J.S. 2005. Modelling glandular epithelial cancers in three-dimensional cultures. *Nat Rev Cancer* 5:675-688.

19. Panorchan, P., Lee, J.S.H., Daniels, B.R., Kole, T.P., Tseng, Y., and Wirtz, D. 2007. Probing cellular mechanical responses to stimuli using ballistic intracellular nanorheology. *Meth. Cell Biol.* 83:115-140.

20. Panorchan, P., Lee, J.S., Kole, T.P., Tseng, Y., and Wirtz, D. 2006. Microrheology and ROCK signaling of human endothelial cells embedded in a 3D matrix. *Biophys J* 91:3499-3507.

21. Lee, J.S., Panorchan, P., Hale, C.M., Khatau, S.B., Kole, T.P., Tseng, Y., and Wirtz, D. 2006. Ballistic intracellular nanorheology reveals ROCK-hard cytoplasmic stiffening response to fluid flow. *J Cell Sci* 119:1760-1768.

22. Tseng, Y., Kole, T.P., and Wirtz, D. 2002. Micromechanical mapping of live cells by multiple-particle-tracking microrheology. *Biophys J* 83:3162-3176.

23. Folkman, J., and Moscona, A. 1978. Role of cell shape in growth control. *Nature* 273:345-349.

24. Kim, S., Bell, K., Mousa, S.A., and Varner, J.A. 2000. Regulation of angiogenesis in vivo by ligation of integrin alpha5beta1 with the central cell-binding domain of fibronectin. *Am J Pathol* 156:1345-1362.

25. Francis, S.E., Goh, K.L., Hodivala-Dilke, K., Bader, B.L., Stark, M., Davidson, D., and Hynes, R.O. 2002. Central roles of alpha5beta1 integrin and fibronectin in vascular development in mouse embryos and embryoid bodies. *Arterioscler Thromb Vasc Biol* 22:927-933.

26. Hynes, R.O. 2002. A reevaluation of integrins as regulators of angiogenesis. *Nat Med* 8:918-921.

27. Takahashi, S., Leiss, M., Moser, M., Ohashi, T., Kitao, T., Heckmann, D., Pfeifer, A., Kessler, H., Takagi, J., Erickson, H.P., et al. 2007. The RGD motif in fibronectin is essential for development but dispensable for fibril assembly. *J Cell Biol* 178:167-178.

28. Clark, R.A., Quinn, J.H., Winn, H.J., Lanigan, J.M., Dellepella, P., and Colvin, R.B. 1982. Fibronectin is produced by blood vessels in response to injury. *J Exp Med* 156:646-651.

29. Risau, W., and Lemmon, V. 1988. Changes in the vascular extracellular matrix during embryonic vasculogenesis and angiogenesis. *Dev Biol* 125:441-450.

30. Neri, D., and Bicknell, R. 2005. Tumour vascular targeting. *Nat Rev Cancer* 5:436-446.

31. Cavalcanti-Adam, E.A., Volberg, T., Micoulet, A., Kessler, H., Geiger, B., and Spatz, J.P. 2007. Cell spreading and focal adhesion dynamics are regulated by spacing of integrin ligands. *Biophys J* 92:2964-2974.

32. Bershadsky, A., Kozlov, M., and Geiger, B. 2006. Adhesion-mediated mechanosensitivity: a time to experiment, and a time to theorize. *Curr Opin Cell Biol* 18:472-481.

33. Chernousov, M.A., Fogerty, F.J., Koteliansky, V.E., and Mosher, D.F. 1991. Role of the I-9 and III-1 modules of fibronectin in formation of an extracellular fibronectin matrix. *J Biol Chem* 266:10851-10858.

34. Mao, Y., and Schwarzbauer, J.E. 2005. Fibronectin fibrillogenesis, a cell-mediated matrix assembly process. *Matrix Biol* 24:389-399.

35. Tomasini-Johansson, B.R., Annis, D.S., and Mosher, D.F. 2006. The N-terminal 70-kDa fragment of fibronectin binds to cell surface fibronectin assembly sites in the absence of intact fibronectin. *Matrix Biol* 25:282-293.

36. Tomasini-Johansson, B.R., Kaufman, N.R., Ensenberger, M.G., Ozeri, V., Hanski, E., and Mosher, D.F. 2001. A 49-residue peptide from adhesin F1 of Streptococcus pyogenes inhibits fibronectin matrix assembly. *J Biol Chem* 276:23430-23439.

37. Korff, T., and Augustin, H.G. 1998. Integration of endothelial cells in multicellular spheroids prevents apoptosis and induces differentiation. *J Cell Biol* 143:1341-1352.

38. Chun, T.H., Sabeh, F., Ota, I., Murphy, H., McDonagh, K.T., Holmbeck, K., Birkedal-Hansen, H., Allen, E.D., and Weiss, S.J. 2004. MT1-MMP-dependent neovessel formation within the confines of the three-dimensional extracellular matrix. *J Cell Biol* 167:757-767.

39. Velling, T., Risteli, J., Wennerberg, K., Mosher, D.F., and Johansson, S. 2002. Polymerization of type I and III collagens is dependent on fibronectin and enhanced by integrins alpha 11beta 1 and alpha 2beta 1. *J Biol Chem* 277:37377-37381.

40. Christopher, R.A., Kowalczyk, A.P., and McKeown-Longo, P.J. 1997. Localization of fibronectin matrix assembly sites on fibroblasts and endothelial cells. *J Cell Sci* 110 (Pt 5):569-581.

41. Bourdoulous, S., Orend, G., MacKenna, D.A., Pasqualini, R., and Ruoslahti, E. 1998. Fibronectin matrix regulates activation of RHO and CDC42 GTPases and cell cycle progression. *J Cell Biol* 143:267-276.

42. Larsen, M., Artym, V.V., Green, J.A., and Yamada, K.M. 2006. The matrix reorganized: extracellular matrix remodeling and integrin signaling. *Curr Opin Cell Biol* 18:463-471.

43. Zhong, C., Chrzanowska-Wodnicka, M., Brown, J., Shaub, A., Belkin, A.M., and Burridge, K. 1998. Rho-mediated contractility exposes a cryptic site in fibronectin and induces fibronectin matrix assembly. *J Cell Biol* 141:539-551.

44. Tan, J.L., Tien, J., Pirone, D.M., Gray, D.S., Bhadriraju, K., and Chen, C.S. 2003. Cells lying on a bed of microneedles: an approach to isolate mechanical force. *Proc Natl Acad Sci U S A* 100:1484-1489.

45. Eliceiri, B.P., Klemke, R., Stromblad, S., and Cheresh, D.A. 1998. Integrin alphavbeta3 requirement for sustained mitogen-activated protein kinase activity during angiogenesis. *J Cell Biol* 140:1255-1263.

46. Hoang, M.V., Whelan, M.C., and Senger, D.R. 2004. Rho activity critically and selectively regulates endothelial cell organization during angiogenesis. *Proc Natl Acad Sci U S A* 101:1874-1879.

47. Corson, L.B., Yamanaka, Y., Lai, K.M., and Rossant, J. 2003. Spatial and temporal patterns of ERK signaling during mouse embryogenesis. *Development* 130:4527-4537.

48. Corbett, S.A., and Schwarzbauer, J.E. 1999. Requirements for alpha(5)beta(1) integrin-mediated retraction of fibronectin-fibrin matrices. *J Biol Chem* 274:20943-20948.

49. Even-Ram, S., Doyle, A.D., Conti, M.A., Matsumoto, K., Adelstein, R.S., and Yamada, K.M. 2007. Myosin IIA regulates cell motility and actomyosin-microtubule crosstalk. *Nat Cell Biol* 9:299-309.

50. Yoneda, A., Ushakov, D., Multhaupt, H.A., and Couchman, J.R. 2007. Fibronectin matrix assembly requires distinct contributions from Rho kinases I and -II. *Mol Biol Cell* 18:66-75.

51. Deroanne, C.F., Lapiere, C.M., and Nusgens, B.V. 2001. In vitro tubulogenesis of endothelial cells by relaxation of the coupling extracellular matrix-cytoskeleton. *Cardiovasc Res* 49:647-658.

52. Ben-Ze'ev, A., Farmer, S.R., and Penman, S. 1980. Protein synthesis requires cell-surface contact while nuclear events respond to cell shape in anchorage-dependent fibroblasts. *Cell* 21:365-372.

53. Clark, K., Langeslag, M., Figdor, C.G., and van Leeuwen, F.N. 2007. Myosin II and mechanotransduction: a balancing act. *Trends Cell Biol* 17:178-186.

54. Georges, P.C., and Janmey, P.A. 2005. Cell type-specific response to growth on soft materials. *J Appl Physiol* 98:1547-1553.

55. Solon, J., Levental, I., Sengupta, K., Georges, P.C., and Janmey, P.A. 2007. Fibroblast adaptation and stiffness matching to soft elastic substrates. *Biophys J* 93:4453-4461.

56. Baneyx, G., Baugh, L., and Vogel, V. 2002. Fibronectin extension and unfolding within cell matrix fibrils controlled by cytoskeletal tension. *Proc Natl Acad Sci U S A* 99:5139-5143.

57. Wu, C., Keivens, V.M., O'Toole, T.E., McDonald, J.A., and Ginsberg, M.H. 1995. Integrin activation and cytoskeletal interaction are essential for the assembly of a fibronectin matrix. *Cell* 83:715-724.

58. Ambesi, A., Klein, R.M., Pumiglia, K.M., and McKeown-Longo, P.J. 2005. Anastellin, a fragment of the first type III repeat of fibronectin, inhibits extracellular signal-regulated kinase and causes G(1) arrest in human microvessel endothelial cells. *Cancer Res* 65:148-156.

59. Mercurius, K.O., and Morla, A.O. 1998. Inhibition of vascular smooth muscle cell growth by inhibition of fibronectin matrix assembly. *Circ Res* 82:548-556.

60. Engler, A., Bacakova, L., Newman, C., Hategan, A., Griffin, M., and Discher, D. 2004. Substrate compliance versus ligand density in cell on gel responses. *Biophys J* 86:617-628.

61. Cai, Y., Biais, N., Giannone, G., Tanase, M., Jiang, G., Hofman, J.M., Wiggins, C.H., Silberzan, P., Buguin, A., Ladoux, B., et al. 2006. Nonmuscle myosin IIA-dependent force inhibits cell spreading and drives F-actin flow. *Biophys J* 91:3907-3920.

62. Galbraith, C.G., Yamada, K.M., and Galbraith, J.A. 2007. Polymerizing actin fibers position integrins primed to probe for adhesion sites. *Science* 315:992-995.

63. Davidson, L.A., Keller, R., and DeSimone, D.W. 2004. Assembly and remodeling of the fibrillar fibronectin extracellular matrix during gastrulation and neurulation in Xenopus laevis. *Dev Dyn* 231:888-895.

64. Gui, L., Wojciechowski, K., Gildner, C.D., Nedelkovska, H., and Hocking, D.C. 2006. Identification of the heparin-binding determinants within fibronectin repeat III1: role in cell spreading and growth. *J Biol Chem* 281:34816-34825.

65. Halliday, N.L., and Tomasek, J.J. 1995. Mechanical properties of the extracellular matrix influence fibronectin fibril assembly in vitro. *Exp Cell Res* 217:109-117.

66. Yang, J.T., Rayburn, H., and Hynes, R.O. 1993. Embryonic mesodermal defects in alpha 5 integrin-deficient mice. *Development* 119:1093-1105.

67. Sottile, J., Hocking, D.C., and Langenbach, K.J. 2000. Fibronectin polymerization stimulates cell growth by RGD-dependent and -independent mechanisms. *J Cell Sci* 113 Pt 23:4287-4299.

68. Hocking, D.C., Sottile, J., and Langenbach, K.J. 2000. Stimulation of integrin-mediated cell contractility by fibronectin polymerization. *J Biol Chem* 275:10673-10682.

69. Deroanne, C.F., Colige, A.C., Nusgens, B.V., and Lapiere, C.M. 1996. Modulation of expression and assembly of vinculin during in vitro fibrillar collagen-induced angiogenesis and its reversal. *Exp Cell Res* 224:215-223.

70. Hynes, R.O., and Zhao, Q. 2000. The evolution of cell adhesion. *J Cell Biol* 150:F89-96.

Chapter 6: Dynamic remodeling of the nucleus during 3-D vasculogenesis

Introduction.

In response to wounding, inflammation or tumor growth, quiescent endothelial cells assume an activated state characterized by the induction of migratory, proliferative and tubulogenic phenotypes (1, 2). In order to effectively interpret exogenous signals, endothelial cells interface with a 3-dimensional (3-D) extracellular matrix (ECM) that supports capillary morphogenesis (3-6). While the structure, topology, and biomechanical properties of the ECM act as key regulators of developmental programs such as those activated during neovascularization (7-15), the ECM is not a static scaffold and undergoes active remodeling by both endothelial cell-dependent pericellular proteolysis and neomatrix deposition (3-6).

Current evidence suggests that cells engaged in morphogenetic programs 'sense' the shifting biophysical properties of the pericellular ECM during remodeling by transmitting mechanical cues from the matrix into their interior via transmembrane receptors that are linked to the actomyosin-cytoskeletal contractile network (11, 13-17). However, the means by which 3-D ECM remodeling relays messages to functionally important downstream targets remains the subject of speculation (2, 3, 11, 13, 17, 18).

Herein, we demonstrate that endothelial cell-dependent remodeling of the pericellular ECM plays a central role in capillary morphogenesis by controlling nuclear compartment organization and architecture in a 3-D-specific fashion. Growth factor-triggered changes in endothelial cell shape are transmitted to the nuclear envelope via a pathway dependent on F-actin, intermediate filaments, microtubules, actomyosin-generated force and the linker of nucleus and cytoskeleton (LINC) complex embedded within the nuclear membrane (19-22).

As the LINC complex is tethered to the nuclear lamina, a meshwork of interconnecting filaments underlying the inner nuclear envelope that bind directly to chromatin (19, 21, 22), we further demonstrate that changes in 3-D cell geometry mediated by pericellular proteolysis and fibronectin matrix assembly co-regulate nuclear organization as well as chromatin structure and function. These results define a new paradigm in which endothelial cells respond to pro-angiogenic signals by remodeling the pericellular 3-D environment to directly transmit permissive environmental cues to the nuclear compartment and its transcriptional machinery.

Methods

Antibodies. Antibodies to the following were used: acetyl histone H3 (Lys 9), acetyl histone H4 (Lys 8), total histone H3, emerin, β-tubulin (Cell Signaling Technologies, Danvers, MA), fibrillarin (Cytoskeleton, Denver, CO), vimentin (Abcam, Cambridge, MA) and SC-35 (Sigma, St. Louis, MO). Nesprin-1 and Nesprin-2 antibodies were generously provided by Dr. Angelika A. Noegel (University of Cologne, Germany). To generate the nesprin-3 antibody, full-length human nesprin-3 from FLJ16564 cDNA was cloned into pGEX-2T and expressed in E.coli strain BL21 codon-plus and purified according to the manufacturer's protocol. Rabbits were injected with the nesprin-3:GST purified fusion proteins at the laboratory of Comparative Pathology at the School of Veterinary Medicine at UC Davis.

Cell culture. Human umbilical vein endothelial cells were isolated from umbilical cords by perfusion of the umbilical vein with type 3 collagenase (Worthington, Lakewood, NJ) and cultured in Medium-199 (Invitrogen, Carlsbad, CA) with 20% human serum and 50 μg/ml endothelial cell growth supplement (ECGS; BD Biosciences, Franklin Lakes, NJ). For 3-D culture, endothelial cells were suspended in a solution of thrombin and aprotinin (Sigma, St. Louis, MO) and mixed with a solution of 6 mg/ml fibrinogen (Calbiochem, Gibbstown, NJ). Vasculogenesis was triggered by treatment with 100 ng/ml VEGF, 50 ng/ml HGF (Genentech, San Francisco, CA). Fibronectin fibrillogenesis was inhibited by treatment with FUD peptide (3) and MMPs were inhibited with GM6001 (Calbiochem). Fibronectin fibrillogenesis was tracked in 3-D by co-culture with human fibronectin (Sigma) labeled with Alexa-594 (Invitrogen). Actomyosin contractility and microtubule assembly were inhibited with blebbistatin and nocodazole, respectively (Calbiochem).

Immunofluorescene, confocal microscopy, and image analysis. For immunofluorescent labeling of protein in endothelial cells in 3-D fibrin, gels were fixed with 4% paraformaldehyde, and endothelial cells were permeabilized with 0.125% Triton X-100. 3-D gels were blocked with 3% normal goat serum, following incubation with primary antibodies for 12 h. After washing with PBS,

gels were incubated with secondary antibodies (Alexa- 488 or 594 -labeled goat anti-mouse or anti-rabbit antibodies; Invitrogen) with Alexa- 488 or 594 -labeled phalloidin, propidium iodide, or DAPI counterstains (Invitrogen). After a final wash, cells in 3-D were visualized using an Olympus FV500 confocal microscope with Fluoview software, using a 60X water immersion objective (1.2 numerical aperture; Olympus, Center Valley, PA). Analysis of chromatin distribution within 2-D and 3-D nuclei was performed using Metamorph software (Molecular Devices, Downingtown, PA).

Transgene expression in primary endothelial cells. For expression of GFP-histone H2B or DsRed-Histone H2B, cells were transfected via Lipofectamine 2000 (Invitrogen, Carlsbad, CA) according to the manufacturer's protocol. To express GFP-KASH (provided by B. Burke, University of Florida) or GFP-lamin (provided by T. Glover, University of Michigan) at high efficiency, endothelial cells were transduced with amphotropic retroviruses in the presence of 50 ng/ml VEGF and 6 μg/ml polybrene (Sigma, St. Louis, MO).

Atomic force microscopy micro-indentation. Fibrin gels were washed briefly with PBS after removing culture medium. Samples were mechanically characterized using an Asylum MFP-3D atomic force microscope (Asylum Research, Santa Barbara, CA) by performing micro-indentation using a sphere-tipped probe (Novascan, Ames, IA) with a sphere diameter of 5 μm and a nominal spring constant of ~60 pN/nm. The cantilever spring constant was confirmed by thermal fluctuation method (23). The AFM system was calibrated by following the manufacturer's recommended standard procedure before each indentation measurement. AFM micro-indentation was performed in PBS solution at room temperature. Individual force-indentation profile was acquired at an indentation rate of 2 μm/s using deflection trigger mode with a trigger value of 200 nm. The AFM tip was positioned either adjacent to or away from a cell. Shear modulus at each position was calculated from fitting force-indentation data using a Hertz sphere model (24).

Cell encapsulation in PEG hydrogels. MMP-resistant or MMP-degradable PEG hydrogels were formed by FXIIIa catalized reaction as described (25).

Briefly, 8-arm PEG-Gln and PEG-Lys were blended to generate stoichiometrically balanced ([Gln]/[Lys]) PEG precursor solutions. The PEG-Lys component was either chosen to contain a linker peptide that is susceptible (GPQG/IWGQ, with / indicating the cleavage site) or resistant (GDQGIAGF) to MMP-mediated degradation. The PEG precursor solutions (1.5, 2.0 and 2% w/v) were cross-linked upon addition of 10 U/mL FXIIIa in presence of 50mM TrisHCl pH 7.6, 50mM $CaCl_2$, 50μM Lys-RGD (Ac-FKGGRGDSPG-NH_2, NeoMPS Strasbourg, France) and cells suspended in medium 12% (v/v) of the total volume. To form hydrogel discs, 20μL drops of the still liquid reaction mixture were sandwiched between sterile, hydrophobic glass microscopy slides that were separated by 1 mm spacers and clamped with binder clips. Polymerization was then allowed to take place for 30min. at 37°C in a humidified incubator. To visualize the matrix, 25μM Lys-FITC (Ac-FKGGGK-FITC-NH_2, NeoMPS Strasbourg, France) was added prior to reaction, leading to a homogenous covalent tethering of FITC to the matrix.

Cell culture of micropatterned substrata. Microcontact printing techniques were used to fabricate substrates patterned with regions that were coated with fibronectin and regions that resisted such adsorption, as previously described (26). 1225 um^2 islands (35um x 35um) were used to constrain cell spreading, while continuous surfaces of fibronectin allowed for full spreading. Briefly, PDMS stamps bearing the relevant pattern of islands were washed with ethanol, dried, immersed for 1 hr in an aqueous solution of 25 mg/ml fibronectin, rinsed thoroughly in water, dried, and placed in conformal contact against the culture substrate, blocked with 0.2% Pluronic F127 (BASF), and used under standard culture conditions.

Results.

Dynamic regulation of nuclear architecture characterizes endothelial cell morphogenetic responses. At sites of tissue damage, inflammation or neoplasia, fibrinogen is converted into a 3-D meshwork of fibrin fibrils that serve as a structural support for endothelial cells undergoing neovascularization (3-5, 27). When endothelial cells are embedded within a 3-D fibrin gel, the cells adopt a spherical shape and assume a dormant phenotype characterized by the absence of either proliferative or apoptotic responses (Figure 6.1)(3). By contrast, in the presence of a pro-angiogenic cocktail comprised of VEGF and HGF, the endothelial cells undergo marked shape changes over the first 48 hrs of the culture period, and subsequently initiate proliferative and tubulogenic programs that result in the formation of an anastomosing network of neovessels over a 6 d culture period (Figure 6.1) (3, 5, 6).

As recent studies have identified a series of direct interactions linking the cell surface to the nuclear envelope (19, 22, 28), a 3-D-specific requirement for VEGF/HGF-dependent induction of endothelial cell morphogenesis is consistent with a hypothetical model wherein cell shape directly or indirectly impacts nuclear architecture. To monitor nuclear morphology in 3-D culture, endothelial cells were either transfected with a GFP-tagged form of the nuclear matrix filament, lamin A, or immunostained for the integral nuclear membrane protein, emerin (19, 22, 28, 29). Unexpectedly, endothelial cells cultured within fibrin gels under basal conditions (i.e., in serum-containing media, but without VEGF/HGF) display an unusual nuclear morphology with numerous lamin A matrix and emerin infoldings and surface irregularities (Figure 6.2). In tandem, the distribution of nuclear pore complexes that regulate the trafficking of proteins and RNA across the nuclear envelope (30-32) is perturbed with aggregates appearing at nuclear membrane invaginations (Figure 6.2). Upon addition of VEGF/HGF, however, the nuclei of fibrin-embedded endothelial cells undergo a dramatic - and 3-D-specific - remodeling in shape to assume a more classic, ovoid morphology complemented by the uniform distribution of nuclear pore complexes (Figure 6.2). Three-dimensional reconstructions of DAPI-stained nuclei confirm that

nuclear architecture transitions between multi-lobed and smooth elliptical shapes in the absence or presence, respectively, of VEGF/HGF (Figure 6.2).

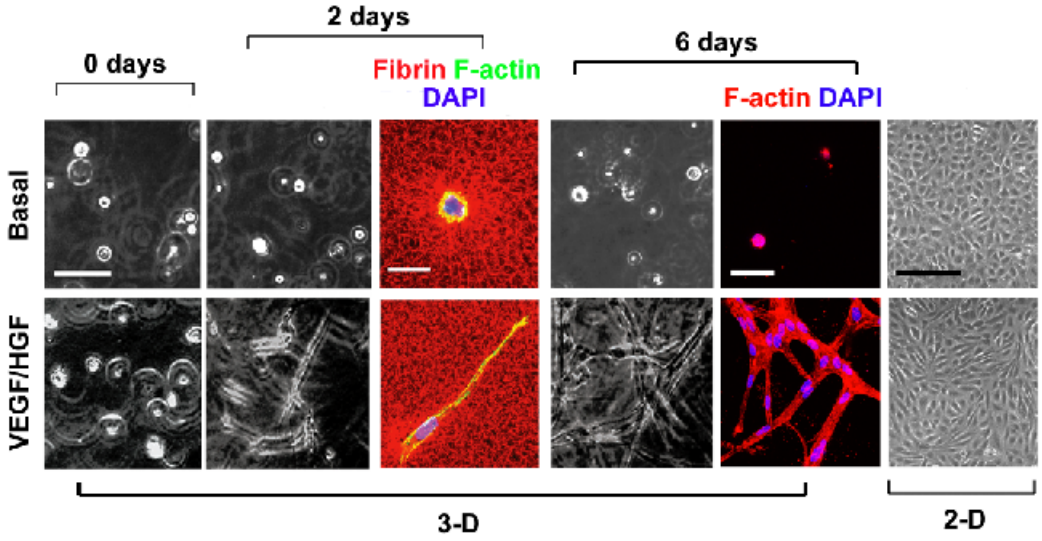

Figure 6.1. Growth factor-dependent 3-D vasculogenesis

Endothelial cells in 3-D fibrin were treated with serum alone (*top panels*), or with serum plus 100 ng/ml VEGF and 50 ng/ml HGF (*bottom panels*) for 6 d. Phase contrast images were taken at 0 d (*First set of panels on left*), 2 d (*second panels*) and 6 d (*fourth set of panels*) incubation (scale bar, 100 μm). (*Third set of panels*) Endothelial cells were embedded in Alexa-594-labeled 3-D fibrin (red) and cell morphology assessed after 48 h treatment with or without VEGF and HGF. Endothelial cells were stained with Alexa-488-labeled phalloidin (green) and 4,6-diamidino-2-phenylindole (DAPI; blue; scale bar, 20 μm). (*Fifth set of panels*) Endothelial cells were embedded in 3-D fibrin for 6 d with or without VEGF and HGF and stained with Alexa-594-labeled phalloidin and DAPI to visualize tubes (scale bar, 50 μm). (*Right panels*) Representative 2-D morphology of endothelial cells cultured atop 2-D fibrin substrata are presented (scale bar, 200 μm).

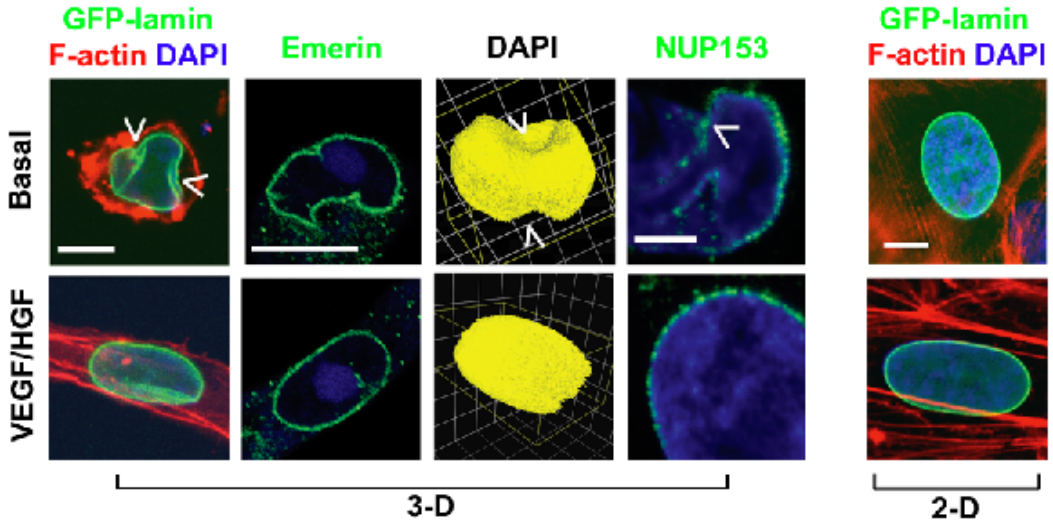

Figure 6.2. Regulation of nuclear architecture during 3-D vasculogenesis

Endothelial cells were cultured atop (2-D, *right panels*) or within 3-D fibrin without growth factors (baseline) or with VEGF and HGF for 2 d. 3-D nuclear architecture (*second column*; scale bar, 10 μm) was assessed by tracking GFP-lamin A distribution (green) and staining F-actin with Alexa-594-labeled phalloidin (red) and DAPI (*left panels*, blue; scale bar, 10 μm). 3-D nuclear structure was further examined by immunostaining for the nuclear matrix protein emerin (*second column of panels*), 3-D reconstruction of DAPI-stained nuclei (*third column of panels*; one unit, 5 μm^2) or immunostaining for NUP153 (green, *fourth set of panels*; scale bar, 2 μm). Nuclear membrane invaginations and NUP153 aggregates are demarcated by arrowheads. 2-D nuclear structure was examined by assessing GFP-lamin A distribution in endothelial cells cultured atop fibrin gels (*far right panels*; scale bar, 10 μm).

Given that changes in nuclear shape can potentially alter chromatin packaging (19, 22, 28), chromatin organization was assessed in basal versus stimulated endothelial cells in 3-D culture by monitoring the localization of GFP-tagged histone H2B or pericentromeric constitutive heterochromatin [visualized by immunostaining for trimethylated lysine 9 of histone H3 (H3K9me3)](33, 34). In unstimulated endothelial cells embedded within 3-D fibrin gels, GFP-H2B as well as H3K9me3 localization reveals chromatin condensation at discrete peripheral locations in the nucleus (Figure 6.3). By contrast, following a 48 h culture period with VEGF/HGF, chromatin is dramatically reorganized in elongating endothelial cells, assuming a diffuse distribution with a relative collapse of the interchromatin space (Figure 6.3). Importantly, endothelial cells

cultured atop – rather than embedded within – fibrin gels (i.e., 2-D culture) display distinct growth requirements from those observed in 3-D culture and generate confluent monolayers in the absence or presence of VEGF/HGF (Figure 6.1). Likewise, under 2-D culture conditions, neither changes in nuclear shape nor nuclear pore complex distribution are dependent on VEGF/HGF (Figure 6.2).

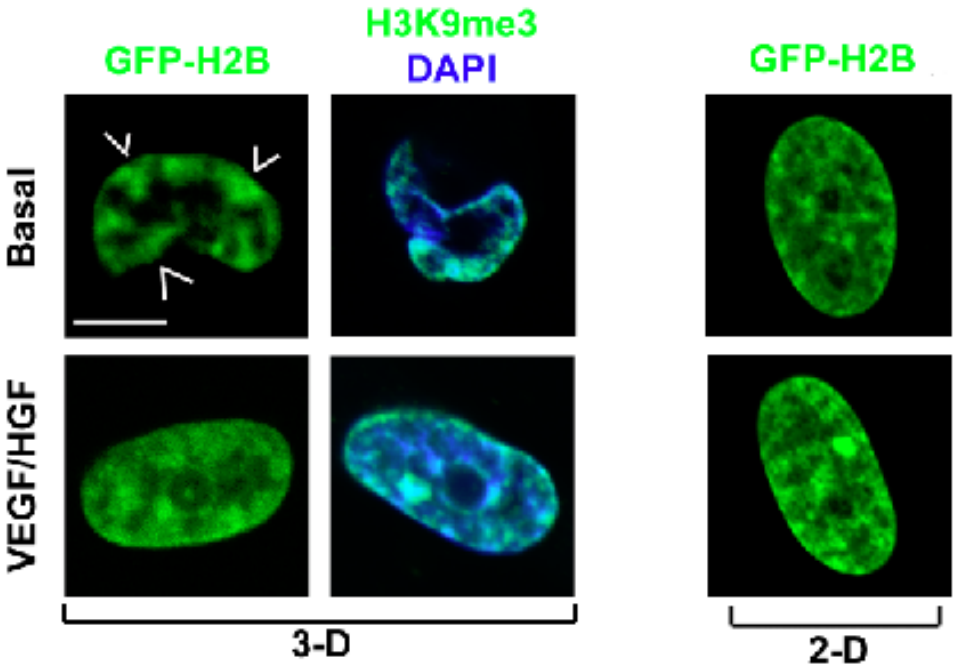

Figure 6.3. Chromatin dynamics during 3-D vasculogenesis

Chromatin distribution in nuclei of endothelial cells in 3-D fibrin under baseline conditions (*top panels*) or with VEGF and HGF (*lower panels*) was assessed by tracking GFP-tagged histone H2B (green, *left panels*) or H3K9me3 [green, *middle panels* with DAPI counterstaining (blue), scale bar, 5 μm]. Peripheral chromatin condensation is marked with arrowheads. Chromatin was also monitored in endothelial cells cultured atop at 2-D fibrin substratum by tracking GFP-H2B distribution (*right panels*).

3-D ECM remodeling controls nuclear organization and function. Within the confines of the 3-D ECM, changes in cell shape necessitate pericellular remodeling of the surrounding fibrin network (35, 36). Indeed, in the presence of VEGF/HGF, endothelial cells mobilize the membrane-anchored matrix metalloproteinases (MT-MMPs), MT1-MMP, MT2-MMP and MT3-MMP, to

mediate fibrinolysis via a process that is abrogated by the pan-specific MMP inhibitor, GM6001 (Figure 6.4)(5, 37). In tandem fashion, VEGF/HGF-stimulated endothelial cells enmesh themselves in an interwoven network of fibronectin fibrils whose assembly can be inhibited specifically by the fibronectin-binding bacterial peptide, FUD (Figure 6.4)(3).

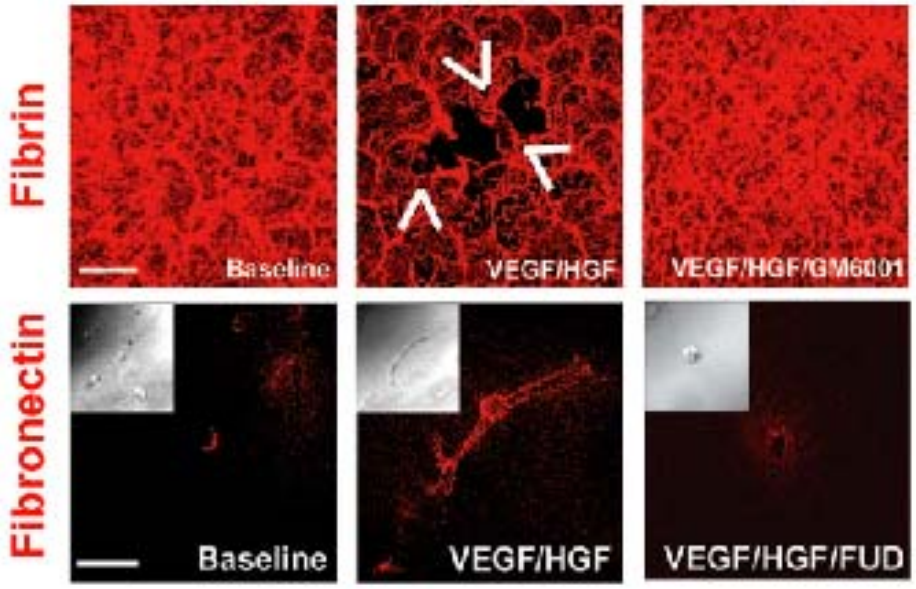

Figure 6.4. Endothelial cells remodel the pericellular ECM during vasculogenesis

Endothelial cells were cultured in the presence of Alexa-594-labeled fibrin (red) under baseline conditions, with VEGF and HGF, or with VEGF and HGF and 5 μ*M* GM6001 for 6 d, and degraded areas (arrowheads) were examined by confocal laser microscopy (*top panels*). Scale bar, 50 μm. (*Bottom panels*) Endothelial cells in 3-D fibrin were cultured under baseline conditions, with VEGF and HGF, or with VEGF, HGF, plus 250 n*M* of the FUD peptide in the presence of 20 μg/ml Alexa-594-labeled fibronectin (red) for 2 d, at which time pericellular fibronectin fibrillogenesis was examined by confocal laser microscopy. Scale bar, 50 μm.

Consistent with a required, and 3-D-specific, role for MT-MMP-dependent fibrinolysis and fibronectin matrix assembly during neovessel formation, the addition of either GM6001 or FUD completely blocks VEGF/HGF-induced changes in cell shape, proliferation or tubulogenesis, but not 2-D cell spreading or proliferation (Figure 6.5). Furthermore, when ECM remodeling is inhibited, VEGF/HGF stimulation is unable to trigger the metamorphosis of nuclear shape or chromatin structure that is normally observed during 3-D tubulogenesis (Figure

6.6). The ability of GM6001 or FUD to block the VEGF/HGF-induced reorganization of nuclear architecture in 3-D culture is not associated with changes in apoptosis (Figure 6.7), and neither inhibitor affects nuclear architecture or chromatin organization under 2-D culture conditions (Figure 6.6).

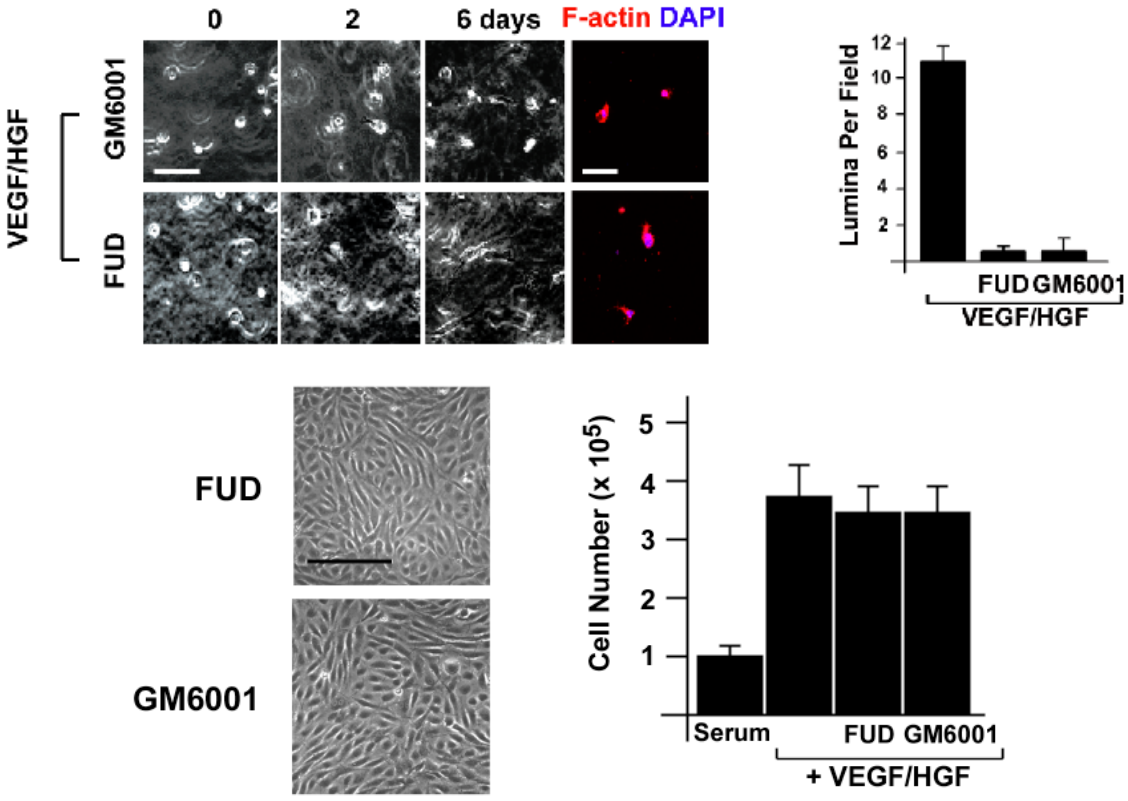

Figure 6.5. Pericellular ECM remodeling is required for 3-D vasculogenesis

(*Top panels*) Endothelial cells were cultured in 3-D fibrin in the presence of VEGF and HGF with either GM6001 or FUD and 3-D morphology monitored by phase contrast microscopy at 0, 2, or 6 days (scale bar, 100 μm), or by staining with Alexa-594-labeled phalloidin (red) and DAPI (blue, *right panels;* scale bar, 50 μm). (*Right*) 3-D fibrin gels were sectioned and lumen formation assessed following hematoxylin and eosin staining. (*Bottom panels*) Endothelial cells were cultured atop fibrin gels and morphology assessed by phase contrast microscopy (scale, 200 μm). Cell growth was monitored by plating 50,000 cells atop a fibrin gel under the indicated conditions, and cell number counted at 72 h incubation.

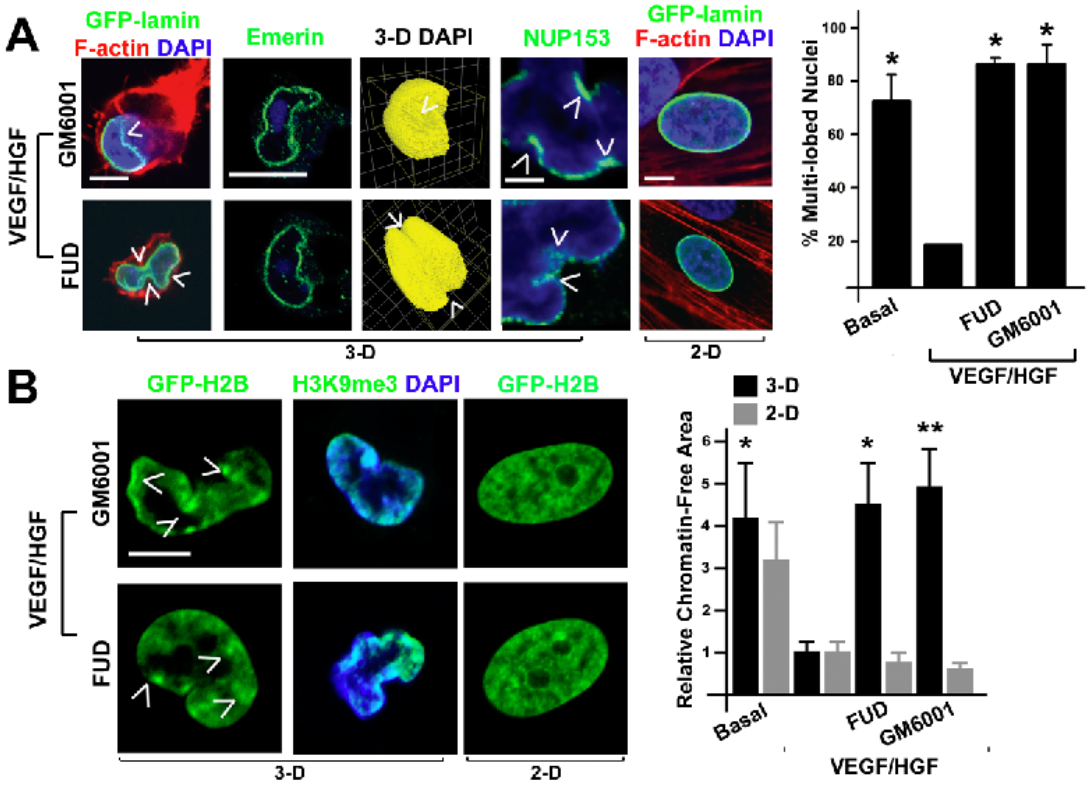

Figure 6.6. Pericellular 3-D ECM remodeling governs nuclear architecture

A. Endothelial cells were cultured in 3-D fibrin with VEGF and HGF with either GM6001 or FUD for 2 days, and nuclear morphology assessed by GFP-lamin staining (*left panels;* scale bar, 10 μm), immunostaining for emerin (*second set of panels;* scale bar, 5 μm), 3-D reconstruction of DAPI-stained nuclei (*third set of panels;* one unit, 5 μm^2) and immunostaining for NUP153 (*fourth set of panels;* scale bar, 2 μm). (*Right panels*) Endothelial cells were cultured atop fibrin gels and nuclear morphology assessed by GFP-lamin tracking (scale bar, 10 μm). Frequency of multi-lobed nuclei for each condition was quantified by tracking GFP-lamin A (n = 3, * $P < 0.005$ compared to VEGF/HGF, student's *t*-test used throughout). **B.** Endothelial cell chromatin architecture in 3-D was analyzed by tracking GFP-H2B distribution (*left panels*) and H3K9me3 (*middle panels*). (*Right panels*) Chromatin was localized in cells cultured atop fibrin gels by visualizing GFP-H2B distribution (scale bar, 5 μm). Chromatin free-area was analyzed by morphometric analysis (n = 5, * $P \leq 0.01$; ** $P < 0.001$ compared to VEGF/HGF).

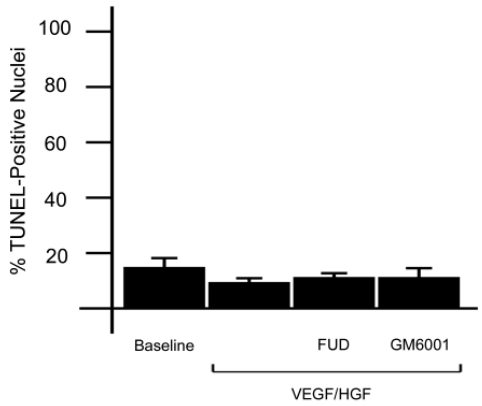

Figure 6.7. ECM remodeling does not affect 3-D apoptosis

Endothelial cells were cultured within 3-D fibrin gels with no growth factors (baseline), VEGF and HGF, VEGF, HGF, and FUD, or VEGF, HGF and GM6001 for 2 d, at which time apoptosis was assessed by TUNEL stain (n = 6).

As histone acetylation plays a critical role in blood vessel formation, and can be regulated by chromatin positioning within the nucleus (38-40), the acetylation status of histones H3 and H4 were assessed as functional markers of changes in chromatin organization. Stimulation of endothelial cells with VEGF/HGF in 3-D, but not 2-D, culture triggers a marked increase in acetylated histone H3 and H4, changes which are attenuated significantly by blocking MT-MMP activity or fibronectin fibrillogenesis (Figure 6.8).

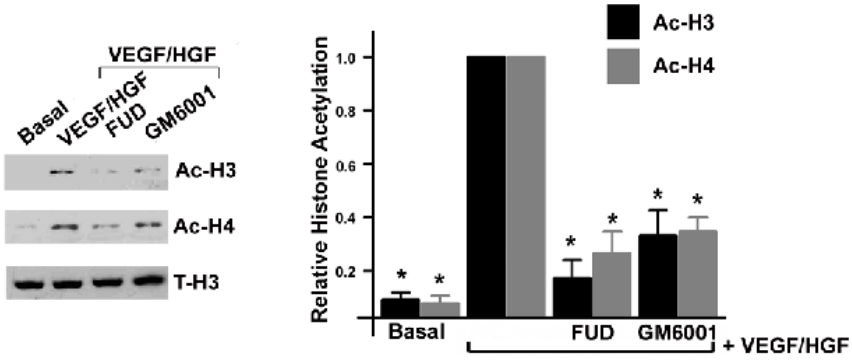

Figure 6.8. VEGF/HGF- and ECM-dependent histone acetylation

Endothelial cells were cultured within 3-D fibrin for 48 h under the indicated conditions. Levels of acetylated histones H3 (Ac-H3) and H4 (Ac-H4) in endothelial cells in 3-D cultures were measured by immunoblotting and levels were normalized to total histone H3 (T-H3; n = 3, * $p < 0.01$ compared to VEGF/HGF).

To correlate global changes in the patterns of histone acetylation with of gene expression, total RNA was isolated from endothelial cells that were embedded in 3-D fibrin gels either without or with VEGF/HGF, and in the absence or presence of either GM6001 or FUD. Following analysis on Affymetrix microarrays, principal component analysis (PCA) mapping demonstrates that VEGF/HGF-stimulated cells display a transcript profile distinct from resting cells (Figure 6.9A). By contrast, growth factor-stimulated cells cultured in the presence of GM6001 or FUD co-align in a distinct cluster, consistent with the inability of 3-D-embedded endothelial cells to respond fully to pro-angiogenic signals in the absence of ECM remodeling (Figure 6.9A). Surprisingly, however, while VEGF/HGF-dependent stimulation alters the expression of more than 500 distinct transcripts, blocking MT-MMP-dependent fibrinolysis or fibronectin matrix assembly significantly affects expression of fewer than 50 of the VEGF/HGF-regulated transcripts with only 12 genes similarly altered by GM6001 and FUD (Figure 6.9B and Table 6.1).

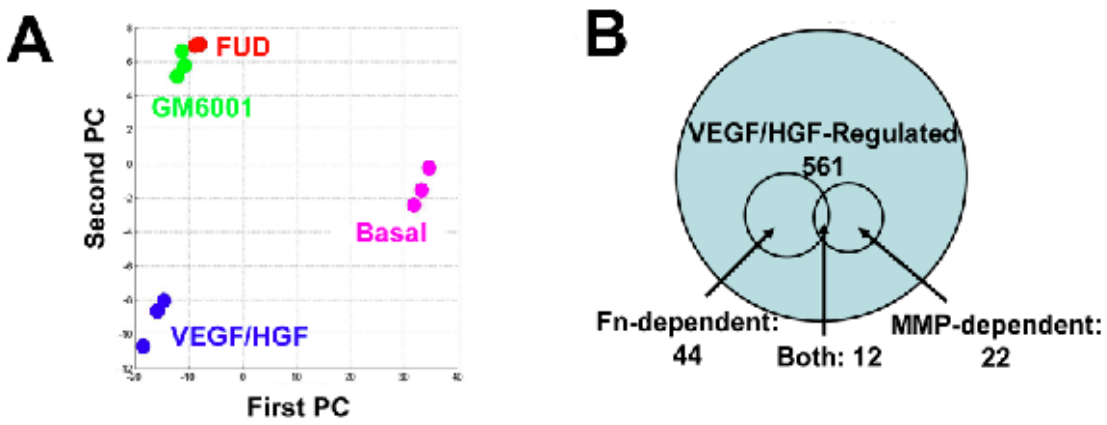

Figure 6.9. Analysis of the VEGF/HGF- and ECM-regulated transcriptomes

A. Endothelial cell transcripts were analyzed by Affymetrix cDNA microarrays. Principal component analysis (PCA) was used to compare global gene expression profiles. **B.** Number of significantly altered genes regulated by VEGF and HGF, FUD, and GM6001 are presented.

ProbeSet Name	UniGene ID	Gene Title	Gene Symbol	RefSeq Transcript ID
216583_x_at	---	unknown transcript	---	---
208898_at	Hs.272630	ATPase, H+ transporting, lysosomal 34kDa, V1 subunit D	ATP6V1D	NM_015994
206913_at	Hs.284712	bile acid Coenzyme A: amino acid N-acyltransferase (glycine N-choloyltransferase)	BAAT	NM_001701
207895_at	Hs.13967	N-acetylated alpha-linked acidic dipeptidase-like 1	NAALADL1	NM_005468
204528_s_at	Hs.524599	nucleosome assembly protein 1-like 1	NAP1L1	NM_004537 /// NM_139207
203228_at	Hs.466831	platelet-activating factor acetylhydrolase, isoform Ib, gamma subunit 29kDa	PAFAH1B3	NM_002573
204612_at	Hs.433700	protein kinase (cAMP-dependent, catalytic) inhibitor alpha	PKIA	NM_006823 /// NM_181839
202101_s_at	Hs.469820	v-ral simian leukemia viral oncogene homolog B (ras related; GTP binding protein)	RALB	NM_002881
206608_s_at	Hs.126035	retinitis pigmentosa GTPase regulator interacting protein 1	RPGRIP1	NM_020366
213874_at	Hs.159628	serpin peptidase inhibitor, clade A (alpha-1 antiproteinase, antitrypsin), member 4	SERPINA4	NM_006215
208495_at	Hs.249125	T-cell leukemia, homeobox 3	TLX3	NM_021025
210609_s_at	Hs.50649	tumor protein p53 inducible protein 3	TP53I3	NM_004881 /// NM_147184

Table 6.1. VEGF/HGF-stimulated gene expression changes dependent on pericellular ECM remodeling.

While more dramatic shifts in gene expression might have been predicted on the basis of the striking changes observed in the morphogenetic programs of GM6001- or FUD- treated endothelial cells, these results are consistent with an alternate model whereby cell shape-dependent inhibition of transcriptional machinery prevents new RNA synthesis while pre-existing transcripts are stabilized (41, 42). Indeed, VEGF/HGF treatment results in a marked induction of RNA transcription, a process attenuated significantly when ECM remodeling events are blocked by either FUD or GM6001 in 3-D, but not 2-D, culture (Figure 6.10). In data not shown, mRNA as well as rRNA synthesis are each inhibited by ~50% in the presence of FUD or GM6001 in 3-D culture.

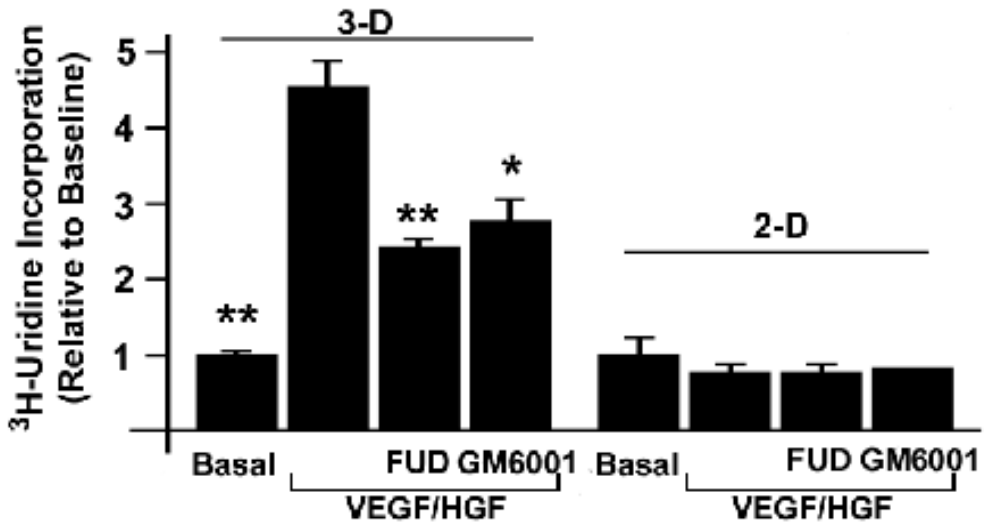

Figure 6.10. ECM remodeling is required for engagement of VEGF/HGF-stimulated RNA synthesis

Cells were either cultured atop (2-D) or within (3-D) fibrin gels, and transcriptional activity was monitored by pulse labeling cells for 2 h with 30 μCi/ml [^{3}H]-uridine.

To directly assess the functional status of ribosomal RNA and pre-mRNA processing sites during dynamic ECM remodeling in 3-D culture, endothelial cells were immunostained for fibrillarin (a pre-rRNA processing protein) or SC-35 (a pre-mRNA splicing protein (33, 43)). Stimulating endothelial cells with VEGF/HGF in 3-D culture results in the expected reorganization of fibrillarin from a single, centrally-located cluster of nucleoli within the interchromatin space to multiple foci distributed throughout the nucleus (Figure 6.11)(33, 43). Likewise, treatment with VEGF/HGF induces the reorganization of nuclear speckle morphology from a basal to activated state wherein a small number of large aggregates are dispersed as small foci throughout the nuclear compartment (Figure 6.11)(33, 43). In both cases, the activated patterns of fibrillarin and SC-35 distribution observed in VEGF/HGF-stimulated endothelial cells in 3-D culture could be reversed to that resembling unstimulated endothelial cells by blocking MMP activity or fibronectin matrix assembly (Figure 6.11). As expected, neither VEGF/HGF, FUD nor GM6001 affect fibrillarin or SC-35 distribution under 2-D culture conditions (Figure 6.12).

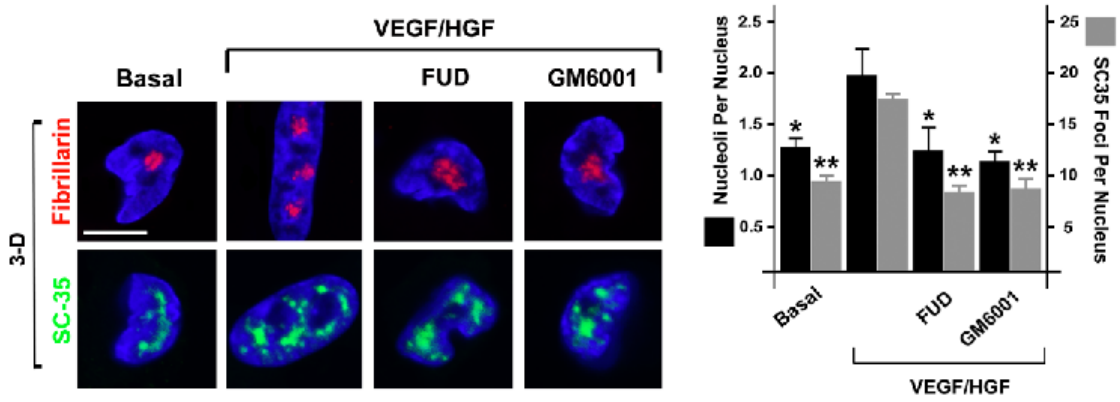

Figure 6.11. VEGF/HGF and ECM-dependent fibrillarin and SC-35 localization

Cells were cultured in 3-D fibrin under various conditions and stained for fibrillarin (red, *upper panels*) or SC-35 (green, *lower panels*) with counterstaining with DAPI (blue; scale = 5 μm). Average number of nucleoli and SC-35 foci per cell are presented.

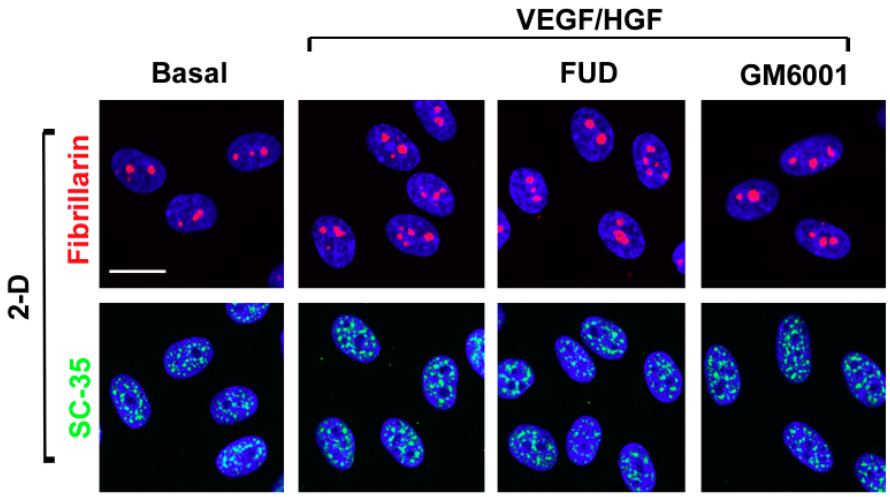

Figure 6.12. Fibrillin and SC-35 distribution are modulated independently of ECM remodeling in 2-D

Endothelial cells were cultured under the indicated conditions and stained for fibrillarin (red, *upper panels*) or SC-35 (green, *lower panels*), scale bar, 20 μm.

The cytoskeleton as a transducer of ECM structural dynamics to the nuclear envelope. Cytoskeletal architecture and tension are closely coupled to cell geometry (10, 12, 13, 44, 45), and can influence nuclear envelope shape under 2-D culture conditions (18, 46). Treatment of 3-D-embedded endothelial cells with VEGF/HGF induces marked cytoskeletal reorganization, with F-actin,

β-tubulin and vimentin redistributing from a diffuse, cortical pattern to a longitudinal fibrous network in tandem with an increase in isometric tension (Figure 6.13). In contrast, VEGF/HGF-triggered cytoskeletal remodeling and force induction in 3-D culture are inhibited completely by abrogating MT-MMP activity or fibronectin fibrillogenesis coincident with a loss of pericellular rigidity as assessed by atomic force microscopy micro-indentation (Figure 6.14), effects that are not observed under 2-D culture conditions (data not shown).

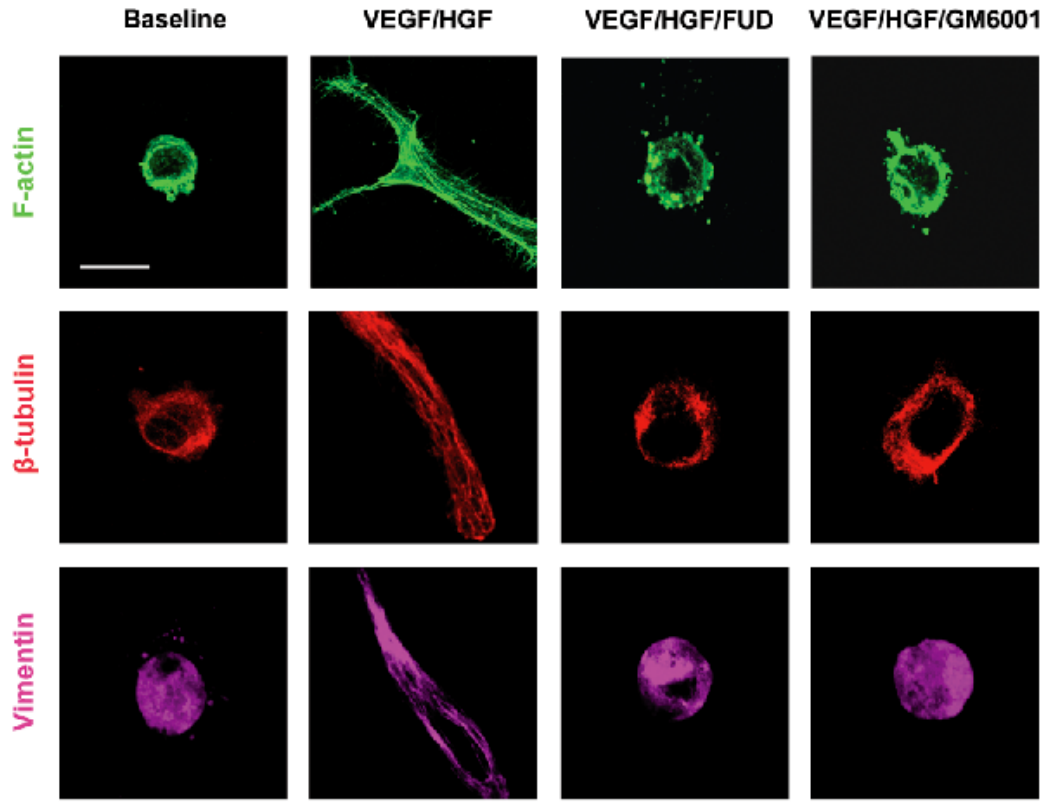

Figure 6.13. Regulation of cytoskeletal structure by 3-D ECM remodeling

Endothelial cells were cultured in 3-D fibrin without growth factors (baseline), with VEGF and HGF, or with VEGF, HGF, and GM6001 or FUD for 2 d, when cell shape and cytoskeletal architecture was examined by confocal laser microscopy following staining for F-actin with Alexa-488-labeled phalloidin (green), and immunocytochemical staining for β-tubulin (red) or vimentin (violet) . Scale = 20 μm.

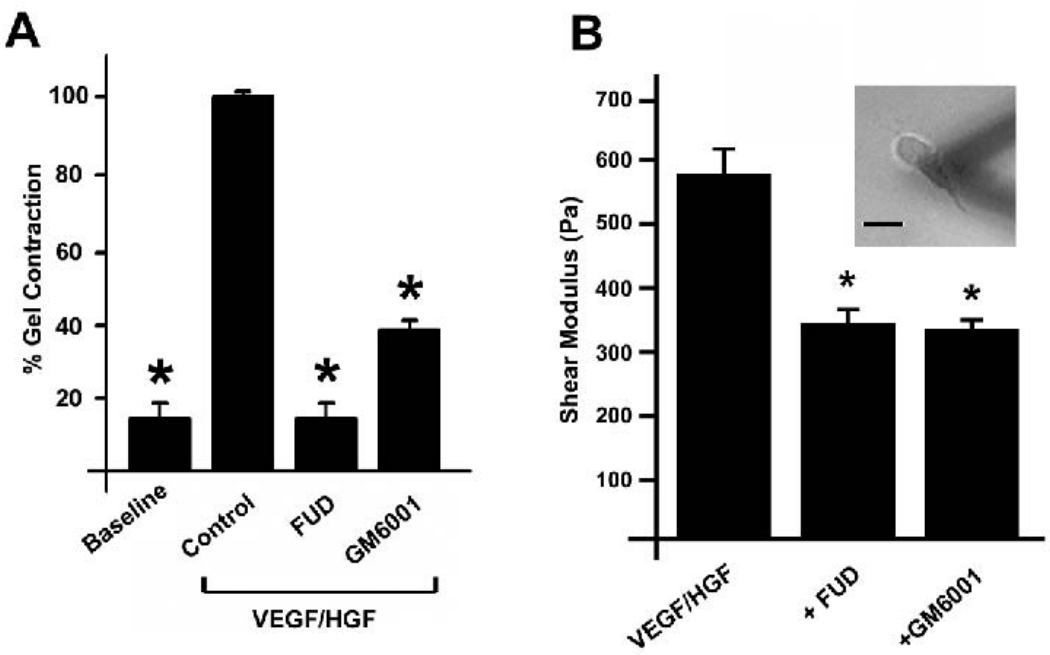

Figure 6.14. Regulation of cytoskeletal function by 3-D ECM remodeling

A. Cells were cultured in 3-D fibrin gels under various conditions for 48 h, at which time the gel was released from the edges of the culture well and allowed to contract for 24 h, when diameter of the contracted gel was measured. **B.** Pericellular ECM rigidity was measured by AFM. Phase contrast image shows probe location relative to 3-D cells (scale = 20 μm).

As cytoskeletal reorganization and contractile tension could serve as the biomechanical effectors that transmit structural and mechanical cues from the pericellular ECM to the nuclear envelope in 3-D culture, VEGF/HGF-stimulated endothelial cells were treated with either blebbistatin to inhibit myosin ATPase function or nocodazole to prevent microtubule assembly (3, 47). Both agents abrogate significantly the contractile force exerted on the 3-D ECM to a similar degree as that observed following treatment with FUD or GM6001 while completely inhibiting endothelial cell 3-D tubulogenesis (Figure 6.15 and data not shown). Further, compared with the ellipsoid nuclear shapes adopted by VEGF/HGF-stimulated endothelial cells in 3-D culture, endothelial cells cultured in the presence of blebbistatin or nocodazole display i) multi-lobed nuclei with perturbations in nuclear pore distribution, ii) chromatin condensations at the nuclear periphery with increased interchromatin space and iii) decreased levels of acetylated histones H3 and H4 (Figures 6.15 and 6.16). *In toto*, these results

demonstrate that the ECM-dependent regulation of cytoskeletal organization is a critical determinant of nuclear as well as chromatin architecture.

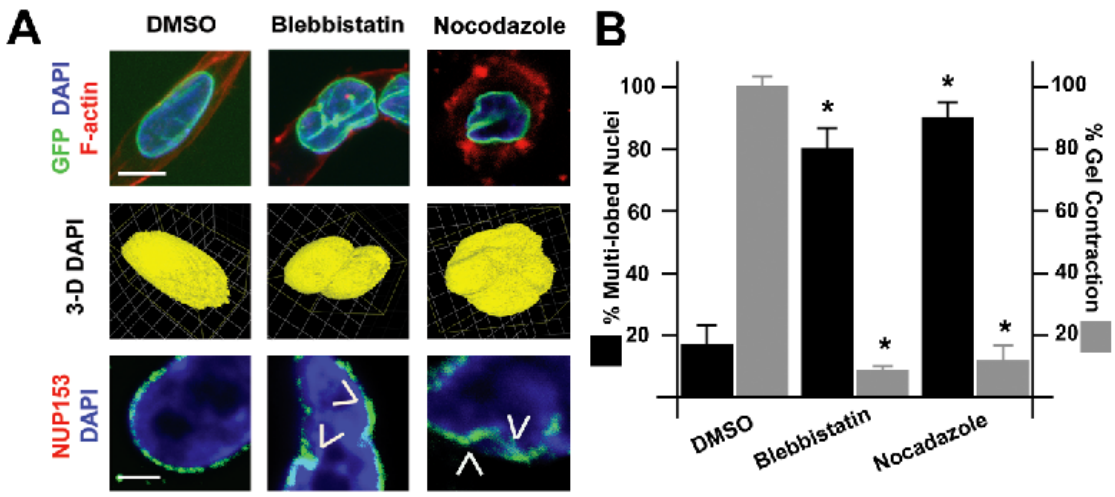

Figure 6.15. Cytoskeletal dynamics regulate nuclear organization

A. Cells were cultured in 3-D fibrin with VEGF and HGF and treated with DMSO vehicle or 50 μ*M* ± blebbistatin or 5 μ*M* nocodazole. Nuclear morphology was assessed by examining GFP-lamin A distribution (green; scale bar, 5 μm). 3-D nuclear structure was assessed by reconstruction of DAPI-stained nuclei (1 unit, 4.2 μm). Nuclear pore complex was examined by staining for NUP153 (green; scale bar, 1 μm). **B.** Endothelial cells were cultured in 3-D fibrin for 48 h with VEGF and HGF alone or with VEGF and HGF in the presence of either nocodazole or blebbistatin. % multi-lobed nuclei were quantified (n = 3; * $P < 0.05$ compared to control). Gel contraction was assessed following release of the 3-D matrix from the edges of the tissue culture well (* $P < 0.005$ compared to control).

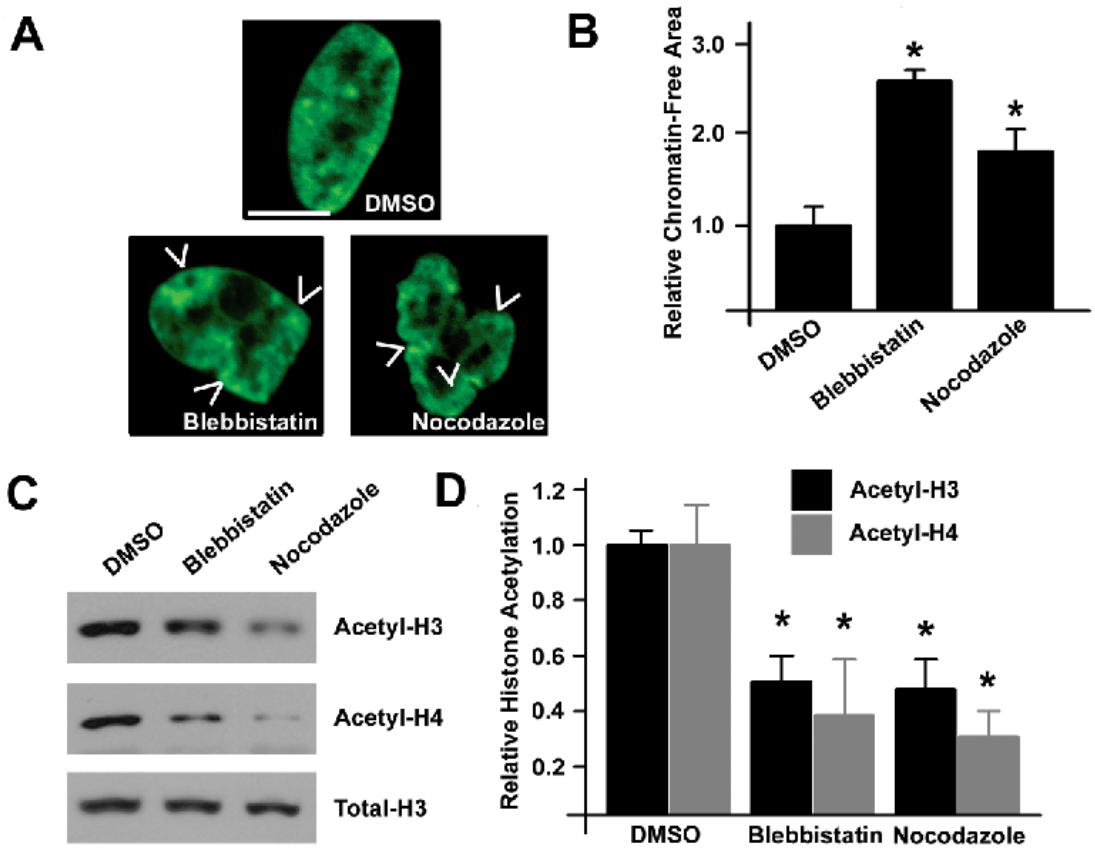

Figure 6.16. Cytoskeletal dynamics regulate chromatin structure

A-B. Cells were engineered to express GFP-H2B. Chromatin distribution was tracked by confocal laser microscopy, and chromatin free area (relative to DMSO vehicle) was measured (scale bar, 5 μm; n ≥ 3; * $P <$ 0.01). **C-D.** Cells in 3-D were lysed, and levels of acetylated histones H3 and H4 were assessed by Western blot.

Nesprins regulate 3-D organization of the nuclear compartment. Physical interactions between cytoskeletal networks and the nucleus can be mediated by a family of Klarsicht, ANC-1, Syne homology (KASH) domain-containing proteins whose C-terminal domains are embedded within the outer nuclear membrane where they interact with the inner nuclear membrane via members of the SUN protein family (19-22, 48). In turn, SUN proteins span the inner nuclear membrane to establish binding interactions with a scaffolding of lamin family members and nuclear pore complexes (19, 21, 22). Endothelial cells express the KASH domain-containing proteins, nesprins-1 and 2 (also termed Syne-1 and 2), which bind F-actin as well as nesprin-3, which indirectly interacts with

intermediate filaments via binding to plectin (Figure 6.17)(19, 22, 49). While VEGF/HGF-treated endothelial cells embedded in 3-D fibrin gels display uniform nesprin distribution within the nuclear envelope, unstimulated endothelial cells, as well as VEGF/HGF-stimulated endothelial cells treated with GM6001 or FUD, exhibit irregular nesprin distributions, with nesprin aggregates accumulating at nuclear membrane invaginations (Figure 6.18).

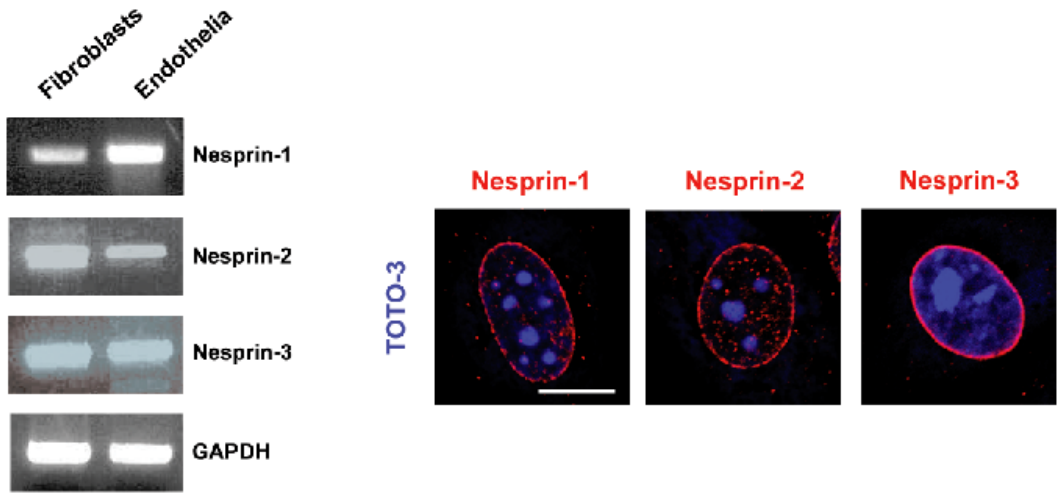

Figure 6.17. Endothelial cells express nesprins 1-3

Expression of nesprins-1,2, and 3 in endothelial cells were assessed by RT-PCR (*left*) or immunocytochemistry (*right*). Scale bar, 5 μm.

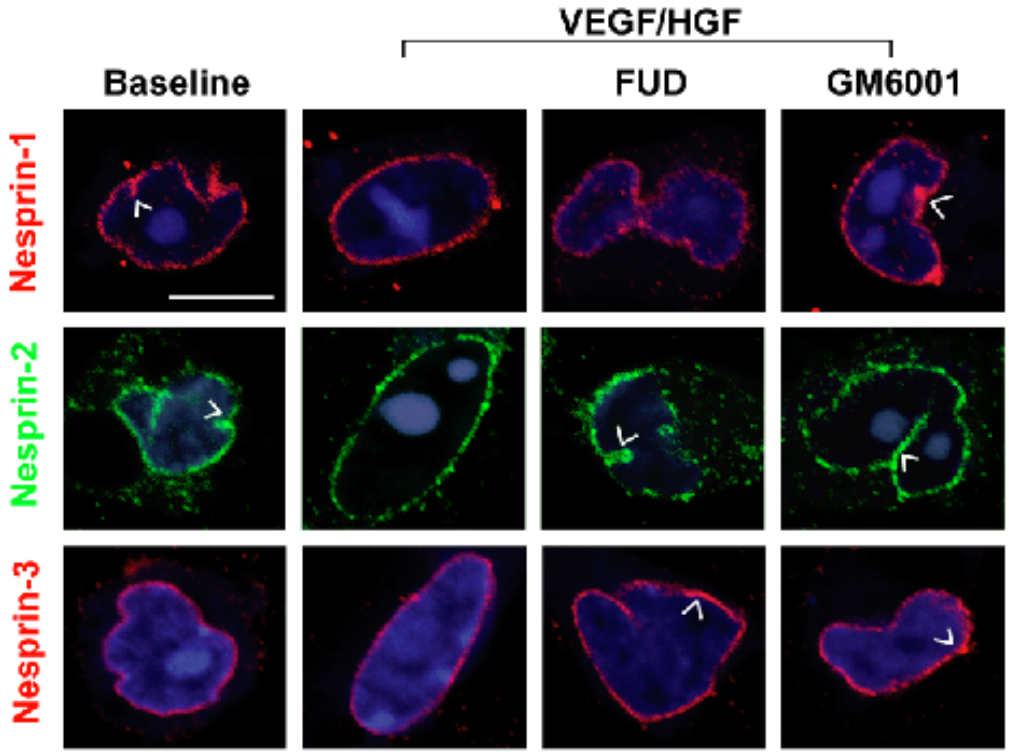

Figure 6.18. 3-D ECM remodeling controls nesprin distribution

Cells in 3-D fibrin were stained with antibodies against nesprins-1,2, or 3 and counterstained with TOTO3. Nesprin localization was assessed by confocal laser microscopy. Arrowheads indicate nesprin accumulation at membrane infoldings (scale bar, 10 μm).

Because endothelial cells remodel their surrounding ECM as a means to organize cytoskeletal structure (3), physical interactions between the cytoskeleton, nesprins, SUN proteins and lamins likely dictate nuclear structure. Hence, the cytoskeleton/nesprin continuum was perturbed by expression of the dominant-negative GFP-KASH, which acts as a truncated nesprin protein that binds to SUN proteins without interacting with cytoskeletal elements (20, 49, 50). Compared to VEGF/HGF-stimulated endothelial cells cultured in 3-D, endothelial cells expressing GFP-KASH fail to trigger nuclear remodeling and adopt the multi-lobed nuclear shape characteristic of unstimulated endothelial cells (Figure 6.19). Further, GFP-KASH expression induces peripheral chromatin condensation and perturbs the distribution of nucleoli and nuclear speckles while inducing marked reductions in acetylated histone H3 or H4 levels (Figure 6.19). Consistent with a proposed role for nuclear organization in regulating endothelial

cell function, KASH-expressing cells are unable to participate in a normal tubulogenic response (i.e., with a 50% transduction efficiency, tubulogenesis is decreased by ~80% of maximal in the targeted endothelial cell population, i.e., from 9.8 ± 2.3 lumina/field to 6.0 ± 2.0 lumina/field; n=3).

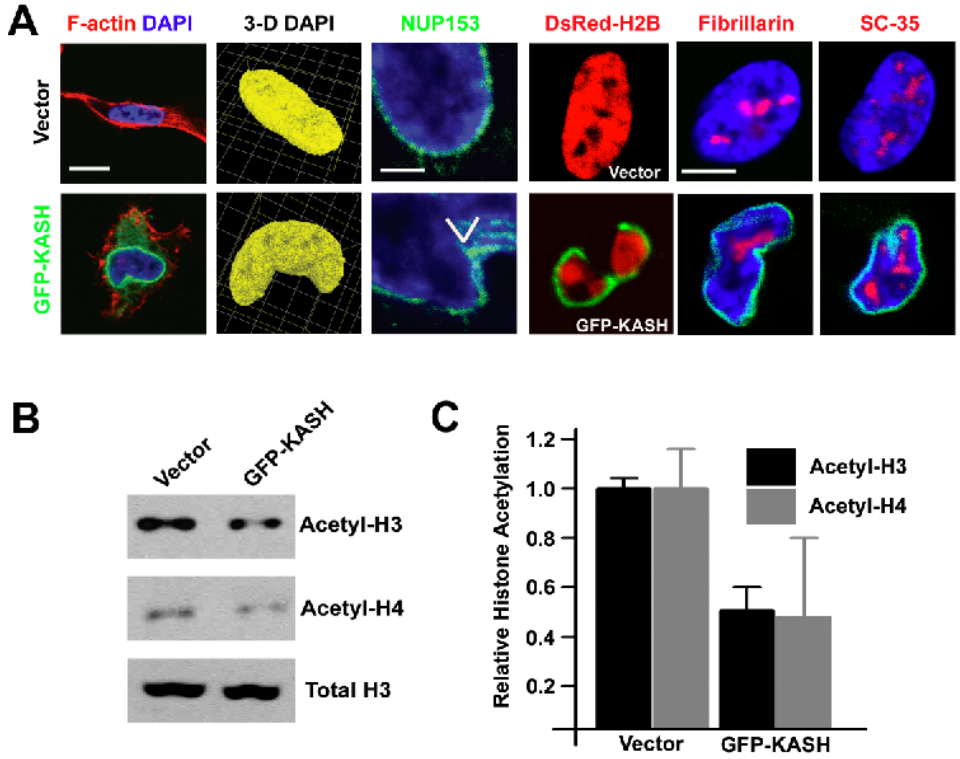

Figure 6.19. LINC complex interactions regulate nuclear organization

A. Cells engineered to express GFP-KASH or the control vector backbone were cultured in 3-D fibrin with VEGF and HGF for 48 h. Nuclear morphology was assessed by examining GFP-KASH distribution (*left panels;* green; scale bar, 10 μm). 3-D nuclear structure was assessed by reconstruction of DAPI-stained nuclei (*second set of panels;* 1 unit, 4.2 μm). Nuclear pore complex was examined by staining for NUP153 (*third set of panels;* green; scale bar, 1 μm). Vector cells contained 31 ± 4 % multi-lobed nuclei, while GFP-KASH cells contained 90 ± 2% (n = 3). Cells were engineered to express DsRed-H2B in addition to control vector or GFP-KASH. Chromatin distribution was tracked by confocal laser microscopy (*fourth set of panels*). Scale bar, 5 μm. GFP-KASH cells exhibited a 7 ± 1.3-fold increase in interchromatin space (n = 5). Cells were stained with antibodies against either fibrillarin (*fifth set of panels;* red; scale bar, 5 μm) or SC-35 (*sixth set of panels*). **B-C.** Cells in 3-D were lysed, and levels of acetylated histones H3 and H4 were assessed by Western blot.

Coupling of cell geometry with nuclear structure and function. If ECM-dependent changes in 3-D cell geometry regulate nuclear architecture, then direct modulation of endothelial cell shape - independent of targeting ECM remodeling proteases, neomatrix assembly or cytoskeletal-nuclear membrane interactions - would be predicted to similarly impact nuclear organization and chromatin structure. Consequently, endothelial cells were cultured within 3-D, biomimetic poly(ethylene glycol) (PEG) hydrogels containing RGD peptides incorporated pendantly within a transglutaminase-crosslinked structure that is engineered to be either susceptible, or resistant, to MMP-mediated hydrolysis (Figure 6.20)(25, 51). In this manner, endothelial cell spreading is controlled specifically as a function of the susceptibility of the 3-D hydrogel to proteolytic remodeling.

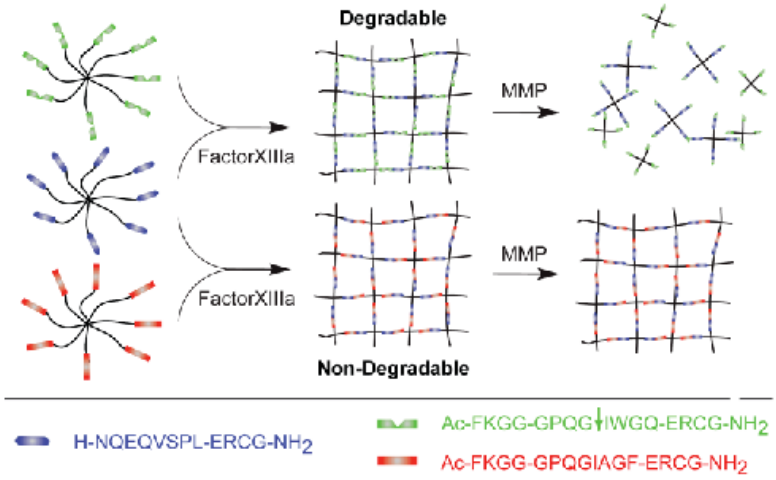

Figure 6.20. Factor XIIIa-catalyzed PEG hydrogel formation

The transglutaminase enzyme factor XIIIa was used to crosslink two multi-arm PEG-peptide conjugates bearing complementary transglutaminase peptide substrates (NQEQVSPL) derived from the N-terminus of α_2-plasmin inhibitor and the synthetic lysine donor peptide Ac-FKGG. Adding FXIIIa to an aqueous precursor solution containing these PEG-peptide conjugates (2.0%) led to gelation within a few minutes at 37°C. To render the gels susceptible to degradation by MMPs, the lysine donor peptide was designed to contain the MMP substrate GPQG↓IWGQ, derived from the native sequence GPQG↓IAGQ found in a1(I) collagen chain (↓ indicates the cleavage site). The sequence GDQGIAGF was chosen as MMP-insensitive control linker. To provide cell adhesion sites to the otherwise inert gels, the integrin-binding peptide H-NQEQVSPL-*RGDSPG*-NH_2 was grafted to both gel types at constant concentration.

Within MMP-sensitive gels, endothelial cells are capable of spreading in response to VEGF/HGF while in MMP-resistant gels, endothelial cells remain locked in a spherical shape (Figure 6.21). As predicted, elongated endothelial cells embedded within MMP-sensitive scaffolds display oval nuclei as revealed by GFP-lamin tracking, while spherical cells embedded in MMP-resistant scaffolds exhibit multi-lobed nuclei (Figure 6.21). Furthermore, genome packaging is regulated as a function of cell shape in 3-D culture with chromatin condensations directed to the nuclear periphery in MMP-resistant hydrogels (Figure 6.21).

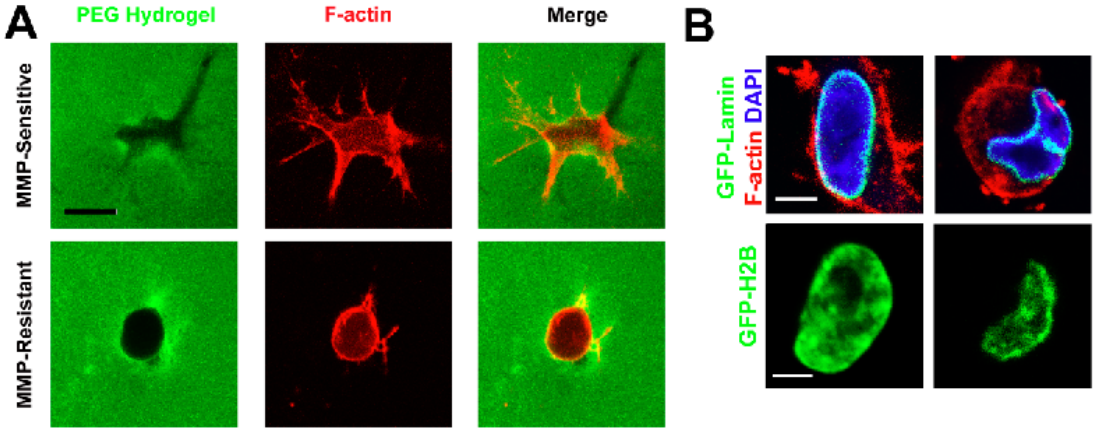

Figure 6.21. 3-D cell shape is the critical regulator of nuclear architecture

A. Endothelial cells were embedded in 3-D PEG hydrogels with MMP-sensitive (top panels) or resistant (bottom panels) linkers. 3-D gels were labeled with FITC (green) and cell shape was monitored following staining with Alexa-594-labeled phalloidin (red). Scale bar, 20 μm. **B.** (*Top panels*) Cells were embedded in 3-D PEG hydrogels and nuclear architecture was tracked by assessing distribution of GFP-lamin (green). Cells were counterstained with Alexa-594-labeled phalloidin (red, F-actin) and DAPI (blue). Scale bar, 10 μm. (*Bottom panels*) Cells were embedded in 3-D PEG hydrogels and chromatin architecture was tracked by examining distribution of GFP-histone H2B by confocal microscopy (green). Scale = 10 μm.

Alternatively, endothelial shape was modulated independently of proteolysis by culturing cells atop micropatterned fibronectin islands printed onto polydimethylsiloxane substrates to generate ECM-adhesive patches surrounded by regions blocked with non-adhesive, Pluronic F127 (10, 13). When endothelial cells are cultured atop surfaces homogeneously coated with monomeric

fibronectin that fully support adhesion and spreading, actin stress fibers are formed and the nucleus assumes a spheroid shape with an ordered distribution of nuclear pore complexes (Figure 6.22). By contrast, when endothelial cells are plated atop microprinted 35 x 35 μm fibronectin islands permissive for cell adhesion, but not spreading (10, 13), a cell shape-dependent perturbed regulation of nuclear and chromatin structure is observed (Figure 6.22). Hence, ECM-directed control of cell geometry directly determines nuclear shape and architecture as well as chromatin structure.

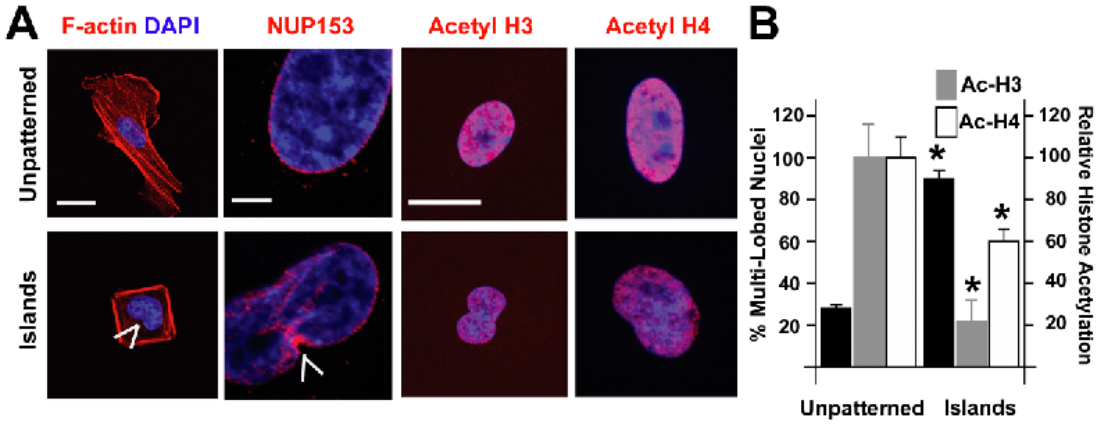

Figure 6.22. 2-D cell shape controls nuclear organization

A. Cells were cultured on either continuously coated fibronectin substrata (*top panels*) or 35 x 35 μm fibronectin islands (*bottom panels*) for 12 h. Cytoskeletal and nuclear architecture was analyzed by staining cells with Alexa-594-labeled phalloidin (red, F-actin) and DAPI (blue) and visualization by confocal laser microscopy (*left panels*; scale bar, 20 μm). Nuclear pore complex distribution was analyzed by staining for NUP153 (red) and visualization by confocal laser microscopy (*second set of panels*; scale bar, 2 μm). Nuclear membrane infoldings and NUP153 aggregation are marked by arrowheads. Endothelial cells were stained for either acetylated histone H3 (*third set of panels*, red) or H4 (*right panels*; red; scale bar, 10 μm). **B.** Relative numbers of multi-lobed nuclei were quantified (n = 3; * $P < 0.001$ compared to cells on unpatterned surface). Relative red fluorescent signal was quantified as an index of histone acetylation (n = 12, * $P < 0.005$ compared to cells on unpatterned surface).

Discussion.

In 2-D culture, cells respond to changes in substrate rigidity and topology by translating mechanical cues from their surrounding environment into transcriptional and morphogenetic responses by largely undefined mechanisms (11, 13, 28). Far less is known, however, regarding the mechanotransduction-dependent pathways engaged by cells embedded within physiologically relevant, 3-D ECM environments. Using vasculogenesis as a model, 3-D morphogenetic program, we unexpectedly find that ECM-embedded endothelial cells adopt a dormant phenotype that is accompanied by a series of distinctive changes in nuclear shape, nuclear pore complex distribution, chromatin organization and RNA biosynthesis. This quiescent state ends abruptly upon the addition of pro-angiogenic growth factors, but only if endothelial cells remodel their pericellular ECM by mobilizing MMPs and assembling a provisional fibronectin matrix. In this fashion, endothelial cells generate their own mechanical cues in order to activate the actomyosin-dependent tractional forces necessary for transmitting information to the nuclear compartment via a relay system of cytoskeletal filaments, KASH-domain containing proteins and SUN family members that bridge the nuclear envelope to bind to the nuclear lamins. In turn, the laminar network of type A and type B lamins directly or indirectly binds chromatin and DNA as well as a variety of inner nuclear membrane proteins and transcription factors that together act as a functional scaffold for chromatin organization, gene regulation, differentiation and DNA replication (21, 22, 49). Interestingly, mutations in the genes encoding lamins or emerin result in a pleiotrophic series of genetic disorders, termed the laminopathies, which are characterized by muscular dystrophies, lipodystrophy and progeria/premature ageing (21, 22, 49). Mutant cells display multi-lobed nuclei and anomalies in nuclear pore complex distribution along with associated alterations in chromatin organization, histone modification and transcriptional activity (21, 22, 49). While these changes in nuclear architecture have been classified as pathognomonic of nuclear membrane or nuclear scaffolding gene mutations, our findings suggest that normal cells purposefully alter nuclear shape and function in a closely related

fashion to regulate growth factor-initiated commands for replication and transcription. From this perspective, we posit that laminopathy-afflicted cells may be “locked” into a nuclear shape more characteristic of dormant cells and as such, are unable to appropriately reshape nuclear architecture in response to soluble or mechanical cues.

Taken together, we propose a new model for the regulation of 3-D cell behavior wherein pericellular remodeling of the ECM represents a required step in allowing cells to initiate the nuclear shape changes that engage the transcriptional machinery responsible for controlling growth and differentiation. While our studies have focused on endothelial cell behavior, these findings likely apply to all cell populations that reside within a 3-D ECM. Indeed, we find that adipocytes as well as human stem cell populations similarly depend on 3-D ECM remodeling to regulate nuclear organization and differentiation (unpublished observation). By linking ECM remodeling to the ordered transmission of mechanical signals to the nuclear envelope, subtle changes in pericellular proteolytic activity would be predicted to profoundly impact phenotype. In this regard, we note that the phenotype of MT1-MMP-null mice – characterized by a markedly shortened lifespan with a profound reduction in growth that is associated with the onset of severe bone, muscle, vascular and adipose tissue-related defects shortly after birth - bear considerable similarity to mouse laminopathy models (4, 35, 52-56). The overlapping phenotypes raise the possibility that nuclei are “hard-wired” to respond to mechanical cues in a precisely orchestrated fashion. As such, modulating nuclear shape by altering ECM remodeling may impact cell function to a degree similar to that observed by directly targeting nuclear envelope-chromatin interactions. We conclude that the complex changes in gene expression and cell function known to accompany 3-D ECM remodeling are interconnected with matrix-derived cues transmitted to the nuclear envelope, chromatin and transcriptional machinery by a continuum of protein:protein interactions that span from the ECM-cell interface to the nuclear interior.

References.

1. Adams, R.H., and Alitalo, K. 2007. Molecular regulation of angiogenesis and lymphangiogenesis. *Nat Rev Mol Cell Biol* 8:464-478.

2. Iruela-Arispe, M.L., and Davis, G.E. 2009. Cellular and molecular mechanisms of vascular lumen formation. *Dev Cell* 16:222-231.

3. Zhou, X., Rowe, R.G., Hiraoka, N., George, J.P., Wirtz, D., Mosher, D.F., Virtanen, I., Chernousov, M.A., and Weiss, S.J. 2008. Fibronectin fibrillogenesis regulates three-dimensional neovessel formation. *Genes Dev* 22:1231-1243.

4. Chun, T.H., Sabeh, F., Ota, I., Murphy, H., McDonagh, K.T., Holmbeck, K., Birkedal-Hansen, H., Allen, E.D., and Weiss, S.J. 2004. MT1-MMP-dependent neovessel formation within the confines of the three-dimensional extracellular matrix. *J Cell Biol* 167:757-767.

5. Hiraoka, N., Allen, E., Apel, I.J., Gyetko, M.R., and Weiss, S.J. 1998. Matrix metalloproteinases regulate neovascularization by acting as pericellular fibrinolysins. *Cell* 95:365-377.

6. Saunders, W.B., Bohnsack, B.L., Faske, J.B., Anthis, N.J., Bayless, K.J., Hirschi, K.K., and Davis, G.E. 2006. Coregulation of vascular tube stabilization by endothelial cell TIMP-2 and pericyte TIMP-3. *J Cell Biol* 175:179-191.

7. Discher, D.E., Janmey, P., and Wang, Y.L. 2005. Tissue cells feel and respond to the stiffness of their substrate. *Science* 310:1139-1143.

8. Folkman, J., and Moscona, A. 1978. Role of cell shape in growth control. *Nature* 273:345-349.

9. Ingber, D.E. 1990. Fibronectin controls capillary endothelial cell growth by modulating cell shape. *Proc Natl Acad Sci U S A* 87:3579-3583.

10. Chen, C.S., Mrksich, M., Huang, S., Whitesides, G.M., and Ingber, D.E. 1997. Geometric control of cell life and death. *Science* 276:1425-1428.

11. Engler, A.J., Sen, S., Sweeney, H.L., and Discher, D.E. 2006. Matrix elasticity directs stem cell lineage specification. *Cell* 126:677-689.

12. Huang, S., Chen, C.S., and Ingber, D.E. 1998. Control of cyclin D1, p27(Kip1), and cell cycle progression in human capillary endothelial cells by cell shape and cytoskeletal tension. *Mol Biol Cell* 9:3179-3193.

13. McBeath, R., Pirone, D.M., Nelson, C.M., Bhadriraju, K., and Chen, C.S. 2004. Cell shape, cytoskeletal tension, and RhoA regulate stem cell lineage commitment. *Dev Cell* 6:483-495.

14. Wozniak, M.A., and Chen, C.S. 2009. Mechanotransduction in development: a growing role for contractility. *Nat Rev Mol Cell Biol* 10:34-43.

15. Wang, N., Tytell, J.D., and Ingber, D.E. 2009. Mechanotransduction at a distance: mechanically coupling the extracellular matrix with the nucleus. *Nat Rev Mol Cell Biol* 10:75-82.

16. Orr, A.W., Helmke, B.P., Blackman, B.R., and Schwartz, M.A. 2006. Mechanisms of mechanotransduction. *Dev Cell* 10:11-20.

17. Paszek, M.J., Zahir, N., Johnson, K.R., Lakins, J.N., Rozenberg, G.I., Gefen, A., Reinhart-King, C.A., Margulies, S.S., Dembo, M., Boettiger, D., et al. 2005. Tensional homeostasis and the malignant phenotype. *Cancer Cell* 8:241-254.

18. Roca-Cusachs, P., Alcaraz, J., Sunyer, R., Samitier, J., Farre, R., and Navajas, D. 2008. Micropatterning of single endothelial cell shape reveals a tight coupling between nuclear volume in G1 and proliferation. *Biophys J* 94:4984-4995.

19. Stewart, C.L., Roux, K.J., and Burke, B. 2007. Blurring the boundary: the nuclear envelope extends its reach. *Science* 318:1408-1412.

20. Crisp, M., Liu, Q., Roux, K., Rattner, J.B., Shanahan, C., Burke, B., Stahl, P.D., and Hodzic, D. 2006. Coupling of the nucleus and cytoplasm: role of the LINC complex. *J Cell Biol* 172:41-53.

21. Dechat, T., Pfleghaar, K., Sengupta, K., Shimi, T., Shumaker, D.K., Solimando, L., and Goldman, R.D. 2008. Nuclear lamins: major factors in the structural organization and function of the nucleus and chromatin. *Genes Dev* 22:832-853.

22. Starr, D.A. 2009. A nuclear-envelope bridge positions nuclei and moves chromosomes. *J Cell Sci* 122:577-586.

23. Thundat, T., Warmack, R.J., Chen, G.Y., and Allison, D.P. 1994. Thermal and ambient-induced deflections of scanning force microscope cantilevers. *Applied Physics Letters* 64:2894-2896.

24. Richert, L., Engler, A.J., Discher, D.E., and Picart, C. 2004. Elasticity of native and cross-linked polyelectrolyte multilayer films. *Biomacromolecules* 5:1908-1916.

25. Ehrbar, M., Rizzi, S.C., Schoenmakers, R.G., Miguel, B.S., Hubbell, J.A., Weber, F.E., and Lutolf, M.P. 2007. Biomolecular hydrogels formed and degraded via site-specific enzymatic reactions. *Biomacromolecules* 8:3000-3007.

26. Singhvi, R., Kumar, A., Lopez, G.P., Stephanopoulos, G.N., Wang, D.I., Whitesides, G.M., and Ingber, D.E. 1994. Engineering cell shape and function. *Science* 264:696-698.

27. Schafer, M., and Werner, S. 2008. Cancer as an overhealing wound: an old hypothesis revisited. *Nat Rev Mol Cell Biol* 9:628-638.

28. Dahl, K.N., Ribeiro, A.J., and Lammerding, J. 2008. Nuclear shape, mechanics, and mechanotransduction. *Circ Res* 102:1307-1318.

29. Glynn, M.W., and Glover, T.W. 2005. Incomplete processing of mutant lamin A in Hutchinson-Gilford progeria leads to nuclear abnormalities, which are reversed by farnesyltransferase inhibition. *Hum Mol Genet* 14:2959-2969.

30. Goldman, R.D., Shumaker, D.K., Erdos, M.R., Eriksson, M., Goldman, A.E., Gordon, L.B., Gruenbaum, Y., Khuon, S., Mendez, M., Varga, R., et al. 2004. Accumulation of mutant lamin A causes progressive changes in nuclear architecture in Hutchinson-Gilford progeria syndrome. *Proc Natl Acad Sci U S A* 101:8963-8968.

31. Hawryluk-Gara, L.A., Shibuya, E.K., and Wozniak, R.W. 2005. Vertebrate Nup53 interacts with the nuclear lamina and is required for the assembly of a Nup93-containing complex. *Mol Biol Cell* 16:2382-2394.

32. Liu, Q., Pante, N., Misteli, T., Elsagga, M., Crisp, M., Hodzic, D., Burke, B., and Roux, K.J. 2007. Functional association of Sun1 with nuclear pore complexes. *J Cell Biol* 178:785-798.

33. Tang, C.W., Maya-Mendoza, A., Martin, C., Zeng, K., Chen, S., Feret, D., Wilson, S.A., and Jackson, D.A. 2008. The integrity of a lamin-B1-dependent nucleoskeleton is a fundamental determinant of RNA synthesis in human cells. *J Cell Sci* 121:1014-1024.

34. Shumaker, D.K., Dechat, T., Kohlmaier, A., Adam, S.A., Bozovsky, M.R., Erdos, M.R., Eriksson, M., Goldman, A.E., Khuon, S., Collins, F.S., et al. 2006. Mutant nuclear lamin A leads to progressive alterations of epigenetic control in premature aging. *Proc Natl Acad Sci U S A* 103:8703-8708.

35. Chun, T.H., Hotary, K.B., Sabeh, F., Saltiel, A.R., Allen, E.D., and Weiss, S.J. 2006. A pericellular collagenase directs the 3-dimensional development of white adipose tissue. *Cell* 125:577-591.

36. Hotary, K.B., Allen, E.D., Brooks, P.C., Datta, N.S., Long, M.W., and Weiss, S.J. 2003. Membrane type I matrix metalloproteinase usurps tumor growth control imposed by the three-dimensional extracellular matrix. *Cell* 114:33-45.

37. Hotary, K.B., Yana, I., Sabeh, F., Li, X.Y., Holmbeck, K., Birkedal-Hansen, H., Allen, E.D., Hiraoka, N., and Weiss, S.J. 2002. Matrix metalloproteinases (MMPs) regulate fibrin-invasive activity via MT1-MMP-dependent and -independent processes. *J Exp Med* 195:295-308.

38. Haberland, M., Montgomery, R.L., and Olson, E.N. 2009. The many roles of histone deacetylases in development and physiology: implications for disease and therapy. *Nat Rev Genet* 10:32-42.

39. Finlan, L.E., Sproul, D., Thomson, I., Boyle, S., Kerr, E., Perry, P., Ylstra, B., Chubb, J.R., and Bickmore, W.A. 2008. Recruitment to the nuclear periphery can alter expression of genes in human cells. *PLoS Genet* 4:e1000039.

40. Somech, R., Shaklai, S., Geller, O., Amariglio, N., Simon, A.J., Rechavi, G., and Gal-Yam, E.N. 2005. The nuclear-envelope protein and transcriptional repressor LAP2beta interacts with HDAC3 at the nuclear periphery, and induces histone H4 deacetylation. *J Cell Sci* 118:4017-4025.

41. Benecke, B.J., Ben-Ze'ev, A., and Penman, S. 1978. The control of mRNA production, translation and turnover in suspended and reattached anchorage-dependent fibroblasts. *Cell* 14:931-939.

42. Ben-Ze'ev, A., Farmer, S.R., and Penman, S. 1980. Protein synthesis requires cell-surface contact while nuclear events respond to cell shape in anchorage-dependent fibroblasts. *Cell* 21:365-372.

43. Lamond, A.I., and Spector, D.L. 2003. Nuclear speckles: a model for nuclear organelles. *Nat Rev Mol Cell Biol* 4:605-612.

44. Tan, J.L., Tien, J., Pirone, D.M., Gray, D.S., Bhadriraju, K., and Chen, C.S. 2003. Cells lying on a bed of microneedles: an approach to isolate mechanical force. *Proc Natl Acad Sci U S A* 100:1484-1489.

45. Nelson, C.M., Pirone, D.M., Tan, J.L., and Chen, C.S. 2004. Vascular endothelial-cadherin regulates cytoskeletal tension, cell spreading, and focal adhesions by stimulating RhoA. *Mol Biol Cell* 15:2943-2953.

46. Dalby, M.J., Gadegaard, N., Herzyk, P., Sutherland, D., Agheli, H., Wilkinson, C.D., and Curtis, A.S. 2007. Nanomechanotransduction and interphase nuclear organization influence on genomic control. *J Cell Biochem* 102:1234-1244.

47. Salpingidou, G., Smertenko, A., Hausmanowa-Petrucewicz, I., Hussey, P.J., and Hutchison, C.J. 2007. A novel role for the nuclear membrane protein emerin in association of the centrosome to the outer nuclear membrane. *J Cell Biol* 178:897-904.

48. Wilhelmsen, K., Ketema, M., Truong, H., and Sonnenberg, A. 2006. KASH-domain proteins in nuclear migration, anchorage and other processes. *J Cell Sci* 119:5021-5029.

49. Crisp, M., and Burke, B. 2008. The nuclear envelope as an integrator of nuclear and cytoplasmic architecture. *FEBS Lett* 582:2023-2032.

50. Stewart-Hutchinson, P.J., Hale, C.M., Wirtz, D., and Hodzic, D. 2008. Structural requirements for the assembly of LINC complexes and their function in cellular mechanical stiffness. *Exp Cell Res* 314:1892-1905.

51. Raeber, G.P., Lutolf, M.P., and Hubbell, J.A. 2007. Mechanisms of 3-D migration and matrix remodeling of fibroblasts within artificial ECMs. *Acta Biomater* 3:615-629.

52. Zhou, Z., Apte, S.S., Soininen, R., Cao, R., Baaklini, G.Y., Rauser, R.W., Wang, J., Cao, Y., and Tryggvason, K. 2000. Impaired endochondral ossification and angiogenesis in mice deficient in membrane-type matrix metalloproteinase I. *Proc Natl Acad Sci U S A* 97:4052-4057.

53. Holmbeck, K., Bianco, P., Caterina, J., Yamada, S., Kromer, M., Kuznetsov, S.A., Mankani, M., Robey, P.G., Poole, A.R., Pidoux, I., et al. 1999. MT1-MMP-deficient mice develop dwarfism, osteopenia, arthritis, and connective tissue disease due to inadequate collagen turnover. *Cell* 99:81-92.

54. Ohtake, Y., Tojo, H., and Seiki, M. 2006. Multifunctional roles of MT1-MMP in myofiber formation and morphostatic maintenance of skeletal muscle. *J Cell Sci* 119:3822-3832.

55. Mounkes, L.C., Kozlov, S., Hernandez, L., Sullivan, T., and Stewart, C.L. 2003. A progeroid syndrome in mice is caused by defects in A-type lamins. *Nature* 423:298-301.

56. Sullivan, T., Escalante-Alcalde, D., Bhatt, H., Anver, M., Bhat, N., Nagashima, K., Stewart, C.L., and Burke, B. 1999. Loss of A-type lamin expression compromises nuclear envelope integrity leading to muscular dystrophy. *J Cell Biol* 147:913-920.

Chapter 7: Generation and Characterization of *Mmp14* and *Mmp15* Conditional Knock-Out Mouse Strains

Introduction.

Epithelial-mesenchymal transition (EMT) is a process by which epithelial cells lose polarity and dedifferentiate to take on a highly-motile, fibroblast-like phenotype (1, 2). Mechanistic dissection of EMT in tissue culture has revealed that epithelial cells repress expression of cell:cell adhesion molecules – including E-cadherin and claudins – as well as cytokeratins, and mucins, reorganize their cytoskeleton to take on a non-polar shape, and activate mesenchymal markers including vimentin and fibronectin (1-5). However, *in vivo*, EMT occurs within the context of highly complex extracellular matrices (ECMs) that vary in structure, composition and biophysical properties and which regulate cell function (6-10). The mechanisms by which EMT is regulated by the ECM niche are only beginning to be elucidated (6-9, 11); however, it is known that EMT involves the activation of transcriptional programs that confer the ability to invade ECM barriers (6, 8, 9, 12). EMT-associated ECM invasion is an integral part of metastatic dissemination during cancer progression as well as population of the interstitial space with epithelium-derived fibroblasts during fibrosis (7-9, 13-20); thus understanding cell-ECM crosstalk during EMT and tissue invasion is a key prerequisite for fully understanding the pathogenesis of these diseases.

Prior to the initiation of EMT *in vivo*, polarized epithelial cells exist atop a basement membrane (BM), a two-dimensional (2-D) sheet of ECM composed primarily of a meshwork of cross-linked type IV collagen with a pore size of approximately 50 nm (6, 18, 21-23) which is subject to remodeling in normal tissue (24, 25) and serves as a structural scaffold for tissue organization (26, 27). During EMT, disruption of the BM barrier promotes the acquisition of mesenchymal characteristics required for growth, migration and survival within the 3-D environment of the underlying interstitial compartment (11, 28). BM

effacement occurs when epithelial cells inactivate BM synthesis and deposition pathways and proteolyze BM barrier components – including the dense meshwork of the collagen IV network - promoting EMT-associated BM transmigration (6, 7, 12, 29-32). Recent evidence suggests that a family of membrane-anchored matrix metalloproteinases (MMPs) – termed the membrane-type MMPs (MT-MMPs) - are essential mediators of proteolytic BM penetration (6, 12). Specifically, MTs1-, 2-, and 3-MMP (encoded by the *Mmp14, Mmp15,* and *Mmp16* genes, respectively in mouse) are effectors of BM transmigration during EMT (6, 12).

Beneath the BM, cells encounter the interstitial ECM- a 3-D meshwork dominated largely by type I collagen (33-36). Cells existing previously in 2-D must adapt for growth, survival, and migration within this 3-D environment (34, 37-39). In addition to serving as proteolytic effectors during BM transmigration, MT-MMPs also serve to remodel pericellular type I collagen barriers to promote cell growth, migration, and differentiation (34, 35, 37, 40). Both MT1-MMP and MT2-MMP express type I collagenolytic activity (33, 35, 41). Hence, cells executing EMT and entering the interstitial compartment must redirect MT-MMP function from degrading the 2-D BM to effectively function in this 3-D environment.

Though previous *in vitro* work suggests a role for these enzymes during pericellular ECM remodeling, it remains unclear whether or not these findings can be extended to the *in vivo* setting. Hence, ablating the function of these enzymes *in vivo* is an essential step to assess their roles in pathologic and homeostatic EMT events. However, mouse models of MT –MMP deficiency are limited. MT1-MMP deficient mice are viable, but die within the first two months of life with defects in multiple mesenchymal tissues, including bone, fat, and muscle (37, 42-44), precluding their use in models of pathologic EMT. MT3-MMP deficient mice are viable and fertile without obvious developmental defects, suggesting that MT3-MMP deficiency is likely compensated by other MT-MMPs (45). The gene for MT2-MMP has yet to be targeted. Herein, we describe the generation and characterization of conditional knock-out alleles of the genes for

MT1-MMP and MT2-MMP in mice. These models will allow for the future study of the roles of MT-MMPs as proteolytic effectors of EMT *in vivo*, and will perhaps verify MT-MMPs as potential therapeutic targets in disease where EMT is an aspect of pathophysiology.

Materials and Methods.

Targeting the mouse *Mmp14* locus by homologous recombination in embryonic stem (ES) cells. A targeting vector was constructed containing exons 2-4 of the mouse *Mmp14* gene as well as an FRT-flanked Phosphoglycerate kinase (PGK-neo) cassette (Figure 7.1). These sequences were flanked by loxp recognition sites for Cre recombinase. To promote homologous recombination in ES cells, 4.9 kb and 3 kb of genomic sequence were inserted 5' and 3' of the loxp-flanked sequences, respectively. The linearized targeting vector was electroporated into W4 (129 strain-derived) mouse ES cells (46), and G418-resistant clones isolated. Targeting of the *Mmp14* locus in ES cells was verified by Southern blot. Targeted ES clones were injected into C57BL/6J donor blastocyts and implanted into adult female mice. Male offspring with > 90% chimerism were crossed to wild-type C57BL/6J females. Progeny with agouti coat color, indicative of conception from a targeted ES cell-derived gamete, were genotyped at the *Mmp14* locus for germline transmission of the $Mmp14^{neo}$ allele. *Mmp14* genotyping primers were 5'-gttgaggcaggaggattgtgagtt-3' (P1; see Figure 6.1) and 5'cctggaaaagtgggcgagaag-3' (P2) used with an annealing temperature of 55.5°. Germline transmission of the $Mmp14^{neo}$ allele was obtained in two independent ES lines. Agouti mice of the genotype $Mmp14^{neo/+}$ were crossed to C57BL/6J β-actin FLPe transgenic mice (Jackson Immunoresearch Laboratories stock No. 003800) for excision of the FRT-flanked PGK-neo cassette. Since FLPe-mediated excision does not occur in every germ cell, $Mmp14^{neo/+}$; FLPe-positive mice are presumably mosaic for the $Mmp14^{neo}$ and $Mmp14^{flox}$ alleles in the germline, and were thus backcrossed to wild-type C57BL/6J mice and progeny screened for the absence of the PGK-neo cassette to indicate the presence of the $Mmp14^{loxp}$ allele. Excision of the PGK-neo cassette was verified with the neo-specific primers 5'-aggatctcctgtcatctcaccttgctcctg-3' and 5'-aagaactcgtcaagaaggcgatagaaggcg-3' with an annealing temperature of 72° to identify $Mmp14^{+/loxp}$ mice.

Targeting the mouse *Mmp15* locus. A targeting vector was constructed containing exons 4 and 5 of the mouse *Mmp15* gene flanked by loxp sites. Immediately 3' of these sequences, an FRT-flanked PGK-neo cassette was inserted. To promote homologous recombination, 3 kb of adjacent genomic sequence was inserted 5' and 3' to the loxp-flanked exons and PGK-neo cassette. The linearized targeting vector was electroporated into W4 ES cells. To generate the *Mmp15*^{neo} allele, three independently-targeted 129 strain-derived ES clones were injected into C57BL/6 donor blastocysts and implanted into adult female mice. Chimeric males produced from injected blastocysts were crossed to wild-type C57BL/6 females. Progeny with agouti coat color were genotyped at the *Mmp15* locus for germline transmission of the *Mmp15*^{neo} allele using primers 5'-aaagccacccacgccatcaaac-3' (P1; see Figure 7.7) and 5'-ccgccaccaagcctcactgtct-3' (P2). *Mmp15*^{neo} mice were crossed to FLPe transgenic mice for excision of the FRT-flanked PGK neo cassette, and *Mmp15*$^{+/loxp}$ mice were isolated. Cre-mediated excision of the loxp-flanked *Mmp15* allele was verified with null allele-specific primers 5'-ccagctggccttgaactttgagat-3' (P3) and 5'-agagctggccttggggagat-3' (P4) with an annealing temperature of 58°.

3-D invasion assay. To measure 3-D invasion, dermal fibroblasts were embedded in a 100 µl type I collagen gel (35). This gel was embedded within an outer cell free gel. Invasion from the outer to the inner gel was stimulated with 10% serum and 10 ng/ml PDGF-BB.

Results.

Conditional inactivation of the *Mmp14* gene. To inactivate the gene encoding MT1-MMP with restricted tissue specificity, a targeting vector was constructed to insert loxp sites flanking exons 2-4 of the mouse *Mmp14* gene (Figure 7.1). Cre-mediated recombination of the targeted allele would be predicted to delete exons 2-4 of the *Mmp14* gene encoding the catalytic domain such that any truncated protein product would be predicted to be catalytically inactive, similar to one of the targeting schemes previously employed to generate a *Mmp14* constitutively deleted allele (42).

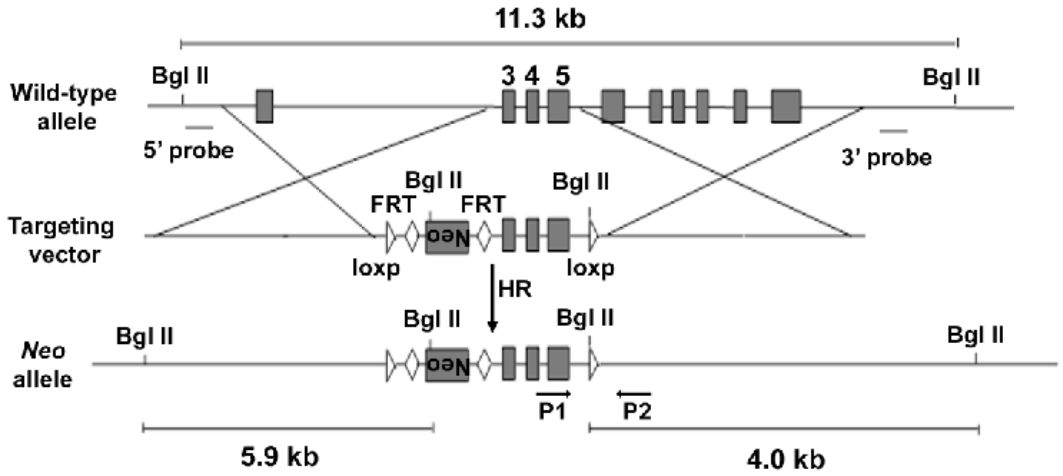

Figure 7.1. Strategy for derivation of the Mmp14^{neo} allele by homologous recombination in ES cells

A targeting vector was constructed to insert loxp sites flanking exons 3-5 of the *Mmp14* gene. After homologous recombination (HR) in ES cells, digestion of genomic DNA with *Bgl* II and hybridization with the 5' probe would be expected to yield bands of 11.3 kb and 5.9 kb upon Southern blotting, while hybridization with the 3' probe should yield fragments of 11.3 and 7.0 kb. FLPe-mediated recombination should excise the PGK-neo selection cassette, allowing expression of the *Mmp14*^{loxp} allele at wild-type levels. Locations of genotyping primers P1 and P2 are shown.

A transcript produced by splicing exon 1 to exon 5 is predicted to contain a premature termination codon. The linearized targeting vector was electroporated into 129 strain-derived embryonic stem cells, and stably-transfected clones were isolated by selection with G418. Targeting of the *Mmp14* locus was screened by Southern blotting following digestion with *Bgl* II and hybridization with either the

5’ probe or 3’ probe (Figure 7.2A). Three clones were identified with accurate targeting at both the 5’ and 3’ ends of the construct, and targeting was confirmed using PCR (Figure 7.2B).

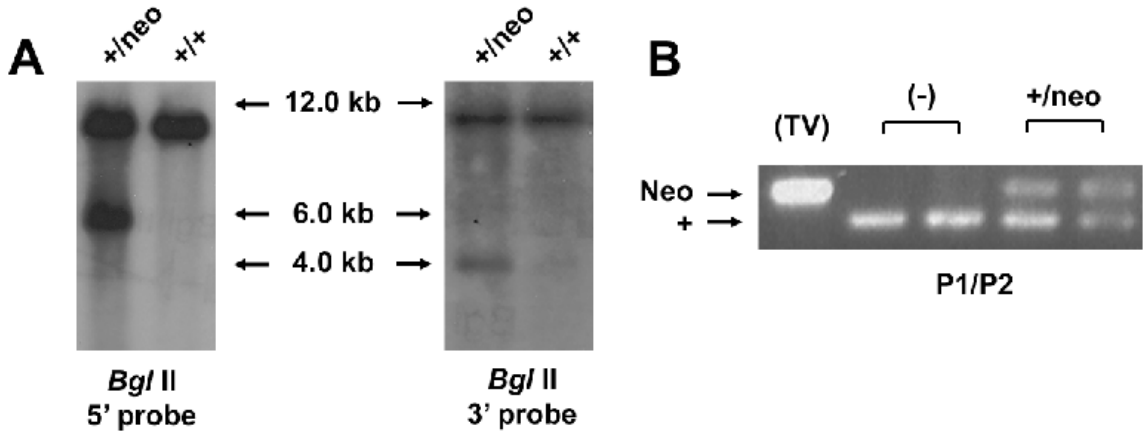

Figure 7.2. Targeting the Mmp14 locus in mouse ES cells

A. DNA from G418-resistant ES cell clones stably transfected with the linearized targeting vector was digested with *Bgl* II and hybridized either with the 5’ probe (left panel; see Figure 6.1) or the 3’ probe (right panel). Fragment sizes were analyzed by Southern hybridization followed by autoradiography. **B.** DNA from G418-resistant ES clones was PCR amplified with primers P1 and P2 to verify the presence of targeting vector-derived sequences within the ES cell genomes. Pure targeting vector was used as a positive control (TV) and DNA from non-transgenic mice as negative controls (-).

The three targeted clones were injected into C57BL/6 donor blastocysts, which were subsequently implanted into adult female mice. These blastocysts yielded 58 chimeras with a chimerism rate of 20-95% as assessed by coat color. Male chimeras with >90% chimerism were crossed to C57BL/6 females, and germline transmission of the *Mmp14*^{neo} allele was observed in offspring from chimeras derived from two independent ES cell lines (Figure 7.3A). To generate the *Mmp14*^{loxp} allele, *Mmp14*$^{+/neo}$ mice were crossed to β-actin-FLPe transgenic mice for Flp recombinase-mediated excision of the PGK-neo cassette (Figure 7.3B). *Mmp14*$^{+/loxp}$ mice were intercrossed, and *Mmp*$^{loxp/loxp}$ mice were born in the expected Mendelian ratios with no discernable defects suggestive of MT1-MMP deficiency (42, 43)(Figure 7.4).

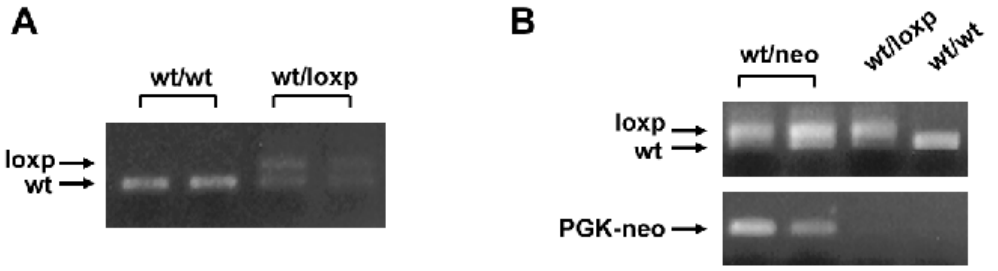

Figure 7.3. Germline transmission of the Mmp14^{neo} allele and FLPe-mediated PGK-neo cassette excision

A. Male chimeras were crossed to wild-type C57BL/6 female mice, and progeny genotyped with primers P1 and P2 to screen for germline transmission of the *Mmp14*^{neo} allele. **B.** *Mmp14*$^{+/neo}$ mice were mated with β-actin-FLPe transgenic mice. FLPe-positive; *Mmp14*$^{+/neo}$ offspring were mated with wild-type mice, and progeny screened for the *Mmp14*^{loxp} allele with P1 and P2 (top panel) and for the absence of an amplification product with primers specific for the PGK-neo cassette (bottom panel).

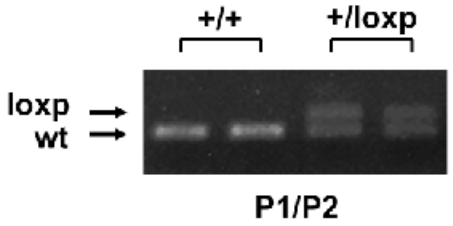

Figure 7.4. Representative genotyping of Mmp14^{loxp} mice

Genomic DNA was PCR amplified with primers P1 and P2 and the presence of the *Mmp14*$^{+}$ and *Mmp14*^{loxp} alleles assessed by agarose gel electrophoresis.

Characterization of the *Mmp14*^{loxp} allele. To determine susceptibility of the *Mmp14*^{loxp} allele to Cre-mediated recombination, we used dermal fibroblasts isolated from *Mmp14*$^{loxp/loxp}$ adult mice. *Mmp14*$^{loxp/loxp}$ fibroblasts were infected either with an adenovirus carrying the cDNA for Cre recombinase to effect recombination at the *Mmp14*^{loxp} allele or a control adenovirus (β-galactosidase). Compared to control-infected fibroblasts, Cre-infected fibroblasts exhibit a > 95% reduction in *Mmp14* mRNA (Figure 7.5), indicating effective recombination at both *Mmp14*^{loxp} loci.

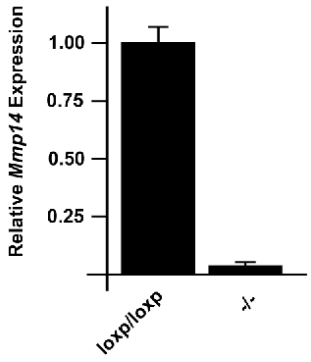

Figure 7.5. Cre-mediated excision of the Mmp14^{loxp} allele in dermal fibroblasts

Mmp14$^{loxp/loxp}$ dermal fibroblasts were isolated and infected either with a control adenovirus (β-galactosidase) or an adenovirus bearing a cDNA encoding Cre recombinase (generating *Mmp14*$^{-/-}$ fibroblasts). Following transduction, mRNA levels of *Mmp14* were measured by quantitative PCR.

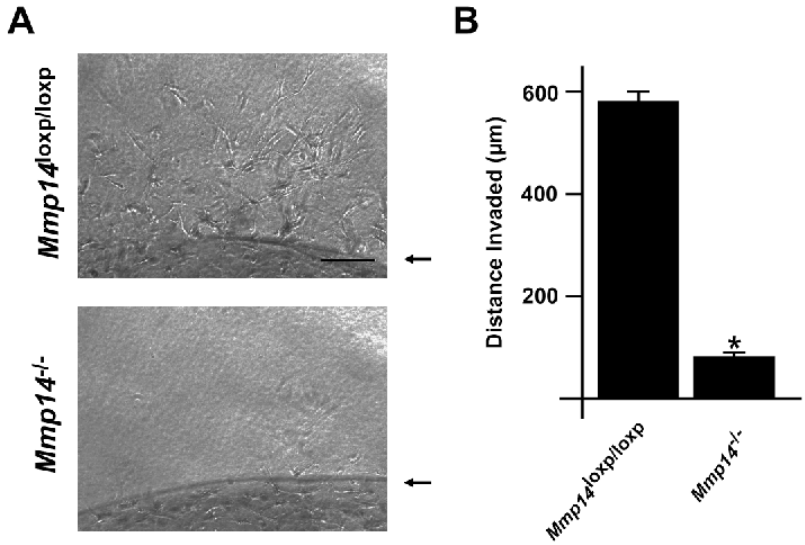

Figure 7.6. Mmp14$^{-/-}$ dermal fibroblasts display defective 3-D tissue invasion

A. *Mmp14*$^{loxp/loxp}$ and *Mmp14*$^{-/-}$ fibroblasts were cultured within a 100 μl gel of type I collagen, which was embedded within a larger, cell-free type I collagen gel. Fibroblast invasion from the inner into the outer gel was stimulated with 10% serum supplemented with 10 ng/ml PDGF-BB, and invasion monitored by phase contrast microscopy for 7 d. Scale = 100 μm. **B.** Invasion distance was measured (* $p < 0.0001$).

MT1-MMP activity is an essential requirement for dermal fibroblast infiltration of type I collagen-rich barriers (35). Hence, the functionality of the

Mmp14^{-} allele was assessed by challenging *Mmp14*$^{fl/fl}$ and *Mmp14*$^{-/-}$ with a 3-D barrier of crosslinked type I collagen. Compared to MT1-MMP expressing fibroblasts, MT1-MMP deficient cells exhibit a nearly complete defect in invasion of type I collagen barriers (Figure 7.6), a defect observed in fibroblasts with a constitutive *Mmp14* null allele (35). Hence, recombination at the *Mmp14*^{loxp} locus results in defective *Mmp14* mRNA production and loss of MT1-MMP functionality required for negotiation of 3-D barriers of type I collagen.

Conditional inactivation of the *Mmp15* gene. To conditionally inactivate the *Mmp15* gene, a targeting vector was constructed containing exons 4 and 5 of the mouse *Mmp15* gene flanked by loxp sites, an FRT-flanked PGK-neo cassette, and two homology arms situated 5' and 3' of these sequences to promote homologous recombination (Figure 7.7). The linearized targeting vector was electroporated into 129 strain-derived ES cells, and stably-transfected clones isolated by antibiotic selection with G418. DNA was isolated from stable clones and screened for *Mmp15* targeting by Southern hybridization.

To verify recombination at the 5' end of the targeting vector, DNA was digested with *Spe* I and hybridized with the 5' probe; to verify the 3' end, *EcoR* I was used to digest DNA for hybridization with the 3' probe (Figure 7.8A). Three clones with accurate targeting were identified, and the presence of targeting vector sequences in genomic DNA was verified by PCR using primers P1 and P2 (Figure 7.8B).

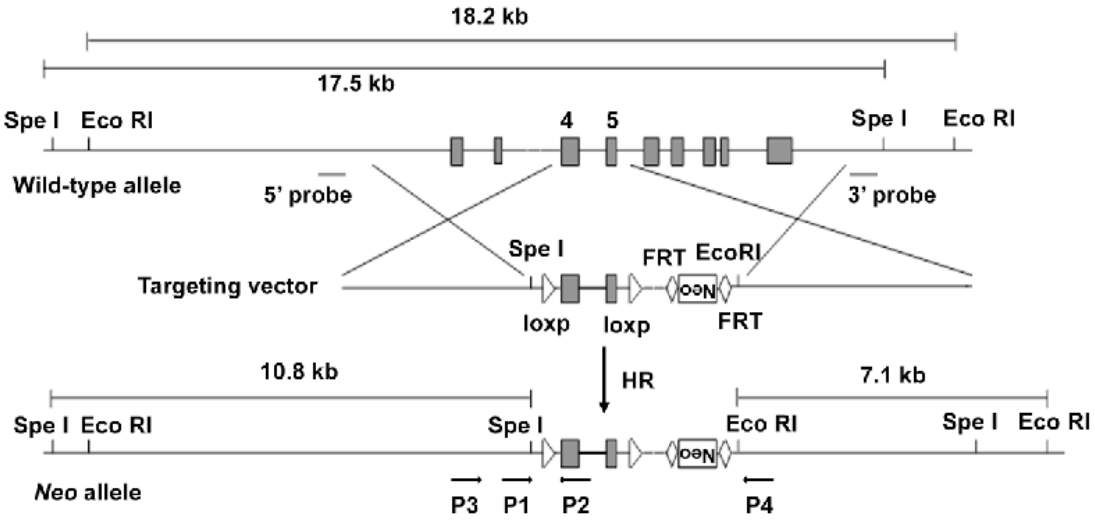

Figure 7.7. Targeting the mouse Mmp15 locus in ES cells

A targeting vector was constructed to insert loxp sites flanking exons 4 and 5 of the mouse *Mmp15* gene. After homologous recombination (HR), digestion of genomic DNA with *Spe* I and Southern hybridization with the 5' probe would be predicted to generate fragments of 17.5 kb for the wild-type allele and 10.8 kb for the $Mmp15^{neo}$ allele. Digestion of genomic DNA with *EcoR* I and Southern hybridization with the 3' probe would be predicted to generate fragments of 18.2 kb for the wild-type allele, and 7.1 kb for the targeted allele. PCR genotyping with P1 and P2 will generate a 400 bp product corresponding to the wild-type allele, and a 500 bp product for the targeted allele. Primers P3 and P4 would generate a 600 bp product for the Cre-excised $Mmp15^{-}$ allele.

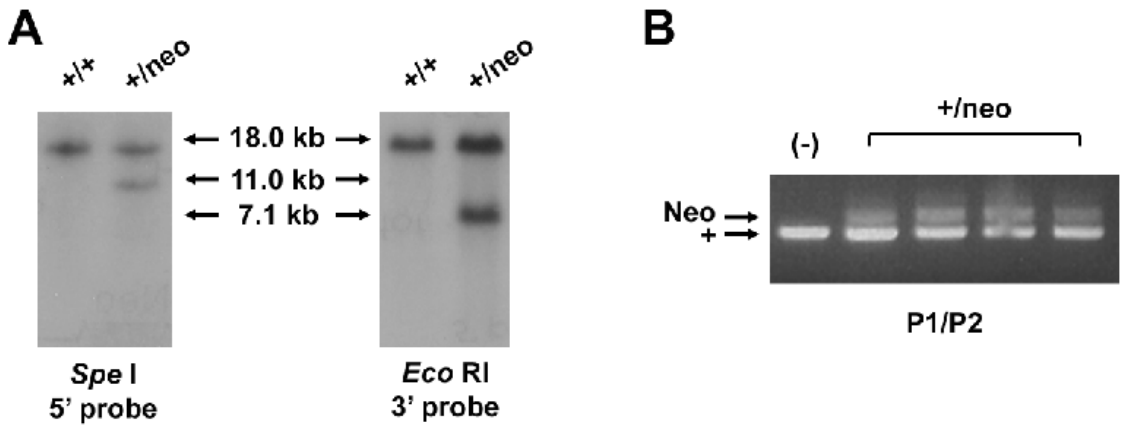

Figure 7.8. Screening ES clones for targeting of Mmp15

A. DNA was isolated from stably-transfected ES cell clones and digested either with *Spe* I for Southern hybridization with the 5' probe (left panel; see Figure 6.7) or *EcoR* I for hybridization with the 3' probe (right panel). Hybridization to digested DNA from targeted clones generates bands of 17.5 and 10.8 kb with the 5' probe, and 18.2 and 7.1 kb with the 3' probe. **B.** DNA from targeted clones identified by Southern blotting was used for PCR using primers P1 and P2 to verify the presence of the *Mmp15*^{neo} allele.

Clones with targeting verified by Southern hybridization and PCR were microinjected into C57BL/6J donor blastocysts which generated chimeras with a chimerism rate ranging from 10-90%. Male chimeras were backcrossed to C57BL/6J females, and germline transmission of the *Mmp15*^{neo} allele confirmed in chimeras derived from two independent ES cell clones (Figure 7.9).

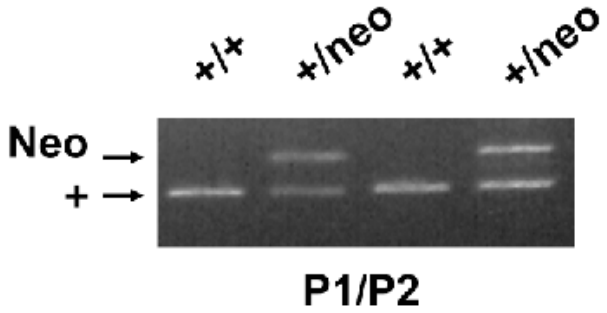

Figure 7.9. Germline transmission of the Mmp15^{neo} allele

Chimeric males were mated with C57BL/6 females, and offspring genotyped with P1/P2 to detect the presence of the *Mmp15*^{neo} allele.

To derive the *Mmp15*^{loxp} allele, *Mmp15*$^{+/neo}$ mice were bred to FLPe transgenic mice for excision of the FRT-flanked PGK-neo cassette. Progeny were isolated that displayed loss of the *neo* gene. *Mmp15*$^{+/loxp}$ mice were intercrossed, and *Mmp15*$^{lxop/loxp}$ mice were isolated (Figure 7.10). To test Cre-mediated excision of the *Mmp15*^{loxp} allele, mice were crossed to the EIIa-Cre strain, where Cre recombinase is driven by the adenoviral EIIa promoter and activated during pre-implantation development (47). *Mmp15*$^{+/-}$ mice were isolated displaying excision of exons 4 and 5 at the PCR level (Figure 7.10). *Mmp15*$^{+/-}$ mice were intercrossed to isolate *Mmp15*$^{i/-}$ offspring; preliminary data suggests that MT2-MMP deficiency may be lethal in the perinatal stage.

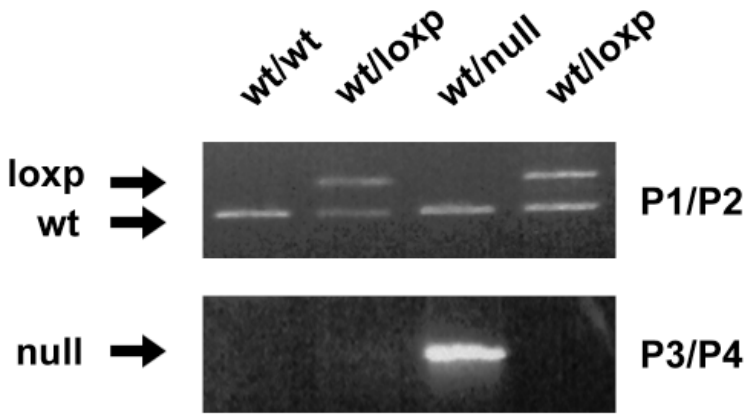

Figure 7.10. Cre-mediated recombination of the Mmp15^{loxp} allele

Mmp15$^{+/loxp}$ mice were mated to EIIa-Cre transgenic mice. EIIa-Cre-positive, *Mmp15*$^{+/loxp}$ offspring were mated with wild-type mice, and offspring of this cross screened for Cre-mediated excision of the *Mmp15*^{loxp} allele with P1 and P2 as well as P3 and P4, which amplify the *Mmp15*$^{-}$ allele.

Discussion.

MT-MMPs are proposed to be critical effectors for proteolysis-associated cell migration through ECM barriers, including the BM and the interstitial ECM during EMT and 2-D-to-3-D transition events (6, 12, 30, 35). However, animal models of MT-MMP deficiency in which the functions of these enzymes can be tested during EMT *in vivo* are currently lacking. MT1-MMP deficient mice exhibit multiple developmental defects in mesoderm-derived tissues - underscoring the importance of MT1-MMP in mesenchymal cell populations and precluding study of this enzyme in models of pathologic EMT *in vivo* (37, 42-44). MT3-MMP-deficient mice do not display developmental defects, suggesting functional redundancy for this enzyme (45). MT2-MMP deficient mice have yet to be characterized. However, given the observation that MT2-MMP might be the predominant MT-MMP expressed in epithelial cells (48), it seems reasonable to predict a potential role for this enzyme in ECM remodeling events during 2-D-to3-D transitions of epithelial cells.

Herein we describe models of conditional inactivation of the genes encoding MT1-MMP and MT2-MMP. *Mmp14* and *Mmp15* were targeted in ES cells by homologous recombination where critical exons encoding the catalytic domains for the enzyme protein products were flanked by loxp sites, and mice bearing targeted alleles susceptible to Cre-mediated recombination were produced. Tissue-specific transgenic expression of Cre recombinase *in vivo* induces deletion of *Mmp14* or *Mmp15* only in selected cell populations where Cre is expressed. Loss of protein function as a result of Cre-mediated recombination of the $Mmp14^{loxp}$ allele was verified by culturing dermal fibroblasts within 3-D cross-linked ECMs of type I collagen, where MT1-MMP function is an absolute requirement for 3-D migration (35). Similar *in vitro* loss-of-function studies are not at this time possible for analysis of the $Mmp15^{loxp}$ allele, as a measurable cell function dependent exclusively on MT2-MMP activity in primary cells without redundant roles for other MT-MMPs has yet to be identified. Hence, future study is required for detailed analysis of the functionality of the proteins produced from the $Mmp15^{loxp}$ and $Mmp15^{-}$ alleles following Cre-mediated recombination.

In response to EMT-inducing signals, epithelial cells transmigrate the BM and invade the underlying interstitial compartment where they assume a mesenchymal-like phenotype (6, 7, 11, 12). Since MT1-MMP does not seem to be required for developmental EMT-associated BM transmigration events - including gastrulation, neural crest migration, and angiogenesis (42, 43) - functional redundancy of MT-MMPs might require targeting of multiple enzymes to assess the role of this MMP family during EMT-associated BM penetration. Indeed, expression of MT1-MMP, MT2-MMP, or MT3-MMP is sufficient to drive BM-invasive events (12), further suggesting functional compensation *in vivo*. Therefore, conditional alleles of the genes encoding these enzymes might be essential for tissue-restricted deficiency of multiple proteases to rigorously interrogate MMP function during EMT *in vivo*.

EMT events contribute to the pathophysiology of multiple diseases including cancer, fibrosis, and atherosclerosis (8, 9, 13, 14, 18, 19, 49, 50). The mouse models of MT-MMP conditional deficiency generated herein will provide valuable tools to assess the potential roles of these effector proteases during EMT within the complex *in vivo* environment.

References.

1. Thiery, J.P. 2002. Epithelial-mesenchymal transitions in tumour progression. *Nat Rev Cancer* 2:442-454.

2. Thiery, J.P., and Sleeman, J.P. 2006. Complex networks orchestrate epithelial-mesenchymal transitions. *Nat Rev Mol Cell Biol* 7:131-142.

3. Nieto, M.A. 2002. The snail superfamily of zinc-finger transcription factors. *Nat Rev Mol Cell Biol* 3:155-166.

4. Peinado, H., Olmeda, D., and Cano, A. 2007. Snail, Zeb and bHLH factors in tumour progression: an alliance against the epithelial phenotype? *Nat Rev Cancer* 7:415-428.

5. Yilmaz, M., and Christofori, G. 2009. EMT, the cytoskeleton, and cancer cell invasion. *Cancer Metastasis Rev*.

6. Rowe, R.G., and Weiss, S.J. 2008. Breaching the basement membrane: who, when and how? *Trends Cell Biol* 18:560-574.

7. Spaderna, S., Schmalhofer, O., Hlubek, F., Berx, G., Eger, A., Merkel, S., Jung, A., Kirchner, T., and Brabletz, T. 2006. A transient, EMT-linked loss of basement membranes indicates metastasis and poor survival in colorectal cancer. *Gastroenterology* 131:830-840.

8. Yook, J.I., Li, X.Y., Ota, I., Fearon, E.R., and Weiss, S.J. 2005. Wnt-dependent regulation of the E-cadherin repressor snail. *J Biol Chem* 280:11740-11748.

9. Yook, J.I., Li, X.Y., Ota, I., Hu, C., Kim, H.S., Kim, N.H., Cha, S.Y., Ryu, J.K., Choi, Y.J., Kim, J., et al. 2006. A Wnt-Axin2-GSK3beta cascade regulates Snail1 activity in breast cancer cells. *Nat Cell Biol* 8:1398-1406.

10. Rowe, R.G., Li, X.Y., Hu, Y., Saunders, T.L., Virtanen, I., de Herreros, A.G., Becker, K.F., Ingvarsen, S., Engelholm, L.H., Bommer, G.T., et al. 2009. Mesenchymal cells reactivate Snail1 expression to drive three-dimensional invasion programs. *J Cell Biol*.

11. Zeisberg, M., Bonner, G., Maeshima, Y., Colorado, P., Muller, G.A., Strutz, F., and Kalluri, R. 2001. Renal fibrosis: collagen composition and assembly regulates epithelial-mesenchymal transdifferentiation. *Am J Pathol* 159:1313-1321.

12. Hotary, K., Li, X.Y., Allen, E., Stevens, S.L., and Weiss, S.J. 2006. A cancer cell metalloprotease triad regulates the basement membrane transmigration program. *Genes Dev* 20:2673-2686.

13. Moody, S.E., Perez, D., Pan, T.C., Sarkisian, C.J., Portocarrero, C.P., Sterner, C.J., Notorfrancesco, K.L., Cardiff, R.D., and Chodosh, L.A. 2005. The transcriptional repressor Snail promotes mammary tumor recurrence. *Cancer Cell* 8:197-209.

14. Olmeda, D., Moreno-Bueno, G., Flores, J.M., Fabra, A., Portillo, F., and Cano, A. 2007. SNAI1 is required for tumor growth and lymph node metastasis of human breast carcinoma MDA-MB-231 cells. *Cancer Res* 67:11721-11731.

15. Schmalhofer, O., Brabletz, S., and Brabletz, T. 2009. E-cadherin, beta-catenin, and ZEB1 in malignant progression of cancer. *Cancer Metastasis Rev*.

16. Zeisberg, E.M., Potenta, S., Xie, L., Zeisberg, M., and Kalluri, R. 2007. Discovery of endothelial to mesenchymal transition as a source for carcinoma-associated fibroblasts. *Cancer Res* 67:10123-10128.

17. Zeisberg, E.M., Potenta, S.E., Sugimoto, H., Zeisberg, M., and Kalluri, R. 2008. Fibroblasts in kidney fibrosis emerge via endothelial-to-mesenchymal transition. *J Am Soc Nephrol* 19:2282-2287.

18. Kalluri, R., and Neilson, E.G. 2003. Epithelial-mesenchymal transition and its implications for fibrosis. *J Clin Invest* 112:1776-1784.

19. Iwano, M., Plieth, D., Danoff, T.M., Xue, C., Okada, H., and Neilson, E.G. 2002. Evidence that fibroblasts derive from epithelium during tissue fibrosis. *J Clin Invest* 110:341-350.

20. Gavert, N., and Ben-Ze'ev, A. 2008. Epithelial-mesenchymal transition and the invasive potential of tumors. *Trends Mol Med* 14:199-209.

21. Abrams, G.A., Goodman, S.L., Nealey, P.F., Franco, M., and Murphy, C.J. 2000. Nanoscale topography of the basement membrane underlying the corneal epithelium of the rhesus macaque. *Cell Tissue Res* 299:39-46.

22. Abrams, G.A., Schaus, S.S., Goodman, S.L., Nealey, P.F., and Murphy, C.J. 2000. Nanoscale topography of the corneal epithelial basement membrane and Descemet's membrane of the human. *Cornea* 19:57-64.

23. Kalluri, R. 2003. Basement membranes: structure, assembly and role in tumour angiogenesis. *Nat Rev Cancer* 3:422-433.

24. Dingemans, K.P. 1988. What's new in the ultrastructure of tumor invasion in vivo? *Pathol Res Pract* 183:792-808.

25. Walker, F. 1972. Basement-membrane turnover in man. *J Pathol* 107:123-125.

26. Vracko, R., and Benditt, E.P. 1972. Basal lamina: the scaffold for orderly cell replacement. Observations on regeneration of injured skeletal muscle fibers and capillaries. *J Cell Biol* 55:406-419.

27. Vracko, R. 1972. Significance of basal lamina for regeneration of injured lung. *Virchows Arch A Pathol Pathol Anat* 355:264-274.

28. Fujiwara, H., Hayashi, Y., Sanzen, N., Kobayashi, R., Weber, C.N., Emoto, T., Futaki, S., Niwa, H., Murray, P., Edgar, D., et al. 2007. Regulation of mesodermal differentiation of mouse embryonic stem cells by basement membranes. *J Biol Chem* 282:29701-29711.

29. Bechetoille, N., Haftek, M., Staquet, M.J., Cochran, A.J., Schmitt, D., and Berthier-Vergnes, O. 2000. Penetration of human metastatic melanoma cells through an authentic dermal-epidermal junction is associated with dissolution of native collagen types IV and VII. *Melanoma Res* 10:427-434.

30. Hlubek, F., Spaderna, S., Jung, A., Kirchner, T., and Brabletz, T. 2004. Beta-catenin activates a coordinated expression of the proinvasive factors laminin-5 gamma2 chain and MT1-MMP in colorectal carcinomas. *Int J Cancer* 108:321-326.

31. Margulis, A., Zhang, W., Alt-Holland, A., Crawford, H.C., Fusenig, N.E., and Garlick, J.A. 2005. E-cadherin suppression accelerates squamous cell carcinoma progression in three-dimensional, human tissue constructs. *Cancer Res* 65:1783-1791.

32. Ikeda, K., Iyama, K., Ishikawa, N., Egami, H., Nakao, M., Sado, Y., Ninomiya, Y., and Baba, H. 2006. Loss of expression of type IV collagen alpha5 and alpha6 chains in colorectal cancer associated with the hypermethylation of their promoter region. *Am J Pathol* 168:856-865.

33. Hotary, K., Allen, E., Punturieri, A., Yana, I., and Weiss, S.J. 2000. Regulation of cell invasion and morphogenesis in a three-dimensional type I collagen matrix by membrane-type matrix metalloproteinases 1, 2, and 3. *J Cell Biol* 149:1309-1323.

34. Hotary, K.B., Allen, E.D., Brooks, P.C., Datta, N.S., Long, M.W., and Weiss, S.J. 2003. Membrane type I matrix metalloproteinase usurps tumor growth control imposed by the three-dimensional extracellular matrix. *Cell* 114:33-45.

35. Sabeh, F., Ota, I., Holmbeck, K., Birkedal-Hansen, H., Soloway, P., Balbin, M., Lopez-Otin, C., Shapiro, S., Inada, M., Krane, S., et al. 2004. Tumor cell traffic through the extracellular matrix is controlled by the membrane-anchored collagenase MT1-MMP. *J Cell Biol* 167:769-781.

36. Wolf, K., and Friedl, P. 2008. Mapping proteolytic cancer cell-extracellular matrix interfaces. *Clin Exp Metastasis*.

37. Chun, T.H., Hotary, K.B., Sabeh, F., Saltiel, A.R., Allen, E.D., and Weiss, S.J. 2006. A pericellular collagenase directs the 3-dimensional development of white adipose tissue. *Cell* 125:577-591.

38. Yamada, K.M., and Cukierman, E. 2007. Modeling tissue morphogenesis and cancer in 3D. *Cell* 130:601-610.

39. Zhou, X., Rowe, R.G., Hiraoka, N., George, J.P., Wirtz, D., Mosher, D.F., Virtanen, I., Chernousov, M.A., and Weiss, S.J. 2008. Fibronectin fibrillogenesis regulates three-dimensional neovessel formation. *Genes Dev* 22:1231-1243.

40. Chun, T.H., Sabeh, F., Ota, I., Murphy, H., McDonagh, K.T., Holmbeck, K., Birkedal-Hansen, H., Allen, E.D., and Weiss, S.J. 2004. MT1-MMP-dependent neovessel formation within the confines of the three-dimensional extracellular matrix. *J Cell Biol* 167:757-767.

41. Li, X.Y., Ota, I., Yana, I., Sabeh, F., and Weiss, S.J. 2008. Molecular dissection of the structural machinery underlying the tissue-invasive activity of membrane type-1 matrix metalloproteinase. *Mol Biol Cell* 19:3221-3233.

42. Holmbeck, K., Bianco, P., Caterina, J., Yamada, S., Kromer, M., Kuznetsov, S.A., Mankani, M., Robey, P.G., Poole, A.R., Pidoux, I., et al. 1999. MT1-MMP-deficient mice develop dwarfism, osteopenia, arthritis, and connective tissue disease due to inadequate collagen turnover. *Cell* 99:81-92.

43. Zhou, Z., Apte, S.S., Soininen, R., Cao, R., Baaklini, G.Y., Rauser, R.W., Wang, J., Cao, Y., and Tryggvason, K. 2000. Impaired endochondral ossification and angiogenesis in mice deficient in membrane-type matrix metalloproteinase I. *Proc Natl Acad Sci U S A* 97:4052-4057.

44. Ohtake, Y., Tojo, H., and Seiki, M. 2006. Multifunctional roles of MT1-MMP in myofiber formation and morphostatic maintenance of skeletal muscle. *J Cell Sci* 119:3822-3832.

45. Shi, J., Son, M.Y., Yamada, S., Szabova, L., Kahan, S., Chrysovergis, K., Wolf, L., Surmak, A., and Holmbeck, K. 2008. Membrane-type MMPs enable extracellular matrix permissiveness and mesenchymal cell proliferation during embryogenesis. *Dev Biol* 313:196-209.

46. Auerbach, W., Dunmore, J.H., Fairchild-Huntress, V., Fang, Q., Auerbach, A.B., Huszar, D., and Joyner, A.L. 2000. Establishment and chimera

analysis of 129/SvEv- and C57BL/6-derived mouse embryonic stem cell lines. *Biotechniques* 29:1024-1028, 1030, 1032.

47. Lakso, M., Pichel, J.G., Gorman, J.R., Sauer, B., Okamoto, Y., Lee, E., Alt, F.W., and Westphal, H. 1996. Efficient in vivo manipulation of mouse genomic sequences at the zygote stage. *Proc Natl Acad Sci U S A* 93:5860-5865.

48. Szabova, L., Yamada, S.S., Birkedal-Hansen, H., and Holmbeck, K. 2005. Expression pattern of four membrane-type matrix metalloproteinases in the normal and diseased mouse mammary gland. *J Cell Physiol* 205:123-132.

49. Mani, S.A., Guo, W., Liao, M.J., Eaton, E.N., Ayyanan, A., Zhou, A.Y., Brooks, M., Reinhard, F., Zhang, C.C., Shipitsin, M., et al. 2008. The epithelial-mesenchymal transition generates cells with properties of stem cells. *Cell* 133:704-715.

50. Xue, C., Plieth, D., Venkov, C., Xu, C., and Neilson, E.G. 2003. The gatekeeper effect of epithelial-mesenchymal transition regulates the frequency of breast cancer metastasis. *Cancer Res* 63:3386-3394.

Chapter 8: Conclusions

Cell dimensionality is an emerging concept in the study of tissue architecture. Cells are capable of assuming two possible dimensional identities: two-dimensional (2-D) and three-dimensional (3-D). 2-D cells line lumina of tubular and glandular organs; and these cells exhibit apicobasolateral polarity, cell:cell adhesion, and interface with a basement membrane (BM) on their basolateral aspect. 3-D cells are found within soft tissues and the interstitial compartment, are encased on all sides by a surrounding fibrillar extracellular matrix (ECM), and possess a multipolar shape. Conversion of 2-D cells into a 3-D phenotype is thought to underlie essential developmental events – including gastrulation and neural crest delamination - as well as the pathogenesis of several diseases – such as tissue fibrosis and cancer. Therefore, recent studies have focused on identifying molecular mechanisms regulating this process (1-4) which as a whole can be termed the 2-D-to-3-D transition. After cells enter the 3-D environment, distinct pathways governing cell growth and differentiation are recruited whereby the structural and mechanical characteristics of the surrounding ECM regulate cell function (5-7). Indeed, pericellular remodeling of the 3-D ECM is required for effective interpretation of soluble signals into high-order biologic outputs (5-8).

Herein, we have provided the first *in vivo* evidence that Snail1 - a transcription factor singularly capable of engaging 2-D-to-3-D transitions - plays a required role in the progression of tissue fibrosis. Furthermore, we have extended this observation by demonstrating that Snail1 is highly expressed in differentiated 3-D mesenchymal cells, and governs the transcriptional programs that regulate fibroblast infiltration of tissue barriers *in vitro* and *in vivo*. In 3-D cells, we have identified a previously unexpected function for endothelial cell deposition of a pericellular ECM of the glycoprotein fibronectin as a required event during 3-D vasculogenesis. In addition to pericellular membrane-type

matrix metalloprotease (MT-MMP)-mediated ECM proteolysis, fibronectin fibrillogenesis is essential for reorganization of the nuclear compartment and chromatin structure for effective engagement of tubulogenic programs. These results provide novel insight into molecular mechanisms of 2-D-to-3-D transitions and regulation of 3-D cell function.

Regulation of Intrinsic Dimensionality by Snail1. It has been proposed that 2-D-to-3-D transitions require the loss of an epithelial phenotype and the concurrent gain of characteristics typical of mesenchymal cells - a transcriptional reprogramming event known as the epithelial-mesenchymal transition (EMT)(1-4). Genetic ablation studies in mice have identified essential roles for a small family of EMT-triggering transcription factors during tissue morphogenesis (9-12); however, whether these factors serve required functions in pathologic EMTs remains unknown. Based on overexpression and RNA interference studies performed in tissue culture and *in vivo*, Snail1 has been postulated to be a key mediator of EMT in disease states (4, 13-16). Consistent with this notion, *in vivo* studies have determined that ectopic overexpression of Snail1 in epithelial cells *in vivo* induces EMT and subsequent fibrosis (17), and Snail1 protein can be found in fibrotic epithelium in a variety of tissues (18, 19). Taken together, these data strongly suggest the Snail1 acts as a positive regulator of epithelial EMT during tissue fibrogenesis. We have tested this hypothesis by utilizing a model of conditional Snail1 inactivation wherein Snail1 expression can be ablated in a tissue-specific manner *via* expression of Cre recombinase (1). We chose a validated model of liver fibrogenesis where mice are chronically treated with the hepatotoxin CCl_4. Mice with hepatocyte-specific Snail1 deficiency displayed a resistance to CCl_4-induced fibrosis coincident with an abrogation of hepatocyte EMT. These data identify the first requirement for Snail1 during progression of a disease characterized by pathologic EMT *in vivo*. Furthermore, these results provide the first proof that an EMT-triggering transcription factor plays a required role during disease evolution induced in response to a pathophysiologically-relevant stimulus *in vivo*, potentially as a direct positive regulator of EMT.

Snail1 is essential for execution of the EMTs required for mesodermal differentiation during development (9). Surprisingly, it has recently been demonstrated that the capacity to express Snail1 is retained in differentiated mesenchymal cells *in vivo* at sites of tissue remodeling (1, 20). Hence, we hypothesized that Snail1 might continue to exert functionally important effects in terminally-differentiated mesenchymal cells following completion of EMT. We analyzed Snail1 expression and function in fibroblasts, and demonstrated that Snail1 expression can be induced by stimuli that induce an 'activated' phenotype in fibroblasts characterized by increased proliferation, neomatrix synthesis, and migration. Indeed, we observed that Snail1 governs the transcriptional programs that oversee mobilization of the essential proteolytic machinery (i.e. MT1-MMP) that promotes fibroblast invasion of ECM constructs *in vitro* and complex tissue barriers *in vivo* (21). Thus, we have defined a novel paradigm whereby EMT-inducing factors seem to additionally act as master transcriptional regulators of mesenchymal cell traffic during tissue remodeling.

EndoMT is a central mechanism by which endothelial cells reprogram intrinsic dimensionality during vascular morphogenesis, pericyte differentiation, and development of the cardiac valves (22-25). Snail1 has been put forth as a central mediator of EndoMT in ECs *in vitro* (25-27), and is highly expressed both in neovessels as well as within endothelial cells undergoing EndoMT *in vivo* (25, 28, 29). However, investigation into whether Snail1 serves a required role in EndoMT *in vivo* has been hampered by a lack of mouse models of tissue-specific Snail1 ablation. We have again employed our model of Snail1 deficiency to identify a required role for endothelial Snail1 during embryonic development, and as a potential mediator of EndoMT in human endothelial cells. These data indicate that Snail1 plays a broad role in regulating intrinsic dimensionality in previously unexpected cell populations.

Control of 3-D Cell Function by Pericellular ECM Remodeling. The 3-D microenvironment governs cell growth, differentiation, migration, and tissue morphogenesis *via* pathways distinct from the 2-D state (5, 7, 8). In 3-D, the structural and biophysical properties of the ECM are central determinants of cell

function and fate (7, 30, 31). Hence, investigating modes of cell:ECM crosstalk in 3-D is essential for understanding mechanisms regulating key functions of 3-D cells. Using our model of 3-D vasculogenesis, we have identified pericellular fibronectin matrix deposition as essential event required for the proliferative and migratory processes underlying 3-D neovessel formation. Indeed, polymeric matrices of unfolded, fibrillar fibronectin are observed at sites of neovessel growth in tumors *in vivo*. Fibronectin fibrillogenesis controls 3-D endothelial cell tubulogenesis by modulating the assembly and function of the cytoskeleton and consequently the stiffness of the intracellular compartment.

With this observation in mind, we sought to investigate the molecular means by which changes in the biophysical properties of the pericellular environment are interpreted into modulation of morphogenetic responses to growth factors using our system of 3-D vasculogenesis as a model. We have demonstrated that – in response to soluble, pro-angiogenic signals – pericellular ECM remodeling is required for the cell shape changes that promote reorganization of nuclear structure and decondensation and activation of chromatin for effective interpretation of growth factor signals. This process is mediated by a novel axis wherein a network of protein:protein interactions physically bridges the ECM, cell surface, cytoskeleton, and nuclear envelope. These results define a novel paradigm wherein remodeling of the 3-D environment dictates cell responses to growth factors by controlling the architecture of the nucleus as well as the packaging and functionality of chromatin.

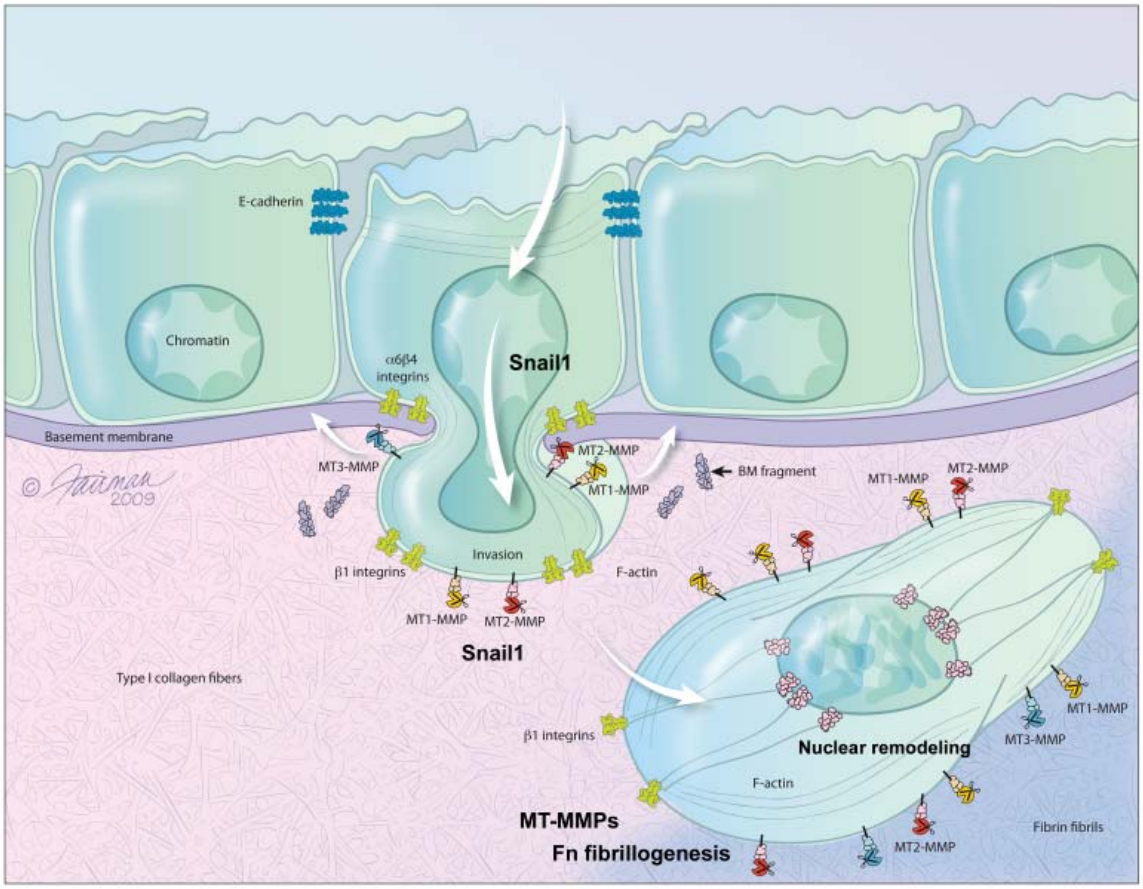

Figure 8.1. Novel insight into the 2-D-to-3-D transition and 3-D cell function

We have identified a novel requirement for Snail1 in mediating the EMTs that occur during tissue fibrogenesis and the EndoMTs that are required for development and remodeling of the vasculature. Snail1 plays an unexpected role in promoting infiltration of tissue barriers following mesenchymal cell differentiation. In 3-D cells, both pericellular MT-MMP-mediated proteolysis and fibronectin (Fn) deposition govern cell proliferation and morphogenesis by controlling the structure and organization of the nuclear and chromatin compoartments.

Future Directions.

We have established a novel tool to ablate Snail1 function *in vivo* with spatial and temporal specificity. Hence, we are in an ideal position for further investigation into Snail1 functionality in specific tissues during developmental events as well as in disease models wherein EMT has been implicated in disease pathobiology. Indeed, our studies are the first to ablate an EMT-inducing transcription factor in a disease model *in vivo* and validate hypotheses suggesting such proteins serve required functions during disease genesis and progression. Therefore, we propose further application of this allele to relevant models of human disease in mice. Studies are underway to generate mice bearing breast carcinomas wherein Snail1 can be inactivated by expression Cre recombinase in isolated cell lines *in vitro* as well as by mammary epithelial-specific Cre expression *in vivo*. Since EMT and 2-D-to-3-D transitions have been implicated as key steps in the progression of this disease (32, 33), these studies will begin to investigate Snail1 as a mediator of carcinoma progression.

Snail1 expression is sufficient to repress the epithelial phenotype and confer a phenotype typical of mesenchymal cells. The majority of studies investigating functions of Snail1 have focused on dissecting its ability to mediate EMT; however, recent data suggest that Snail1 expression can be re-activated in differentiated mesenchymal cells at sites of tissue remodeling. Indeed, we have demonstrated that Snail1 is required for mobilization of the transcriptional programs responsible for fibroblast tissue invasion. Since Snail1 protein function is controlled by several layers of regulation - including transcriptional and post-translational mechanisms (4, 16, 34, 35) - current studies are focused on the means by which Snail1 activity is modulated in fibroblasts. Further, we are using our novel *Snai1* allele in mouse models of wound healing to investigate Snail1 function in stromal cell populations *in vivo*.

We have identified a requirement for Snail1 expression within the endothelium for mouse viability during embryonic development. However, studies aimed at identifying the specific process(es) regulated by Snail1 during

cardiovascular development were hampered by experimental variability when embryos were isolated from timed pregnancies. Hence, the conditional Snail1 allele was inbred to a pure genetic background within which vascular development studies are typically pursued. Ongoing studies will aim to identify cardiovascular defects present in Snail1-deficient endothelial cells *in vivo*.

Following BM perforation, EMT, BM transmigration, and infiltration of underlying tissue, cells find themselves embedded within the 3-D ECM wherein pathways modulating growth, survival, and differentiation are distinct from the 2-D condition (5, 7, 8). We have identified a novel ECM deposition pathway essential for 3-D vasculogenesis whereby endothelial cells deposit a pericellular scaffold of fibrillar fibronectin to adjust intracellular stiffness to a degree permissive for the proliferative and migratory responses required for neovessel formation. Since this pathway seems to be recruited only by the actively forming vasculature, this presents a potential therapeutic opportunity. Studies are ongoing to investigate the practicality of targeting fibronectin fibrillogenesis as an anti-angiogenic therapy.

During angiogenesis, pericellular 3-D ECM remodeling events govern structure and function of the nucleus and chromatin. Though the idea that cues from the pericellular niche might communicate with the nuclear compartment has been posited previously (36, 37), we provide the first experimental demonstration of this idea, and extend this notion to demonstrate that cells actively fine tune their microenvironment for effective interpretation of soluble signals. Further study will identify the applicability of this axis to other cell types and differentiation processes, potentially including stem cell function. Indeed, cell shape and biophysical properties of the pericellular environment modulate mesenchymal stem cell lineage commitment (30, 31). Accordingly, our preliminary data suggest that pericellular proteolysis of the 3-D ECM regulates mesenchymal stem cell differentiation. Hence, determining the relative role of ECM-dependent regulation of nuclear architecture during 3-D mesenchymal stem cell lineage selection will serve to bolster understanding of ECM-dependent differentiation. Additionally, analysis of ECM-regulated changes in nuclear structure that occur

during the 2-D-to-3-D transition might provide deeper comprehension of the phenotypic shift that occurs during this process. Since this novel axis seems to govern several aspects of 3-D cell function in endothelial cells, further understanding of the regulation of the nuclear compartment by the pericellular ECM in additional systems will provide insight developmental events and disease states that involve 2-D-to-3-D transitions.

We have generated novel mouse strains wherein expression of MT1-MMP or MT2-MMP can be ablated in a tissue-specific fashion. These systems will allow *in vivo* verification of models of MT-MMP function derived from *in vitro* and *ex vivo* tissue culture constructs. MT-MMP family members are effectors of the pericellular proteolytic events required for BM transmigration and 3-D cell functions including proliferation, differentiation, survival, and tissue morphogenesis (2, 5, 8, 21, 38-42). These ideas seem to be validated by the phenotype of mice deficient for MT1-MMP, which exhibit defects in a variety of tissues populated by 3-D cells, including bone, adipose tissue, and skeletal muscle (8, 43-45). However, the widespread severity of the MT1-MMP-deficient phenotype suggests that many of these observed tissue-specific defects might not be cell- or tissue-autonomous, perhaps evolving secondary to a state of chronic stress and morbidity. Hence, tissue-specific ablation of MT1-MMP will serve to further elucidate MT1-MMP's *in vivo* roles during development.

MT2-MMP expression is sufficient to promote BM transmigration as well as infiltration of 3-D ECM barriers (2, 40, 41, 46). However, no *in vivo* model of MT2-MMP deficiency has yet been derived. We have generated MT2-MMP-constitutive null mice and are currently assessing the consequences of MT2-MMP deficiency during development. In preliminary studies, we have yet to isolate MT2-MMP-deficienct mice at the age of weaning, suggesting potential lethality early in life or during embryogenesis.

Expression of MT1-MMP, MT2-MMP, or MT3-MMP is sufficient to drive proteolytic BM transmigration in epithelial cells (2, 41). The phenotype of the deficient mouse strain demonstrates that MT1-MMP is dispensable for the essential BM transmigration events that occur during development – such as

during gastrulation - suggesting possible functional redundancy of MT-MMPs during these events. Hence, deletion of these MT-MMPs in combination might be necessary to unequivocally identify the proteolytic effector(s) of developmental BM transmigration *in vivo*. Indeed, as an example of MT-MMP redundancy *in vivo*, deletion of MT3-MMP in a background of MT1-MMP ablation enhances the MT1-MMP-deficient phenotype (47). These studies will serve to identify further developmental events wherein MT-MMPs play redundant roles.

MT-MMP proteolysis of BMs and constraining ECM barriers promotes local carcinoma invasion and subsequent expansive growth in 3-D tissues (2, 5, 21, 41). Thus, application of these tissue-specific alleles of MT1-MMP and MT2-MMP to mouse models of carcinogenesis will serve to validate the hypothesized pro-tumorigenic and pro-metastatic roles of these enzymes in tumor progression. Using validated model systems that recapitulate the pathologic features of human skin and breast carcinogenesis in mice, studies have been initiated to investigate functions for MT-MMPs at various stages of tumor evolution *in vivo*, including BM penetration, primary tumor growth, and distant metastasis. These studies will be the first to either prove or disprove proposed functions of MT-MMPs during neoplastic disease *in vivo*.

Ingrowth of neovasculature supplies tumors with oxygen and nutrients, and is a required event for growth of primary and secondary tumors (48, 49). Using *in vitro* and *ex vivo* culture systems, it has been demonstrated that MT-MMP activity governs endothelial cell navigation of tissue barriers during postnatal angiogenesis (38, 39). However, due to the limited lifespan of MT1-MMP-deficienct mice, and the lack of MT2-MMP-deficient mice, *in vivo* investigation of MT-MMP proteolysis-driven neovessel formation has yet to be undertaken (43, 45). We are currently deriving mice with deficient MT1-MMP and/or MT2-MMP expression ablated specifically in endothelial cells for assessment of vascular structure and function as a function of the activity of these enzymes.

Our data suggest that Snail1-mediated EMT might contribute significantly to the accumulation of 3-D myofibroblast-like cells in fibrosis. However, for

effective 2-D-to-3-D transition, this intrinsic reprogramming must be accompanied by proteolytic removal of ECMs comprising tissue barriers, in this case the hepatocyte BM (2). Hence, we hypothesize that MT-MMPs might serve as the essential proteolytic effectors of this process. Thus, we have initiated studies to test this idea using our model of CCl_4-induced fibrosis. We are generating mice with hepatocyte-specific deficiency of MT1-MMP in order to investigate its role in mediating the 2-D-to-3-D transitions underlying liver fibrogenesis.

Summary.

The conversion of a 2-D cell to the phenotype of a 3-D cell is a recurring theme in development and disease. During the 2-D-to-3-D transition, acquisition of a 3-D phenotype requires recruitment of distinct mechanisms of regulating growth, migration, survival, and differentiation that depend on remodeling of the pericellular niche. We have identified Snail1 as playing a central role in promoting 2-D cell acquisition of a 3-D phenotype during development and disease. Additionally, Snail1 exerts control over pathways regulating infiltration of 3-D ECM barriers. Further, we have discovered a novel ECM deposition pathway essential for 3-D capillary tubulogenesis. Finally, we have uncovered a new paradigm wherein ECM remodeling-dependent changes in cell shape dictate structure and function of the nucleus and chromatin as a component of the cellular response to morphogenetic growth factors. These data begin to elucidate the molecular mechanisms underlying 2-D-to-3-D transitions as well as key pathways governing cell function in 3-D. These findings will be extended and reinforced by use of our novel models of tissue-specific MT1-MMP and MT2-MMP ablation.

References.

1. Rowe, R.G., Li, X.Y., Hu, Y., Saunders, T.L., Virtanen, I., Garcia de Herreros, A., Becker, K.F., Ingvarsen, S., Engelholm, L.H., Bommer, G.T., et al. 2009. Mesenchymal cells reactivate Snail1 expression to drive three-dimensional invasion programs. *J Cell Biol* 184:399-408.

2. Rowe, R.G., and Weiss, S.J. 2008. Breaching the basement membrane: who, when and how? *Trends Cell Biol* 18:560-574.

3. Thiery, J.P., and Sleeman, J.P. 2006. Complex networks orchestrate epithelial-mesenchymal transitions. *Nat Rev Mol Cell Biol* 7:131-142.

4. Yook, J.I., Li, X.Y., Ota, I., Hu, C., Kim, H.S., Kim, N.H., Cha, S.Y., Ryu, J.K., Choi, Y.J., Kim, J., et al. 2006. A Wnt-Axin2-GSK3beta cascade regulates Snail1 activity in breast cancer cells. *Nat Cell Biol* 8:1398-1406.

5. Hotary, K.B., Allen, E.D., Brooks, P.C., Datta, N.S., Long, M.W., and Weiss, S.J. 2003. Membrane type I matrix metalloproteinase usurps tumor growth control imposed by the three-dimensional extracellular matrix. *Cell* 114:33-45.

6. Yamada, K.M., and Cukierman, E. 2007. Modeling tissue morphogenesis and cancer in 3D. *Cell* 130:601-610.

7. Zhou, X., Rowe, R.G., Hiraoka, N., George, J.P., Wirtz, D., Mosher, D.F., Virtanen, I., Chernousov, M.A., and Weiss, S.J. 2008. Fibronectin fibrillogenesis regulates three-dimensional neovessel formation. *Genes Dev* 22:1231-1243.

8. Chun, T.H., Hotary, K.B., Sabeh, F., Saltiel, A.R., Allen, E.D., and Weiss, S.J. 2006. A pericellular collagenase directs the 3-dimensional development of white adipose tissue. *Cell* 125:577-591.

9. Carver, E.A., Jiang, R., Lan, Y., Oram, K.F., and Gridley, T. 2001. The mouse snail gene encodes a key regulator of the epithelial-mesenchymal transition. *Mol Cell Biol* 21:8184-8188.

10. Murray, S.A., and Gridley, T. 2006. Snail family genes are required for left-right asymmetry determination, but not neural crest formation, in mice. *Proc Natl Acad Sci U S A* 103:10300-10304.

11. Murray, S.A., Oram, K.F., and Gridley, T. 2007. Multiple functions of Snail family genes during palate development in mice. *Development* 134:1789-1797.

12. Wakamatsu, N., Yamada, Y., Yamada, K., Ono, T., Nomura, N., Taniguchi, H., Kitoh, H., Mutoh, N., Yamanaka, T., Mushiake, K., et al.

2001. Mutations in SIP1, encoding Smad interacting protein-1, cause a form of Hirschsprung disease. *Nat Genet* 27:369-370.

13. Moody, S.E., Perez, D., Pan, T.C., Sarkisian, C.J., Portocarrero, C.P., Sterner, C.J., Notorfrancesco, K.L., Cardiff, R.D., and Chodosh, L.A. 2005. The transcriptional repressor Snail promotes mammary tumor recurrence. *Cancer Cell* 8:197-209.

14. Olmeda, D., Montes, A., Moreno-Bueno, G., Flores, J.M., Portillo, F., and Cano, A. 2008. Snai1 and Snai2 collaborate on tumor growth and metastasis properties of mouse skin carcinoma cell lines. *Oncogene* 27:4690-4701.

15. Olmeda, D., Moreno-Bueno, G., Flores, J.M., Fabra, A., Portillo, F., and Cano, A. 2007. SNAI1 is required for tumor growth and lymph node metastasis of human breast carcinoma MDA-MB-231 cells. *Cancer Res* 67:11721-11731.

16. Yook, J.I., Li, X.Y., Ota, I., Fearon, E.R., and Weiss, S.J. 2005. Wnt-dependent regulation of the E-cadherin repressor snail. *J Biol Chem* 280:11740-11748.

17. Boutet, A., De Frutos, C.A., Maxwell, P.H., Mayol, M.J., Romero, J., and Nieto, M.A. 2006. Snail activation disrupts tissue homeostasis and induces fibrosis in the adult kidney. *Embo J* 25:5603-5613.

18. Dooley, S., Hamzavi, J., Ciuclan, L., Godoy, P., Ilkavets, I., Ehnert, S., Ueberham, E., Gebhardt, R., Kanzler, S., Geier, A., et al. 2008. Hepatocyte-specific Smad7 expression attenuates TGF-beta-mediated fibrogenesis and protects against liver damage. *Gastroenterology* 135:642-659.

19. Yoshino, J., Monkawa, T., Tsuji, M., Inukai, M., Itoh, H., and Hayashi, M. 2007. Snail1 is involved in the renal epithelial-mesenchymal transition. *Biochem Biophys Res Commun* 362:63-68.

20. Franci, C., Takkunen, M., Dave, N., Alameda, F., Gomez, S., Rodriguez, R., Escriva, M., Montserrat-Sentis, B., Baro, T., Garrido, M., et al. 2006. Expression of Snail protein in tumor-stroma interface. *Oncogene* 25:5134-5144.

21. Sabeh, F., Ota, I., Holmbeck, K., Birkedal-Hansen, H., Soloway, P., Balbin, M., Lopez-Otin, C., Shapiro, S., Inada, M., Krane, S., et al. 2004. Tumor cell traffic through the extracellular matrix is controlled by the membrane-anchored collagenase MT1-MMP. *J Cell Biol* 167:769-781.

22. Arciniegas, E., Frid, M.G., Douglas, I.S., and Stenmark, K.R. 2007. Perspectives on endothelial-to-mesenchymal transition: potential

contribution to vascular remodeling in chronic pulmonary hypertension. *Am J Physiol Lung Cell Mol Physiol* 293:L1-8.

23. Potenta, S., Zeisberg, E., and Kalluri, R. 2008. The role of endothelial-to-mesenchymal transition in cancer progression. *Br J Cancer* 99:1375-1379.

24. Romano, L.A., and Runyan, R.B. 2000. Slug is an essential target of TGFbeta2 signaling in the developing chicken heart. *Dev Biol* 223:91-102.

25. Timmerman, L.A., Grego-Bessa, J., Raya, A., Bertran, E., Perez-Pomares, J.M., Diez, J., Aranda, S., Palomo, S., McCormick, F., Izpisua-Belmonte, J.C., et al. 2004. Notch promotes epithelial-mesenchymal transition during cardiac development and oncogenic transformation. *Genes Dev* 18:99-115.

26. Kokudo, T., Suzuki, Y., Yoshimatsu, Y., Yamazaki, T., Watabe, T., and Miyazono, K. 2008. Snail is required for TGFbeta-induced endothelial-mesenchymal transition of embryonic stem cell-derived endothelial cells. *J Cell Sci* 121:3317-3324.

27. Lopez, D., Niu, G., Huber, P., and Carter, W.B. 2009. Tumor-induced upregulation of Twist, Snail, and Slug represses the activity of the human VE-cadherin promoter. *Arch Biochem Biophys* 482:77-82.

28. Parker, B.S., Argani, P., Cook, B.P., Liangfeng, H., Chartrand, S.D., Zhang, M., Saha, S., Bardelli, A., Jiang, Y., St Martin, T.B., et al. 2004. Alterations in vascular gene expression in invasive breast carcinoma. *Cancer Res* 64:7857-7866.

29. Zidar, N., Gale, N., Kojc, N., Volavsek, M., Cardesa, A., Alos, L., Hofler, H., Blechschmidt, K., and Becker, K.F. 2008. Cadherin-catenin complex and transcription factor Snail-1 in spindle cell carcinoma of the head and neck. *Virchows Arch* 453:267-274.

30. Engler, A.J., Sen, S., Sweeney, H.L., and Discher, D.E. 2006. Matrix elasticity directs stem cell lineage specification. *Cell* 126:677-689.

31. McBeath, R., Pirone, D.M., Nelson, C.M., Bhadriraju, K., and Chen, C.S. 2004. Cell shape, cytoskeletal tension, and RhoA regulate stem cell lineage commitment. *Dev Cell* 6:483-495.

32. Brabletz, T., Jung, A., Spaderna, S., Hlubek, F., and Kirchner, T. 2005. Opinion: migrating cancer stem cells - an integrated concept of malignant tumour progression. *Nat Rev Cancer* 5:744-749.

33. Thiery, J.P. 2002. Epithelial-mesenchymal transitions in tumour progression. *Nat Rev Cancer* 2:442-454.

34. Peinado, H., Quintanilla, M., and Cano, A. 2003. Transforming growth factor beta-1 induces snail transcription factor in epithelial cell lines: mechanisms for epithelial mesenchymal transitions. *J Biol Chem* 278:21113-21123.

35. Zhou, B.P., Deng, J., Xia, W., Xu, J., Li, Y.M., Gunduz, M., and Hung, M.C. 2004. Dual regulation of Snail by GSK-3beta-mediated phosphorylation in control of epithelial-mesenchymal transition. *Nat Cell Biol* 6:931-940.

36. Dahl, K.N., Ribeiro, A.J., and Lammerding, J. 2008. Nuclear shape, mechanics, and mechanotransduction. *Circ Res* 102:1307-1318.

37. Nelson, C.M., and Bissell, M.J. 2006. Of extracellular matrix, scaffolds, and signaling: tissue architecture regulates development, homeostasis, and cancer. *Annu Rev Cell Dev Biol* 22:287-309.

38. Chun, T.H., Sabeh, F., Ota, I., Murphy, H., McDonagh, K.T., Holmbeck, K., Birkedal-Hansen, H., Allen, E.D., and Weiss, S.J. 2004. MT1-MMP-dependent neovessel formation within the confines of the three-dimensional extracellular matrix. *J Cell Biol* 167:757-767.

39. Hiraoka, N., Allen, E., Apel, I.J., Gyetko, M.R., and Weiss, S.J. 1998. Matrix metalloproteinases regulate neovascularization by acting as pericellular fibrinolysins. *Cell* 95:365-377.

40. Hotary, K., Allen, E., Punturieri, A., Yana, I., and Weiss, S.J. 2000. Regulation of cell invasion and morphogenesis in a three-dimensional type I collagen matrix by membrane-type matrix metalloproteinases 1, 2, and 3. *J Cell Biol* 149:1309-1323.

41. Hotary, K., Li, X.Y., Allen, E., Stevens, S.L., and Weiss, S.J. 2006. A cancer cell metalloprotease triad regulates the basement membrane transmigration program. *Genes Dev* 20:2673-2686.

42. Hotary, K.B., Yana, I., Sabeh, F., Li, X.Y., Holmbeck, K., Birkedal-Hansen, H., Allen, E.D., Hiraoka, N., and Weiss, S.J. 2002. Matrix metalloproteinases (MMPs) regulate fibrin-invasive activity via MT1-MMP-dependent and -independent processes. *J Exp Med* 195:295-308.

43. Holmbeck, K., Bianco, P., Caterina, J., Yamada, S., Kromer, M., Kuznetsov, S.A., Mankani, M., Robey, P.G., Poole, A.R., Pidoux, I., et al. 1999. MT1-MMP-deficient mice develop dwarfism, osteopenia, arthritis, and connective tissue disease due to inadequate collagen turnover. *Cell* 99:81-92.

44. Ohtake, Y., Tojo, H., and Seiki, M. 2006. Multifunctional roles of MT1-MMP in myofiber formation and morphostatic maintenance of skeletal muscle. *J Cell Sci* 119:3822-3832.

45. Zhou, Z., Apte, S.S., Soininen, R., Cao, R., Baaklini, G.Y., Rauser, R.W., Wang, J., Cao, Y., and Tryggvason, K. 2000. Impaired endochondral ossification and angiogenesis in mice deficient in membrane-type matrix metalloproteinase I. *Proc Natl Acad Sci U S A* 97:4052-4057.

46. Li, X.Y., Ota, I., Yana, I., Sabeh, F., and Weiss, S.J. 2008. Molecular dissection of the structural machinery underlying the tissue-invasive activity of membrane type-1 matrix metalloproteinase. *Mol Biol Cell* 19:3221-3233.

47. Shi, J., Son, M.Y., Yamada, S., Szabova, L., Kahan, S., Chrysovergis, K., Wolf, L., Surmak, A., and Holmbeck, K. 2008. Membrane-type MMPs enable extracellular matrix permissiveness and mesenchymal cell proliferation during embryogenesis. *Dev Biol* 313:196-209.

48. Hanahan, D., and Folkman, J. 1996. Patterns and emerging mechanisms of the angiogenic switch during tumorigenesis. *Cell* 86:353-364.

49. Hanahan, D., and Weinberg, R.A. 2000. The hallmarks of cancer. *Cell* 100:57-70.